v. 1

PFC/RR-87-7 DOE/ID-01570-1

SAFETY AND ECONOMIC COMPARISON OF FUSION FUEL CYCLES

Sandra J. Brereton and Mujid S. Kazimi

August 1987

Plasma Fusion Center
and the
Department of Nuclear Engineering
Massachusetts Institute of Technology
Cambridge, Massachusetts 02139 USA

*This work was supported by EG&G Idaho, Inc. and the U.S. Department of Energy, Idaho Operations Office under DOE Contract No. DE–AC07–76ID01570

SAFETY AND ECONOMIC COMPARISON OF FUSION FUEL CYCLES

Abstract

The DT, DD and DHe fusion fuel cycles are compared on the basis of safety and economics. The designs for the comparison employ HT-9 structure and helium coolant; liquid lithium is used as the tritium breeder for the DT fuel cycle. The reactors are pulsed superconducting tokamaks, producing 4000 MW thermal power. The DT and DD designs are developed utilizing a plasma beta of 5 %, 10 % and 20 %, assuming first stability scaling laws; a single value of 10 % for beta is used for the DHe design. Modest extrapolations of current day technology are employed, providing a reference point for the relative ranking of the fuel cycles. Technological advances and improved understanding of the physics involved may alter the relative positions from what has been determined here.

The cost of electricity (COE) produced by the DT fuel cycle is projected to be 57 mills/kWh in 1986 dollars. This cost is a decreasing function of plasma beta up to a value of 10 %, beyond which no further improvement is seen. The lowest COE for the DD fuel cycle is 85 mills/kWh at 20 % beta. The cost of electricity produced by the DHe fuel cycle is 79 mills/kWh, assuming a helium-3 cost of 40 kS/kg. The COE is shown to increase by roughly 10 % as the helium-3 fuel cost increases by ten fold. Parametric studies indicate a strong dependence of the COE on the mass utilization factor, or fusion island mass per unit of thermal power produced. A fusion island mass of ~ 10,000 tonne and a fusion island volume of ~ 3,000 m^3 place DT tokamaks in the economically competitive region. The DD tokamaks appear to be too large and massive to be economically viable. A strong influence of the neutron fluence limit on the COE for the DT fuel cycle is evident up to 15 $\frac{MW \cdot yr}{m^2}$; above this value, the decrease in COE per unit increase in fluence limit is not large. The neutron fluence limit has an impact on the COE for the DD fuel cycle up to a value of 5 $\frac{MW \cdot yr}{m^2}$.

Tritium inventories for the advanced fuel plants are considerably reduced from the DT plants. The total vulnerable inventory is reduced by a factor of 20 for the DD and DHe fuel cycles compared to DT. The total onsite inventory, including both vulnerable and non-vulnerable forms, is reduced by nearly two orders of magnitude for the advanced fuels. Tritium breeding and blanket processing are not the major contributors to the DT plant tritium inventory. In all cases, the bulk of the tritium resides in the exhaust processing system. The average tritium source term at the DD and DHe plants is roughly one one-hundredth that at the DT plants. A single detritiation unit is needed to maintain the plant atmospheric tritium concentration at an acceptable level for the DT plants; the steady state tritium concentration in the atmospheres of the advanced fuel reactor halls is low enough without the use of a detritiation unit to permit access of unprotected personnel.

There appears to be no great advantage in terms of blanket activation with the advanced fuels for the materials considered in this study. These conclusions are a reflection of the material used and cannot be regarded as a generalization. Because of the large volume of structure used, activity and afterheat levels in the DD blankets exceed that in the DT blankets. The levels found in the DHe blanket

are lower than both DT and DD, but are still of significance. Since equal volume fractions of structural material are found in the first walls, activity and afterheat levels are greater for DT. This reflects the high neutron energy and greater flux intensity associated with the DT designs. Higher levels of activity are seen at higher values of beta for a given fuel cycle. None of the wastes produced at the fusion plants qualifies for shallow land burial, although material modifications may allow the criteria to be met. Waste from the DD plants poses the greatest threat, while that from the DHe plant is least hazardous. Gamma dose rates encountered by plant workers are greatest for the DT fuel cycle. Steam generator dose rates dominate the occupational exposures.

The use of an alternate blanket, consisting of a reduced activation ferritic steel (RAF) first wall and an Fe2Cr1V alloy blanket, for the 10 % beta DD design, reduces the COE from 94 mills/kWh (with an HT-9 blanket) to 85 mills/kWh. The savings is due to a higher blanket multiplication factor, resulting in a smaller reactor size, and a lower cost blanket material. The safety analysis for normal plant conditions revealed that this alternate blanket results in similar levels of short lived species (compared to HT-9), but leads to a significant reduction in long lived isotopes. Shutdown decay heat levels are similar for both blanket materials. No reduction in occupational exposures is expected with the RAF/Fe2Cr1V blanket compared to the HT-9 case. However, the alternate blanket does considerably reduce waste disposal hazards.

Investigation of a loss of coolant accident (LOCA) for the HT-9 designs indicated that the DHe fuel cycle presents the least risk. Little difference is seen in the total onsite dose incurred subsequent to the accident for the DT and DD fuel cycles. The largest economic impact of the LOCA results for the DD fuel cycle, mainly as a consequence of the greater repair costs. Offsite impacts of this accident are minimal in all cases.

A methodology for cost/benefit analysis is applied to determine if the increased costs of the alternate HT-9 designs relative to the 20 % beta DT case are justified by the improved safety which they provide. Normal conditions and the health and economic risks posed by a loss of coolant accident are considered. It is revealed that, of the HT-9 designs considered in this study, only the 10 % beta DT design is cost effective. A rough assessment of the cost effectiveness of the DD and DHe designs using an unspecified, very low cost, very low activation blanket and shield material still indicated that use of the advanced fuels is unjustified. This conclusion may be altered, however, if consideration is given to cost reductions during construction of the advanced fuel plants due to application of less costly practices employed in non-nuclear power plants.

Acknowledgements

Several people assisted in various phases of this work. We sincerely appreciate the time and effort taken by these individuals. Several people at the M.I.T. Plasma Fusion Center contributed to this effort. We would like to thank Dr. Dan Cohn for his input and comments. We appreciate the invaluable support work of Lisa Porter. The assistance of Rene LeClaire with the work dealing with economics is greatly appreciated. We thank Steve Fetter for the use of, and help with, his FUSEDOSE calculational methodology. We also acknowledge John Massidda for the use of, and assistance with, his heat transfer code. As well, we wish to express our gratitude to Steve Piet of EG & G, Idaho for his input and comments on this research.

The financial support of Ontario Hydro and the National Science and Engineering Research Council of Canada (NSERC) are gratefully acknowledged, as is the support and encouragement of Kam Wong and the staff of the Canadian Fusion Fuels Technology Project (CFFTP). Finally, we would like to thank the Fusion Safety Program of EG & G, Idaho for funding this research.

Table Of Contents

		Page
	Abstract	2
	Acknowledgements	4
	Summary, Conclusions and Recommendations	20
	Summary and Conclusions	21
	Recommendations	34
Chapter One:	Introduction	38
1.1	Fuel Cycles for Fusion Reactors	39
1.2	Design Considerations for Advanced Fuel Reactors	47
1.3	Safety and Economic Considerations	51
1.4	Recent Design Studies	53
1.5	Scope of Present Work	54
1.6	References	56
Chapter Two:	Reference Reactor Designs	60
2.1	Reactor Parameters	61
2.1.1	Plasma Beta	61
2.1.2	Blanket Materials	64
2.1.3	Plasma Operation	67
2.1.4	Other Considerations	68
2.2	DT Designs	69
2.2.1	The Effect of Varying Beta	73
2.2.2	The Effect of Varying Aspect Ratio	80
2.2.3	The Effect of Varying Plasma Elongation	85
2.3	DD Designs	91
2.3.1	The Effect of Varying Beta	95
2.3.2	The Effects of Varying Aspect Ratio and Elongation	96

		Page
2.4	A DHe Design	97
2.4.1	Comparison of the DHe Design to the Other Fuel Cycles	101
2.4.2	Ohmic Heating in Advanced Fuel Reactors	102
2.5	Design Summary	105
2.6	References	107
Chapter Three:	**Economic Evaluation of Alternate Fuel Cycles**	113
3.1	Costing Methodology	114
3.2	Economics of DT Designs	121
3.2.1	The Effect of Varying Beta	121
3.2.2	The Effects of Varying Aspect Ratio and Elongation	130
3.2.3	Other Effects	135
3.3	Economics of DD Designs	141
3.3.1	The Effect of Varying Beta	141
3.3.2	The Effects of Varying Aspect Ratio and Elongation	151
3.3.3	Other Effects	154
3.4	Economics of the DHe Design	157
3.5	General Discussion of Fuel Cycle Economics	162
3.6	Summary of Economic Analysis	173
3.7	References	177
Chapter Four:	**Fuel Cycle Systems**	180
4.1	Vacuum System	185
4.2	Impurity Removal System	192
4.3	Isotope Separation Systems	195

		Page
4.3.1	Hydrogen Isotope Separation	196
4.3.2	Helium Isotope Separation	203
4.4	Fuel Storage and Delivery System	208
4.5	Atmospheric Tritium Recovery Systems	211
4.6	Tritiated Waste Treatment System	217
4.7	Blanket Tritium Recovery System	219
4.8	Economic Evaluation of Fuel Cycle Systems	221
4.9	Summary of Fuel Cycle Systems	225
4.10	References	226
Chapter Five:	**Radiological Hazards of Fusion Fuel Cycles**	230
5.1	Tritium Hazards	231
5.1.1	Tritium Inventory	232
5.1.1.1	Tritium Inventory in the Fuel Handling System	233
5.1.1.2	Tritium Inventory in the Blanket and Breeder Processing Systems	237
5.1.1.3	Tritium Inventory in the Blanket Structure and Coolant System	237
5.1.2	Tritium Releases	240
5.1.2.1	Tritium Releases from the Fuel Handling Systems	245
5.1.2.2	Tritium Releases from the Blanket and Breeder Processing Systems	250
5.1.2.3	Tritium Releases from the Coolant System	251
5.1.2.4	Tritium Releases from Waste Handling	252
5.1.2.5	Atmospheric Tritium Releases from the Plant	254
5.1.3	Doses Due to Tritium Exposure	260
5.1.4	Tritium Hazard Summary	264
5.2	Induced Radioactivity Hazards	268

		Page
5.2.1	Activation Product Inventories	269
5.2.2	Releases of Activated Material	280
5.2.3	Occupational Doses	283
5.2.4	Waste Management	290
5.2.5	Induced Radioactivity Hazard Summary	304
5.3	References	308
Chapter Six:	**Accident Hazards of Fusion Fuel Cycles**	313
6.1	Sources of Stored Energy	314
6.2	Mechanisms for the Release of Stored Energy	316
6.2.1	Plasma Disruptions	317
6.2.2	Magnet System Accidents	318
6.2.3	Lithium Fires	320
6.2.4	Cryogenic Depressurization	321
6.2.5	Auxiliary System Accidents	322
6.2.6	Hydrogen Explosions	323
6.3	Consequences of a Loss of Coolant Accident	323
6.3.1	Discussion of the Problem	324
6.3.2	Assumptions Involved and Method of Analysis of the Loss of Coolant Accident	326
6.3.2.1	First Wall Temperature Response	328
6.3.2.2	Mobility of Oxides	329
6.3.2.3	Stuctural Creep Considerations	333
6.3.3	Immediate Consequences of the Coolant System Accident	335
6.3.4	Health Effects due to the Loss of Coolant Accident	348
6.3.5	Economic Consequences of the Loss of Coolant Accident	356

		Page
6.3.5.1	Onsite Economic Consequences	356
6.3.5.1.1	Replacement Power	357
6.3.5.1.2	Decontamination Costs	358
6.3.5.1.3	Repair Costs	366
6.3.5.1.4	Health Effects Costs	368
6.3.5.2	Offsite Economic Consequences	368
6.4	Accident Hazard Summary	369
6.5	References	374
Chapter Seven:	**Cost/Benefit Safety Analysis of Fusion Fuel Cycles**	378
7.1	Discussion of Approaches to Cost/Benefit Analysis	379
7.1.1	Cost/Benefit Analysis for Routine Occupational Exposure Reduction	380
7.1.2	Application of Cost/Benefit Analysis to Accident Conditions	388
7.1.3	Economic Considerations in Cost/Benefit Analysis	390
7.1.4	Shortcomings of Cost/Benefit Analysis	394
7.2	Methodology for Cost/Benefit Analysis	396
7.2.1	Cost/Benefit Figure of Merit for a Proposed Design	396
7.2.1.1	Economic Factor for the Figure of Merit	397
7.2.1.2	Safety Factor for the Figure of Merit	399
7.2.1.3	Cost/Benefit Figure of Merit	401
7.2.2	Cost/Benefit Expenditure Limit	402
7.2.3	The Design Decision Process	407
7.3	Application of Cost/Benefit Methodology to Advanced Fusion Fuel Cycles	408
7.3.1	Ceiling on Safety Expenditures	408

		Page
7.3.2	Cost/Benefit Figure of Merit for Alternate Designs	412
7.4	Summary and Conclusions Regarding the Cost Effectiveness of Alternate Designs	420
7.5	References	425
Appendix A:	**Description of Reactor Designs**	430
A.1	Reactor Design Code	430
A.2	Lifetime Fluence Limits	475
A.2.a	Neutron Fluence Limit	475
A.2.b	Thermal Fluence Limit	478
A.3	References	481
Appendix B:	**Cost Accounts and Costing Algorithms**	483
B.1	Cost Accounts and Costing Algorithms	483
B.2	References	569
Appendix C:	**Maintenance Assessment**	571
C.1	Plant Capacity Factor	571
C.2	Personnel Requirements	591
C.3	References	594
Appendix D:	**Fuel Cycle Systems**	595
D.1	Vacuum System Conductance Analysis	595
D.2	Isotope Separation Systems	612
D.2.a	Hydrogen Isotope Separation	612
D.2.b	Helium Isotope Separation	614
D.3	Atmospheric Tritium Removal System	619
D.4	References	636
Appendix E:	**Tritium Dose Estimates**	638
E.1	Occupational Exposures Under Normal Operating Conditions	638

		Page
E.2	References	671
Appendix F:	**Gamma Dose Estimates**	672
F.1	Gamma Dose Rates During Normal Operation	672
F.1.a	Dose Rates During Near Reactor Maintenance	672
F.1.b	Dose Rates During Coolant/Steam Generator Maintenance	673
F.1.c	Dose Rates During Blanket Changeouts	674
F.1.d	Dose Rates During Blanket Processing	675
F.1.e	Dose Rates During Waste Handling	675
F.2	Occupational Gamma Exposures Under Normal Operating Conditions	677
F.3	References	681
Appendix G:	**Accident Consequences**	682
G.1	First Wall Structural Response to the LOCA	682
G.2	Determination of Occupational Doses During the LOCA	692
G.2.a	Activity Concentrations and Doses Incurred During the Initial Release Phase of the LOCA	692
G.2.b	Activity Concentrations and Doses Incurred Subsequent to the LOCA	697
G.3	References	711

List of Tables

		Page
1.1	Terrestrial Resources of Helium-3	42
2.1	Beta Scaling Laws	63
2.2	Reactor Parameters for DT Designs	70
2.3	Reactor Parameters for DD Designs	92
2.4	Reactor Parameters for DT, DD and DHe Designs with 10 % Beta	98
2.5	Reactor Parameters for STARFIRE, WILDCAT and the EPRI D $-^3$ He Tokamak	103
3.1	Costing Factors for Determination of COE	118
3.2	Economics for DT Designs	122
3.3	Economics for DD Designs	142
3.4	Economics for DT, DD & DHe Designs with 10 % Beta	158
3.5	Fuel Cycle Costs	163
3.6	Waste Handling Information	166
3.7	Economic Scaling Factors	169
3.8	Relative Ranking of Economic Scaling Factors of Advanced Fuels Compared to the DT Fuel Cycle	170
4.1	Vacuum System Parameters for DT Reactors	189
4.2	Vacuum System Parameters for DD Reactors	190
4.3	Vacuum System Parameters for DT, DD and DHe Reactors for 10 % Beta	191
4.4	Isotope Separation System Parameters	199
4.5	Working Environment and Protective Clothing Requirements	214
4.6	Economics of Fuel Cycle Systems	223
4.7	Comparison of Fuel Handling Systems Cost Estimates	224

		Page
5.1	Tritium Inventory in Various Plant Components	239
5.2	Design Parameters That Affect Tritium Releases	243
5.3	Tritium Release Estimates from the Fuel Handling Systems	248
5.4	Tritium Release Estimates from Various Plant Locations	253
5.5	Atmospheric Tritium Releases From Fusion Plants	258
5.6	Comparison of Tritium Releases to the Environment from Fusion and Fission Plants	259
5.7	Doses Incurred Due to Routine Tritium Releases	263
5.8	Major Contributors to First Wall Radioactive Inventory at End of Blanket Lifetime	271
5.9	Relative Reaction Rates Producing Major Short Lived Isotopes	273
5.10	Major Contributors to First Wall Decay Heat Levels at End of Blanket Lifetime	275
5.11	Average Inboard Blanket Activity and Decay Heat Levels at End of Blanket Lifetime	278
5.12	Gamma Dose Rates at Various Plant Locations	286
5.13	Maintenance Time Estimates and Annual Cumulative Doses Incurred During Maintenance Activities	287
5.14	Concentrations of Important Nuclides in the Blanket One Year After Shutdown and 10CFR61 Class C Shallow Land Burial Limits	293
5.15	Concentrations of Important Nuclides in the Blanket Thirty Years After Shutdown and 10CFR61 Class C Shallow Land Burial Limits	297
5.16	Wastes Generated from Fusion Plant Operation	299
5.17	Doses Incurred During Handling of Blanket Wastes	303
6.1	Sources of Stored Energy	315
6.2	Assumptions Made for the Loss of Coolant Accident	327
6.3	Mobilization Rates of HT-9 First Wall Elements	332
6.4	Nuclides Released Subsequent to the LOCA	345

		Page
6.5	Thermal Effects on First Wall During LOCA	347
6.6	Occupational Exposures Due to LOCA	351
6.7	Weather Conditions Assumed During LOCA	354
6.8	Offsite Health Impacts of LOCA for Scenarios (1) and (3)	355
6.9	Summary of Surface Decontamination Methods	361
6.10	Decontamination Program	365
6.11	Economic Impact of LOCA	367
7.1	Summary of Cost/Benefit Methodologies	381
7.2	Advantages and Disadvantages of Cost/Benefit Analysis	395
7.3	Representative Occupational Exposure Rate for Base Case Design	410
7.4	Cost/Benefit Expenditure Ceiling	413
7.5	Changes in Economic and Health Parameters Required for Evaluation of the Cost/Benefit Figure of Merit	414
7.6	Routine Dose Savings for Alternate Designs	415
7.7	Accident Related Dose Savings for Alternate Designs	416
7.8	Accident Related Cost Increases	417
7.9	Cost/Benefit Figure of Merit	419
7.10	Optimistic Cost/Benefit Parameters for Advanced Fuel Designs	423
A.1	Superconducting Design Code Input	438
A.2	Blanket Material Compositions	441
A.3	Reactor Parameters for DT Designs With Varying Beta	443
A.4	Reactor Parameters for DT Designs With Varying Aspect Ratio	446
A.5	Reactor Parameters for DT Designs With Varying Plasma Elongation	449
A.6	Reactor Parameters for DD Designs With Varying Beta	452
A.7	Reactor Parameters for DD Designs With Varying Aspect Ratio	455
A.8	Reactor Parameters for DD Designs With Varying Plasma Elongation	458
A.9	Fluence Limits	480
B.1	Variables Used in Cost Accounts	511

		Page
B.2	Economics for DT Designs With Varying Beta	515
B.3	Economics for DT Designs With Aspect Ratio	518
B.4	Economics for DT Designs With Varying Plasma Elongation	521
B.5	Economics for DD Designs With Varying Beta	524
B.6	Economics for DD Designs With Varying Aspect Ratio	527
B.7	Economics for DD Designs With Varying Plasma Elongation	530
C.1	Unscheduled Downtime Estimates for Reactor Plant Equipment Maintenance	573
C.2	Estimated Staff Size for 1200 MWe Fusion Plant	592
C.3	Estimate of Total Exposed Work Force and Most Exposed Work Group	593
D.1	Vacuum System Dimensions	596
D.2	Hydrogen Isotope Separation System Parameters	613
D.3	Helium Isotope Separation System Parameters	615
E.1	Scheduled Downtime Tritium Dose Estimates	641
E.2	Unscheduled Downtime Tritium Dose Estimates	651
F.1	Gamma Dose Rates at Various Plant Locations	678
F.2	Scaling Factors Used to Determine Gamma Dose Rates	679
F.3	Annual Maintenance Time Estimates and Resultant Gamma Doses	680
G.1	Thermal Effects on First Wall During LOCA	691

List of Figures

		Page
1.1	Cross Sections for DT, DD (total) and DHe Reactions	44
1.2	Values of $\bar{\sigma v}$ based on a Maxwellian Distribution for DT, DD (total) and DHe Reactions	45
2.1	Major Radius vs Beta	74
2.2	Minor Radius vs Beta	74
2.3	Fusion Power Density vs Beta	75
2.4	Toroidal Field vs Beta	75
2.5	Plasma Current vs Beta	76
2.6	Total Average Plasma Density vs Beta	76
2.7	Confinement Time vs Beta for DT Reactors	77
2.8	Confinement Time vs Beta for DD Reactors	77
2.9	Neutron Wall Loading vs Beta	78
2.10	Thermal Wall Loading vs Beta	78
2.11	Neutron Wall Loading vs Power Density of Fusion Island	79
2.12	Major Radius vs Aspect Ratio	79
2.13	Minor Radius vs Aspect Ratio	81
2.14	Toroidal Field vs Aspect Ratio	81
2.15	Plasma Current vs Aspect Ratio	82
2.16	Total Average Plasma Density vs Aspect Ratio	82
2.17	Confinement Time vs Aspect Ratio for DT Reactors	83
2.18	Confinement Time vs Aspect Ratio for DD Reactors	83
2.19	Neutron Wall Loading vs Aspect Ratio	84
2.20	Thermal Wall Loading vs Aspect Ratio	84
2.21	Major Radius vs Plasma Elongation	86
2.22	Minor Radius vs Plasma Elongation	86

		Page
2.23	Toroidal Field vs Plasma Elongation	87
2.24	Total Average Plasma Density vs Plasma Elongation	87
2.25	Plasma Current vs Plasma Elongation	88
2.26	Confinement Time vs Plasma Elongation for DT Reactors	88
2.27	Confinement Time vs Plasma Elongation for DD Reactors	89
2.28	Neutron Wall Loading vs Plasma Elongation	89
2.29	Thermal Wall Loading vs Plasma Elongation	90
3.1	Cost of Electricity vs Beta for the DT Fuel Cycle	126
3.2	Cost of Electricity vs Neutron Wall Loading for the DT Fuel Cycle	126
3.3	Cost of Electricity vs Toroidal Field for the DT Fuel Cycle	128
3.4	Cost of Electricity vs Minor Radius for the DT Fuel Cycle	128
3.5	Cost of Electricity vs Mass of Fusion Island for the DT Fuel Cycle	129
3.6	Cost of Electricity vs Volume of Fusion Island for the DT Fuel Cycle	129
3.7	Cost of Electricity vs Power Density of Fusion Island for the DT Fuel Cycle	131
3.8	Cost of Electricity vs Mass Power Density for the DT Fuel Cycle	131
3.9	Cost of Electricity vs Aspect Ratio for the DT Fuel Cycle	132
3.10	Direct Capital Cost vs Mass Per Unit Thermal Power for the DT Fuel Cycle	132
3.11	Cost of Electricity vs Plasma Elongation for the DT Fuel Cycle	134
3.12	Cost of Electricity vs Capacity Factor for the DT Fuel Cycle	134
3.13	Cost of Electricity vs Construction Time for the DT Fuel Cycle	136
3.14	Cost of Electricity vs Lifetime Neutron Fluence Limit for the DT Fuel Cycle	136
3.15	Cost of Electricity vs Blanket/First Wall Lifetime for the DT Fuel Cycle	138
3.16	Cost of Electricity vs Neutron Wall Loading for the DT Fuel Cycle	138
3.17	Cost of Electricity vs Cost of Shielding for the DT Fuel Cycle	140

		Page
3.18	Cost of Electricity vs Cost of Deuterium for the DT Fuel Cycle	140
3.19	Cost of Electricity vs Beta	146
3.20	Cost of Electricity vs Neutron Wall Loading	146
3.21	Cost of Electricity vs Toroidal Field	148
3.22	Cost of Electricity vs Minor Radius	148
3.23	Cost of Electricity vs Mass of Fusion Island for the DD Fuel Cycle	149
3.24	Cost of Electricity vs Volume of Fusion Island	149
3.25	Cost of Electricity vs Power Density of Fusion Island	150
3.26	Cost of Electricity vs Mass Power Density	150
3.27	Cost of Electricity vs Aspect Ratio	152
3.28	Direct Capital Cost vs Mass Per Unit Thermal Power	152
3.29	Cost of Electricity vs Plasma Elongation	153
3.30	Cost of Electricity vs Blanket/First Wall Lifetime	153
3.31	Cost of Electricity vs Lifetime Neutron Fluence Limit	155
3.32	Cost of Electricity vs Cost of Deuterium	155
3.33	Cost of Electricity vs Cost of Helium-3 for the DHe Fuel Cycle	161
3.34	Cost of Electricity vs Beta for Fusion Fuel Cycles	161
4.1	Schematic of DT Fuel Processing System	182
4.2	Schematic of DD Fuel Processing System	183
4.3	Schematic of DHe Fuel Processing System	184
4.4	Geometric Representation of Limiter/Vacuum System	186
4.5	Schematic of Impurity Removal System	194
4.6	DT Hydrogen Isotope Separation System	200
4.7	DD Hydrogen Isotope Separation System	201
4.8	DHe Hydrogen Isotope Separation System	202
4.9	DD Helium Isotope Separation System	206
4.10	DHe Helium Isotope Separation System	207
4.11	Reactor Building Detritiation System	216
4.12	Schematic of the Tritium Waste Treatment System	218

		Page
4.13	Schematic of Molten Salt Tritium Extraction Method for Fusion Reactors with Liquid Lithium Blankets	220
5.1	Schematic Pathways of Tritium Release During Normal Operation	241
5.2	Relative Contributions to Total Tritium Inventory	266
6.1	Initial First Wall Temperature Response During LOCA for DT Designs	336
6.2	Initial First Wall Temperature Response During LOCA for DD Designs	337
6.3	Initial First Wall Temperature Response During LOCA for 10 % Beta Designs	338
6.4	First Wall Temperature During LOCA for DT Designs	339
6.5	First Wall Temperature During LOCA for DD Designs	340
6.6	First Wall Temperature During LOCA for 10 % Beta Designs	341
6.7	Blanket Responses Midway Through LOCA for 5 % and 20 % Beta DT and DD Designs	343
6.8	Blanket Responses Midway Through LOCA for 10 % Beta Designs	344
7.1	Allowable Spending on Safety	384
7.2	Range of Spending on Safety	385
7.3	Allowable Spending on Reducing Plant Financial Risk	392
7.4	Reactor Economic Risk Spectrum	393
A.1	Blanket Configuration for Neutronics Analysis	442
D.1	Vacuum Pumping System	598
D.2	McCabe-Thiele Analysis for Helium Isotope Separation for the DD Fuel Cycle	618
D.3	Atmospheric Tritium Removal	621
G.1	Plasma Shutdown Mode After LOCA	683

Summary, Conclusions and Recommendations

The aim of this study was to compare, on an equal basis, the safety and economic characteristics of the DT, DD and DHe fusion fuel cycles. Representative designs were established based on consistent design criteria using only modest extrapolations of present day technologies. An economic analysis of these designs was performed within a consistent framework, with some flexibility in areas where the fuel cycles differed so that an accurate determination of the cost of electricity could be made. Safety analyses were performed to evaluate tritium inventories, routine tritium releases, inventories of activation products and the level of hazard associated with plant wastes. The annual dose incurred by plant workers was estimated for all fuel cycles. The impact of the use of an alternate blanket material on the economics and safety during normal conditions of the DD fuel cycle was examined. A loss of coolant accident (LOCA) was investigated to determine the relative safety and economic impact of this event for the various fuel cycles for designs employing the same structural material. Finally, a cost/benefit analysis was performed to assess the cost effectiveness of the alternate designs and to determine if the increased costs associated with these designs is justified by the improved safety which they provide. A summary of the findings and conclusions from the study are discussed in the next section. This is followed by recommendations for future work.

Summary and Conclusions

The representative reactors on which the safety and economic comparison was based were pulsed superconducting tokamaks. The DT designs employed a lithium breeder for tritium production with HT-9 structure and helium coolant. The blankets of the DD and DHe reactors were designed for energy multiplication and utilized HT-9 structure with helium coolant. An alternate DD design which employed a reduced activation ferritic steel (RAF) first wall and Fe2Cr1V alloy blanket with helium coolant was also studied. The advanced fuel reactors are larger than their DT counterparts because of the lower fusion power density associated with these fuel cycles. Although the designs all produced a thermal power of 4000 MW, the power produced by fusion in the plasma was not the same in each case. The DD reactors show a larger total gain in energy from neutron interactions in the blanket. This reflects the blanket material, the neutron energy spectrum and the total number of neutrons entering the blanket. The DT designs have the greatest blanket/shield thickness due to the greater quantity and higher energy of the fusion neutrons. Designs were developed for a range of values of plasma beta, assuming first stability scaling laws. As beta was increased, the reactor size decreased but the wall loading increased. This was found to have an important effect on reactor economics.

The fuel handling systems were characterized for the various fuel cycles. The blanket tritium recovery system and coolant tritium removal capabilities are needed only for the DT fuel cycle. Other fuel handling components, including the vacuum system, impurity removal system, isotope separation systems, storage facilities, fuel delivery system, tritium waste treatment system and atmospheric tritium recovery system are needed at the advanced fuel plants because a circulating tritium inventory exists. Some of these components, however, may be scaled down from those needed for the DT fuel cycle because of the lower tritium throughput. Others, such as the vacuum system, are larger for the advanced fuels because of the more severe

plasma purity requirements. The hydrogen isotope separation systems do not differ greatly amongst the fuel cycles. A third column for the advanced fuels is only needed during and shortly after pulse initiation, since tritium is being fueled at this time and the plasma exhaust will contain a higher tritium concentration which must be reduced before discharge to the environment. Helium isotope separation capabilities are greatest for the DHe fuel cycle. Since ^{3}He is present in the plasma exhaust from the DT reactor chamber in very small quantities, no helium isotope separation equipment is needed for this fuel cycle. Other components of the fuel cycle systems are not expected to be largely different amongst the fuel cycles. No difference in equipment needs is seen for the different values of beta for a given fuel cycle.

The economic comparison was founded on the projected cost of electricity (COE) for each fuel cycle. The COE was determined from the plant capital cost, the operating and fuel costs, the plant capacity factor, the plant lifetime and financing parameters. The costing generally followed a standard set of accounts. Assumptions included a six year construction time, 30 year plant lifetime and 6 % inflation for current dollar calculations. Results of the economic analysis indicated that the advanced fuels are at a clear economic disadvantage with respect to the DT fuel cycle. The COE in 1986 dollars obtained for the DT fuel cycle was 57 mills/kWh (at 10 % and 20 % beta). At best, the DD fuel cycle produced electricity at a cost of 85 mills/kWh (48 % greater than for DT). This occurred for the 20 % beta HT-9 design and for the 10 % beta RAF/Fe2Cr1V design. Both of these tokamaks were smaller as a result of the higher power density in the 20 % beta HT-9 case, and as a result of the higher blanket multiplication factor in the 10 % beta RAF/Fe2Cr1V case. The cost of electricity produced by the DHe fuel cycle was 79 mills/kWh at 10 % beta (38 % greater than for DT), with a cost of helium-3 of 40 k$/kg. The COE will be higher if the cost of helium-3 fuel is much greater than this. It should be noted that these costs are for pulsed systems, which are more costly than steady state systems because of the large investment required for the thermal storage sys-

tem and greater poloidal field magnet costs. It was estimated that the pulsed burn mode adds 8 to 10 mills/kWh to the COE compared to that for a steady state system.

Several parametric studies were performed for DT fuel cycle. It was revealed that for the designs considered in this work (Li/He/HT-9, aspect ratio of 4, elongation of 2.5, 4000 MWt) there is no economic incentive for pursuing values of plasma beta above 10 %. This optimum results from the competition between decreasing costs due to a smaller reactor versus the increasing costs due to more frequent component replacement as beta is increased. It was found that for 10 % beta, a high aspect ratio and an elongation of 2.0 are desirable. The COE for DT was found to be linearly dependent on the cost of shielding, and almost unaffected by the cost of deuterium fuel. A fairly strong dependence of the COE on the mass utilization factor ($\frac{M_{FI}}{P_T}$) was seen. The fusion island mass of a 4000 MWt plant must be in the area of 10,000 tonne, and the fusion island volume must be on the order of 3,000 m^3 in order for DT tokamaks employing conventional power conversion systems to be competitive with fission. The neutron fluence limit was seen to have a large impact on the COE up to values of $\sim$ 15 $\frac{MW \cdot yr}{m^2}$. Above this value, the decrease in the COE per unit increase in fluence limit is not large.

Higher beta appears to have a greater impact on reducing the COE for the DD fuel cycle than for DT. However, the unit reduction in cost per unit increase in beta becomes small beyond a beta of 10 - 15 %. This is again a consequence of the competing effects of decreasing costs due to smaller component sizes and increasing costs due to more frequent replacement at high beta. To minimize the COE for DD reactors, a moderate value of beta (10 - 15 %), a high aspect ratio and elongation of 2.0 to 2.5 should be sought. A longer blanket lifetime is more important for this fuel cycle because the larger reactor components result in more costly blanket changeouts. Varying the fluence limit showed that no impact on the COE is felt beyond a value of $\sim$ 12 $\frac{MW \cdot yr}{m^2}$. The use of a material having a higher blanket multiplication factor (Fe2Cr1V vs HT-9) resulted in an improved COE. This

is due to the lower fusion power, and hence smaller and less costly reactor, required to produce 4000 MWt. The lower unit cost of the blanket material (20 $/kg for Fe2Cr1V vs 50 $/kg) also contributes to the reduction in the COE. The mass and volume of the least costly DD designs (20 % beta HT-9 and 10 % RAF/Fe2Cr1V) were seen to be far too large to result in a competitive COE.

The DHe fuel cycle was found to produce electricity at a cost lower than for DD, but still significantly above that for DT. An important factor in determining the COE for this fuel cycle is the cost of fuel. An increase of 7 mills/kWh in the COE was seen as the cost of helium-3 was increased from 40 k$/kg to 500 k$/kg. A major concern is the availability of fuel to supply an economy dependent on this fuel cycle. Terrestrial reserves may be sufficient to support an experimental research program, but would be insufficient to support a mature fusion economy based on this fuel cycle. The lunar soil has been identified as a potential source of helium-3. However, the feasibility of mining and transporting this helium-3 back to earth has not been determined at this time.

A recategorization of costs from the standard accounts allowed for a direct comparison of costs directly associated with the fuel cycle. Fuel cycle costs included initial and replacement first wall/blanket, limiter and auxiliary heating costs, miscellaneous scheduled replaceable items costs, fuel costs and waste handling costs. These were seen to be similar for DT and DHe, both being much below the costs for DD. The greater cost for DD is mainly a consequence of the larger volume of materials use for components compared to DT, and the greater replacement frequency compared to DHe. These costs are somewhat lower for the RAF/Fe2Cr1V DD design (compared to the HT-9 DD design) due both to the smaller blanket and the lower unit cost of the blanket material. The contribution of fuel costs to the fuel cycle costs are greatest for DHe; the contribution of waste handling costs are least for this fuel cycle. This reflects the reduced volume and activity of the wastes to be handled.

An advantage of using an advanced fuel is that there is no need to breed tritium. This is a major difficulty for DT reactors which strive to achieve a tritium breeding ratio of one. This constraint is alleviated for the advanced fuels, giving more flexibility in the blanket design. However, for the designs considered here, the advanced fuels have more costly blankets and produce energy more expensively despite the elimination of tritium breeding and the potential for enhanced neutron energy multiplication. The absence of a lithium compound and breeder tritium extraction equipment do not result in a great cost reduction for the DD and DHe fuel cycles. To provide for plasma exhaust purification, tritium handling and hydrogen isotope separation equipment is still required, although on a smaller scale than for DT. Some cost savings is seen, but these are largely overshadowed by the much larger expense associated with the advanced fuel blankets and other components of the fusion island.

An economic benefit of the lower occupational hazards of the DD and DHe fuel cycles is seen in the improved plant capacity factor experienced with these fuel cycles. Lower tritium inventories and release rates allow workers to perform tasks unencumbered by bubble suits, as they would be performing the same tasks at a DT plant. The reduced gamma dose rates at various locations throughout the plant for the DD fuel cycle, and especially for the DHe fuel cycle, allow for contact maintenance in areas where the same task would be performed remotely at a DT plant. This results in substantial savings in downtime. After consideration of these effects, improved plant capacity factors of 69 % for DD and 72 % for DHe, compared to 65 % for DT, were found. This partially offsets the increased costs for the advanced fuel cycles seen in other areas, but does not have a strong enough impact to render the advanced fuels economically competitive.

The DT fuel cycle is superior in terms of material and volume utilization per unit power produced. It also requires much less magnetic energy for power production. The DT fusion island is less capital intensive, but has a greater need for component replacement as reflected through the wall loading. Nevertheless, the

economics of the DT fuel cycle are far more attractive than that of the advanced fuels.

Although the advanced fuels are at an economic disadvantage with respect to DT, they have a clear advantage over the DT fuel cycle in terms of tritium hazard. The tritium circulating throughout the plant, tritium inventories in plant components, tritium release rates from these components and tritium exposures incurred during maintenance activities are all significantly reduced for the DD and DHe fuel cycles.

The tritium exhausted from the DD and DHe reactor chambers is over two orders of magnitude lower than for DT. This is a consequence of reduced tritium fueling and the higher fractional burnup of tritium for the advanced fuels due to their higher operating temperatures. This is important because the tritium inventories established throughout the plant are largely dependent on the tritium exhaust rate from the plasma.

Reductions in tritium inventories for the advanced fuels relative to DT are found at all locations in the fuel cycle. The first wall tritium inventory is reduced by two orders of magnitude; the tritium retained in the blanket structure is reduced by three orders of magnitude. A large reduction in the quantity of tritium found in the cryopumps and fuelers is seen for the advanced fuels. Although the amount of tritium found in the coolant is small for all fuel cycles, the two orders of magnitude reduction for the DD and DHe fuel cycles is significant because permeation of tritium into the steam cycle and subsequent leakage from this system is a major tritium pathway to the environment. Concerns associated with tritium in the breeding blanket and blanket processing systems are completely eliminated for the advanced fuels. The total vulnerable tritium inventory is reduced by over a factor of twenty for the DD and DHe fuel cycles compared to DT. The total inventory at the site, including both vulnerable and non-vulnerable forms, is reduced by nearly two orders of magnitude for DD and DHe. The tritium throughput and resultant tritium

inventories throughout the DHe plant are very near to that for the DD plant. The plasma exhaust rate on which the tritium inventory is largely dependent, is based on the tolerable level of alpha ash in the plasma. The higher formation rate of alpha ash in the plasma of a DHe reactor requires a greater plasma exhaust rate to maintain the ash concentration at an acceptable level. This results in relatively high recirculation rates of all species and a higher tritium inventory throughout the plant than would be expected from the tritium concentration in the DHe plasma.

Upon examination of the distribution of the tritium inventory throughout the plant, it was shown that the tritium inventory in the DT blanket and blanket processing system is somewhat less than that in the exhaust processing system and much smaller than that in storage. Tritium breeding and blanket processing are not the major contributors to the plant tritium inventory. It is the need for tritium as a component of the fuel, and the relatively high tritium concentration in the exhaust which leads to the higher tritium inventories. For the advanced fuels, the bulk of the inventory is also located in the exhaust processing systems. However, this is much reduced relative to DT so that the advanced fuels are much more desirable from a tritium handling viewpoint. The elimination of the tritium breeding function for the advanced fuels does not eliminate the need for tritium handling equipment such as cryopumps, molecular sieves, cryogenic distillation columns and fuelers. These components are required whether or not tritium is bred, although on a smaller scale than for DT.

The occupational tritium hazard and tritium releases to the environment are dependent upon the releases to the reactor building during normal operation and maintenance. The average tritium source term is reduced by two orders of magnitude for the advanced fuels. As a consequence of this, the steady state tritium concentration in the reactor hall is low enough that unprotected personnel access is permitted, and the building atmosphere can be directly vented to the environment without processing. Emergency tritium removal capabilities were assessed based on the release of the maximum vulnerable tritium inventory. This was located in

the blanket processing system for the DT reactors, and in the cryopumps for the advanced fuels. Eight units would be needed to reduce the tritium concentration to 500 $\mu Ci/m^3$ within 48 hours for the DT designs; four units would accomplish this objective for the advanced fuels. A single unit would be used during normal operation at the DT plants. The others would be on standby for off normal events. This would be the case for all units found at the DD and DHe plants.

Tritiated wastes are significantly reduced for the advanced fuels, as would be expected from their lower tritium inventories. This results in reduced exposures during waste handling. Some cost savings also results for these activities for the advanced fuels because of the lower volume and activity of the wastes being handled.

The HT-9 DD and DHe designs considered in this work showed no distinct advantage in terms of induced radioactivity hazard over the DT fuel cycle. A considerable reduction in long term concerns resulted with the RAF/Fe2Cr1V DD design compared to the HT-9 design. A similar reduction in long term hazards would also be expected with this materials change for the other fuel cycles.

The higher energy neutrons and greater flux intensity associated with the DT designs lead to a greater concentration of radionuclides in their first walls. With the increase in flux at high beta, activity concentrations are greatest for these designs. The design presenting the most concentrated first wall activity level is the 20 % beta DT design. Short lived species dominate at shutdown in all cases. The relative contribution of these short lived isotopes to the total shutdown activity is greatest for DT. Long lived isotopes are present in equal or greater amounts in the HT-9 DD first walls compared to the DT first walls. This is not the case for the DD design with an RAF first wall where a reduction of nearly four orders of magnitude is seen in the long lived species compared to the HT-9 first wall. The DHe first wall contains a non-negligible amount of long lived species. This is both a consequence of the softer neutron spectrum characteristic of the advanced fuels and of the longer blanket lifetime. As would be expected from the higher level of activity associated

with the DT designs, decay heating levels in the first wall at shutdown are greatest for this fuel cycle.

The bulk of the blanket presents a slightly different situation than does the first wall. The average blanket activity is lower than the first wall activity for the DT designs because of the reduced amount of HT-9 structure located here. The case is reversed for the advanced fuels, where the volume fraction of steel is much greater in the blanket and the resulting activity levels are higher than in the first wall. The activity concentrations and decay heat levels are greatest for the 20 % beta DD design. As with the first wall, short lived species dominate the shutdown activity of the blanket. Both short and long lived species are present in greater quantities for the DD and DHe fuel cycles. This may be surprising, especially for the DHe fuel cycle. It strongly suggests using a lower activation material in the blanket, or employing boron to capture neutrons in the DHe case, where useful energy multiplication is not crutial. The use of a Fe2Cr1V blanket, with a reduced nickel and molybdenum content, showed reduced levels of long lived isotopes compared to the HT-9 DD case, but resulted in higher levels than the DT case (due to the higher fraction of structure in the DD blanket). These levels would likely fall below the DT HT-9 levels if RAF was used in the blanket (RAF has an even lower nickel and molybdenum content, so that long lived species would be produced in smaller amounts). This, however, would come at a cost penalty.

Dose rates encountered by plant workers during normal operation were found to be highest for the DT fuel cycle. Steam generator doses, followed by those incurred during blanket changeouts, dominate occupational exposures in all cases. This suggests that doses incurred during maintenance could be significantly reduced by the use of a lower activation material. The RAF first wall/Fe2Cr1V blanket DD design resulted in slightly higher doses to plant workers because of slightly higher levels of short lived species compared to the HT-9 case. An additional hazard also exists for the DT fuel cycle, during processing of the breeder material. However, the dose incurred while carrying out breeder processing tasks is not large relative

to doses resulting from other maintenance activities. Offsite impacts of induced radioactivity are expected to be negligible for all fuel cycles. Routine releases of aqueous effluents and releases of activated atmospheric gases are expected to be low. The hazard presented to the public from induced activity under normal conditions was not evaluated, but is expected to be small for all fuel cycles.

None of the wastes produced at the fusion plants qualifies for shallow land burial. The advantage of the RAF/Fe2Cr1V design is seen in the reduced levels of long lived isotopes. However, shallow land burial is not possible since the disposal limit was still exceeded with this material. Shallow land burial may be possible if the blanket had been made entirely of RAF. The economic penalty of using this more expensive blanket material (compared to Fe2Cr1V) may be offset by the savings in waste disposal costs. This would be true for all fuel cycles. Because the quantities of long lived species are greatest for the HT-9 DD designs, it poses the greatest waste disposal hazard. Blanket wastes from the DHe design still pose a waste disposal threat. These conclusions should be regarded with caution since they are dependent on the material used.

The effect of plasma beta on plant safety is more evident in terms of component activation than tritium hazard. Very little difference was seen in tritium inventories, release rates and occupational exposures for a given fuel cycle at various values of beta. Hazards due to material activation and waste handling were seen to increase with plasma beta. This is a consequence of the decreased reactor size, resulting in a higher first wall flux and greater activity concentration. Because doses incurred at the advanced fuel plants are almost exclusively due to exposure to gamma fields, high beta designs for these fuel cycles are less desirable from a safety standpoint.

The advanced fuels appear to have greater quantities of stored energy in their reactor systems and hence, a greater potential for release of radioactive material. This is largely a consequence of the greater magnetic fields and the higher operating temperature associated with these fuel cycles. The DD fuel cycle has the greatest

quantity of stored energy in the form of decay heat, for the blanket material used here (HT-9). This is a result of the larger amount of structural material relative to DT and the higher neutron flux relative to DHe. An additional source of stored energy exists in the lithium blankets of the DT designs. The chemical energy which could be released upon burning lithium presents a potential concern for this fuel cycle. The magnitude of this source of stored energy is comparable to that stored as kinetic and magnetic energy in the advanced fuel plasmas.

To evaluate the impact of a potential accident, a loss of coolant accident was investigated. The scenario envisioned was a complete loss of coolant to all modules with a simultaneous breach of the vacuum vessel. This would allow ingress of air, resulting in oxidation and volatilization of radioactive species. In terms of overall impact of the accident, the DHe fuel cycle presents the least hazard. The temperature achieved during the transient was the least for this fuel cycle. Although the relative amounts of the different nuclides released are different, the total amount volatilized is nearly the same for DT and DD. The total activity released for these cases is over three orders of magnitude higher than for the DHe fuel cycle, but significantly less than that released during the accident at Three Mile Island. The impact of this accident was not evaluated for the RAF/Fe2Cr1V DD design. However, a similar first wall temperature response to the HT-9 case would be expected due to the similar levels of short lived species. It would be expected that similar quantities of the isotopes contributing most to the dose would be released so that the impact of this accident would not be largely different between the two materials considered.

Because of the very small radioactive release for the DHe fuel cycle, decontamination was not required after the accident. The clean up effort was greatest for the high beta DT and DD designs. They required a longer duration decontamination program because of the greater amount of material mobilized, and resulted in a greater occupational exposure. It was determined that the structural damage from the accident would be limited to the single breached module. Repair then involved

the replacement of a single module in all cases. Doses during repair were found to be higher for the low beta cases, mainly because of the longer time required to replace the larger modules.

Little difference is seen in the total onsite dose incurred subsequent to the accident for the DT and DD fuel cycles. There is a significant reduction in the onsite dose incurred for the DHe fuel cycle. The doses are slightly greater for the high beta designs, although the variation over the range of betas examined is less than 20 % for both the DT and DD fuel cycles. Offsite doses are small in all cases. However, the offsite impact is least for the DHe fuel cycle. It should be stressed that the impact of this accident is minimal. The chronic dose at the site boundary for the worst case just exceeds the limiting annual dose for a member of the general public. If this scenario is representative of a design base accident, the minimal offsite impact may allow less restrictive codes to be employed for construction.

The economic impact of the accident appears to be greatest for the DD fuel cycle. This is largely due to the replacement component costs. Replacement power costs are also a significant contributor to the accident costs. These are fairly similar for the DT and DD designs at a given value of beta. This cost is somewhat lower for DHe because there is no need for a decontamination program and the outage duration is somewhat reduced. The economic benefit of the lower accident hazard associated with the DHe design is clear.

A cost/benefit analysis was carried out to determine if the increased costs associated with the alternate designs were justified by the improved safety which they provided. The analysis was performed relative to the 20 % beta DT case, the design which results in the lowest COE and the highest exposures. A cost/benefit expenditure ceiling was evaluated which included an allowance for spending to improve plant safety under normal conditions and accident conditions, as well as an allowance to provide some protection for the utility's financial investment in the plant. Spending limits ranged from 5.07 $\frac{\$}{MW \cdot man-rem}$, where no consideration was

given to financial risk, to 11.4 $\frac{\$}{MW \cdot man-rem}$, where some protection was provided for the entire capital investment. When consideration is given only to normal conditions, the spending limit was found to be 4.79 $\frac{\$}{MW \cdot man-rem}$. A cost/benefit figure of merit was evaluated for each alternate design. This figure of merit considered normal operation costs (COE) and doses incurred during normal operation, maintenance and waste handling activities. For the HT-9 designs, costs and doses resulting from the loss of coolant accident were also included. The results showed that for the designs considered in this work, only the 10 % beta DT design is cost effective. The main reason why the other designs are not cost effective stems from their higher COE's. If the COE of the alternate designs can be reduced, they may then approach the region of cost effectiveness. Note that this conclusion would still apply if only normal operation had been considered for the HT-9 designs. However, it may not be the case if more accident scenarios had been examined. Other accidents may result in a lower economic impact relative to the high beta DT design in addition to some dose savings. This would lower the cost/benefit figure of merit, and perhaps would render some of the other designs cost effective.

Examining the results of the cost/benefit analysis for the DT fuel cycle alone, previous indications of an optimum value of plasma beta of 10 % are confirmed. Based on the outcome of the safety/economic tradeoffs, determined by the cost/benefit analysis, a plasma beta of 10 % is most cost effective. This result is also seen for the DD fuel cycle. The 10 % beta case results in the lowest cost/benefit figure of merit of the three DD designs considered. A value of plasma beta of 10 % is also most cost effective for the DD fuel cycle for the designs considered here.

A rough estimate of the cost effectiveness of the advanced fuel designs using a low cost, low activation blanket material was made. Assuming a cost of 10 \$/kg, no operational gamma doses to workers, and no accident health impacts, it was still found that the advanced fuel designs were not cost effective. It appears that the safety advantages potentially available with the advanced fuel designs cannot overcome their economic disadvantage. The low cost, low activation case was not

examined for the DT fuel cycle. However, it is expected that designs with both 10% and 20% beta would be cost effective relative to the base case design.

Including the effects of potential financial losses in determining the expenditure ceiling did not affect the outcome of this study. However, it is important that this aspect of the accident consequences be considered. The contribution of the capital investment loss to the economic impact of the accident studied here is significant. With the potential for large financial losses, it would be wise to provide some allowance for their protection.

The overall conclusion from this study is that a fusion plant utilizing the DT fuel cycle with a plasma beta of 10 % is the most cost effective option of the alternatives considered here. This conclusion applies to the designs studied in this work and should not be taken as a generalization. Optimized designs using different materials and/or energy conversion systems may well lead to a different conclusion.

Recommendations for Future Work

The broad nature of this study uncovered many areas which require further study. These will be highlighted in this section.

The designs compared in this study were based on a consistent set of criteria such that the differences between each would solely be a consequence of the difference in the fuel cycle or the difference in plasma beta. Materials used and plant systems which were not dependent on the fuel cycle, were the same for the comparison amongst the fuel cycles so that the impact of the change in fuel cycle would be clearly seen. An alternate material was investigated for a single fuel cycle (DD) to determine the impact of such a change. Knowing the relative positions of the fuel cycles with respect to safety and economics, it may now be useful to carry out the analysis with the optimized designs for all fuel cycles. This would involve a

substantial amount of design work and consideration of potential tradeoffs.

A rough assessment of the cost effectiveness of the advanced fuel designs using a low cost, low activation material was made. It may be appropriate to more carefully examine the use of such a material. The HT-9 structure was chosen for the comparison amongst the fuel cycles in this work so as not to introduce a materials variation into the analysis. As the results indicated here, this lead to considerable activity in the advanced fuel blankets, impacting occupational hazards, waste disposal concerns and accident consequences. However, in choosing a material, the purpose of the blanket as an energy multiplication medium must be kept in mind. The DD reactors illustrated the advantage of high energy gain in the blanket in that smaller reactors producing less fusion power were needed to produce the same amount of thermal power from the plant. The DD reactors also illustrated the safety disadvantages resulting from a high level of activity in the blanket. An alternate material (reduced activation ferritic (RAF) first wall/Fe2Cr1V alloy blanket) was examined for the DD fuel cycle. This showed improved blanket multiplication and reduced long term hazards, but the short term concerns were still present. A material less subject to neutron activation, but still an effective energy multiplication medium would be desirable. These may be opposing constraints, so that some tradeoffs will be necessary in selecting the most appropriate blanket material. The importance of using a low cost material must also be given attention. Although utilizing a lower activation material may result in some loss of blanket energy gain, this loss may be offset by economic gains from reduced occupational hazards and waste disposal issues. In fact, some materials may result in wastes qualifying for shallow land burial which would likely lead to considerable savings. The challenge is then to find a suitable low cost/low activation material. The RAF/Fe2Cr1V design showed a reduction in cost and long term safety concerns, but a material which resulted in lower short lived inventories would be more desirable. The cost/benefit approach proposed in this work is well suited for application to problems such as this and it may be useful to apply it to designs employing a vanadium alloy or ceramic (such

as silicon carbide).

A more efficient energy conversion system could be employed to take advantage of the larger fraction of energy released as charged particles with the advanced fuels. Use of direct conversion of charged particle energy or MHD conversion of radiated energy, especially in the case of the DHe fuel cycle, may be a much more effective way of obtaining the energy released in the plasma. An investigation into different energy conversion options should be undertaken. The use of a more efficient energy conversion system in combination with a low cost, low activation blanket material would take advantage of the safety benefits offered by the advanced fuel cycles (especially DHe) and may render these designs costs effective.

It may be interesting to explore different operating regimes for the DHe fuel cycle. Operating at a higher temperature where the reactivity is greater may be more economical. Furthermore, enriching the fuel to a larger fraction of helium-3 may improve the cost effectiveness of this fuel cycle. A higher concentration of helium-3 would suppress the neutron yielding DD side reactions, further improving this fuel cycle's standing in the safety arena.

The potential for high q, and hence low current operation in the second stability regime at high beta is presently being investigated. Should operation in this mode be realized, cost reductions can be expected. Lower current will impact magnet, power conditioning and current drive (for steady state operation) costs. This will be important for the advanced fuels.

A further area where recent strides have been made is in superconducting magnet technology. Higher temperature superconductors will result in significant reductions in magnet operating costs. This again would be of greater significance for the advanced fuels, which utilize higher magnetic fields.

An additional aspect which was not considered here for the DHe design was the possibility of reduced construction time. Since there is the potential for lower

activation, the construction time may be reduced because of easier siting and licensing. Furthermore, the use of readily obtainable non-nuclear grade components in many areas of the plant may avoid unnecessary delays during plant construction. It may be worthwhile investigating this consideration.

The negative conclusion on advanced fuels may be changed if N-stamp construction requirements are reduced. This could provide considerable savings in both construction time and materials costs. Additional economic savings could be envisioned if consideration was given to reduced safety systems costs for the advanced fuels.

It may be enlightening to include additional accident scenarios. The loss of coolant accident studied here represents only one of an entire spectrum of possible offnormal events. Examining the impact of a several forced outages or small consequence events, and the consequences of a more severe accident would provide more evidence for the relative ranking of the fuel cycles in terms of safety and economics.

Chapter 1
Introduction

Fusion's ultimate acceptance as an energy source will depend on how successfully its potential safety and environmental advantages are utilized. More specifically, it will depend on whether achieving ambitious environmental and safety goals in fusion reactors can be managed economically. Fusion studies to date have generally focussed on the DT fuel cycle because of its high energy release and high reactivity at relatively low temperatures. While these factors seem significant at this stage of fusion reactor development, the ultimate goal of advanced fuel cycle operation cannot be ignored. If physics and technology issues do not preclude their use, advanced fuel cycles may enhance fusion's position in the area of safety. Elimination of the need to breed tritium avoids having to deal with the hazards of lithium or its compounds, and reduces radioactive gas handling and inventory. These considerations, in addition to the potential for lower structural activation due to a reduction in the high energy neutron flux, provide a strong impetus for examining alternate fuels. However, there may be an economic penalty associated with the use of such a scheme.

The DD fuel cycle is the advanced fuel cycle which has received the most attention to date. In this study, the economics and safety of this advanced fuel cycle will be examined and compared to that of the DT fuel cycle. Some investigation of the DHe fuel cycle, in which interest has recently grown, will also be undertaken. It is hoped that some conclusions regarding the cost effectiveness of the advanced fuel cycles relative to the DT fuel cycle will emerge.

1.1 Fuel Cycles for Fusion Reactors

Most efforts in the fusion community have been devoted to the development of the DT fuel cycle. The large reaction cross section at relatively lower temperatures makes DT fuel the easiest of fusion fuels to ignite. Furthermore, the relatively large energy release of the DT reaction provides the highest possible fusion power density. The reaction between deuterium and tritium is given by:

$$D + T \longrightarrow {}^4He\ (3.5\ MeV) + n\ (14.1\ MeV)$$

The advanced fuel cycle which appears the most attractive for use in fusion reactors is the DD fuel cycle since its ignition requirements are not vastly greater than for the DT fuel cycle and are potentially achievable. DD fusion is advantageous since deuterium, a naturally occurring and easily separable isotope of hydrogen, is the only fuel required. Two possible reactions, the neutron branch and the proton branch, take place with almost equal probability. The tritium produced in the proton branch and the helium-3 formed from the neutron branch can also react within the plasma. The sum of all these reactions form the catalyzed-deuterium or cat-D fuel cycle:

$$D - D \longrightarrow T\ (1.01\ MeV) + H\ (3.02\ MeV)$$

$$D - D \longrightarrow {}^3He\ (0.82\ MeV) + n\ (2.45\ MeV)$$

$$D - T \longrightarrow {}^4He\ (3.5\ MeV) - n\ (14.1\ MeV)$$

$$D - {}^3He \longrightarrow {}^4He\ (3.6\ MeV) - H\ (14.7\ MeV)$$

At sufficiently high temperatures, the four nuclear reactions shown above would occur, with the two neutrons produced leaving the plasma and depositing their energy elsewhere. From six reacting deuterons, the total energy release would be 43.2 MeV or 7.2 MeV per deuteron.

The possibility of utilizing a cat-D-T mode of operation also exists [1.1, 1.2]. This mode operates in the regime between the DT and cat-D fuel cycles where the DD and DT reactions occur simultaneously in the plasma. The relative rates at which these two reactions occur would be determined by the average number of tritons fed into the reactor. The cat-D-T mode of operation may alleviate some of the difficulties encountered with both the DT and cat-D fuel cycles and may be envisioned as an optimum fuel cycle. Feeding the plasma with externally produced tritium can increase its average reactivity and power density relative to a cat-D plasma and may lead to a relaxation of the confinement requirements of cat-D reactors. On the other hand, a simpler and possibly safer and cheaper blanket design compared to DT may result from a reduction in the number of tritons which must be produced per fusion neutron. A further alternative known as the semi-catalyzed deuterium (SCD) fuel cycle has also been given some attention [1.1]. In this case, all the tritium, but little of the helium-3 produced in the DD reactions, fuses in the plasma. If tritium produced by external sources is also added to the plasma, the fraction of the DT reactions occurring can be increased, causing the plasma to be operated in the SCD-T mode. Since the helium-3 reaction rate is low at moderate temperatures compared to DT, the use of tritium to improve the plasma reactivity appears more effective than the use of helium-3.

In the case of the DHe fuel cycle, the fourth reaction indicated above would dominate. DD side reactions and the subsequent burning of tritium produced in the proton branch of the DD fuel cycle result in the DHe fuel cycle not being completely neutron free. However, undesirable neutron production can be minimized by enriching the fuel in helium-3 and/or operating at a much higher temperature where the DHe reaction cross section far exceeds the DD reaction cross section.

The advantages of the DHe fuel cycle have been emphasized in previous work [1.3, 1.4, 1.5-1.12]. The high fraction of energy released as charged particles make the use of direct conversion techniques attractive, providing the potential for more

efficient energy recovery. The main advantages lie in the greatly reduced neutron production, leading to decreased shielding and lower material activation, and the large amount of energy released in charged particles, making more efficient energy conversion schemes possible. However, there are several disadvantages associated with this fuel cycle. The low power density, compared to DT, necessitates high magnetic fields or high beta. High beta would allow the magnetic field to be reduced, leading to lower magnet costs and reduction of cyclotron radiation losses. However, the attainability of high beta is uncertain at this time. There is some concern about the relatively high heat fluxes impinging on the first wall of DHe reactors. These surface heats loads may be tolerable, in light of the the low neutron fields [1.3, 1.4, 1.13] which also exist. The use of materials with relatively high thermal conductivities will further mitigate this issue because they will lead to lower temperature differentials and thermal stresses [1.14]. The major shortcoming which has deterred research efforts on this fuel cycle is the supply of fuel. The availability of helium-3 on earth is limited. Sources are listed in table 1.1. The quantity available could supply an experimental research program, but would be insufficient to support a mature fusion economy based on the DHe fuel cycle. The idea of using DHe satellite reactors with DT or DD reactors as generators of helium-3 has been the only suggestion up to this point to circumvent the fuel supply problem [1.3, 1.7-1.9]. However, a recent study [1.10] has identified the lunar soil as being a potentially large source of helium-3. The moon has served as a collector of solar wind particles for more than four billion years. The helium nuclei in this wind impinge upon the lunar surface at a flux of 6 x 10^{10} particles/$cm^2 \cdot$ s, and the isotopic abundance of helium-3 is high ($\sim$ 480 appm). It is estimated that the soil of the moon contains a million tonnes of helium-3, enough to provide 10^7 GWe$\cdot$ yr of electrical power (in a 50 % efficient DHe fusion reactor). Expressed in a different manner, the entire U.S. electrical consumption in 1985 could come from mining an area on the moon's surface equivalent in area to the size of Washington D.C. If it is possible to efficiently mine and transport the helium-3 back to earth, then the major drawback of this fuel cycle would be overcome.

Table 1.1: Terrestrial Resources of Helium-3 [1.10]

Source	Isotopic Abundance $\frac{^3He}{^4He}$ (appm)	Cumulative Amount to Year 2000 (kg)	Production Rate Post year 2000 (kg/yr)
U.S Stored Helium Reserves	0.2	29	-
U.S Natural Gas Wells	0.2	187	-
Volcanic Gases	~ 16	-	3
Atmosphere	1.4	4×10^6	-
Decay of T_2:			
DOE	-	> 13.4	1.3
CANDU Reactors	-	10	2
U.S. Weapons	-	~ 300	~ 15

The probability of a reaction occurring is given by the reaction cross section. Values for the reactions of interest here are shown in figure 1.1 (from reference [1.16]). The DT curve exhibits a maximum at an energy of 110 keV. Below about 100 keV, the total DD cross section is roughly 100 times smaller than the DT cross section. The DHe cross section in this same energy range is less than the DD value and much below the DT value. However, the DHe cross section is a rapidly increasing function of energy and exceeds the DD cross section above 120 keV. The DD curve gives the sum of the cross sections for the two DD reactions. Up to deuteron energies of 120 keV, the value for each individual reaction may be taken as half the total.

The rate of a particular reaction is reflected by the value of the reaction rate parameter ($\bar{\sigma v}$), which is simply the reaction cross section averaged over the particle velocity distribution. Often a maxwellian velocity distribution is assumed. Integration of the cross sections of figure 1.1 over a maxwellian distribution of velocities leads to the results shown in figure 1.2 (also taken from reference [1.16]). The peak of the DT curve occurs at roughly 70 keV. The DD and DHe curves peak at much higher temperatures. The reaction rate parameter, along with the energy released per interaction, is important in determining fusion power density. Since both of these factors are reduced for the DD reactions compared to the DT reaction, the fusion power density for a DD reactor would be somewhat lower than that for a DT reactor. Hence, to obtain the same total power output, a DD reactor would have to be larger if other factors affecting power output remain fixed. This results in an economic penalty due to the greater materials needs of a larger reactor, but may provide the benefit of lower specific activation. Although the DHe reactivity is lower than DT, the energy yield for this reaction is large (18.3 MeV compared to 3.6 MeV on average for DD, and 17.6 MeV for DT). Above about 22 keV, the DHe reactivity exceeds that of the DD reaction. Thus, for the same fusion power, the DHe reactor would be smaller than its DD counterpart, but still somewhat larger than its DT counterpart.

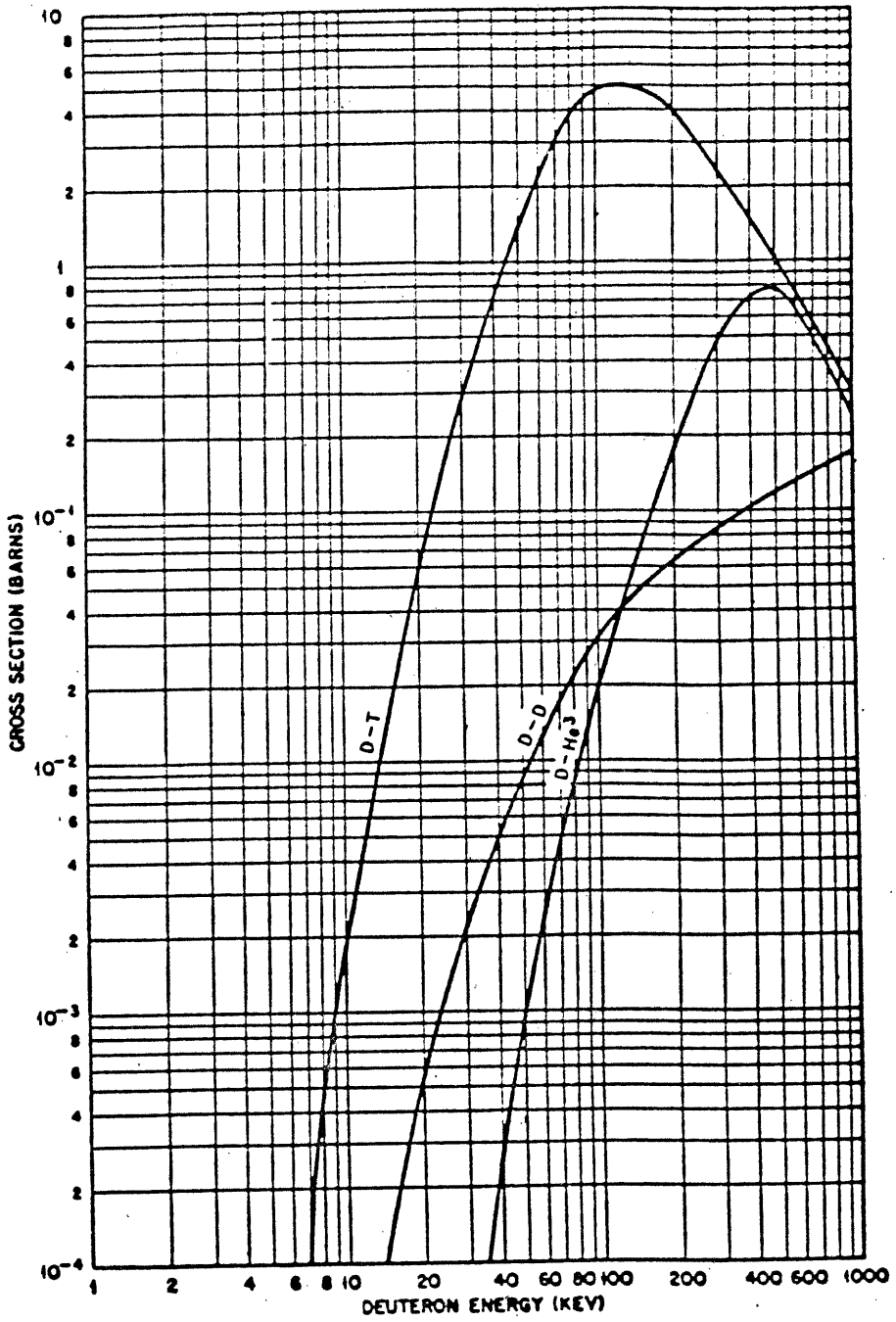

Figure 1.1: Cross Sections for DT, DD (total) and DHe Reactions (from [1.16])

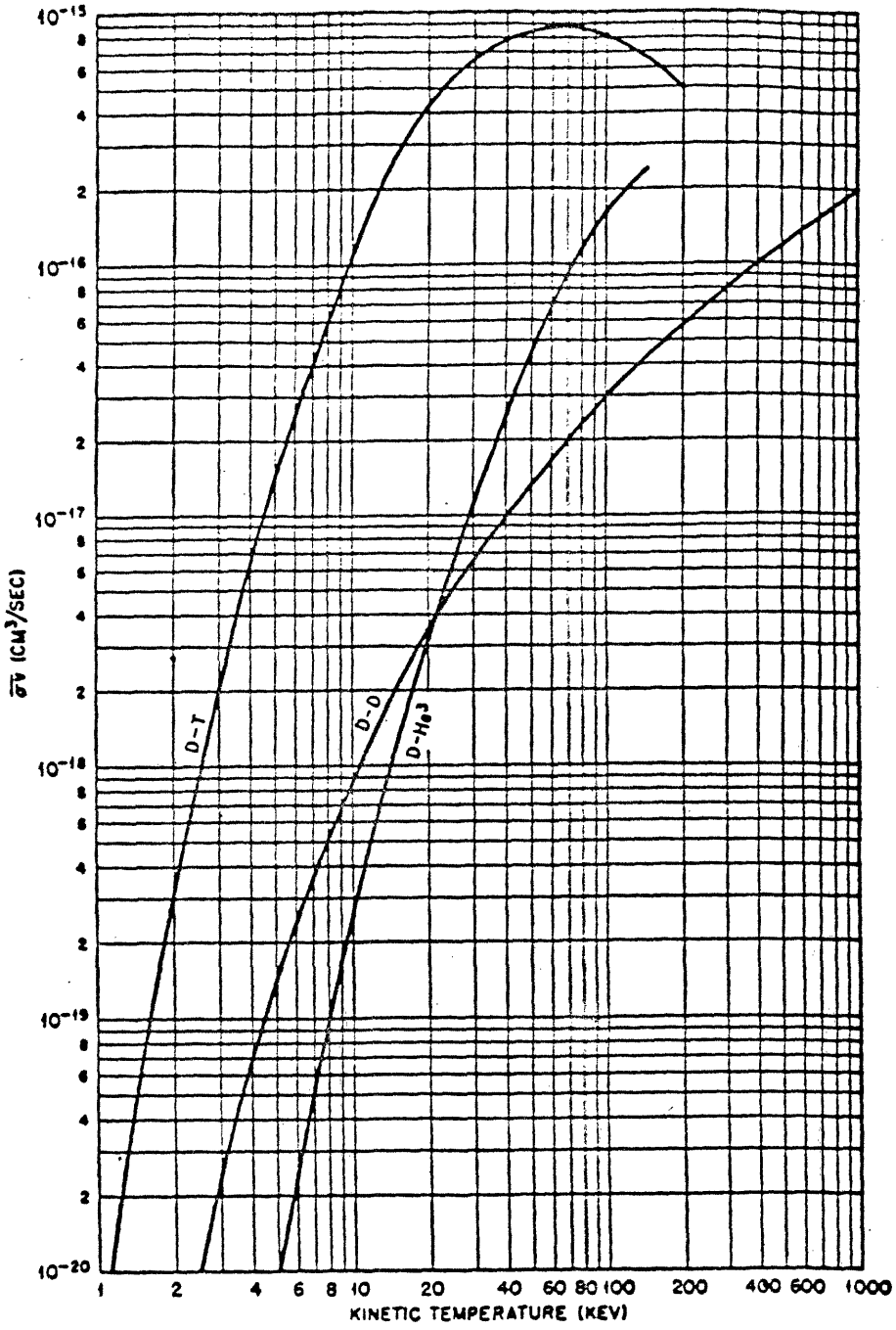

Figure 1.2: Values of $\bar{\sigma v}$ based on a Maxwellian Distribution for DT, DD (total) and DHe Reactions (from [1.16])

The lower reactivity of the advanced fuels could be partially compensated for by operating at a higher temperature. This is technologically more difficult to achieve and would result in larger radiative losses, requiring a correspondingly longer energy confinement time [1.17]. Because of the higher ignition temperature, greater heating is required to achieve ignition in a DD or DHe reactor. This problem is not insurmountable, however, since it may be possible to minimize external heating by igniting a DT plasma and allowing thermal runaway.

Energy losses are of greater concern for advanced fuel reactors. At temperatures above 10 keV, bremsstrahlung losses are insignificant compared to fusion power in a DT reactor ($T^{ideal}_{ign-DT} = 4$ keV). Bremsstrahlung losses become equivalent to the energy released from DD fusion at 36 keV ($T^{ideal}_{ign-DD} = 36$keV, $T^{ideal}_{ign-cat-D} = 25$ keV) and at 29 keV for DHe fusion ($T^{ideal}_{ign-DHe} = 29$ keV) [1.18]. Above this temperature, fusion power produced exceeds bremsstrahlung power, but by less than an order of magnitude, so that these losses are significant in an advanced fuel system. In the presence of high fields, cyclotron losses also become large.

The distribution of energy between charged particles and neutrons is of importance. Since charged particles can be confined in a magnetic field, they will be retained in the reaction region, while the neutrons will escape and liberate their energy in a different location. Thus, only the energy of the charged particles will be available internally to compensate for energy losses and to sustain the reacting plasma. In a thermonuclear reacting system consisting of deuterium alone, the two DD reactions would occur at nearly equal rates, and the tritium formed in the proton branch would then react, relatively rapidly, with deuterium. In this system (semi-catalyzed DD), 8.3 MeV out of the total 24.9 MeV released, or about 33 %, would be carried by charged particles; the other 16.6 MeV of energy (67 %) carried by neutrons, would be recoverable only as heat. In a reacting system consisting of an equal mixture of deuterium and helium-3, the majority of reactions would result in no neutron production. However, the unavoidable DD side reactions produce 2.45 MeV neutrons and tritons, which then react to pro-

duce 14 MeV neutrons. The relative importance of the DD side reactions and the consequent neutron production depend on the operating temperature. However, the fraction of energy carried by neutrons for the DHe fuel cycle is below 10 % at modest temperatures and can be as low as 1 - 2 % if high temperatures and helium-3 rich fuel are utilized. The higher fraction of energy carried by charge particles imply high surface particle and radiation loads for advanced fuel reactors. Countering this, neutron damage and activation in a DT reactor would be more severe due to the greater number of high energy neutrons.

1.2 Design Considerations For Advanced Fuel Reactors

The design of an advanced fuel reactor involves the consideration of many factors. These include reduced high energy neutron production, increased fusion energy carried by charged particles and the elimination of the need for tritium breeding. The contribution of a lower reaction cross section, higher required plasma temperature and increased radiation losses make efficient confinement more difficult. Thus, advanced fuel cycles provide simplification in some reactor design aspects, but lead to greater complexities in other areas.

Upon considering technology issues for various fuel cycles, neutron yield is of prime importance. In the DT cycle, approximately 80 % of the power is given to the neutrons. In the cat-D cycle, the neutrons carry away roughly 40 % of the total power, while less than 10 % of the energy resides with the neutrons for the DHe fuel cycle. This impacts the design of the first wall/blanket and shielding requirements. Lower neutronic heating puts a less severe demand on the blanket heat transport system. The smaller number of energetic neutrons per unit area impinging on the first wall reduces damage and lengthens the first wall and blanket lifetime. An assessment by Baxter et al. [1.19] indicated that the first wall and blanket lifetime would be four to five times longer for a DD tokamak compared to a DT tokamak.

This situation would be even more favorable for the DHe tokamak, and lifetime blankets may even be possible. Furthermore, maintenance and replacement operations for a DHe device may be more easily and quickly accomplished, resulting in improved availability. However, the high surface heat loads present a concern for first wall materials and require an efficient heat removal system. The lower bulk neutron heating in the advanced fuel blanket necessitates the use of materials that produce a high energy multiplication in order to improve the economic viability of the system. Removing the need for tritium breeding in the advanced fuel designs allows the system to be optimized for energy multiplication. Optimization can be achieved by selecting materials with a high (n,γ) reaction potential since this type of reaction generally releases a large amount of energy. Since the (n,γ) cross sections generally decrease as neutron energy increases ($\sigma \propto \frac{1}{v}$), energy multiplication can be maximized if measures are taken to moderate the neutrons. However, careful material selection is essential so that material activation and afterheat do not present a major concern.

The higher fraction of energy carried by charged particles suggest alternate approaches to energy conversion for the advanced fuel reactor. Direct conversion of charged particle energy provides more efficient conversion from fusion to electric power. If this option is not employed, elimination of the breeder function of the blanket allows more freedom in materials choice so that, in the case of the DD reactor, which still has a relatively high neutron yield, the blanket can be designed to optimize energy gain. This will offset the lower fusion power density of the DD reactor, allowing for a smaller reactor to produce the same total thermal power. In the case of the DHe fuel cycle, which has a relatively low neutron yield, clever schemes of obtaining the radiative energy released, such as MHD conversion, may be more efficient. This would alleviate concerns due to high surface wall loads.

In a previous study [1.20], a nuclear analysis was performed to identify the impact on technology requirements of alternate fuels. It was found that cat-D systems yield relatively high nuclear heating and atomic displacement rates when

compared to DT systems having a neutron wall load as much as twice as high. However, the radiation damage due to gas production was found to be more severe in DT systems since the associated damage cross sections have high threshold energies. The reduced damage in the DD reactor may lead to increased first wall lifetime and improved plant maintenance capability. The study also assessed reactor shielding requirements for the alternate cycles. For an epoxy-based insulator for superconducting magnets with a limiting dose of 5 x 10^9 rad and a plant lifetime of 30 MW $\cdot$ yr/m^2, about 1 m of shielding would be required for the cat-D cycle. With the low neutron yield of the DHe fuel cycle, radiation damage, induced activity and shielding requirements are considerable reduced. Baker et al. [1.20] estimated a shielding thickness of 0.7 m for this fuel cycle. A smaller blanket can also be used since there will be little neutron heating and the radiative energy can be captured in a relatively small thickness [1.7]. The smaller blanket/shield thickness reduces materials costs and will also allow for smaller, less costly magnet structures. According to Baker et al. [1.20], the breeding blanket and shield would be about 1.5 m thick for the DT cycle. The smaller thickness of the advanced fuel blankets would allow for greater coupling between the magnet, other auxiliary systems and the plasma. A thinner inboard shield would permit higher fields in the plasma and thus would enhance its power density. Since the thickness of the outboard blanket/shield is less critical, this portion of the blanket could be designed to increase neutron multiplication.

An advanced fuel tokamak reactor will require toroidal magnetic fields and plasma currents larger than those contemplated in design studies for DT tokamak reactors. To initiate and sustain the larger plasma current, a larger flux swing in the ohmic heating (OH) coil system will be required. This will necessitate a larger area within the OH solenoid. The larger toroidal field will require thicker TF coils, with a larger radius of curvature, demanding more support. The cost of these magnets would be high. If such high fields were employed in DT designs, a higher power density would result leading to shorter first wall and blanket lifetimes. Hence, the

high field option for DT reactors may not be beneficial.

To alleviate fatigue problems associated with pulsed operation, considerable attention has been given to steady state current drive. The STARFIRE reactor [1.21] employs lower hybrid waves for steady state operation with DT fuel. The very large toroidal current in an advanced fuel reactor makes the rf power prohibitive for this type of current drive. The WILDCAT reactor design [1.22], which is the DD counterpart to STARFIRE, employs the compressional alfven wave rf current drive for steady state operation. Use of this mode presents a larger penalty in terms of percentage of total plant output required for current drive power. This is unfortunate, since the DD reactor has a higher fraction of the total wall load in the form of charged particles and radiation which provides incentive to operate in the steady state mode in order to prevent encroaching on heat load limitations.

Another important parameter to be considered in fusion reactor studies is the plasma beta. This parameter contains constraints imposed by both physics and technology. The value of beta can never exceed unity, since the plasma energy density cannot be larger than the magnetic energy density in a stable tokamak plasma. However, the closer beta approaches unity, the more effectively the existing magnetic field is being utilized. It can be easily shown that the power density of a fusion reactor scales with $\beta^2 B^4$. Since current designs employ magnetic fields of 14 - 15 T, which represent the upper limit of current superconducting magnet technology, a larger total power output can be achieved with a higher value of beta. It has been shown [1.23] that over the range of beta which is permitted by tokamak stability considerations (0.02 - 0.09), DT tokamaks have power densities ranging from 0.6 MW/m^3 to 5.0 MW/m^3. It was also noted that the power density of 5.0 MW/m^3 can be achieved in a cat-D tokamak at a value of beta of about 0.2. Hence, if high beta can be achieved, the advanced fuel reactor should be competitive with the DT tokamak on the basis of maximum achievable power density. Furthermore, this study indicated that if high beta fusion reactors become feasible, the DT reaction loses its primary attraction of high reactivity, since wall loading limitations

prevent this advantage from being fully exploited.

A further consideration for advanced fuel reactor designs is the maximum impurity concentration in the plasma that will permit ignition. The allowable concentration decreases exponentially with the charge of the impure species. It has been shown that a DD reactor must be an order of magnitude cleaner than a DT reactor [1.24]. The ash products to be removed from a DD reactor are protons and alphas, compared to only alphas for DT. Since protons charge exchange, they are more difficult to remove. However, since the average mass of a DD plasma is lower than the average mass of a DT plasma, sputtering of the boundary coating is somewhat less of a problem for a DD reactor. This is an advantage since it alleviates, to a degree, the more stringent requirements on the impurity control system needed to ensure a cleaner plasma. In the DHe plasma, almost as much alpha ash is produced as in a DT reactor. However, because of the need for a much cleaner plasma for this system (to minimize radiative losses at the higher operating temperature), demands on the impurity removal system are greater than for DT.

1.3 Safety and Economic Considerations

A viable reactor system would produce sufficient fusion power to overcome plasma losses, supply enough electric power to operate the fusion plant and have a sufficient amount of net power available for sale so that the cost of building and maintaining the plant are justified. Safety and environmental concerns must also be considered when assessing the cost effectiveness of the fusion plant. A safety benefit of employing the cat-D fuel cycle is the possibility of reduced structural activation resulting from the decreased high energy neutron flux [1.25, 1.26]. Baxter et al., [1.19] have stated that the inventories of activated structural materials and activated corrosion products are less for a DD tokamak than for a DT tokamak for short times after shutdown (less than 10 years) since the inventory is dominated by short half-

life radionuclides with an equilibrium inventory proportional to the neutron flux (which is smaller for DD than for DT reactors). However, they also indicated that for the same total neutron fluence (15 $MW \cdot yr/m^2$ for STARFIRE and 20 full power years for a DD tokamak operated at a thermal wall loading of 1 $MW \cdot yr/m^2$), the long-lived radioactive inventories are approximately the same. Baker et al. [1.20] have shown that the hazard associated with the induced radioactive inventory of a DHe device (as indicated by the BHP) is one to two orders of magnitude lower than for a DD or DT device. For the same total power output, the specific afterheat of DD and DHe reactors will be lower than the DT design due to the decreased neutron power, resulting in smaller radioactive inventories and the larger volume in which they are contained. The reduced specific activity also has beneficial implications for waste disposal. There may also be a reduction in total waste volume due to longer blanket lifetime. Further gains in alleviating waste disposal concerns can be achieved through the flexibility of the advanced fuel reactor blanket, allowing low activation materials to be more easily accommodated.

The tritium inventory in the advanced fuel reactor may be more than two orders of magnitude lower than in a DT reactor. Systems for recovery and processing of tritium from vacuum exhaust are still required for the DD and DHe reactors. However, systems for recovery and containment of tritium in the blanket and heat transport system are not needed. Consequences of tritium accidents would be much less for the advanced fuel cycles compared to the DT cycle.

Sources of stored energy provide a mechanism for the release of radioactivity. The advanced fuel reactors have greater plasma kinetic energy. For example, WILDCAT has approximately 8300 MJ in plasma kinetic energy compared to approximately 900 MJ for STARFIRE [1.27]. Additionally, the DD and DHe reactors have more energy stored in the magnets due to the higher fields used (e.g. 14.4 T for WILDCAT compared to 11 T for STARFIRE). Another source of stored energy is decay heat. This is expected to be lower for the advanced fuel reactors than for DT; blanket damage or melting would take much longer. Hazards associ-

ated with the chemical reactivity of lithium and its compounds can be completely avoided with the elimination of tritium breeding in the advanced fuel designs. Overall, it appears that advanced fuel tokamaks present a lesser risk than DT tokamaks.

1.4 Recent Design Studies

Since the tokamak is the reactor concept currently closest to realization, tokamak reactors have been most studied. The most well known DT tokamak reactor study is STARFIRE [1.21]. Some smaller scale studies have been performed for DD reactors, the most well known of which is the WILDCAT study [1.22]. Even less work has been performed for the DHe fuel cycle. The STARFIRE reactor was designed with a relatively low plasma beta of 6.7 % and a magnetic field of 11 T. The net electric power output of the STARFIRE reactor is 1200 MW. WILDCAT was designed with a plasma beta of 11.5 %. A magnetic field of 14.4 T, which represents the upper limit on superconducting magnet technology, was necessary to obtain a favorable power balance. WILDCAT was designed to produce 810 MWe and the cost was determined to be 62 mills/kWh. If the reactor is scaled up to a net power production of 1200 MWe, as for STARFIRE, the COE drops to 44 mills/kWh [1.19]. This is only marginally above the COE for STARFIRE of 35 mills/kWh (1980 $). If beta is increased to 15 % in STARFIRE, and the maximum magnetic field is decreased from 11 to 7.5 T to maintain a constant fusion power density and plasma size, the COE is only slightly reduced [1.25]. It is apparent, then, that the effects of high beta operation are more strongly felt by DD reactors. If high beta can be achieved, DD reactors may be more cost effective than DT reactors.

Another DD tokamak reactor assessment was performed by Science Applications; Inc [1.26]. Their study was based on a 1200 MWe DD reactor. Variations in magnetic field, beta and reactor size were investigated. They determined that the cost decrease per unit increase in beta is small for beta larger that 15 %, where the

COE is roughly equal to 37 mills/kWh. Hence in agreement with the WILDCAT study conclusions, if high plasma beta can be achieved, the COE of DD tokamaks approach that of DT tokamaks.

Some smaller scale studies have been performed for the DHe fuel cycle [1.3, 1.4]. The main reason that designs for this fuel cycle have not been developed to the same extent as for the DD fuel cycle is the inability to guarantee a supply of fuel. To circumvent this problem, some studies have focussed on the DD breeder/DHe satellite system [1.7, 1.12]. This scenario utilizes free neutrons from a cat-D reactor to breed tritium which is then allowed to decay to helium-3, supplying fuel for a satellite DHe reactor. Other DHe reactors have been designed assuming fuel would be available. Values of plasma beta from 0.1 to 0.3 have been used, with on axis fields of 5.5 to 7.0 T [1.3, 1.4]. No estimates for the cost of electricity from these designs was made.

1.5 Scope of Present Work

The advantages and disadvantages of the DD and DHe fuel cycles relative to the DT fuel cycle have been briefly presented in this introductory chapter. For a given geometry, size, toroidal field and plasma beta, the power production of an advanced fuel reactor is substantially lower than that of a tritium fueled reactor. Consequently, a DD or DHe reactor must be significantly larger and/or operate at higher magnetic fields or higher plasma betas than a DT reactor of comparable fusion power. Larger devices with higher field magnets are more difficult to design. Larger devices would also imply larger auxiliary systems and higher parasitic power losses resulting in lower efficiency and reduced net electric power. Higher temperature operation for the advanced fuel reactor results in greater cyclotron and bremsstrahlung losses and necessitates a larger confinement parameter, $n\tau$, and fewer impurities in the plasma in order to achieve ignition. The larger fraction

of total power in the form of charged particles and radiation makes heat load a concern in the first wall/blanket design. The overall result of these factors may be to increase the cost of electricity for advanced fuel reactors. However, no cost studies have estimated the economic benefits of lower occupational, accident and waste disposal hazards anticipated for the advanced fuel cycles. Furthermore, even if these effects do not make DD or DHe reactors a cheaper source of electricity, it has yet to be determined if the safety benefits from these fuel cycles justify a more expensive source of power. An attempt to achieve some conclusions with regards to the cost effectiveness of the DD and DHe fuel cycles is made in this work.

The representative designs for the comparison are described in chapter 2. In chapter 3, a discussion of the economic evaluation is given. Chapter 4 discusses in more detail, the components of the fuel handling system required for each fuel cycle. In chapter 5, the tritium hazards of the fuel cycles are estimated by scaling and extension of previous studies. Induced radioactivity hazards and waste management issues are also addressed. In chapter 6, the safety and economic repercussions of a loss of coolant accident are assessed and compared. Chapter 7 applies an approach to cost/benefit analysis to determine the cost effectiveness of the various designs. Conclusions and recommendations are are summarized at the beginning of the report.

1.6 References

(1.1) E. Greenspan et al., Cat-D-T Tokamaks, Proceedings of the Fourth Topical Meeting on the Technology of Controlled Nuclear Fusion, King of Prussia Pennsylvania, October 1980.

(1.2) E. Bobrov et al., High Field Tokamaks with DD-DT Operation and Reduced Tritium Breeding Requirements, Massachusetts Institute of Technology Plasma Fusion Center, PFC/RR-83-5, 1983.

(1.3) C. Choi et al., Exploratory Studies of High-Efficiency Advanced Fuel Fusion Reactors, Electric Power Research Institute, EPRI ER-581, November 1977.

(1.4) J. Fillo et al., Exploratory Studies of High-Efficiency Advanced Fuel Fusion Reactors, Electric Power Research Institute, EPRI ER-919, December 1978.

(1.5) R.W Conn et al., Alternate Fusion Fuel Cycle Research, IAEA-CN-38/V-5.

(1.6) B. Brunelli and G. Leotta, eds., Unconventional Approaches to Fusion, Plenum Press, 1981.

(1.7) G. Miley et al., Advanced Fuel Fusion Systems - The D^3He Satellite Approach, Proceedings of the Review Meeting on Advanced Fuel Fusion, p. 39, Electric Power Research Institute, EPRI ER-536 SR, June 1977.

(1.8) G. Sheu et al., Conceptual Design of a Deuterium - ^3He Fueled Tandem Mirror Reactor Satellite/Breeder System, Fusion Technology, 9, May 1986.

(1.9) K. Schoepf et al., Reaction Balance and Efficiency Analysis of a DD Fusion/Fission with Satellite D^3He Reactors, Journal of Fusion Energy, 2, No. 3, 1982.

(1.10) L. Wittenberg et al., Lunar Source of ^3He for Commercial Fusion Power, Fusion Technology, 10, September 1986.

(1.11) B. Logan, An Advanced-Fuel Variant for ESECOM: D^3He Fusion Using Direct Conversion of Microwave Synchrotron Radiation, Presentation of ESECOM, April 1986.

(1.12) R. Scott et al., Advanced Fuel Fusion Systems - The D^3He Satellite Approach, Proceedings of the Review Meeting on Advanced Fuel Fusion, p. 455, Electric Power Research Institute, EPRI ER-536 SR, June 1977.

(1.13) C.C. Baker at al., Fusion Reactor Technology Impact of Alternate Fusion Fuels, Proceedings of the Eighth IEEE Symposium on the Engineering Problems of Fusion Research, p. 861, November 1979.

(1.14) J. Fillo and J. Powell, Fusion Blankets for Catalyzed DD and DHe Reactors, Proceedings of the Review Meeting on Advanced Fuel Fusion, p. 57, Electric Power Research Institute, EPRI ER-536, June 1977.

(1.15) G.M. M^{c}Cracken et al., Princeton Plasma Physics Laboratory, PPPL1569, 1979.

(1.16) S. Glasstone and R. Lovberg, Controlled Thermonuclear Reactions, D. Van Norstrand and Co., 1960.

(1.17) D. Rose and M. Clark Jr., Plasmas and Controlled Fusion, M.I.T. Press, 1961.

(1.18) J. Reece Roth, The Influence of Engineering Constraints on Confinement Time Requirements of Advanced Fuel Fusion Reactors, Nuclear Technology/Fusion, 4, p. 258, September 1983.

(1.19) D. Baxter et al., DD Tokamak Reactor Assessment, Nuclear Technology/Fusion, 4, September 1983.

(1.20) C.C. Baker at al., Fusion Reactor Technology Impact of Alternate Fusion Fuels, Proceedings of the Eighth Symposium on Engineering Problems of Fusion Research, San Francisco California, November 1979.

(1.21) C.C. Baker et al., STARFIRE - A Commercial Tokamak Fusion Power Plant Study, Argonne National Laboratory, ANL/FPP-80-1, September 1980.

(1.22) K.E. Evans et al., WILDCAT: A Catalyzed DD Tokamak Reactor, Argonne National Laboratory, ANL/FPP/TM-150, November 1981.

(1.23) C.J. Reece Roth and H. Roland, The Effect of Wall Loading Limitations and Choice of Beta on the Feasibility of Advanced Fuel Fusion Reactors, Proceedings of the Eighth Symposium on Engineering Problems of Fusion Research, San Francisco California, November 1979.

(1.24) C.C Baker at al., Implications of the DD fuel Cycle on Tokamak Reactor Technology Considerations, Proceedings of the Fourth Topical Meeting on the Technology of Controlled Nuclear Fusion, King of Prussia Pennsylvania, October 1980.

(1.25) D. Dobrott, Alternate Fuels in Fusion Reactors, Nuclear Technology/Fusion, 4, September 1983.

(1.26) D. Baxter at al., DD Tokamak Reactor Assessment, Final Report, Science Applications, Inc., SAI25082-213LJ, March 1983.

(1.27) B. Jenson and R. Endicott, Utility Evaluation of the DT STARFIRE and DD WILDCAT Reactors, Nuclear Technology/Fusion, 4, September 1983.

(1.28) K.E. Evans et al., DD Tokamak Reactor Studies, Argonne National Laboratory, ANL/FPP/TM-138, November 1981.

(1.29) G. Miley, Potential Status of Alternate-Fuel Fusion, Proceedings of the Fourth Topical Meeting on the Technology of Controlled Nuclear Fusion, King of Prussia Pennsylvania, October 1980.

(1.30) J. Jung, Nuclear Design and Analysis of a Deuterium-Deuterium Tokamak Reactor, WILDCAT, Nuclear Technology/Fusion, 4, July 1983.

(1.31) J. Gordon, Advanced Fuel Fusion Fuels and Reactor Concepts, Proceedings of the Fourth Topical Meeting on the Technology of Controlled Nuclear Fusion, King of Prussia Pennsylvania, July 1981.

(1.32) G. Miley et al., Confinement Approaches for Burning Alternate Fuels, Proceedings of the Fourth Topical Meeting on the Technology of Controlled Nuclear Fusion, King of Prussia Pennsylvania, July 1981.

(1.33) S. Allenberger and W. Houlberg, Plasma Physics Sensitivity Analysis of Catalyzed-D Operation in Tokamaks, Proceedings of the Fourth Topical Meeting on the Technology of Controlled Nuclear Fusion, King of Prussia Pennsylvania, July 1981.

(1.34) S. Fetter, The Radiological Hazards of Magnetic Fusion Reactors, proposed for publication in Fusion Technology, January 1986.

Chapter 2

Reference Reactor Designs

The primary objective of this study is to assess the impact of the fusion fuel cycle on reactor safety and economics. In order to investigate the impact of using an advanced fuel instead of DT fuel, the fusion reactors for each fuel cycle must first be defined. Several reactor designs have been developed for this purpose, each being a pulsed, superconducting tokamak. The designs were characterized using the superconducting design code described in appendix A, and are discussed in this chapter. An effort has been made to develop consistent designs. Thus, only necessary modifications to a base case DT design were made in order to accommodate DD and DHe fuel cycles. In this way, it is hoped, the impact of changing the fuel cycle will not be obscured. It should be noted that these designs do not represent the optimum scheme for each fuel cycle, but rather provide the foundation for comparing the fuel cycles on an equal basis. In this section, the parameters common to all designs will be outlined. Specific designs for each of the fuel cycles will be presented. The reasoning for the choice of specific values of parameters will be discussed.

2.1 Reactor Parameters

2.1.1 Plasma Beta

The effectiveness of utilizing the magnetic field for confinement of a plasma, as measured by the plasma beta, is a key physics parameter which impacts overall cost. This is particularly true for schemes like the tokamak which rely primarily on strong magnetic fields generated by external conductors for confinement of the plasma. Experimental values of plasma beta achieved to date have been limited to 5 % [2.1]. Studies [2.2, 2.3] have suggested that a substantial decrease in the cost of energy could be realised by operating at a higher value of beta than currently possible, since a greater fusion power density would be achieved (fusion power $\sim \beta^2$). A smaller reactor could be used to produce a given amount of power. This issue is more important when considering the advanced fuel cycles, because the economics may only be attractive with higher beta [2.4 - 2.8]. Furthermore, high beta would relax the requirement for high magnetic fields for advanced fuel devices, lowering magnet costs and reducing synchrotron losses. If limitations on beta imposed by the physics render such high values unattainable, the design is driven to a more expensive region of parameter space. It is possible, however, that a very high beta may not be beneficial for DT reactors [2.8]. As beta is increased, the power density increases, allowing the reactor to be smaller for the same total power output. Wall loading and materials limitations may then be encountered. Although operation at higher beta permits the use of lower magnetic fields for the same power output, more frequent replacement of components at higher wall loadings may render high beta DT reactors uneconomical.

Because MHD instabilities have the potential to limit beta to low values, extensive studies at several laboratories have been performed to determine ideal MHD limits for various configurations. The maximum stable value of beta has been found to increase with inverse aspect ratio, elongation and triangularity. Scaling laws for the beta limit have been developed as a function of principal geometric factors.

Several are given in table 2.1. These apply to the first region of stability. Experiments on Doublet III covered a wide range of plasma shapes in order to compare experiments with theory [2.9]. Betas of up to 4.7 % were achieved [2.9] and good agreement with the theoretical ballooning mode predictions of Tuda and Sykes was found [2.10].

The existence of a high beta second region of stability has been predicted by various theoretical studies [2.5, 2.9, 2.11 - 2.13]. For the BIG DEE tokamak, which will be constructed from the Doublet III tokamak, the theoretical beta limit was found to vary from 11 % to over 21 % [2.5]. Yamazaki et al. [2.11] indicate that higher elongation and more pronounced triangularity of the plasma shape are favourable for achieving higher beta values. Furthermore, they propose that strong bean shaping has the essential feature of allowing access to the second stability region.

Grimm et al. [2.12] suggest that bean shaping could provide for a ballooning-mode-stable path to very high beta values ($\beta > 20\%$) in medium aspect ratio, slightly elongated tokamak plasmas. Chance et al. [2.13] state that indentation of a tokamak plasma on its inboard side aids in achieving high beta stability against ballooning modes and that moderate indentation provides accessibility to the second region of stability. Sheffield [2.17], Dobrott [2.6] and Baxter et al. [2.7] appear optimistic regarding the achievability of higher beta. However, others [2.18, 2.19] have expressed their skepticism towards the attainment of the second stability regime.

No scaling laws describing achievable beta in the second stability region as a function of relevant parameters currently exist. Because of this, and the relatively large uncertainties associated with second stability beta, it is difficult to explore possible commercial reactor designs using the high beta approach. The second stability regime is significantly displaced from present tokamak physics and a number of theoretical questions remain. Despite this, it was felt important to examine the potential of high beta designs. Representative high beta cases have been generated

Table 2.1: Beta Scaling Laws

Name	Beta Scaling	Basis
Troyan [2.14]	$\beta = 2.7\frac{I_p}{a \cdot B_T}$	Kink mode stability
Sykes [2.15]	$\beta = 4.4\frac{I_p}{a \cdot B_T}$	Ballooning mode limits with optimized pressure profile
Doublet III [2.9]	$\beta = 27 q_s^{-1.1} \epsilon^{1.3} \kappa^{1.2}(1 + 1.5\delta)$	Experimental data
Tuda [2.16]	$\beta = 30\frac{\kappa^{1.5}}{A \cdot q_s}\left(1 + 0.9(\kappa - 1)\delta - 0.6\left(\frac{\kappa^{0.75}}{q_s}\right) + 14(\kappa - 1)(1.85 - \kappa)\frac{\delta^{1.5}}{q_s^2}\right)$ (2.1)	Ballooning mode limits with plasma shaping
Yamazaki [2.11]	$\beta = 4.7\frac{I_p}{a \cdot B_T}\left(1 - \frac{0.065 \cdot A \cdot I_p}{\sqrt{\kappa} \cdot a \cdot B_T}\left(1 - \frac{(\kappa - 1 + 0.05\delta)}{\sqrt{\kappa}}\left(\frac{1 + 1.5\delta}{\kappa}\right)^{2.5}\right)\right)$	Ballooning mode limits with plasma shaping

where
- β = plasma beta (%)
- I_p = plasma current (MA)
- a = plasma minor radius (m)
- B_T = toroidal field on axis (T)
- κ = plasma elongation
- A = aspect ratio
- ϵ = inverse aspect ratio
- q_s = safety factor at the edge
- δ = plasma triangularity

assuming confinement continues to follow present trends at high beta. Access to the second stability regime was assumed to be obtained through strong plasma shaping.

In all fairness, the fuel cycle comparison should be made at the same value of beta. It appears to be most desirable to operate at high beta, but whether or not such values can be achieved is uncertain. Consequently, reactor designs for a range of values of beta were developed for the DT and DD fuel cycles (from 3 % to 20 %). A single intermediate value of beta of 10 % was chosen for the DHe fuel cycle since it was felt that scoping the entire range for this fuel cycle would not reveal any new information in addition to that found for the DD fuel cycle. In a recent DD reactor assessment [2.7], it was shown that economic gains beyond a beta value of 20 % are small. At values of beta in this vicinity, the cost of energy from a DD tokamak was shown to approach that of a DT tokamak. For this reason, an upper limit for beta of 20 % was chosen.

2.1.2 Blanket Materials

The blanket concept selected for the DT designs employs a liquid lithium breeder, helium coolant and HT-9 (ferritic steel) as the structural material. This combination of breeder/coolant/structure was one of the top ranked tokamak blanket designs recommended for further investigation by the Blanket Comparison and Selection Study [2.20]. It was selected as the most attractive option for the present study over Li/Li/V (ranked #1) and Li_2O/He/HT-9 (ranked #2). The use of He as blanket coolant was desirable since it can be used for all fuel cycles, and the safety concerns associated with a liquid lithium coolant in the DD and DHe designs would be avoided. The use of a liquid breeder for the DT designs was felt to be advantageous since it can be circulated through the blanket, allowing for the bred tritium to be extracted external to the blanket.

With the advanced fuel designs, the need for tritium breeding is eliminated. The blanket can be designed to maximize energy multiplication. The material chosen for the DD and DHe blankets is HT-9, cooled by helium. By keeping the structure and coolant the same as in the DT designs, the effect of eliminating tritium breeding should be evident.

It was also of interest to investigate the impact of a materials change on safety and economics. This was carried out only for the DD fuel cycle. The alternate first wall material selected was a reduced activation ferritic steel (RAF) (see appendix A for exact composition). Relative to HT-9, the major differences in this material are that it contains much less molybdenum (0.00027 % compared to 1.0 % by weight) and less nickel (0.006 % versus 0.5 %). Because of the less severe environment in the blanket compared to the first wall, a lower cost material having reduced performance characteristics could be employed in the blanket region. The material used in the bulk of the blanket was the alloy Fe2Cr1V. Relative to HT-9, the iron content of this material is greater (95.13 % compared to 85.0 % by weight), the chromium content is reduced (2.4 % versus 11.5 %), as is the manganese content (0.3 % versus 0.55 %). The quantities of nickel and molybdenum are greatly reduced (nickel from 0.5 % to 0.05 %, molybdenum from 1.0 % to 0.02 %) and the alloy contains no tungsten. With these alterations to the material composition, it is expected that there may be an increase in short lived species, but a significant reduction in long lived isotopes (which arise mainly from nickel and molybdenum). Thus, for this design, a reduction in long term waste disposal hazards can be envisioned.

The main shielding material used was Fe1422 (Fe/14% Mn/2% Ni/2% Cr). A previous study [2.21] recommended this material based on satisfactory performance, low cost and resource availability. A further motivation for its use is the low concentration of Ni and Cr. Low chromium content minimizes the consumption of strategic materials; low nickel content reduces the dose equivalent after shutdown and the production of long-lived isotopes. The shield is comprised of several sections. The main section is the steel shield, consisting of water coolant (20 % by

volume) and Fe1422 (80 %). Behind this is a B_4C shield consisting of 60 % B_4C, 20 % Fe1422 and 20 % H_2O. The B_4C acts as a neutron absorber to decrease the activation of reactor components and structural materials. A density factor of 0.7 was assumed for the B_4C to avoid the fabrication costs associated with the high density form. The outboard shield has one further section, comprised entirely of lead, which acts as a gamma ray attenuator.

It has been suggested [2.22] that the Fe1422 in the shield be replaced by HT-9. The afterheat in the shield during the first several hours after shutdown is dominated by ^{56}Mn, which is produced primarily by reactions with Mn in Fe1422. The Mn content of HT-9 is 26 times less than Fe1422 (0.54 % vs 14.0 %). If the Fe1422 in the shield is replaced by HT-9, it has been shown that the short term afterheat is reduced by an order of magnitude [2.22]. Furthermore, the maximum temperature of the blanket during a post accident scenario has been shown to be lowered by 500 K. This lower post accident blanket temperature reduces release fractions of most constituents from 30 to 150 times. Massidda [2.23] has shown that nearly an order of magnitude of reduction in decay heat density at shutdown will result in the manifold region if HT-9 is used in place of Fe-1422 for designs with lithium coolant and vanadium structure. The temperature rise of the first wall subsequent to a loss of coolant accident was found to be reduced by 550 °C for the same designs. Because of these potential safety benefits, several reactors were designed using HT-9 as the major shielding material. There appears to be little difference in shielding performance between the HT-9 and the Fe1422, but the cost of HT-9 is somewhat greater. There may be a cheaper alternative to HT-9 which is also low in manganese. However, further investigation of this issue was beyond the scope of the present work.

2.1.3 Plasma Operation

DT ignition will be achieved via ohmic heating with some supplemental rf heating. The start-up scheme proposed for advanced fuel tokamaks involves DT ignition followed by thermal runaway [2.24]. The "matchhead effect" is achieved by first igniting a low density DT core. The excess of fusion energy can then be used to heat new cold fuel, building up the plasma density. Simultaneously, the core can be expanded and transformed to a non-circular shape. This can be followed by non-circular burn propagation and thermal runaway. As the desired temperature is approached, some supplemental heating may be applied and the fueling rates of components can be adjusted to the level required by the particular advanced fuel cycle.

The plasma burn mode adopted for all designs is a 5000 second pulse. A major concern with a pulsed reactor is material fatigue. A comparative study for tokamak burn modes [2.25] has indicated that if the fusion period is greater than $\sim$ 1 h, thermal fatigue is not life limiting for the first wall and limiter. Their study was performed with PCA (Prime Candidate Alloy, an austenitic stainless steel) as the structural material. Thermal wall loadings of 1.5 - 3.5 MW/m^2 on the limiter front face were considered. Since HT-9, the structural material chosen for this work, has superior thermal performance properties compared to PCA [2.20], these conclusions should still apply to the designs examined here. Since plasma disruptions may also contribute to the thermal fatigue of materials, a 5000 second pulse length was used to provide some allowance for these events. The pulsed mode of operation was also adopted in the BCSS [2.20] since it was felt that this design basis would be more credible to the fusion physics community. The long pulse can be achieved by driving a toroidal current with a transformer and then maintaining the current with a non-inductive current driver while the transformer is being reset (at low plasma temperature and density). During the reset period ($\sim$ 40 seconds), the thermal storage system will ensure a steady flow of steam to the turbine. The cost of this

system and the additional pumping power required for its operation are significant. However, there is a considerable reduction in the power consumed to charge the coils, compared to the power consumed by the steady state current drive system. Since the same burn mode is utilized for all fuel cycles, the decision to have a pulsed design will not affect the comparison between fuel cycles.

2.1.4 Other Considerations

The designs employ a pumped limiter as the means of impurity control. This has been shown to be an attractive concept with many inherently simple features which would be desirable in a commercial power reactor [2.26].

An aspect ratio of 4 was chosen for all designs. At low beta, where first stability physics applies, a low aspect ratio is attractive, since devices can be smaller and less costly. Because of the inverse scaling of beta with aspect ratio (see Doublet III and Tuda scalings in table 2.1), lower fields can also be used to achieve the same power output. LeClaire [2.27] has performed some design optimization work. He chose an aspect ratio of 3 for his low beta designs. At high beta, the second stability regime is not accessible at low aspect ratio [2.12]. LeClaire selected an aspect ratio of 5 for his high beta designs. For the main designs considered in the present work, an aspect ratio of 4 was chosen after consideration of these issues. The impact of varying the aspect ratio on other design parameters and economics has been examined for the DT and DD fuel cycles and is discussed later in this report (see Sections 2.2.2, 2.3.2, 3.2.2 and 3.3.2).

Because of the scaling of beta with elongation, the maximum value of this parameter is desirable. Yamazaki et al., [2.11] used values of elongation up to 3 in their investigations. The BIG DEE tokamak is to have a plasma elongation of 2.15 [2.4]. The Generomak study chose an intermediate value of 2.5 for the elongation of their tokamak variation [2.28]. This value was also chosen for the current study. With the elongation and aspect ratio fixed, the different values for beta can be

achieved from scaling laws by varying the plasma indentation. Yamazaki considered strong bean shaping, with triangularities up to 1.5 [2.11]. Strong bean shaping will result in more complex coil systems. Some consideration is given to this in the costing of the reactor designs.

A plasma scrape-off distance of 10 cm was used for all designs. The charged particle flux in this zone has been shown to fall off exponentially. An e-folding distance of $\sim$ 2 cm has been measured [2.29]. In the Fusion Engineering Device (FED) [2.30], a scrape-off distance of 10 cm was assumed. This would correspond to roughly 5 times the particle flux exponential falloff distance, resulting in a small particle flux to the wall.

The balance of plant for all fuel cycles is similar. A conventional steam cycle transfers the energy from the primary helium coolant to the turbine. The balance of plant for each reactor uses state-of-the-art technology wherever possible. Other approaches to energy conversion could potentially be used for the DHe fuel cycle to take advantage of the large fraction of energy released in charged particles (e.g. direct conversion, MHD conversion). However, a conventional steam cycle was assumed here so that all fuel cycles would be compared on an equal basis.

The safety and economic comparison will be based on the designs described in the following sections. Reactor parameters and parametric variations will be discussed. In subsequent chapters, the effects of these variations on reactor safety and economics will be clarified.

2.2 DT Designs

The major reactor parameters for the DT designs having plasma betas of 5%, 10% and 20% are listed in table 2.2. For these designs, the aspect ratio has been set at 4, the elongation is 2.5, the plasma scrape off distance is 10 cm, the shielding material is Fe1422, and the thermal power is 4000 MW. The operating temperature,

Table 2.2: Reactor Parameters For DT Designs

Parameter	Low Beta (5 %)	Medium Beta (10 %)	High Beta (20 %)
Major Radius (m)	7.64	6.51	5.68
Minor Radius (m)	1.91	1.63	1.42
Inboard Blanket (cm)	26.0	26.0	26.0
Outboard Blanket (cm)	101.0	100.0	100.0
Inboard Shield (cm)	68.0	69.0	70.0
Outboard Shield (cm)	104.0	106.0	107.0
Plasma Scaling Constant ($\beta^2 B^4 a^2$) ($T^4 \cdot m^2$)	4.37	5.14	5.89
Toroidal Field at coil (T)	8.03	6.77	5.61
Toroidal Field on axis (T)	4.68	3.73	2.92
$B^2 a$ ($T^2 \cdot m$)	41.8	22.7	12.1
T_{OH} (keV)	2.4	1.9	1.5
OH Flux Swing ($\dot{V} \cdot s$)	558	406	298
Plasma Current (MA)	18.4	12.5	8.6
Total Wall Loading (MW/m^2)	3.80	5.20	6.76
Neutron Wall Loading (MW/m^2)	3.04	4.16	5.41
Surface Heat Flux (MW/m^2)	0.76	1.04	1.35
$n_D \tau_E$ (Neo-Alcator) (sec/m^3)	2.85×10^{21}	2.85×10^{21}	2.85×10^{21}
Neo-Alcator Ignition Margin	9.4	9.5	9.5
τ_E (Neo-Alcator) (sec)	36.0	28.3	23.1
$n_D \tau_E$ (Mirnov) (sec/m^3)	7.21×10^{20}	7.21×10^{20}	5.27×10^{20}
Mirnov Ignition Margin	3.2	2.4	1.7
τ_E (Mirnov) (sec)	12.4	7.1	4.3
τ_P (sec)	2.9	2.3	1.9
Total Average Density (m^{-3})	1.70×10^{20}	2.16×10^{20}	2.65×10^{20}

Parameter	Low Beta (5 %)	Medium Beta (10 %)	High Beta (20 %)
Murakami Density Limit (m^{-3})	6.12×10^{19}	5.74×10^{19}	5.15×10^{19}
Deuteron Density (m^{-3})	7.92×10^{19}	1.01×10^{20}	1.24×10^{20}
Triton Density (m^{-3})	7.92×10^{19}	1.01×10^{20}	1.24×10^{20}
Helium-3 Density (m^{-3})	3.08×10^{16}	3.92×10^{16}	4.81×10^{16}
Proton Density (m^{-3})	7.71×10^{16}	9.81×10^{16}	1.20×10^{17}
Alpha Density (m^{-3})	1.11×10^{19}	1.41×10^{19}	1.73×10^{19}

	Common Parameters
Aspect Ratio	4.0
Scrape off (cm)	10
Plasma Elongation	2.5
Safety Factor at edge	2.5
Peak Electron Temperature (kev)	15.2
Average Electron Temperature (kev)	10.1
Peak Ion Temperature (kev)	17.0
Average Ion Temperature (kev)	11.3
Fusion Power (MW)	3645
Blanket Multiplication Factor	1.122
System Multiplication Factor	1.098
Thermal Power (MW)	4000
Net Electric Power (MW)	1225
Fraction of Energy due to DT Fusion	0.9989
Fraction of Energy due to DD Fusion	0.0011
Fraction of Energy due to DHe Fusion	~ 0
Tritium Burned (g/day)	559
Tritium Bred (g/day)	634

Parameter	Common Parameters
Deuterium Burned (g/day)	378
Tritium Produced in Plasma (g/day)	1.6
Helium-3 Produced in Plasma (g/day)	1.6
Protium Produced in Plasma (g/day)	0.5
Alphas Produced in Plasma (g/day)	742
Tritium Exhausted (g/day)	1598
Deuterium Exhausted (g/day)	1067
Helium-3 Exhausted (g/day)	1.6
Protium Exhausted (g/day)	0.5
Helium-4 Exhausted (g/day)	742
Total Gas Load ($Pa \cdot m^3/s$)	32.7
Tritium Fueled (g/day)	2156
Deuterium Fueled (g/day)	1445
Tritium Fractional Burn-up	0.259
Deuterium Fractional Burn-up	0.261

was selected to maximize the fusion power density ($\sim \frac{<\sigma v>}{T^2}\beta^2 B^4$ [2.31]). For DT reactors, this occurs at roughly 15 keV (ideal ignition occurs at $\sim$ 4 keV). All machines are ignited, according to both Neo-Alcator and Mirnov scaling, with a comfortable ignition margin. Blanket and shield thicknesses were determined from neutronics calculations using the Los Alamos code ONEDANT [2.32]. The blanket configuration for the neutronics analysis is shown in figure A.1 of appendix A. The blanket and shield sizes were based on sufficient tritium breeding (1-D tritium breeding ratio of 1.25) and adequate magnet shielding ($\sim$ 10^{10} rad to magnet thermal insulation). Other details are given in appendix A. It should be noted that two-thirds of the outboard blanket and shield were assumed to lie between the coils and one-third beneath the coils. The shield thickness beneath the coils on the outboard side is the same as the inboard shield thickness; the external lead shield employed between the coils for gamma ray attenuation is only found between the coils. The outboard shield thickness in the table refers to the shielding between the coils.

The DT reactor with 5 % beta is not greatly different from STARFIRE. Major reactor parameters for STARFIRE are listed in table 2.6 at the end of this chapter. Although STARFIRE operates in the steady state mode, thus alleviating the inner bore radius constraint, its major radius is still relatively large. A value of 7 m for STARFIRE was selected based on wall loading considerations.

2.2.1 The Effect Varying of Beta

Additional DT reactor designs were determined for plasma betas of 3 %, 7 %, 12 % and 16 %. The variations of reactor parameters with beta are indicated in figures 2.1 through 2.10; more information regarding these designs is given in appendix A. As beta is increased, both the major and minor radii are seen to decrease. This occurs since as beta increases, the fusion power density also increases, as indicated in figure 2.3. Hence, for the same total power, a smaller plasma volume

FIGURE 2.1: MAJOR RADIUS VS BETA

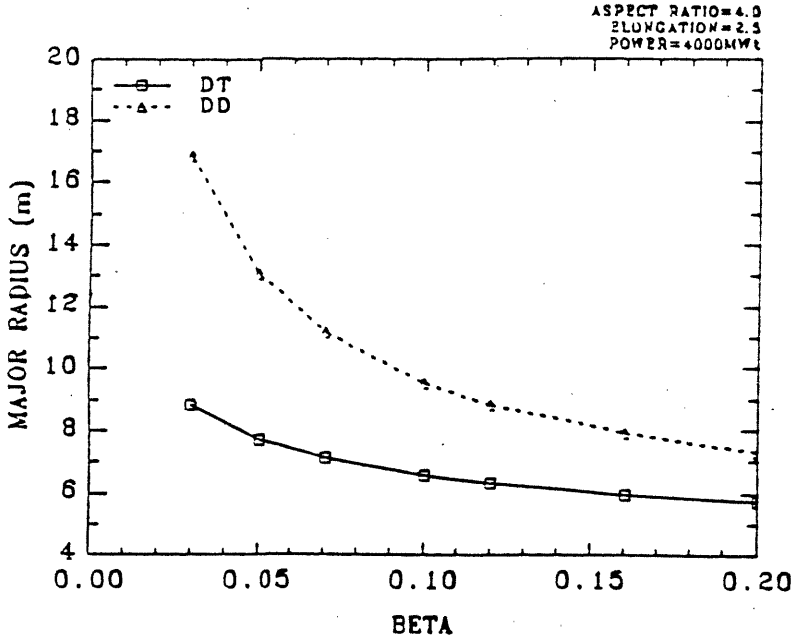

FIGURE 2.2: MINOR RADIUS VS BETA

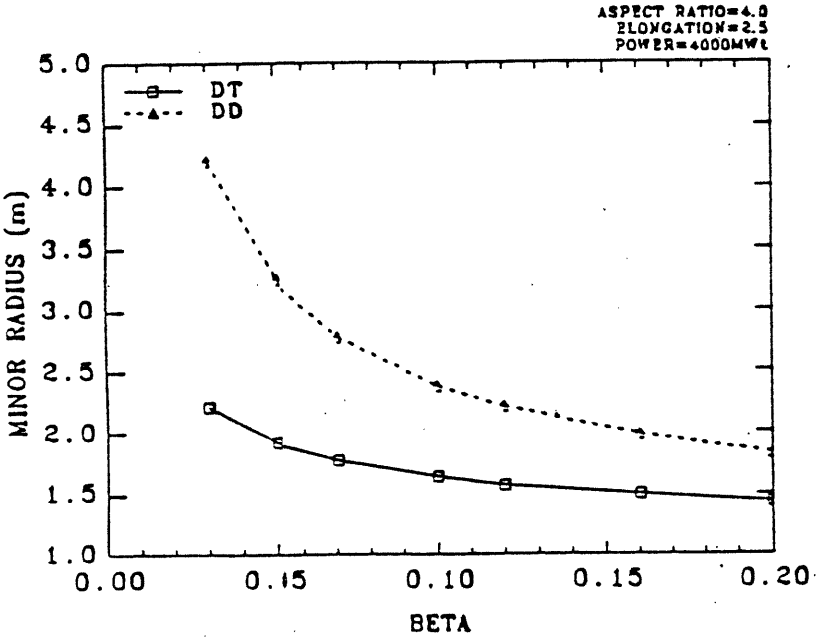

FIGURE 2.3: FUSION POWER DENSITY VS BETA

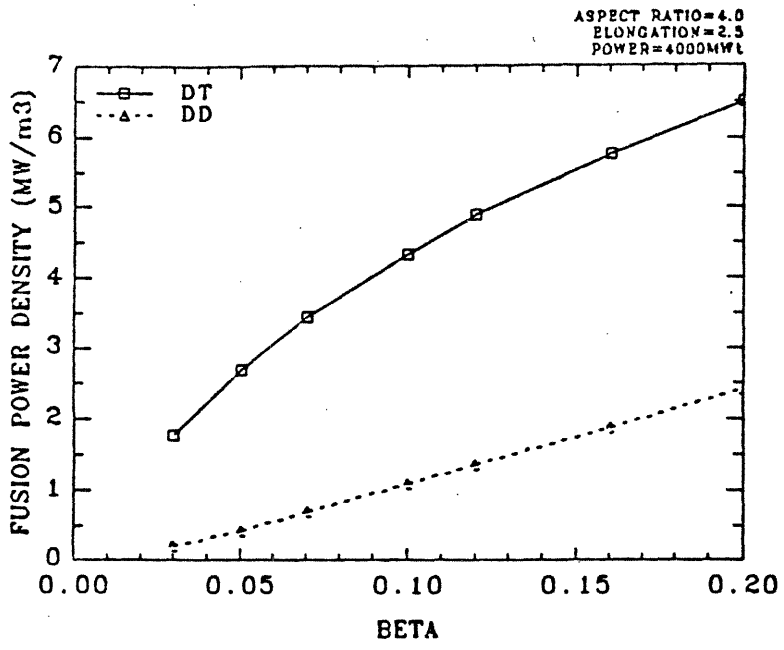

FIGURE 2.4: TOROIDAL FIELD VS BETA

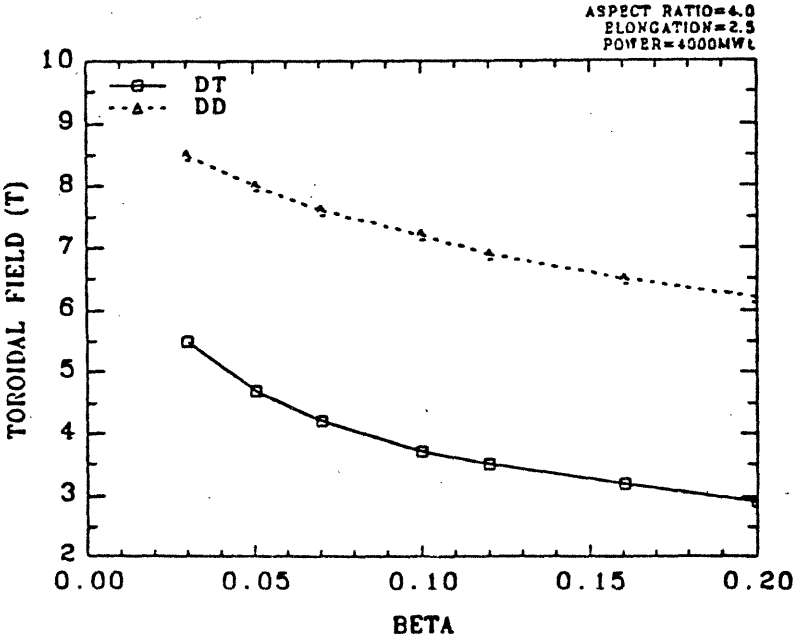

FIGURE 2.5: PLASMA CURRENT VS BETA

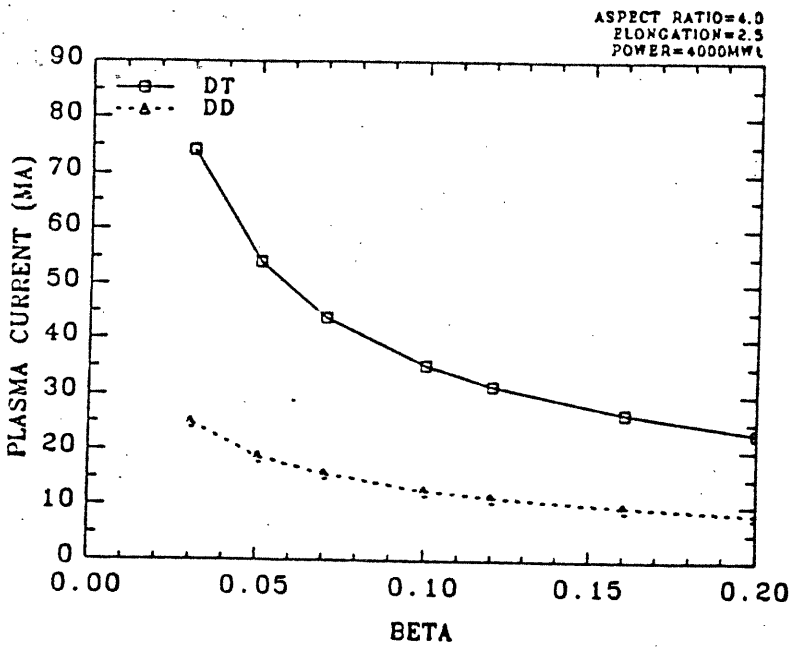

FIGURE 2.6:
TOTAL AVERAGE PLASMA DENSITY VS BETA

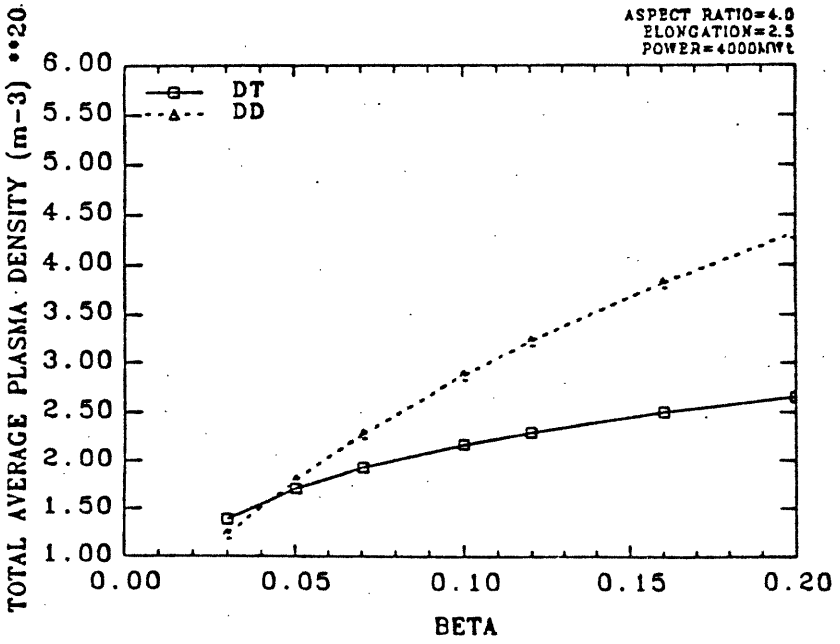

FIGURE 2.7: CONFINEMENT TIME VS BETA FOR DT REACTORS

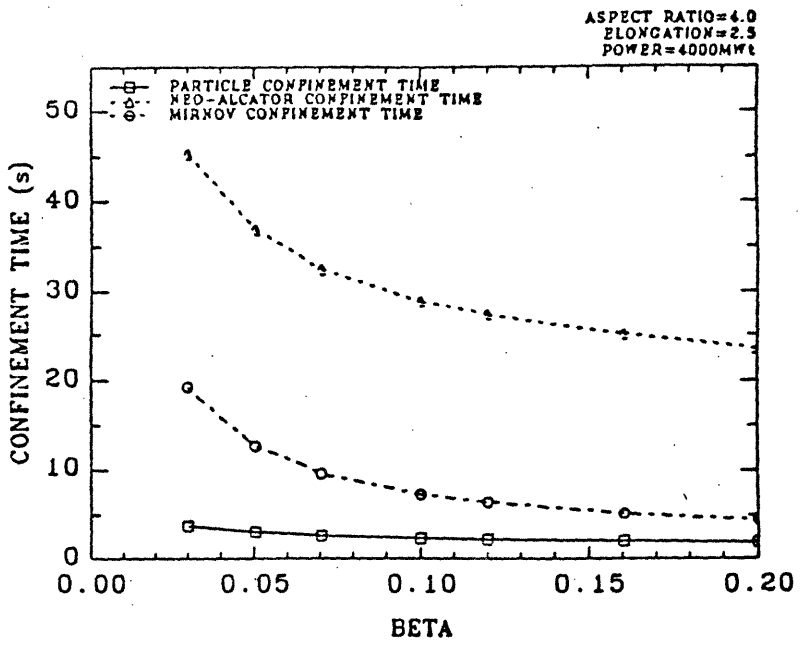

FIGURE 2.8: CONFINEMENT TIME VS BETA FOR DD REACTORS

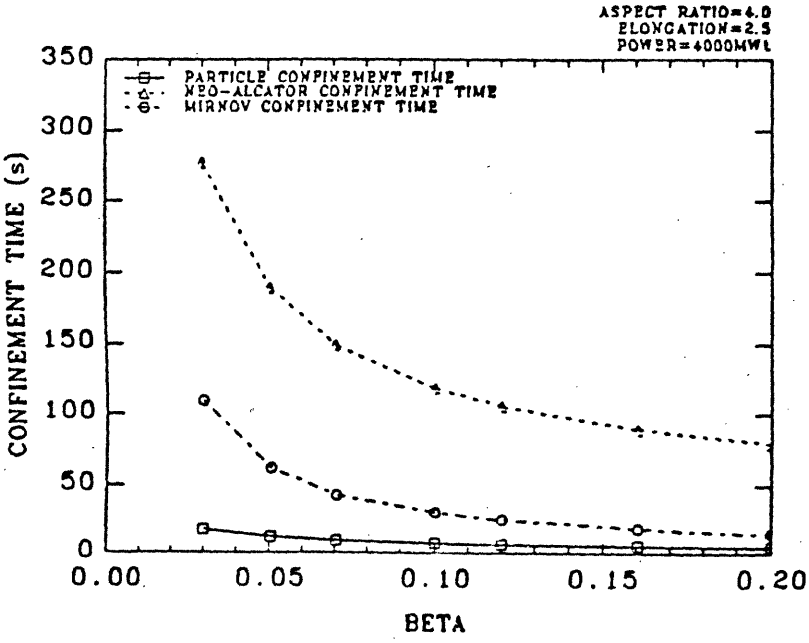

FIGURE 2.9: NEUTRON WALL LOADING VS BETA

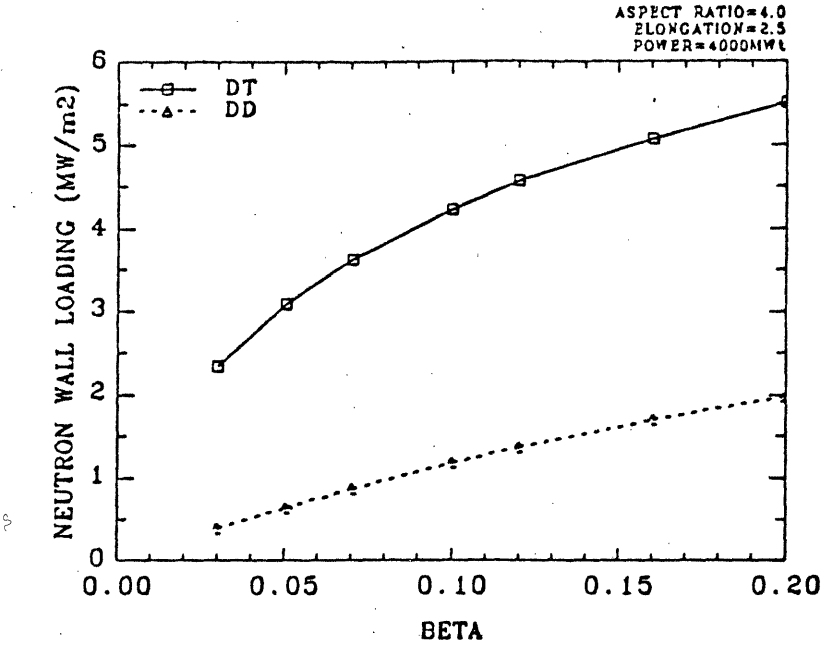

FIGURE 2.10: THERMAL WALL LOADING VS BETA

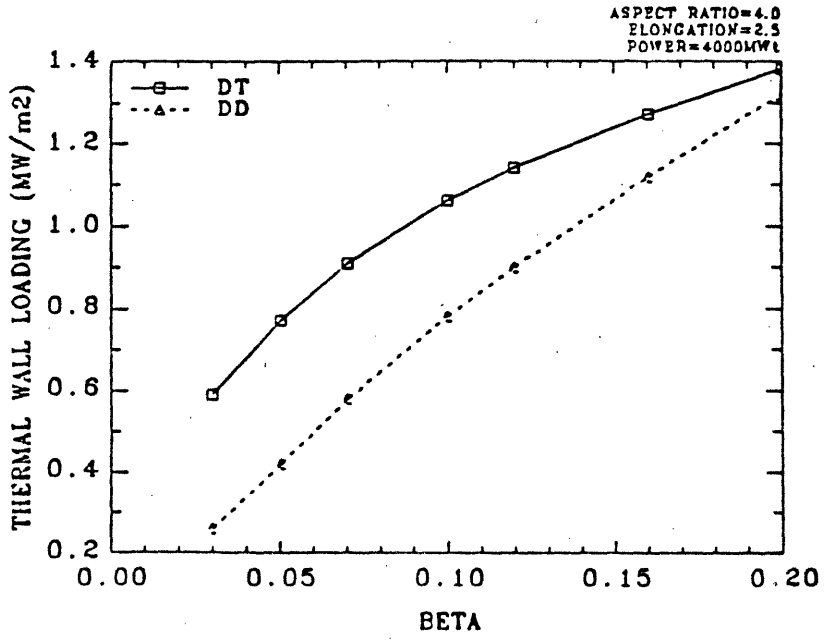

FIGURE 2.11:
NEUTRON WALL LOADING VS POWER DENSITY OF FUSION ISLAND

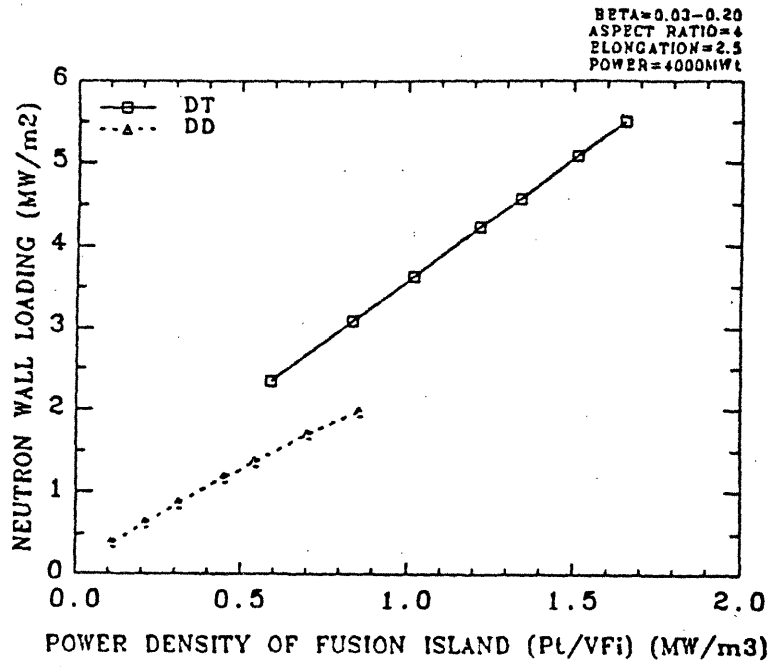

FIGURE 2.12: MAJOR RADIUS VS ASPECT RATIO

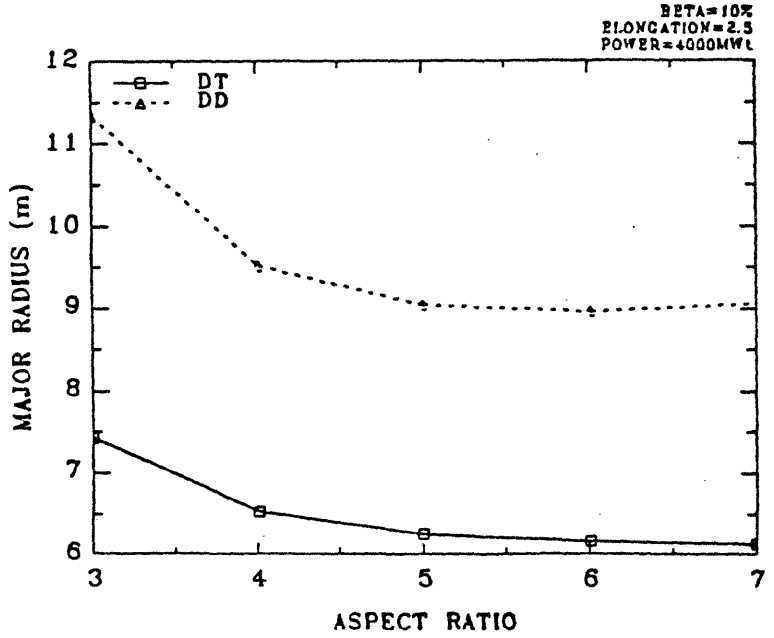

is required. This also explains the decrease in toroidal field as beta becomes larger, since fusion power density is also proportional to the toroidal field to the fourth power. As a result of the decreasing plasma size and toroidal field, the plasma current also decreases ($I_p \sim \frac{a^2 B_T}{R_0}$). Increasing beta has the effect of increasing the plasma density. Since the fusion power density, which is proportional to the square of the plasma density, is seen to increase with increasing beta, this corresponds to an increase in the density of the fusing particles. At higher betas, a deterioration in particle and energy confinement is apparent (see figure 2.7). For neo-alcator scaling ($\tau_E \sim n \cdot a \cdot R^2$), the effect of the decrease in reactor size is greater than the effect of the increasing density, leading to an overall reduction in confinement time. Mirnov scaling ($\tau_E \sim a \cdot I_p$) depends on plasma current and minor radius, both of which decrease as beta increases, leading to a decrease in confinement time. Particle confinement is also reduced as the reactor size decreases. Wall loading is seen to increase with plasma beta, as the first wall area decreases. In figure 2.11, the neutron wall loading is plotted against the power density of the fusion island (fusion power divided by volume of plasma, blanket, shield, structure and coils) for the designs corresponding to the range of values of beta examined. The power density of the fusion island reflects the efficiency of using volume for power production. A high value would be desirable, indicating that more power is produced in a smaller volume. Larger values of the power density of the fusion island correspond to higher values of beta, but come at the price of higher wall loadings. The greater wall loadings result in more frequent changeouts for the first wall due to the greater damage which results from the higher neutron and thermal fluxes. Because of this consideration, very high beta DT reactors may not be economically attractive.

2.2.2 The Effect of Varying Aspect Ratio

The effect of varying aspect ratio (from 3 to 7) on other reactor design parameters has been investigated. Results are displayed in figures 2.12 to 2.20 and the

FIGURE 2.13: MINOR RADIUS VS ASPECT RATIO

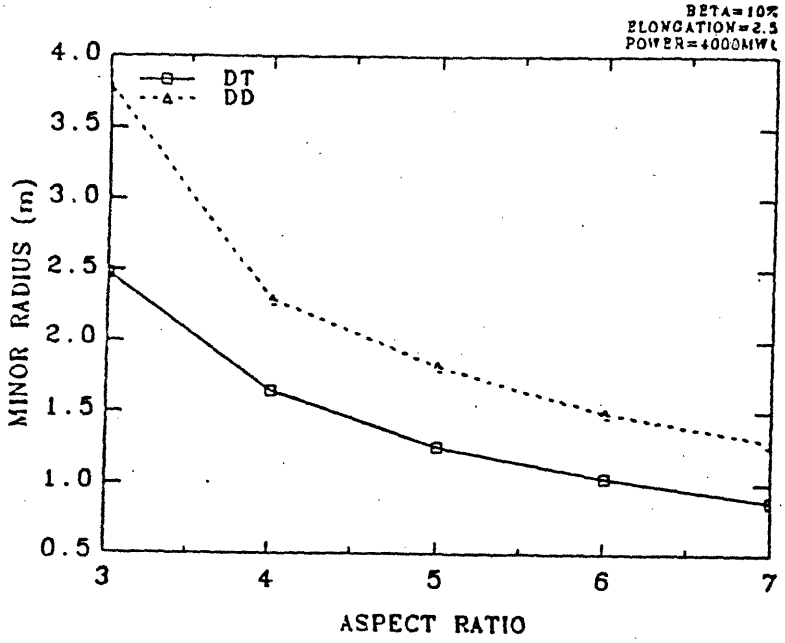

FIGURE 2.14: TOROIDAL FIELD VS ASPECT RATIO

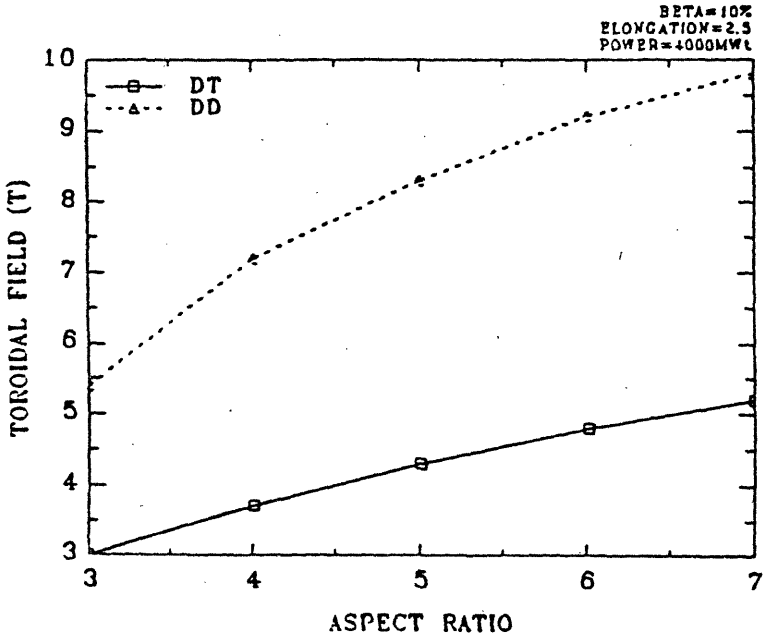

FIGURE 2.15: PLASMA CURRENT VS ASPECT RATIO

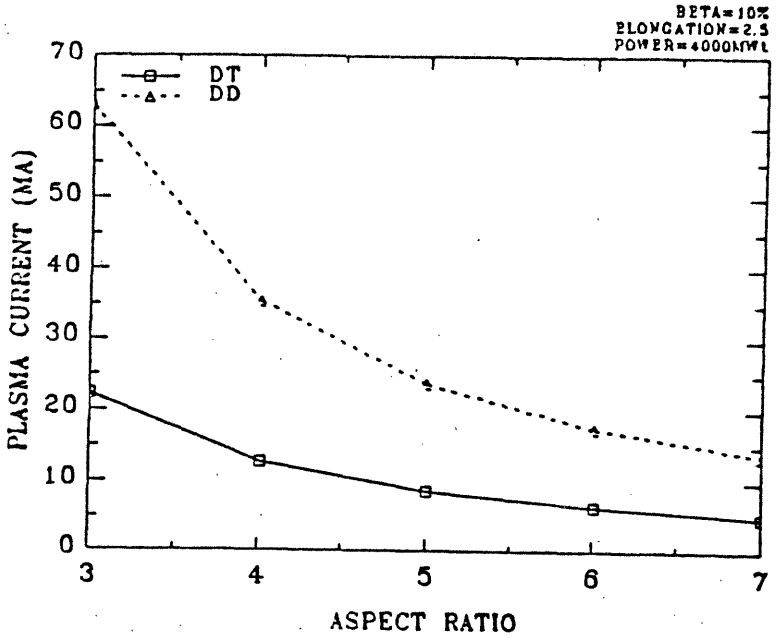

FIGURE 2.16:
TOTAL AVERAGE PLASMA DENSITY VS ASPECT RATIO

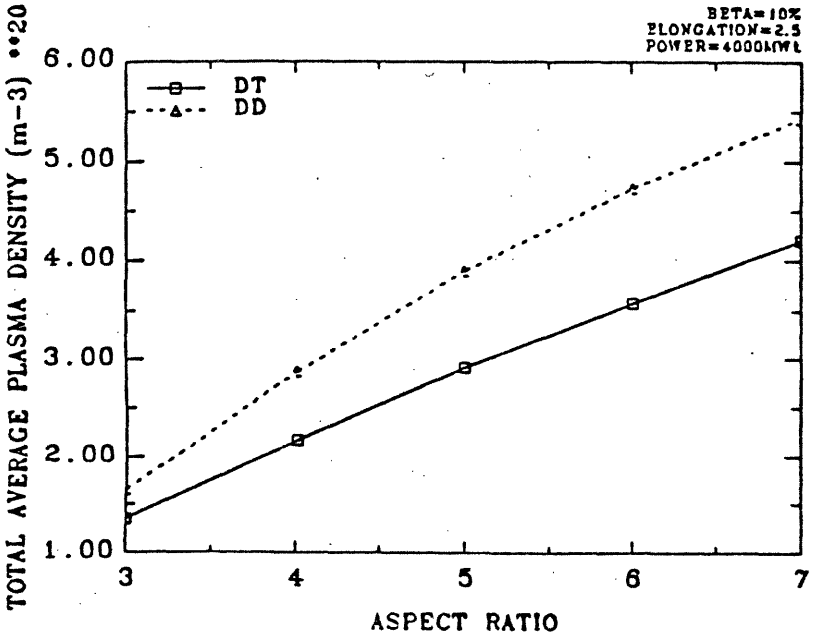

FIGURE 2.17:
CONFINEMENT TIME VS ASPECT RATIO FOR DT REACTORS

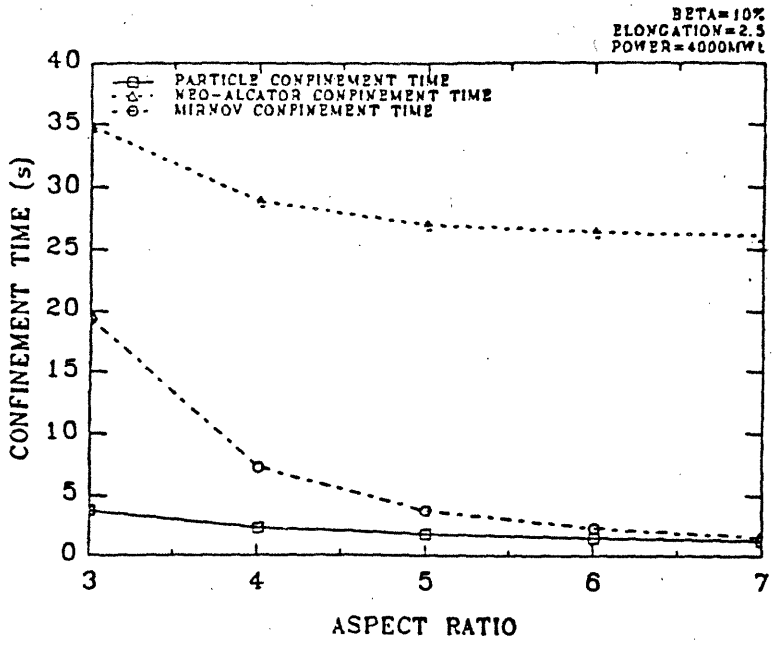

FIGURE 2.18:
CONFINEMENT TIME VS ASPECT RATIO FOR DD REACTORS

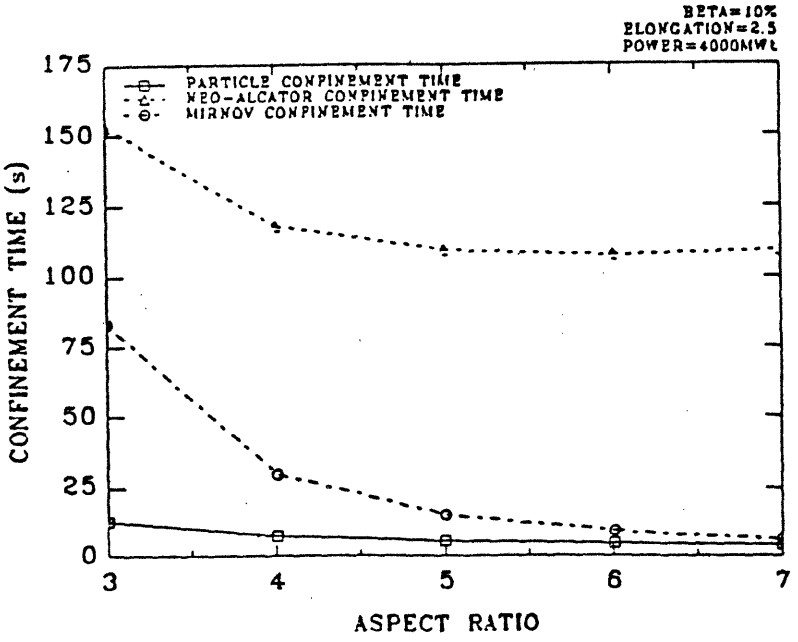

FIGURE 2.19: NEUTRON WALL LOADING VS ASPECT RATIO

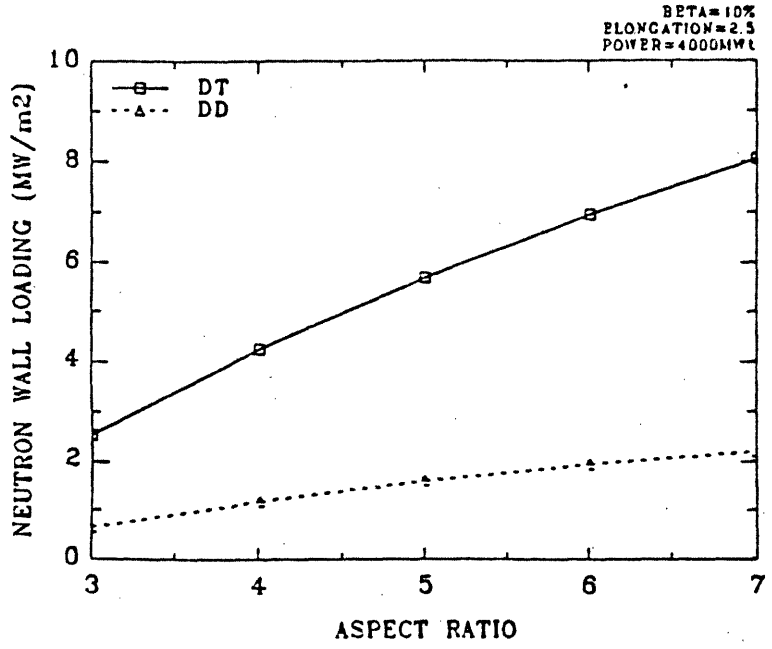

FIGURE 2.20: THERMAL WALL LOADING VS ASPECT RATIO

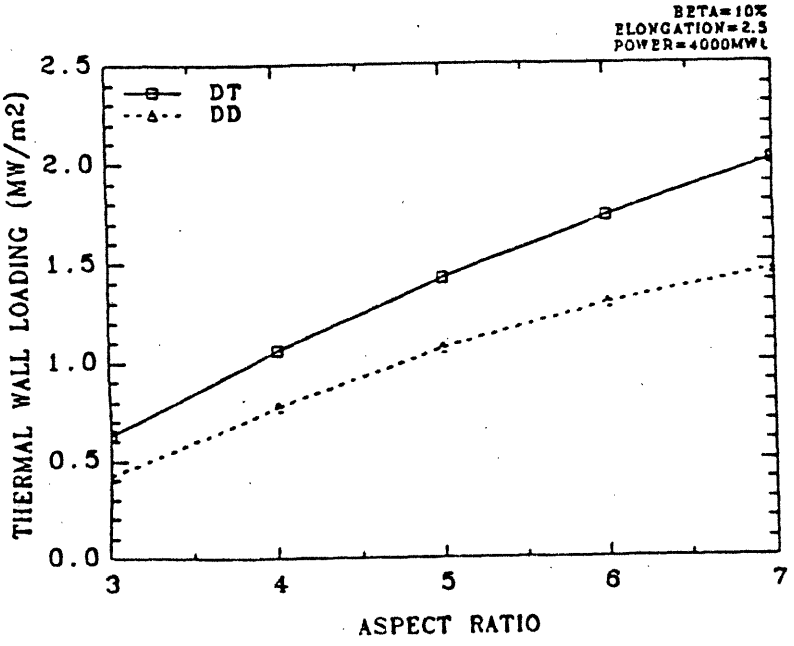

design information is given in appendix A. These designs assume a plasma beta of 10 %, plasma elongation of 2.5, scrape off distance of 10 cm and thermal power of 4000 MW. The shielding material used in these designs is HT-9. However, the same trends would be observed if Fe1422 was used as the shielding material. As the aspect ratio becomes larger, both the major and minor radii are seen to decrease. This occurs because at higher aspect ratios, there is more space available for the OH coil in the central bore. Thus, in a high aspect ratio machine, the major radius can be smaller before the minor radius and inboard blanket/shield come in contact with the OH coil/bucking cylinder. This effect seems to be less dramatic beyond an aspect ratio of 4 or 5. Because beta is held constant and the reactor is becoming smaller as the aspect ratio is increased, the toroidal field must necessarily increase in order for the same total power to be obtained. This implies a higher power density for a higher aspect ratio machine. Examining the expression for plasma current for its dependence on aspect ratio ($I_p \sim \frac{1}{A(1-\frac{1}{A^2})^2}$), it is evident that a decrease in current should be expected with an increase in aspect ratio. The higher power density of the higher aspect ratio designs requires a more dense plasma, as is evidenced in figure 2.16. The deterioration in confinement observed with increasing aspect ratio shown in figure 2.17 is due mainly to the reduction in reactor size. At aspect ratios greater than 4, the reduction in confinement time is less severe. Finally, at larger aspect ratios, higher wall loadings result from the decrease in first wall area associated with the smaller reactor size.

2.2.3 The Effect of Varying Plasma Elongation

Plasma elongation may be varied to assess the effects of changing the plasma cross section on reactor parameters. The trends exhibited by the design parameters as elongation is varied are shown in figures 2.21 to 2.29. Designs were defined having a beta of 10 %, an aspect ratio of 4, a scrape off distance of 10 cm and a thermal power of 4000 MW (see table A.4 in appendix A). Once again, HT-9 was employed

FIGURE 2.21: MAJOR RADIUS VS PLASMA ELONGATION

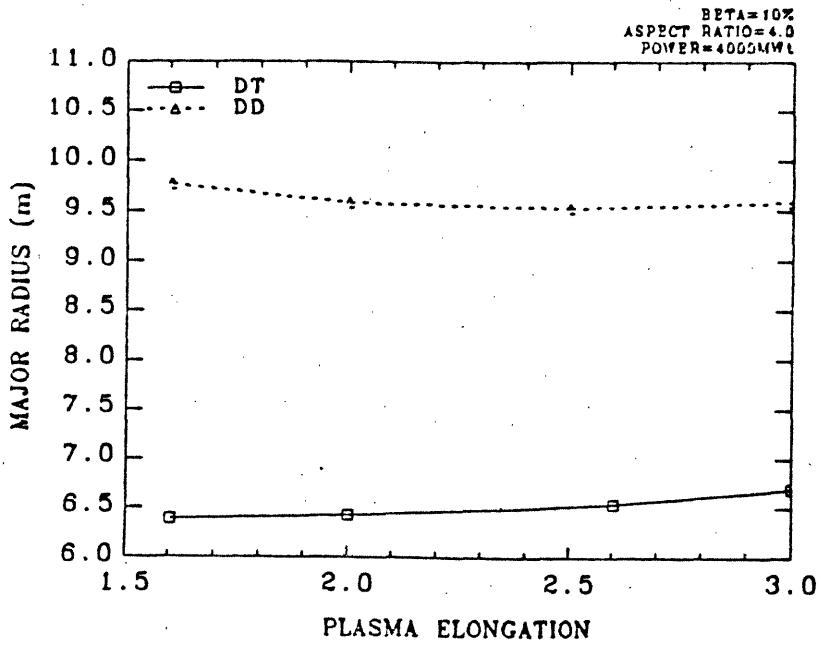

FIGURE 2.22: MINOR RADIUS VS PLASMA ELONGATION

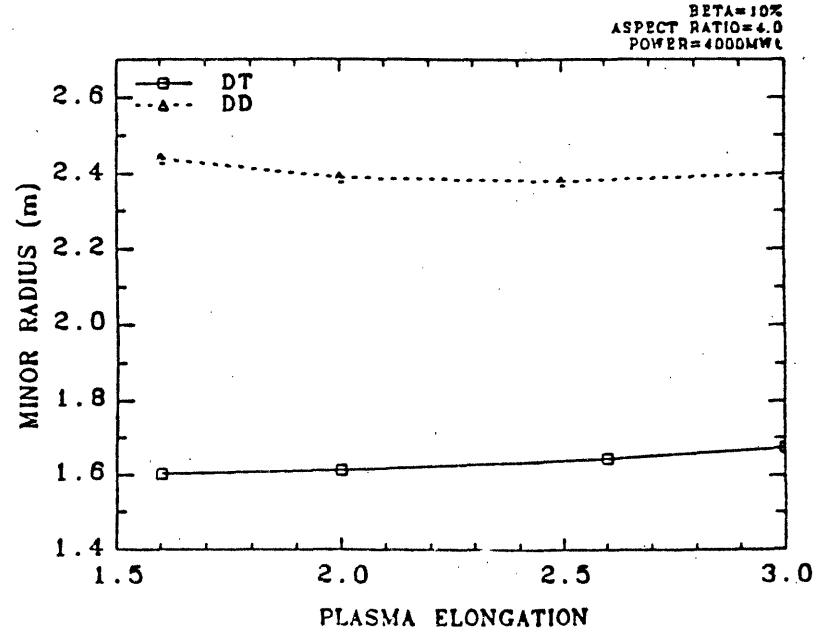

FIGURE 2.23: TOROIDAL FIELD VS PLASMA ELONGATION

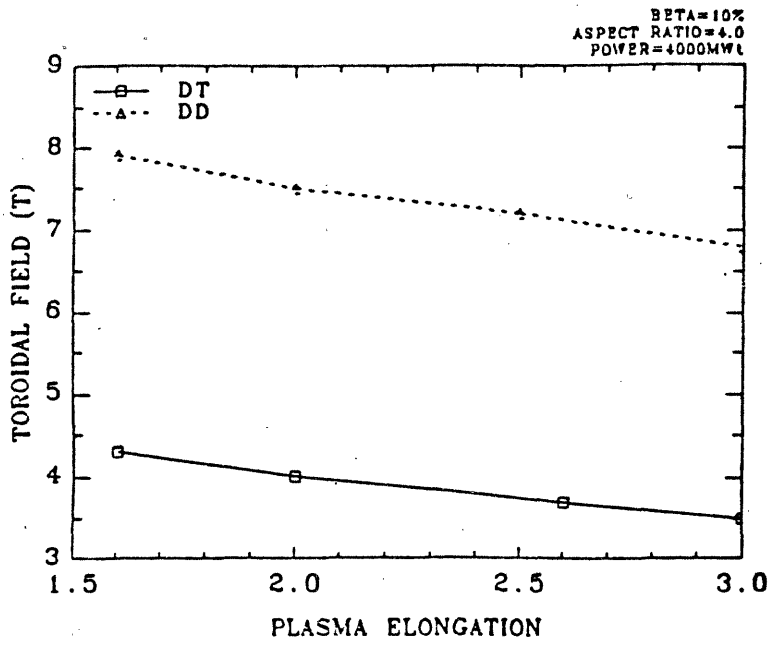

FIGURE 2.24:
TOTAL AVERAGE PLASMA DENSITY VS PLASMA ELONGATION

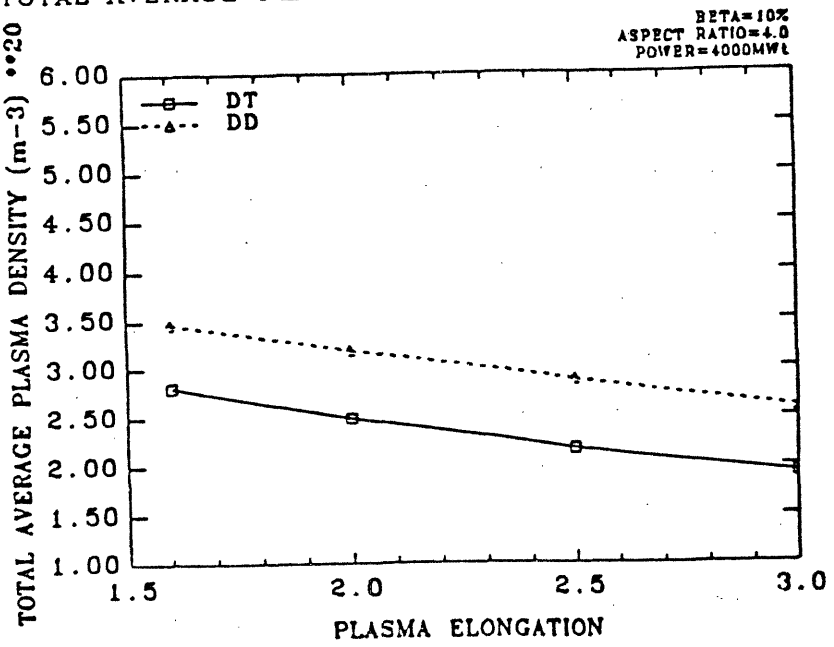

FIGURE 2.25: PLASMA CURRENT VS PLASMA ELONGATION

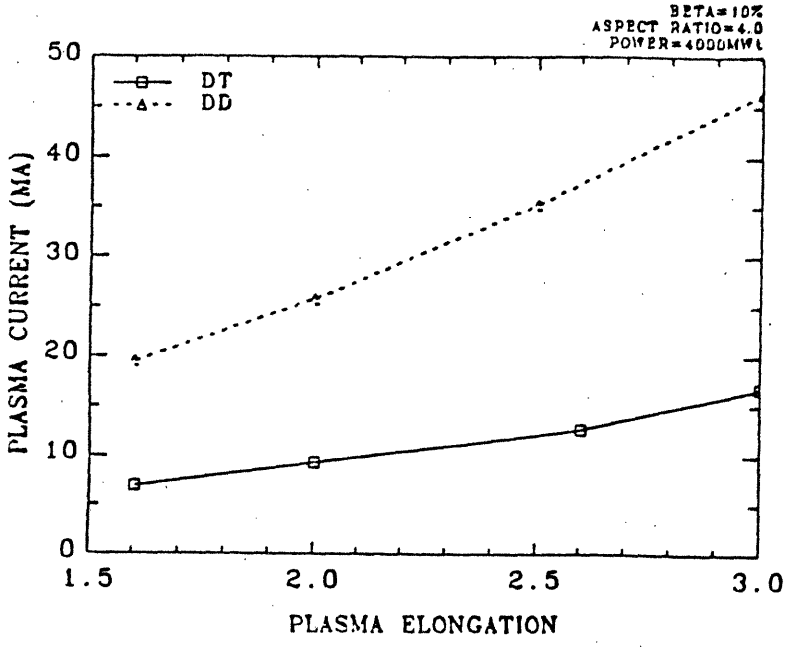

FIGURE 2.26:
CONFINEMENT TIME VS PLASMA ELONGATION FOR DT REACTORS

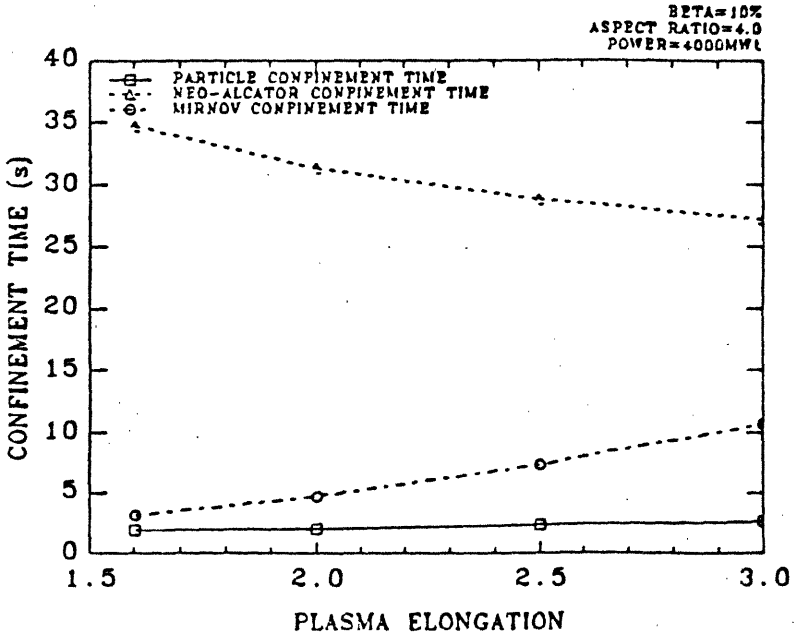

FIGURE 2.27:
CONFINEMENT TIME VS PLASMA ELONGATION FOR DD REACTORS

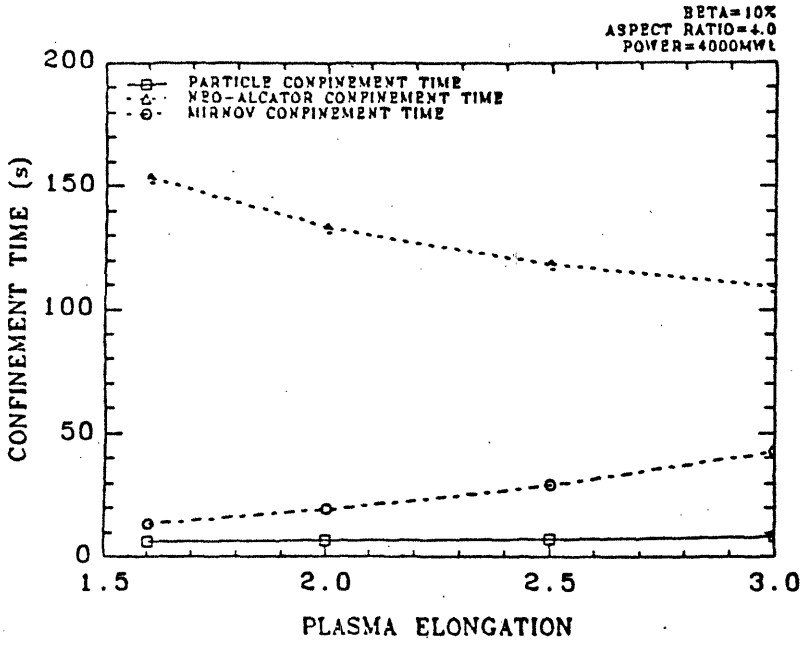

FIGURE 2.28: NEUTRON WALL LOADING VS PLASMA ELONGATION

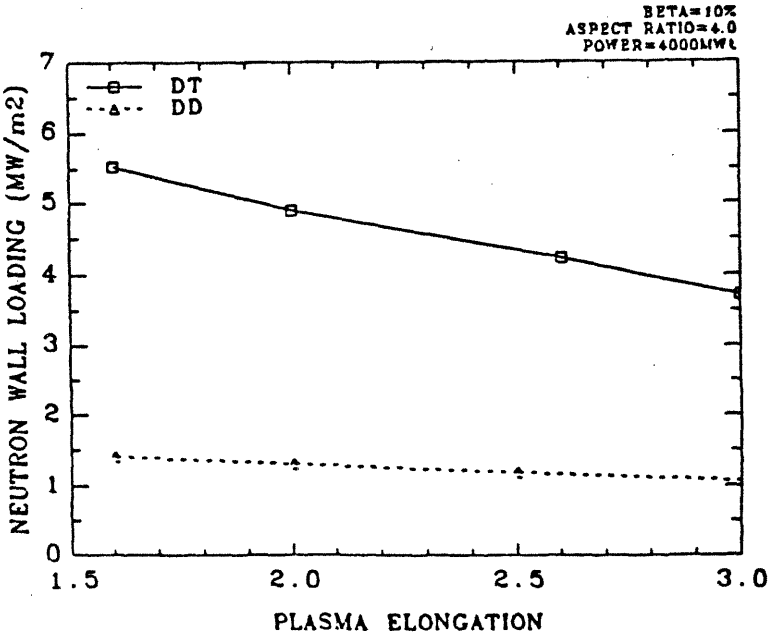

FIGURE 2.29: THERMAL WALL LOADING VS PLASMA ELONGATION

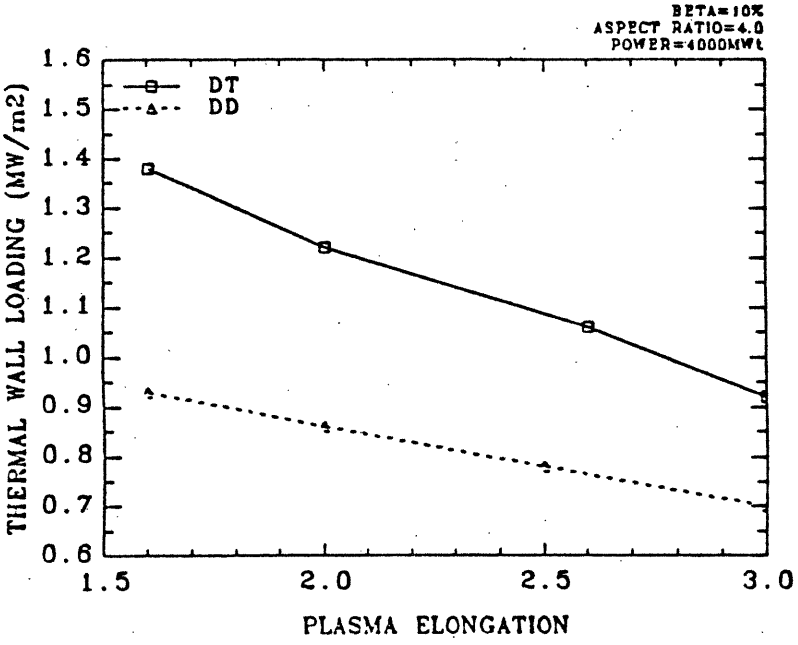

as the shielding material, but this should not bias the results. Over the range of elongation examined (from 1.5 to 3.0), both major and minor radii exhibit a very small increase. The plasma is becoming larger in volume and the plasma power density is decreasing slightly, allowing for a decrease in toroidal field. This decrease in power density also leads to a slight reduction in plasma density for the same total power output. Plasma current, being most strongly affected by geometric factors ($I_p \sim \frac{a(1+\kappa^2)}{A(1-\frac{1}{A^2})^2}$), is seen to increase with elongation. The larger reactor size results in slightly improved particle confinement. According to the Mirnov confinement law ($\tau_E \sim a \cdot \kappa^{\frac{1}{2}} \cdot I_p$), improved energy confinement will also result. Neo-Alcator scaling ($\tau_E \sim n \cdot a \cdot R^2$) shows a dimunition in energy confinement time because the fractional decrease in plasma density over the range of elongation scanned (44 %) is greater than the fractional increase in the geometric factor ($a \cdot R^2$ increases by 13 %). As expected, both neutron and thermal wall loadings decrease with elongation as the available wall area increases.

2.3 DD Designs

The major reactor parameters for the DD designs considered for this comparison are listed in table 2.3. As with the DT designs, the aspect ratio has been set at 4, the elongation is 2.5, the plasma scrape off distance is 10 cm, the shielding material is Fe1422, and the thermal power is 4000 MW. With the DD designs, the need for tritium breeding is eliminated. The blanket employed for three of the designs for this fuel cycle is HT-9 cooled by helium. The RAF DD design uses a reduced activation ferritic steel (RAF) first wall and a Fe2Cr1V blanket (see appendix A for compositions), cooled by helium. It employs a plasma beta of 10 %.

The DD reactors utilize the semi-catalyzed fuel cycle and are operated near the maximum of the $\frac{<\sigma v>}{T^2}$ curve, at a peak ion temperature of $\sim$ 50 keV (ideal ignition occurs at $\sim$ 25 keV [2.31]). According to both Neo-Alcator and Mirnov scaling, all machines are ignited with a comfortable ignition margin. Blanket and shield

Table 2.3: Reactor Parameters For DD Designs

Parameter	Low Beta (5 %)	Medium Beta (10 %) HT-9	Medium Beta (10 %) RAF	High Beta (20 %)
Major Radius (m)	13.01	9.52	9.44	7.28
Minor Radius (m)	3.25	2.38	2.36	1.82
Inboard Blanket (cm)	40.0	40.0	35.0	40.0
Outboard Blanket (cm)	125.0	125.0	120.0	125.0
Inboard Shield (cm)	37.0	39.0	45.0	40.0
Outboard Shield (cm)	56.0	57.0	65.0	59.0
Plasma Scaling Constant ($\beta^2B^4a^2$) ($T^4 \cdot m^2$)	109.0	149.0	139.8	194.5
Toroidal Field at coil (T)	12.1	11.3	11.3	10.4
Toroidal Field on axis (T)	8.0	7.2	7.1	6.2
B^2a ($T^2 \cdot m$)	209	122	118	70
T_{OH} (keV)	4.7	3.8	3.7	3.0
OH Flux Swing ($V \cdot s$)	1018	538	525	311
Plasma Current (MA)	53.8	35.2	34.5	23.2
Total Wall Loading (MW/m^2)	1.06	1.95	1.84	3.30
Neutron Wall Loading (MW/m^2)	0.64	1.17	1.10	1.98
Surface Heat Flux (MW/m^2)	0.42	0.78	0.74	1.32
$n_D\tau_E$ (Neo-Alcator) (sec/m^3)	3.05×10^{22}	3.05×10^{22}	2.84×10^{22}	3.05×10^{22}
Neo-Alcator Ignition Margin	23.7	23.7	22.0	23.7
τ_E (Neo-Alcator) (sec)	188.6	118.0	112.4	78.9
$n_D\tau_E$ (Mirnov) (sec/m^3)	9.93×10^{21}	7.59×10^{21}	7.21×10^{21}	5.74×10^{21}
Mirnov Ignition Margin	7.7	5.9	5.6	4.5
τ_E (Mirnov) (sec)	61.3	29.4	28.5	14.8
τ_P (sec)	11.8	7.4	7.6	4.9

Parameter	Low Beta	Medium Beta (10 %)		High Beta
	(5 %)	HT-9	RAF	(20 %)
Total Average Density (m^{-3})	$1.80x10^{20}$	$2.88x10^{20}$	$2.81x10^{20}$	$4.31x10^{20}$
Murakami Density Limit (m^{-3})	$6.16x10^{19}$	$7.52x10^{19}$	$7.50x10^{19}$	$8.51x10^{19}$
Deuteron Density (m^{-3})	$1.62x10^{20}$	$2.59x10^{20}$	$2.53x10^{20}$	$3.87x10^{20}$
Triton Density (m^{-3})	$6.48x10^{17}$	$1.04x10^{18}$	$1.01x10^{18}$	$1.55x10^{18}$
Helium-3 Density (m^{-3})	$3.19x10^{18}$	$5.09x10^{18}$	$4.97x10^{18}$	$7.61x10^{18}$
Protium Density (m^{-3})	$1.04x10^{19}$	$1.66x10^{19}$	$1.62x10^{19}$	$2.48x10^{19}$
Alpha Density (m^{-3})	$4.05x10^{18}$	$6.47x10^{18}$	$6.32x10^{18}$	$9.67x10^{18}$
Fusion Power (MW)	2876	2876	2675	2876
Blanket Multiplication Factor	1.65	1.65	1.83	1.65
System Multiplication Factor	1.39	1.39	1.50	1.39
Thermal Power (MW)	4001	4001	3999	4001
Net Electric Power (MW)	1213	1213	1213	1213
Tritium Burned (g/day)	221	221	206	221
Deuterium Burned (g/day)	777	777	723	777
Helium-3 Burned (g/day)	30	30	28	30
Tritium Produced in Plasma (g/day)	228	228	212	228
Helium-3 Produced in Plasma (g/day)	228	228	212	228
Protium Produced in Plasma (g/day)	86	86	80	86
Alphas Produced in Plasma (g/day)	334	334	310	334
Tritium Exhausted (g/day)	16	16	15	16
Deuterium Exhausted (g/day)	2687	2687	2499	2687
Helium-3 Exhausted (g/day)	198	198	184	198
Protium Exhausted (g/day)	86	86	80	86
Helium-4 Exhausted (g/day)	334	334	310	334
Total Gas Load ($Pa \cdot m^3/s$)	41.3	41.3	38.5	41.3
Tritium Fueled (g/day)	9.4	9.4	8.7	9.4
Deuterium Fueled (g/day)	3465	3465	3222	3465

Aspect Ratio	4.0
Scrape off (cm)	10
Plasma Elongation	2.5
Safety Factor at edge	2.5
Peak Electron Temperature (kev)	46.3
Average Electron Temperature (kev)	30.0
Peak Ion Temperature (kev)	50.0
Average Ion Temperature (kev)	33.3
Fraction of Energy due to DT Fusion	0.6368
Fraction of Energy due to DD Fusion	0.2728
Fraction of Energy due to DHe Fusion	0.0904
Deuterium Fractional Burn-up	0.224
Tritium Fractional Burn-up	0.932
Helium-3 Fractional Burn-up	0.132

thicknesses were determined using ONEDANT and were based on adequate heat removal and magnet shielding. Since tritium breeding is not an issue, the blanket thickness was adjusted until 90 - 94 % of the neutron energy was deposited in the blanket region. The higher neutron multiplication factor for the RAF DD design allows for a thinner blanket and lower fusion power to meet the 4000 MWt criterion. A slightly smaller reactor may result in some economic savings. As with the DT designs, two-thirds of the outboard blanket and shield were assumed to lie between the coils and one-third beneath the coils. The shield thickness beneath the coils on the outboard side is the same as the inboard shield thickness. The outboard shield thickness in the table refers to the shielding between the coils and includes an additional lead shield for gamma ray attenuation.

The DD reactors with 10 % beta are not greatly different from the pulsed version of WILDCAT. Major reactor parameters for WILDCAT are listed in table 2.6 at the end of this chapter. Many of the small differences can be attributed to the lower fusion power of WILDCAT.

2.3.1 The Effect Varying of Beta

The variations of reactor parameters with beta for the DD designs are indicated along with those for the DT designs in figures 2.1 through 2.11 and reactor parameters are given in appendix A. The reactors are consistently larger than their DT counterparts for the same thermal power output as as consequence of the lower DD fusion power density. With a constant total fusion power, both the major and minor radii decrease as plasma beta increases. The decrease is more dramatic for DD than for DT, where a reduction by 57 % is seen in major radius going from a beta of 3 % to a beta of 20 % (compared to a 36 % reduction for DT). Increasing beta increases the fusion power density so that a smaller plasma volume is required to produce the same total power. The fusion power density is higher for DT, being 8.8 times larger at a beta of 3% and 2.7 times larger at a beta of 20 % (note that

the DT and DD reactors are not operating at the same temperature). As beta becomes larger, the fusion power density increases, allowing for a reduction in the toroidal field. The rate of decrease is nearly the same for DT and DD, although higher fields are needed for DD. The plasma current decreases as a result of the decreasing plasma size and toroidal field. The sharper decrease for DD reflects the more dramatic change in plasma size with beta for this fuel cycle. Increasing beta results in an increase in the plasma density because of the decreasing size of the reactor. Particle and energy confinement is seen to be degraded at higher betas, due mainly to the decrease in reactor size. Confinement times are greater for DD, due to the scaling with reactor size. Wall loading is seen to increase with plasma beta, as the first wall area becomes smaller. However, values of both the neutron and thermal wall loadings for DD are still below those for the DT reactors over the range of betas examined. The DD machines may be able to operate for their entire life without requiring a blanket changeout, even at high beta. Thus, high beta operation may be more advantageous to the DD fuel cycle than to the DT fuel cycle. This is also expressed in figure 2.11. The highest power density of the fusion island for DD is obtained at a neutron wall loading less than 2 MW/m^2, corresponding to the design at 20 % beta. Obtaining more energy per unit volume for DD may not result in an economic penalty from damage due to neutron exposure.

2.3.2 The Effects of Varying Aspect Ratio and Elongation

Figures 2.12 through 2.20 illustrate the effect of varying aspect ratio for the DD designs as well as the DT designs. The trends and rates of change of the parameters with aspect ratio are similar for both fuel cycles.

Elongation also has a similar effect on reactor parameters for both fuel cycles, as shown in figures 2.21 through 2.29. For the most part, the effect is very small. Plasma current is more strongly affected for DD than for DT, increasing with elongation ($I_p \sim (1 + \kappa^2)$). The other factors upon which the plasma current depends

decrease as the elongation increases. Because this decrease is slightly smaller in the DD case, the effect of the scaling with elongation is more evident for this fuel cycle. The neo-alcator confinement time is seen to decrease with increasing elongation, reflecting the slight reduction in major and minor radii ($\tau_E \sim n \cdot a \cdot R^2$). The mirnov confinement time increases because of its dependence on plasma current ($\tau_E \sim I_p$). These effects, however are not large.

2.4 A DHe Design

A DHe tokamak design has been characterized as part of this work. A single value of plasma beta of 10 % has been adopted. Due to time constraints, a complete scan of the major design parameters was not made for this fuel cycle. However, some insight as to the relative position of this fuel cycle compared to the DT and DD fuel cycles with regards to safety and economics can be obtained by a comparison of the 10 % beta designs. Other parameters of the DHe design are listed in table 2.4.

The DHe design was assumed to operate at a peak temperature of $\sim$ 50 keV (average ion temperature of $\sim$ 33 keV) so that the plasma reactivity would be maximized (ignition occurs at $\sim$ 29 keV [2.31]). As with the DD designs, the need for tritium breeding is eliminated. An HT-9/helium cooled blanket is used. The advantages related to improved energy recovery for the DHe fuel cycle have not been exploited in this design. It was felt that an extensive evaluation of the energy recovery system was beyond the scope of this study. Elaborate schemes to take advantage of the energy released as charged particles (via divertor/direct conversion) and to efficiently utilize the radiative energy release (via rectification using solid-state circuitry or in-situ MHD conversion [2.33]) have been proposed. These, in addition to other techniques for energy conversion will likely render the DHe fuel cycle more attractive than is indicated here [2.34]. A conventional thermal cycle is also possible for energy conversion, if the first wall temperature can be kept

Table 2.4:

Reactor Parameters For DT, DD and DHe Designs With 10 % Beta

Parameter	DT	DD	DHe
Major Radius (m)	6.51	9.52	10.02
Minor Radius (m)	1.63	2.38	2.50
Inboard Blanket (cm)	26.0	40.0	30.0
Outboard Blanket (cm)	100.0	125.0	50.0
Inboard Shield (cm)	69.0	39.0	34.0
Outboard Shield (cm)	106.0	57.0	76.0
Peak Electron Temperature (kev)	15.2	46.3	46.5
Average Electron Temperature (kev)	10.1	30.9	31.0
Peak Ion Temperature (kev)	17.0	50.0	50.0
Average Ion Temperature (kev)	11.3	33.3	33.3
Plasma Scaling Constant ($\beta^2 B^4 a^2$) ($T^4 \cdot m^2$)	5.14	149.0	210.0
Toroidal Field at coil (T)	6.77	11.34	11.67
Toroidal Field on axis (T)	3.73	7.16	7.61
$B^2 a$ ($T^2 \cdot m$)	22.7	122.1	144.9
T_{OH} (keV)	1.9	3.8	4.0
OH Flux Swing ($V \cdot s$)	406	538	619
Plasma Current (MA)	12.5	35.2	39.3
Total Wall Loading (MW/m^2)	5.20	1.95	2.31
Neutron Wall Loading (MW/m^2)	4.16	1.17	0.18
Surface Heat Flux (MW/m^2)	1.04	0.78	2.13
Fusion Power (MW)	3645	2876	3763
Blanket Multiplication Factor	1.122	1.651	1.818
System Multiplication Factor	1.097	1.391	1.063
Net Electric Power (MW)	1225	1213	1213

Parameter	DT	DD	DHe
Fraction of Energy due to DT Fusion	0.9989	0.6368	0.0766
Fraction of Energy due to DD Fusion	0.0011	0.2728	0.0472
Fraction of Energy due to DHe Fusion	~ 0	0.0904	0.8762
$n_D\tau_E$ (Neo-Alcator) (sec/m^3)	2.85×10^{21}	3.05×10^{22}	1.66×10^{22}
Neo-Alcator Ignition Margin	9.5	23.7	7.3
τ_E (Neo-Alcator) (sec)	28.3	118.0	132.2
$n_D\tau_E$ (Mirnov) (sec/m^3)	7.21×10^{20}	7.59×10^{21}	4.34×10^{21}
Mirnov Ignition Margin	2.4	5.9	1.9
τ_E (Mirnov) (sec)	7.1	29.4	34.5
τ_P (sec)	2.3	7.4	2.3
Total Average Density (m^{-3})	2.16×10^{20}	2.88×10^{20}	2.77×10^{20}
Murakami Density Limit (m^{-3})	5.74×10^{19}	7.52×10^{19}	7.60×10^{19}
Deuteron Density (m^{-3})	1.01×10^{20}	2.59×10^{20}	1.26×10^{20}
Triton Density (m^{-3})	1.01×10^{20}	1.04×10^{18}	3.49×10^{17}
Helium-3 Density (m^{-3})	3.92×10^{16}	5.09×10^{18}	1.38×10^{20}
Proton Density (m^{-3})	9.81×10^{16}	1.66×10^{19}	9.00×10^{18}
Alpha Density (m^{-3})	1.41×10^{19}	6.47×10^{18}	3.46×10^{18}
Tritium Burned (g/day)	559	221	42
Deuterium Burned (g/day)	378	777	506
Helium-3 Burned (g/day)	~ 0	30	464
Tritium Produced in Plasma (g/day)	1.6	228	63
Helium-3 Produced in Plasma (g/day)	1.6	228	63
Protium Produced in Plasma (g/day)	0.5	86	176
Alphas Produced in Plasma (g/day)	742	334	672
Tritium Exhausted (g/day)	1598	16	20
Deuterium Exhausted (g/day)	1067	2687	4920
Helium-3 Exhausted (g/day)	1.6	198	20261

Parameter	DT	DD	DHe
Protium Exhausted (g/day)	0.5	86	176
Helium-4 Exhausted (g/day)	742	334	672
Total Gas Load ($Pa \cdot m^3/s$)	32.7	41.3	253.5
Tritium Fueled (g/day)	2156	9.4	0
Deuterium Fueled (g/day)	1445	3464	5426
Helium-3 Fueled (g/day)	0	0	20663
Tritium Fractional Burn-up	0.259	0.932	0.674
Deuterium Fractional Burn-up	0.261	0.224	0.093
Helium-3 Fractional Burn-up	-	0.132	0.022

Common Parameters	
Aspect Ratio	4.0
Scrape off (cm)	10
Plasma Elongation	2.5
Safety Factor at edge	2.5
Thermal Power (MW)	4000

within bounds [2.24, 2.35]. As with the other fuel cycles, this type of thermal system has been adopted here. In this way, the comparison amongst the fuel cycles will be made on an equal basis.

2.4.1 Comparison of the DHe Design to the Other Fuel Cycles

Table 2.4 also list the parameters for the DT and DD designs having a 10 % beta. The DHe reactor is slightly larger than its DD counterpart due to the lower overall energy multiplication and the criterion for producing the same total amount of power (4000 MWt). The shield thickness is least for the DHe design, since only 7.7 % (i.e. 291 MW) of its fusion power is produced in neutrons. The shielding required by the DD design is somewhat greater since 60 % (i.e. 1726 MW) of the power is released in the form of neutrons. Both are significantly less than the shielding required by the DT machine which releases 80 % (i.e. 2916 MW) of the power as neutrons. Due to the lower reactivity of the advanced fuels, higher magnetic fields and larger reactors are required to produce the same total power, at a fixed value of beta. This will have an impact both in terms of economics, due to the larger size of the reactors and the magnets, and in terms of safety, due to the larger stored energy in the magnets. Larger plasma currents are found in the DD and DHe fuel cycles due to the larger toroidal fields and reactor sizes. The total wall loading of the DT reactor is greatest due to the large fusion power and the relatively small size of the reactor. The total wall loading of the DHe reactor exceeds that of the DD reactor despite its slightly larger size because of the greater fusion power. Such a high fusion power is required since the fraction of the power carried by the neutrons is small. Consequently, the total multiplication of power in the blanket is low compared to the DD case, and a larger fusion power is needed to achieve the 4000 MWt criterion. The blanket multiplication factor refers to the amplification of neutron energy per neutron entering the blanket. Although the DT reactor releases the greatest fraction of energy in the form of neutrons, it has the

lowest blanket multiplication factor. The DHe reactor releases the fewest neutrons but it has the largest blanket multiplication factor i.e. more energy is released per neutron interaction in the blanket. This effect is the result of the difference in neutron energy spectra associated with the fuel cycles. In the DT fuel cycle, the source neutrons are entirely 14.06 MeV (the temperature is too low for DD or DHe side reactions to occur to any significant extent). With the semi-catalyzed DD fuel cycle the neutron energy split is 49 % 14.06 MeV neutrons and 51 % 2.45 MeV neutrons. The neutron source of the DHe machine is 40 % 14.06 MeV neutrons and 60 % 2.45 MeV neutrons. Since the interaction cross sections of many isotopes vary as $\frac{1}{v}$, the lower energy neutrons react more strongly. Because the fraction of lower energy neutrons in the DHe blanket is largest, a higher energy multiplication per neutron is seen.

Reactor parameters for a DHe tokamak from a previous study [2.24] are listed in table 2.5 for comparison. It should be noted that the thermal power, plasma beta, aspect ratio, elongation and some plasma physics parameters are different than those assumed for the DHe design presented here.

2.4.2 Ohmic Heating in Advanced Fuel Reactors

The anticipated start-up scheme for the advanced fuel reactors will involve DT ignition followed by thermal runaway [2.24]. Achieving DT ignition will require some form of auxiliary heating because the intrinsic heating mechanism provided by collisional friction (i.e. ohmic heating) will fall short of heating to thermonuclear temperatures. Examining the energy balance containing the ohmic heating term, the maximum temperature achievable from this heating mechanism is found to be a function of B^2a:

$$T_{OH} = \left(\frac{k \cdot J^2 \cdot \tau_E}{3 \cdot n \cdot \alpha}\right)^{\frac{2}{5}}$$
$$= 0.55 \left(B_T^2 \cdot a\right)^{\frac{2}{5}} \qquad (2.1)$$

Table 2.5: Reactor Parameters For STARFIRE, WILDCAT and the EPRI D $-^3$ He Tokamak

Parameter	STARFIRE	WILDCAT	EPRI D $-^3$ He
Plasma Beta	0.067	0.11	0.12
Major Radius (m)	7.0	8.58	8.24
Minor Radius (m)	1.94	2.64	2.75
Aspect Ratio	3.6	3.25	3.0
Inboard Blanket (cm)	35.0	20.0	incl. with shield
Outboard Blanket (cm)	53.0	40.0	incl. with shield
Inboard Shield (cm)	60.0	39.0	100
Outboard Shield (cm)	118.0	97.0	-
Scrape off (cm)	20	20	50
Plasma Elongation	1.6	1.6	3.0
Safety Factor at edge	5.0	3.0	3.0
Electron Temperature (kev)	17.3	30.0	-
Ion Temperature (kev)	24.1	32.0	45
Plasma Scaling Constant ($T^4 \cdot m^2$)	19.119	345.42	261.47
Toroidal Field at coil (T)	11.1	14.0	14.5
Toroidal Field on axis (T)	5.8	8.0	7.0
Plasma Current (MA)	10.1	29.2	53
Total Wall Loading (MW/m^2)	4.5	1.5	1.1
Neutron Wall Loading (M/m^2)	3.6	0.55	0.046
Surface Heat Flux (MW/m^2)	0.9	0.83	1.054
Fusion Power (MW)	3510	1285	$\sim$ 1887
Multiplication Factor	1.14	2.024	$\sim$ 1.06
Thermal Power (MW)	4000	2600	2000
Net Electric Power (MW)	1200	850	800

where

T_{OH} = temperature achievable by ohmic heating (keV)

k = proportionality constant relating plasma resistivity to plasma temperature ($\eta = k \cdot T^{\frac{-3}{2}}$) ($\frac{J^{\frac{3}{2}} \cdot \Omega}{m}$)

J = current density (assumed constant) ($\frac{A}{m^2}$)

τ_E = energy confinement time (s)

= 1.9×10^{-21} n a R^2 (Neo-Alcator scaling)

n = plasma density (m^{-3})

α = fraction of plasma cross section subject to ohmic heating (assumed to be two-thirds)

a = plasma minor radius (m)

B_T = toroidal field on axis (T)

From this expression, the maximum temperature achievable by ohmic heating for the DT designs considered in this study are 2.4 keV for 5 % beta, 1.9 keV for 10 % beta and 1.5 keV for 20 % beta. The declining temperature as beta increases is a consequence of the decreasing reactor size (a) and toroidal field (B^2) (for constant power output of 4000 MWt). In all cases, the temperature falls short of the minimum required temperature (ideal) for ignition of $\sim$ 4 keV. However, it may be possible to achieve this temperature in the advanced fuel reactors, which must be larger and require higher magnetic fields for the same power output. If ohmic heating to DT ignition can in fact occur in the advanced fuel machines, then this could be followed by thermal runaway until the DD or DHe fuel mixture was ignited. The temperatures achievable for the designs examined here are indicated in tables 2.4 and 2.5. The 5 % beta DD design can be heated ohmically to 4.7 keV. This surpasses the ideal ignition temperature for DT, at which time the fusion power released as

charged particles can heat the plasma sufficiently to balance bremsstrahlung losses. The other DD designs ohmically heat to a slightly lower temperature because of the smaller size and the lower magnetic fields of these reactors. They do not quite heat the plasma to the extent of reaching DT ignition. However, the temperatures which can be achieved by ohmic heating are roughly twice as high as those in the DT machines of the same beta.

It has been shown [2.36, 2.37] that confinement is degraded as auxiliary power input to the plasma increases. Since the scheme employing DT ignition and thermal runaway requires less auxiliary power to achieve ignition of the advanced fuel (than would be the case without first igniting a DT plasma), confinement degradation will not be as severe as it could be. This is important when considering the advanced fuels because of the longer confinement time needed to maintain the burn.

2.5 Design Summary

Representative design parameters for the various fuel cycles over the range of values of beta have been summarized in tables 2.2, 2.3 and 2.4. All designs are pulsed, superconducting tokamaks, employing a 5000 second pulse. Each design has an aspect ratio of 4, an elongation of 2.5, a safety factor at the edge of 2.5, and produces 4000 MW of thermal power. For the DT and DD designs, the reactor size and on axis toroidal field are seen to decrease with plasma beta. The increasing fusion power density with increasing beta results in an increase in wall loading. It is evident that the DT reactors are smaller than their advanced fuel counterparts at a give beta. This is a consequence of the lower power density of the advanced fuels, despite the higher operating temperature and magnetic fields associated with these reactors.

The DT blankets were composed of lithium breeder with HT-9 structure and helium coolant. The thickness was determined from neutronics calculations with

a one-dimensional tritium breeding ratio of 1.25 as the design criteron. Tritium breeding is not a design issue for the advanced fuels. Their blankets were designed for deposition and removal of energy released in the plasma. They utilize HT-9 as the blanket material, cooled by helium. The blanket thickness was determined such that $\sim$ 94 % of the neutron energy was deposited in this zone. Shield thicknesses were based on attenuation of the high energy neutron flux to ensure adequate magnet protection in all cases. The total blanket/shield thickness is greatest for the DT designs, reflecting the greater quantity and higher energy of the fusion neutrons. The DD designs show the largest total gain in energy from neutron interactions in the blanket. This is a consequence of the blanket material, the neutron energy spectrum and the total number of neutrons entering the blanket. Because of this, the DD reactors can be designed to produce a lower fusion power, but still result in the same thermal power output as the other fuel cycles. An even greater blanket multiplication factor is achieved with the use of the RAF first wall/Fe2Cr1V blanket DD design. This is largely due to the greater iron content of the Fe2Cr1V blanket compared to the HT-9 blanket.

The designs presented here have been developed on a consistent design basis. The minimum number of changes to the DT fuel cycle were made to accommodate the advanced fuels, so that any design changes are a direct consequence of the change in fuel cycle. These designs can then be compared, in terms of safety and economics, on an equal basis. The economic and safety analyses are presented in the forthcoming chapters.

2.6 References

(2.1) M. Okabayashi et al., Studies of Bean-Shaped Tokamaks and Beta Limits for Reactor Design, Proceedings of the Tenth Conference on Plasma Physics and Controlled Nuclear Fusion Research, London, England, September 1984.

(2.2) J. Sheffield et al., Cost Assessment of a Generic Magnetic Fusion Reactor, Fusion Technology, 9, p. 199, March 1986.

(2.3) J.P. Freidberg and J.A. Wesson, Minimum Required Beta in a Tokamak Reactor, Nuclear Fusion, 25, No. 7, p. 759, 1985.

(2.4) D.C. Baxter et al., d-d Tokamak Reactor Assessment, Science Applications Inc., SAI25082-213LJ, March 1983.

(2.5) F.J. Helton et al., Beta Limits for the BIG DEE, Nuclear Fusion, 25, No. 3, p. 299, 1985.

(2.6) D. Dobrott, Alternate Fuels in Fusion Reactors, Nuclear Technology/Fusion, 4, p. 399, September 1983.

(2.7) D.C Baxter et al., D-D Tokamak Reactor Assessment, Nuclear Technology/Fusion, 4, p. 246, September 1983.

(2.8) K.E. Evans et al., WILDCAT: A Catalyzed D-D Tokamak Reactor, Argonne National Laboratory, ANL/FPP/TM-150, November 1981.

(2.9) L.C. Bernard et al., MHD Beta Limits: Scaling Laws and Comparison With Doublet III Data, Nuclear Fusion, 23, No. 11, p. 1475, 1983.

(2.10) R.D. Stambaugh et al., Tests of Beta Limits as a Function of Plasma Shape in Doublet III, Proceedings of the Tenth International Conference on Controlled Fusion and Plasma Physics, 1984.

(2.11) K. Yamazaki et al., Ballooning Beta Limits of Dee- and Bean- Shaped Tokamaks, Nuclear Fusion, 25, No. 11, p. 1543, 1985.

(2.12) R.C. Grimm et al., MHD Stability Properties of Bean Shaped Tokamaks, Nuclear Fusion, 25, No. 7, p. 805, 1985.

(2.13) M. Chance et al., Ballooning Mode Stability of Bean-Shaped Cross Sections for High-β Tokamak Plasmas, Phys.Rev.Lett., 51, No. 21, p. 1963, November 1983.

(2.14) F. Troyan et al., MHD Limits to Plasma Confinement, Proceedings of the Eleventh European Conference on Controlled Fusion and Plasma Physics, 1983.

(2.15) A. Sykes et al., Beta Limits in Tokamaks due to High-N Ballooning Modes, Proceedings of the Eleventh European Conference on Controlled Fusion and Plasma Physics, 1983.

(2.16) T. Tuda et al., Accessible Beta Value of Tokamaks Proceedings of the Tenth International Conference on Controlled Fusion and Plasma Physics, 1984.

(2.17) J. Sheffield, Physics Requirements for an Attractive Magnetic Fusion Reactor, Nuclear Fusion, 25, No. 12, p. 1733, 1985.

(2.18) Prof. K. Molvig, P. Hakkarainen, J. Crotinger, Private Communication, March 1986.

(2.19) C. Baker, Private Communication by letter, March 1986.

(2.20) D.L. Smith et al., Blanket Comparison and Selection Study (BCSS) - Final Report, Argonne National Laboratory, ANL/FPP-84-1, September 1984.

(2.21) Y. Gohar, Low Cost Shield for Tokamak Fusion Reactors, Nuclear Technology/Fusion, 4, p. 373, September 1983.

(2.22) S. Fetter, The Radiological Hazards of Magnetic Fusion Reactors, Ph.D. Thesis, University of California, Berkeley, 1985.

(2.23) J. Massidda, private communication, M.I.T., September 1986.

(2.24) C. Choi et al., Exploratory Studies of High-Efficiency Advanced Fuel Fusion Reactors, Electric Power Research Institute, EPRI ER-581, November 1977.

(2.25) D. Ehst et al., A Comparative Study of Pulsed and Steady-State Tokamak Reactor Burn Cycles, Argonne National Laboratory, ANL/FPP/TM-185, May 1984.

(2.26) C. Baker et al., STARFIRE - A Commercial Tokamak Fusion Power Plant Study, Argonne National Laboratory, ANL/FPP-80-1, September 1980.

(2.27) R. LeClaire, Conceptual Design of a Commercial Tokamak Reactor Using Resistive Magnets, M.I.T. Plasma Fusion Center, PFC/RR-86-17, June 1986.

(2.28) R.A. Krakowski, Parametric Results Using Generomak Model with Emphasis on Power Density Versus Inherent-Safety Tradeoffs, Memorandum to ESECOM, March 1986.

(2.29) G.M. M^{c}Cracken et al., Princeton Plasma Physics Laboratory, PPPL1569, 1979.

(2.30) C.A. Flanagan et al., Fusion Engineering Device Design Description, Oak Ridge National Laboratory, ORNL/TM-7948, December 1981.

(2.31) J. Reece Roth and H.C. Roland, The Effect of Wall Loading Limitations and Choice of Beta on the Feasibility of Advanced Fuel Fusion Reactors, Proceedings of the Eighth Symposium on the Engineering Problems of Fusion Research, San Francisco California, p. 869, November 1979.

(2.32) R.D. O'Dell et al., User's Manual for ONEDANT: A Code Package for ONE–Dimensional, Diffusion-Accelerated, Neutral- Particle Transport, Los Alamos National Laboratory, LA-9184-M, February 1982.

(2.33) B. Logan, An Advanced-Fuel Variant for ESECOM: D^3He Fusion Using Direct Conversion of Microwave Synchrotron Radiation, Presentation of ESECOM, April 1986.

(2.34) R. Scott et al., Advanced Fuel Fusion Systems - The D^3He Satellite Approach, Proceedings of the Review Meeting on Advanced Fuel Fusion, p. 455, Electric Power Research Institute, EPRI ER-536 SR, June 1977.

(2.35) L. Wittenberg et al., Lunar Source of ^3He for Commercial Fusion Power, Fusion Technology, 10, September 1986.

(2.36) R.J. Bickerton et al., Latest Results from JET, JET Joint Undertaking, JET-P(85)15, September 1985.

(2.37) D.R. Cohn, Future Directions in Fusion Research: Super High Field Tokamaks, M.I.T. Plasma Fusion Center, PFC/CP-86-14, October 1986.

(2.38) J. Fillo et al., Exploratory Studies of High-Efficiency Advanced Fuel Fusion Reactors, Electric Power Research Institute, EPRI ER-919, December 1978.

(2.39) R.W Conn et al., Alternate Fusion Fuel Cycle Research, IAEA-CN-38/V-5.

(2.40) B. Brunelli and G. Leotta, eds., Unconventional Approaches to Fusion, Plenum Press, 1981.

(2.41) G. Miley et al., Advanced Fuel Fusion Systems - The D^3He Satellite Approach, Proceedings of the Review Meeting on Advanced Fuel Fusion, p. 39, Electric Power Research Institute, EPRI ER-536 SR, June 1977.

(2.42) G. Sheu et al., Conceptual Design of a Deuterium - ^3He Fueled Tandem Mirror Reactor Satellite/Breeder System, Fusion Technology, 9, May 1986.

(2.43) K. Schoepf et al., Reaction Balance and Efficiency Analysis of a DD Fusion/Fission with Satellite D^3He Reactors, Journal of Fusion Energy, 2, No. 3, 1982.

(2.44) C.C. Baker at al., Fusion Reactor Technology Impact of Alternate Fusion Fuels, Proceedings of the Eighth IEEE Symposium on the Engineering Problems of Fusion Research, p. 861, November 1979.

(2.45) J. Fillo and J. Powell. Fusion Blankets for Catalyzed DD and DHe Reactors, Proceedings of the Review Meeting on Advanced Fuel Fusion, p. 57, Electric Power Research Institute, EPRI ER-536, June 1977.

(2.46) K.E. Evans et al., D-D Tokamak Reactor Studies, Argonne National Laboratory, ANL/FPP/TM-138, November 1980.

(2.47) W. M Stacey, FUSION : An Introduction to the Physics and Technology of Magnetic Confinement Fusion, John Wiley & Sons, 1984.

(2.48) R.A. Gross, Fusion Energy, John Wiley & Sons, 1984.

(2.49) D. Smith et al., Overview, BCSS, Fusion Technology, 8, July 1985.

(2.50) J. Jung and J. Foley, A Comparative Multidimensional Nuclear Analysis of Candidate Blanket Designs for Tokamak and Mirror Reactor Concepts, Fusion Technology, 8, p. 1998, September 1985.

(2.51) N.M. Schaeffer, Reactor Shielding for Nuclear Engineers, US Atomic Energy Commission, 1973.

(2.52) N. Uckan and J. Sheffield, A Simple Procedure for Establishing Ignition Conditions in Tokamaks, Oak Ridge National Laboratory, ORNL/TM-9722, September 1985.

(2.53) R.L. Reid et al., Large Aspect Ration Tokamak Study, Oak Ridge National Laboratory, ORNL/TM-7278, June 1980.

(2.54) E. Greenspan et al., Tritium Catalyzed Deuterium Tokamaks, Argonne National Laboratory, ANL/FPP/TM-183, April 1984.

(2.55) T. Shiba et al., Neutronics Optimization Study for D-D Fusion Reactor Blanket/Shield, Journal of Fusion Energy, 4, No. 6, p. 389, 1985.

(2.56) Y. Gohar and S. Yang, Energy Deposition and Shielding Requirements for all Concepts of the Blanket Comparison and Selection Study, Fusion Technology, 8, p. 2010, September 1985.

(2.57) D. Ehst et al., Tokamak Burn Cycle Study: A Data Base for Comparing Long Pulse and Steady State Power Reactors, Argonne National Laboratory, ANL/FPP/TM-178, November 1983.

(2.58) A.E. Dabiri, Economic Considerations of Commercial Tokamak Options, Oak Ridge National Laboratory - Fusion Engineering Design Center, ORNL/FEDC-86/2, May 1986.

Chapter 3
Economic Evaluation of Alternate Fuel Cycles

In order to ascertain the overall attractiveness of a given fuel cycle, an economic analysis must be performed. A costing code to assess the cost of electricity has been developed. Flexibility for application to costing of fusion plants utilizing the DT, DD and DHe fuel cycles has been incorporated. Details of the code can be found in appendix B. The following section outlines the costing methodology employed.

3.1 Costing Methodology

The competitiveness of fusion as a source of electrical power will be dependent on the cost of the electricity which it provides. The cost of electricity, COE, is determined from the plant capital cost, the operating and fuel costs, the plant capacity factor and lifetime, and the financing parameters. The plant capital cost is dependent on the cost to construct the plant as well as the economic conditions during construction (inflation/escalation and interest rates). The elements of the constructed cost are direct cost, indirect cost and contingency. These are discussed further below. The effects of time related considerations, such as interest and inflation, are also described.

The direct costs are associated with permanent components of the plant and include equipment, materials, engineering and labor. Equipment and materials costs include the basic purchase price, expenses associated with shipment to the site, research and development expenses incurred during the development of a component for the facility being costed and quality assurance and testing costs. The engineering component includes first-of-a-kind, nonrecurring engineering costs for any items not commercially available. Labor costs for construction and acceptance testing of the permanent plant are also included in the direct costs.

Indirect costs result from support activities required to accomplish the direct cost activities. The support activities include: (1) construction facilities, equipment and services (15 % of the direct costs for an eight year construction period); (2) home office engineering services; (3) field office engineering and construction management services (a total of 25 % of the direct costs for elements (2) and (3) for an eight year construction period); (4) project administration costs (10 % of the direct costs for an eight year construction period), spare parts and inventories. Spare parts and inventories were estimated as proposed in reference [3.1]. The indirect costs for construction times other than eight years can be determined by linear scaling:

$$C_{indir} = 0.15 \cdot \frac{Y}{8} \cdot C_{dir} + 0.25 \cdot \frac{Y}{8} \cdot C_{dir} + 0.10 \cdot \frac{Y}{8} \cdot C_{dir} + C_{SPINV} \quad M\$ \qquad (3.1)$$

These indirect charge percentages are raised from those recommended in references [3.2] and [3.3] (10 % for construction facilities, equipment and services, 8 % for engineering and construction management services and 5 % for project administration). This increase should more accurately reflect present day experience in the power industry [3.4].

Allowance for uncertainties in project definition, unit pricing and execution is included in the contingency cost. Such unforeseen and unpredictable expenses are expected to occur during the facility construction and start-up. As recommended in reference [3.4], the contingency allowance adopted in this study was 15 % of direct and indirect costs.

The costing procedure generally follows the methodology developed at the Fusion Engineering Design Center [3.5]. This approach is based mainly on the parametric cost estimating method which estimates on a cost-per-unit (weight, volume, area, power, etc.) and incorporates a generic code of accounts. The accounts are based on the standard fusion accounts set out in a previous document [3.2] and on present power industry practice [3.6]. Some modifications have been made to facilitate comparison of fusion power reactor costs to other sources of electricity. Specific changes concern the indirect costs elements (four separate elements instead of three), a completely different set of subaccounts for reactor plant equipment (accounts 221-229) and the use of account 26 for total plant heat reject system rather than special materials (which are now included in account 25, with miscellaneous plant equipment). The accounts and the algorithms used for costing are discussed in the appendix.

As suggested in references [3.2], [3.3] and [3.5], and as adopted by major design studies ([3.7] and [3.8]), the levelized revenue requirement method for calculating

the COE has been employed in this work. The COE is the unit cost of generating electricity from the fusion reactor facility and represents the necessary yearly revenues required by the utility to pay operating costs, taxes, return on undepreciated capital investment and capital investment depreciation. The COE can be calculated in two ways. In the current dollar approach, inflation is explicitly included and the purchasing capability of the dollar changes with time. The COE is quoted in dollars of a future year (dollars of year of completion of construction or first year of plant operation), the capital costs are levelized to account for inflation/escalation during the plant lifetime, the operating and maintenance costs are also levelized to account for inflation and escalation during the plant lifetime and are quoted in dollars of the first year of operation. The constant dollar approach allows for easy comparison with present day costs. In this approach, no inflationary effects are incorporated, but the time value of money is considered (i.e. interest on borrowing capital for plant construction). Operating costs are calculated in current-day dollars (as opposed to dollars of the first year of operation).

For the Current Dollar COE:

$$\mathrm{COE_{current}} = \frac{C_C \cdot \mathrm{FCR} + (C_{OM} + C_F) \cdot \mathrm{LN}}{P_e \cdot 8760 \cdot F_{cap}} \ \text{mills/kWh} \tag{3.2}$$

For the Constant Dollar COE:

$$\mathrm{COE_{constant}} = \frac{C_C \cdot \mathrm{FCR} + C_{OM} + C_F}{P_e \cdot 8760 \cdot F_{cap}} \ \text{mills/kWh} \tag{3.3}$$

where

$\mathrm{COE_{current}}$= levelized revenue requirement or cost of electricity (mills/kWh, dollars of first year of operation)

$\mathrm{COE_{constant}}$= levelized revenue requirement or cost of electricity (mills/kWh, dollars of present day)

C_C= total capital cost of plant (M$)

FCR= levelized annual fixed charge rate (see below)

C_{OM}= annual operating and maintenance costs (M$/yr)

C_F= annual fuel costs (M$/yr)

LN= thirty year levelizing factor (see below)

P_e= plant net electrical output (MW)

F_{cap}= plant capacity factor

The total construction cost of the plant is determined from the direct, indirect and contingency costs. The total capital cost is obtained from the total construction cost of the plant by including time related costs incurred during plant construction. The plant cost factors used to account for these time related effects were taken from reference [3.5] and are listed in table 3.1. The current dollar calculation uses the factors which include inflation/escalation as well as interest during construction. It is assumed that power plant escalation in excess of general inflation is 0 % (i.e. escalation and inflation rates are equal). For the constant dollar calculation, only interest during construction is included.

The levelized annual fixed charge rate converts the capital cost of the plant to an equivalent annual expenditure over the 30 year plant lifetime. In the current dollar calculation, both inflation and interest are included. Only interest is considered in the constant dollar mode. Also, return on capital, local property taxes, income taxes, book depreciation, investment tax credit and tax writeoff are reflected through the fixed charge rate. The financial parameters on which the fixed charge rates used in this study are based are listed in table 3.1.

The annual operating and maintenance costs include expenditures associated with plant operating personnel (salaries, benefits, administration, overtime, travel,

Table 3.1: Costing Factors for Determination of COE [3.5]

Parameter	Inflation Rate		
	0 %	6 %	10 %
Effective Cost of Money (%/yr)	4.2	9.0	12.2
Fixed Charge Rate (%/yr) (FCR)	8.3	14.4	19.1
Thirty Year Levelizing Factor (LN)	1.000	1.950	2.822
Four Year Construction Plant Cost Factor†	1.070	1.324	1.517
Six Year Construction Plant Cost Factor†	1.109	1.523	1.866
Eight Year Construction Plant Cost Factor†	1.148	1.751	2.296
Ten Year Construction Plant Cost Factor†	1.188	2.014	2.824

† factor applied to the total constructed cost of the plant to account for interest/inflation

retraining, cost of contract personnel, workman's compensation insurance); supplies, equipment and interim replacement parts; coolant makeup; process materials; licensing; liability insurance; miscellaneous costs such as equipment rental; and a decommissioning allowance.

The cost of fuel cycle materials that must be replaced during operation are included in the annual fuel costs. This includes the blanket/first wall replacement cost and the costs of other replaceable components that are part of the energy gain system such as the limiter, auxiliary heating equipment and the fuel components. Eighty percent of the miscellaneous scheduled replaceable items cost is included with the fuel costs, the remainder being evaluated as part of the miscellaneous plant equipment costs. Replacement of these components results from neutron damage and erosion. The fluence limit of the first wall and components of the auxiliary heating system which are bombarded by neutrons is set by the average neutron wall loading. The first wall also receives heat as electromagnetic radiation from the plasma. The remaining thermal power is handled by the targets and limiters. Their fluence limit is set by erosion damage from plasma bombardment. Erosion can be minimized by maintaining a cold plasma edge temperature. When erosion cannot be avoided, it must be localized to easily replaceable components such as targets and limiters. The lifetime of these components is set by the average thermal power (particles and radiation) on the surface.

The cost of waste disposal has also been assessed as part of the annual fuel costs, and has been evaluated as in reference [3.9]. To estimate these costs, it was assumed that 5 % of plant personnel work in waste handling and that the materials, labor and overhead costs for these activities are 5 % of those for operation and maintenance. Volumes of low activity, tritiated and first wall/blanket wastes were determined by scaling the estimates given by Cannon [3.10] with net electric power and tritium inventory. The cost for transport of these wastes to the disposal site was taken to be $ 635 per shipment (see reference [3.9] for details). Disposal costs were 241 $/m^3 for low level wastes qualified for shallow land burial and

473,400 $/m^3 for high level wastes requiring geologic disposal (from reference [3.9], updated to current dollars).

In this study, it was desirable to know the total costs associated with a given fuel cycle. The total fuel cycle cost would include the initial blanket, first wall, limiter and auxiliary heating system, in addition to the elements mentioned above in the discussion on the cost of fuel cycle materials. A separate calculation was performed to evaluate these costs together. For simplicity, no inflation was included so that the levelized annual repayment is simply the average yearly cost, in constant dollars. This recategorization facilitates the comparison of fuel cycle costs between alternate fusion fuels, and between fusion and fission.

The thirty year levelizing factor levelizes the annual costs which may be subject to inflation during the plant lifetime. An equivalent annual cost is obtained so that the present value of the time-varying cost is equal to the present value of the resulting levelized cost. The factors used to account for this are listed in table 3.1, and assume that costs change at the same rate as inflation (i.e. no additional escalation of costs). Note that this factor is equal to one for the constant dollar calculation (i.e. no inflation).

The cost of electricity has been evaluated for the DT, DD and DHe fuel cycles. A construction lead time of 6 years and inflation rate of 6 % have been employed. Reference [3.6] has recommended a plant capacity factor of 65 %. This value was adopted for the DT designs. Some improvement in the capacity factor is anticipated for the advanced fuel cycles resulting from the absence of the breeder, lower induced activity and reduced tritium inventory. The capacity factor has been evaluated as 69 % for the DD fuel cycle and 72 % for the DHe fuel cycle. These values were assessed based on estimates of scheduled and unscheduled maintenance times required for the same number of activities (see appendix C). Results of the economic analysis are given in tables 3.2, 3.3 and 3.4 and are discussed below.

3.2 Economics of DT Designs

3.2.1 The Effect of Varying Beta

For the DT designs, the COE has been determined for reactors having values of plasma beta of 5 %, 10 % and 20 %. The designs costed have an aspect ratio of 4, elongation of 2.5, plasma scrape of of 10 cm, employ an Fe1422 shield and have a thermal power of 4000 MW. Reactor parameters are listed in table 2.2 and the corresponding economic information is found in table 3.2.

The trend observed is that as beta is increased, the COE decreases. In going from beta of 5 % to 10 %, there is a 7 % drop in the cost of electricity, from 61.6 mills/kWh to 57.2 mills/kWh. Further increasing beta to 20 % from 10 % results in no additional improvement in the COE. This trend can be explained by examining the changes to the reactor parameters and how these changes affect the cost accounts contributing to the COE. As beta is increased, the reactor dimensions are reduced for a fixed power output. Hence, any costs scaling with the volume of material used will decrease as beta is increased. These costs include: structures and site facilities ($\sim$ fusion island volume), first wall/blanket ($\sim$ first wall/blanket volume) shield ($\sim$ shield volume), structure and support ($\sim$ toroidal field coil volume + plasma volume), particle removal and control ($\sim$ major radius + minor radius), magnet systems ($\sim$ toroidal field coil volume), and vacuum system ($\sim$ fusion island volume). These costs comprise the bulk of the direct costs. The cost of electricity for DT reactors appears to level off as beta is increased beyond 10 %. This occurs as a result of the increasing importance of other factors in the cost scaling as beta is increased. Poloidal field coil costs scale with plasma shaping, which is increased in order to achieve higher beta. Plasma shaping also strongly affects power conditioning costs (for conversion/regulation of ac line power, distribution of power to magnets, protection of magnets and supply of power) for the EF and CF coils. Some of the replaceable items costs scale with wall loading, which increases with beta, as the reactor size and hence first

Table 3.2: Economics for DT Designs

Parameter	Low Beta (5 %)	Medium Beta (10%)	High Beta (20 %)
Direct Costs (1986 M$)	2385	2165	2159
Land & Land Rights	5.0	5.0	5.0
Structures & Site Facilities	407	346	307
Reactor Plant Equipment	1346	1182	1210
Blanket & First Wall	31	24	19
Shielding	216	168	135
Structure & Support	79	48	31
Particle Removal/Control	3.5	3.0	2.6
Magnet Systems	247	169	162
Power Injection System	153	131	110
Vacuum System	11.2	8.6	7.0
Power Conditioning Systems	191	221	336
Heat Transport System	179	174	172
Fuel Handling & Storage	143	143	143
Instrumentation & Control	30	30	30
Maintenance Equipment	63	63	63
Turbine Plant Equipment	399	399	399
Electric Plant Equipment	110	110	110
Misc. Plant Equipment	64	69	73
Heat Rejection System	54	54	54
Indirect Costs (1986 M$)	996	910	909
Contingency (1986 M$)	507	461	460

Parameter	Low Beta (5 %)	Medium Beta (10%)	High Beta (20 %)
Total Constructed Cost (1986 M$)	3889	3536	3528
Total Capital Cost (constant 1986 M$)	4313	3922	3912
Total Capital Cost (current 1992 M$)	5923	5386	5373
Annual Operation & Maintenance (1986 M$/yr)	57.9	57.7	57.5
Fuel Cycle (1986 M$/yr)	20.2	21.5	21.9
COE (mills (1992)/kWh)	142	132	132
COE (mills (1986)/kWh)	61.6	57.2	57.2
Relevant Design Information:			
Plasma Volume (m^3)	1375	854	565
First Wall/Blanket Volume (m^3)	754	574	458
Shield Volume (m^3)	1800	1399	1129
TF Coil Volume (m^3)	250	111	51
Fusion Island Volume (m^3)	4699	3225	2378
Major Radius (m)	7.64	6.51	5.68
Minor Radius (m)	1.91	1.63	1.42
Toroidal Field (T)	4.68	3.73	2.92
Plasma Current (MA)	18.4	12.5	8.6
Triangularity	0	0.3	1.2
Plasma Density (m^{-3})	1.70×10^{20}	2.16×10^{20}	2.65×10^{20}
Neutron Wall Loading (MW/m^2)	3.04	4.16	5.41
Thermal Wall Loading (MW/m^2)	0.76	1.04	1.35

wall area, decrease. These considerations play an increasing role at higher values of beta, driving the COE up and countering the reduced capital costs from the smaller sized reactor. Hence, for the DT fuel cycle, there is not a large economic incentive for achieving a more than moderately high value of plasma beta (i.e. $\sim$ 10 %).

It must be stressed, however, that this conclusion assumes that first stability scaling laws can be extrapolated to high values of beta (i.e. an estimate of the degree of triangularity required to obtain a given value of beta, knowing the aspect ratio, elongation and safety factor, was obtained using first stability scaling laws regardless of the value of beta). Theoretical studies of beta-saturation mechanisms associated with resistive ballooning modes and internal kink modes have lead to exploration of possible approaches to the second stability region for high beta tokamak configurations [3.11]. One possible route to this regime assumes high values of the on axis safety factor coincident with lower plasma current and indentation. Studies are currently underway to examine the feasibility of this scheme [3.12]. Relaxation of plasma indentation and a reduction in plasma current will lead to reduced capital costs because of a smaller central solenoid and fewer plasma shaping magnets. This consideration may improve the economic position of the high beta design. However, because it is not clear that the second stability regime can be achieved, this approach was not examined here. The high beta designs were based on extrapolation of first stability physics.

As part of the economic analysis, the total costs associated with the fuel cycle were evaluated. These costs include those components which are part of the energy gain system such as initial and replacement costs for the first wall/blanket, the limiter and 25 % of the auxiliary heating components (vacuum windows, launching structures, klystrons, gyrotrons, etc., which suffer neutron damage), as well as 80 % of miscellaneous scheduled replaceable items, fuel costs and waste handling costs. For the three reactors assessed, the fuel cycle costs were least for beta of 5 % (20.2 M$/yr), and greatest for beta of 20 % (21.9 M$/yr). The slight increase in fuel cycle costs at higher beta can be explained if the factors which contribute to the

total fuel cycle costs are examined. Initial first wall/blanket, limiter and auxiliary heating components costs scale with reactor size, and hence decrease with increasing beta (see table 3.5). However, replacement frequency and therefore replacement costs for these components also depend on wall loading, which increases with beta. At high beta, total replacement costs represent a larger fraction of the total fuel cycle costs than the initial costs (49 % at 20 % beta and 37 % at 5 % beta) due to the more frequent replacement of components (see table 3.5). Other miscellaneous replaceable items costs also scale with wall loading, thus tending to increase the fuel cycle costs at higher beta. Another difference is in the area of waste handling. Despite the smaller volume of the reactor, the waste handling costs are greater at higher beta. This is a result of the greater number of blanket/first wall changeouts which take place during the lifetime of the higher beta reactor. However, for the DT designs, the overall impact of this consideration is not large and the total fuel cycle cost is nearly the same for all values of betas.

The cost model was used to examine the dependence of the COE on several parameters. The designs described in chapter 2, for beta ranging from 3 % to 20 %, with HT-9 as the shielding material, have been costed. Economic information pertaining to these designs can be found in appendix B. It was found that the use of HT-9 as the shield material increased the COE compared to that when Fe1422 is used. An adjustment to the COE can be made (see section 3.2.3) to account for this difference, and give the expected COE for the design using Fe1422 shielding. The Fe1422 adjusted COE's have been used in the parametric plots. The same trends should be exhibited regardless of the shielding material used.

In figure 3.1, the COE is seen to decrease with beta, illustrating the importance, in terms of cost, of obtaining a value of beta higher than what is currently achievable ($\sim$ 5 %). Beyond a beta of 10 %, however, the cost decrease is minimal, coming at the expense of increased wall loading (see figure 3.2). This will lead to more frequent replacement of components. However, the volume of material required per changeout decreases as beta increases, due to the decreasing

FIGURE 3.1:
COST OF ELECTRICITY VS BETA FOR THE DT FUEL CYCLE

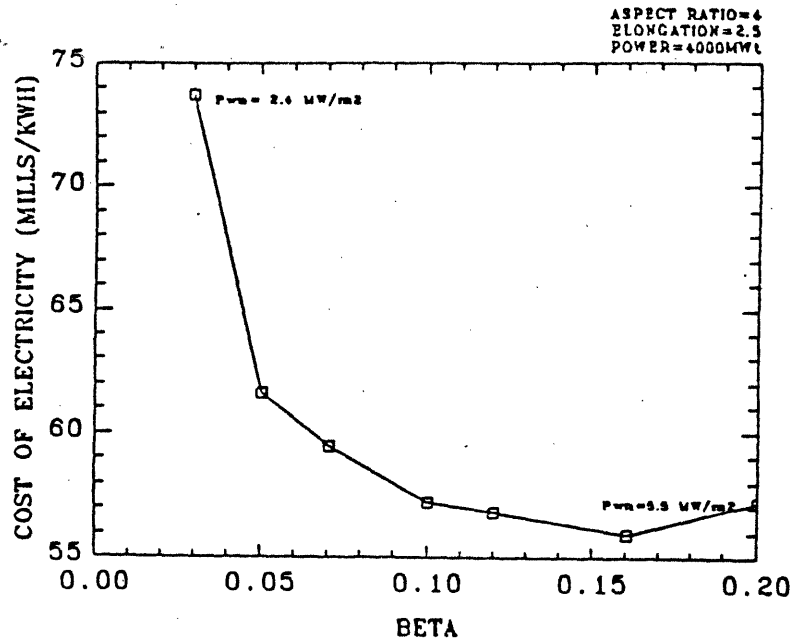

FIGURE 3.2:
COST OF ELECTRICITY VS NEUTRON WALL LOADING
FOR THE DT FUEL CYCLE

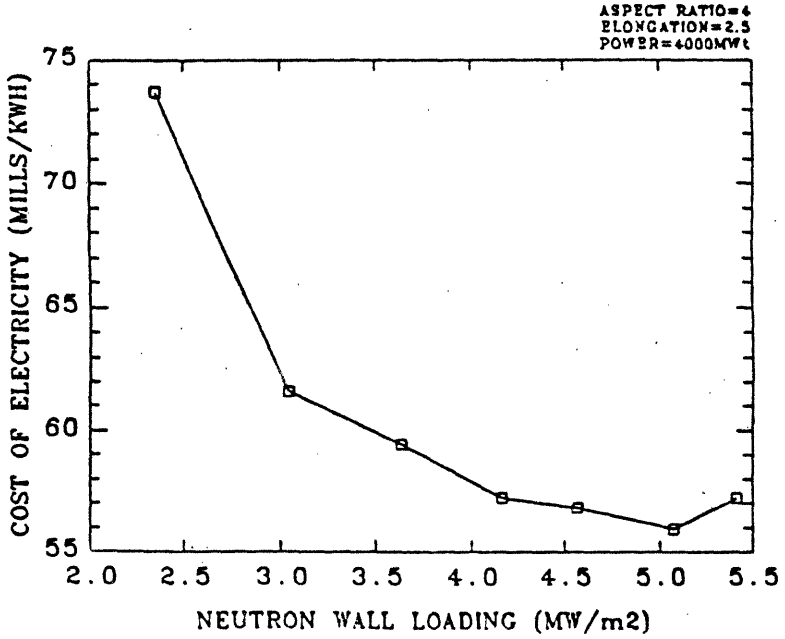

reactor size. These competing effects contribute to the appearance of a slight minimum in the COE at a beta of 16 %, but the improvement of the COE at this minimum over that at 10 % beta is not large. The main advantage of high beta operation is that lower toroidal fields may be used for the same size device, thereby lowering the COE. This effect is illustrated in figure 3.3. The highest on axis magnetic field indicated (5.5 T) corresponds to a beta of 3 % and results in the highest COE. At a beta of 20 %, the toroidal field on axis can be reduced to 3.2 T, leading to a lower COE. The toroidal field costs are somewhat reduced but stronger plasma shaping is required to achieve higher beta. This increases the poloidal field and power conditioning costs. These considerations also contribute to the slight occurrence of the minimum at 16 %. The effect of reactor size on the cost of electricity is indicated in figure 3.4. The COE is plotted against minor radius for the series of reactors having values of beta ranging from 3 % to 20 %. It is evident that larger sized reactors produce more expensive electricity.

Fission costs are expected to rise from the current level of $\sim$ 40 mills/kWh to $\sim$ 50 mills/kWh or higher in the future [3.6, 3.13]. Figure 3.5 indicates that the fusion island mass must be in the area of 10,000 tonne for a 4000 MWt plant in order to be competitive with fission. From this figure which plots the COE versus the fusion island mass for the series of reactors discussed above, it can be seen that the fusion island is responsible for a small fraction of the COE. The rest of the COE is comprised of the cost of auxiliary systems, power supplies, turbine plant, electric plant, operation and maintenance costs, indirect costs and contingency costs.

Although it is the neutron and thermal fluences which determine the total number of first wall and blanket components, limiters and other targets cycled through the plant during its lifetime, the mass and volume of these components and hence, their cost, would be greater for a more massive fusion island. Since many of the cost components scale with volume, it is not unexpected that a larger fusion island volume would correspond to a higher COE, as is exhibited in figure 3.6. In order for the COE to fall in the competitive range, the fusion island volume

FIGURE 3.3:
COST OF ELECTRICITY VS TOROIDAL FIELD
FOR THE DT FUEL CYCLE

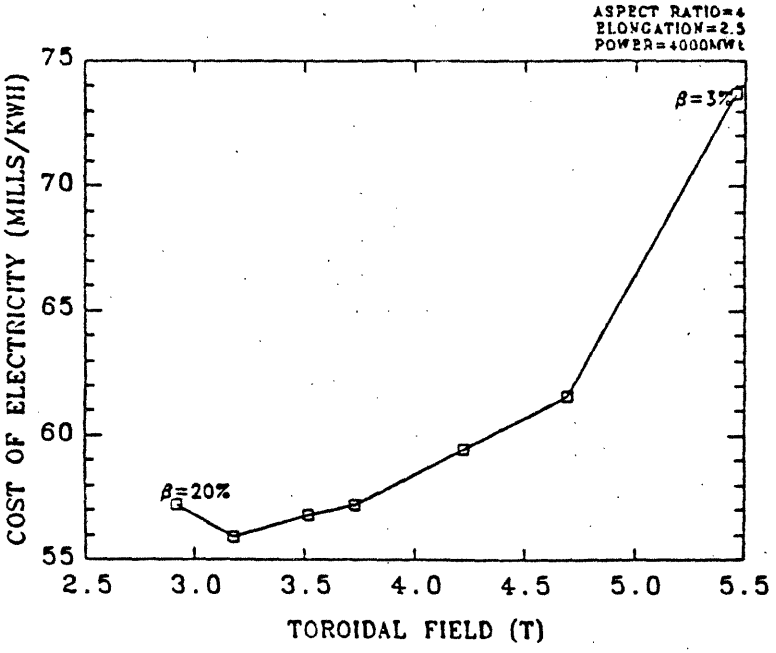

FIGURE 3.4:
COST OF ELECTRICITY VS MINOR RADIUS FOR THE DT FUEL CYCLE

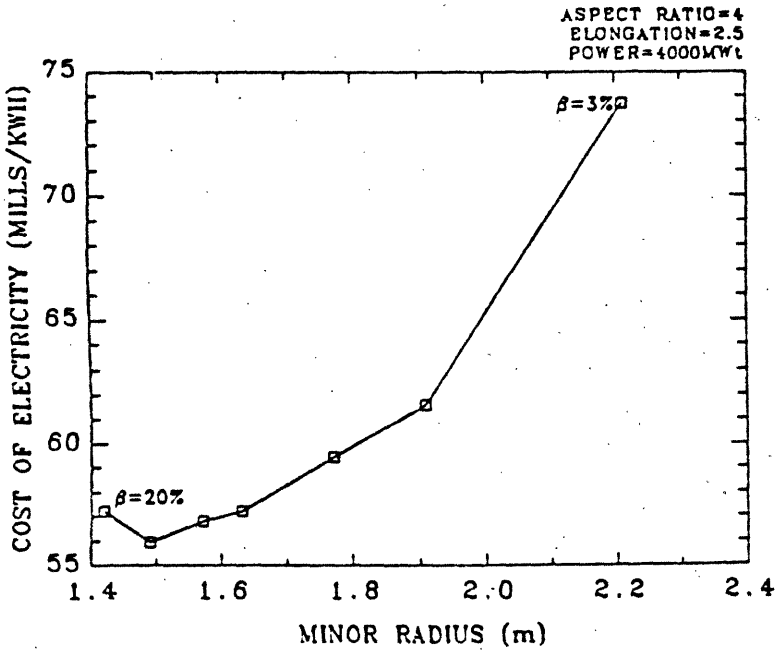

FIGURE 3.5: COST OF ELECTRICITY VS MASS OF FUSION ISLAND
FOR THE DT FUEL CYCLE

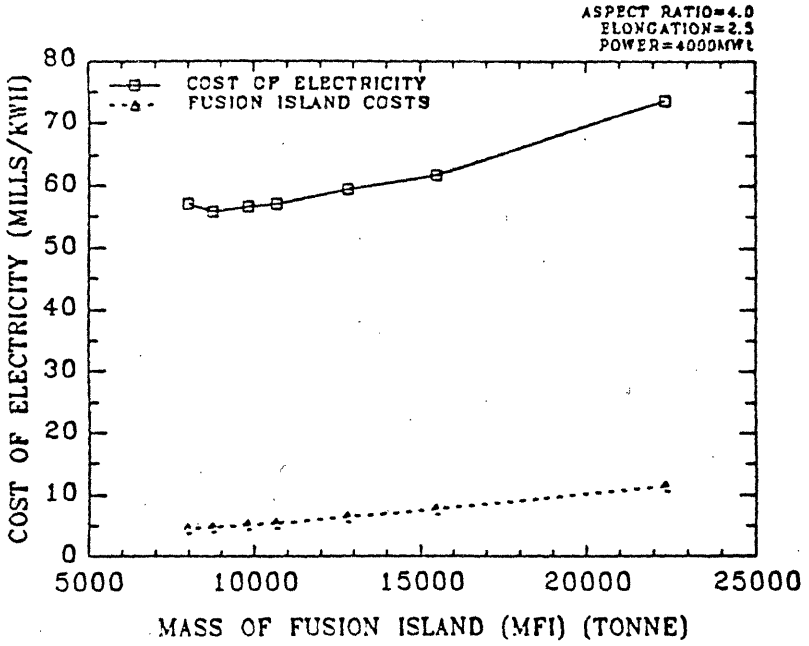

FIGURE 3.6:
COST OF ELECTRICITY VS VOLUME OF FUSION ISLAND
FOR THE DT FUEL CYCLE

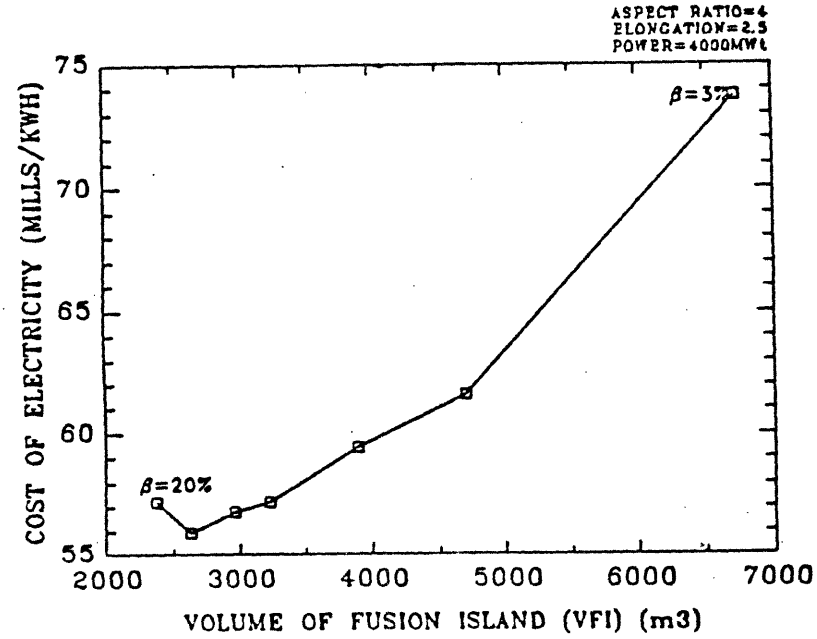

must be on the order of 3000 m^3.

The power density of the fusion island (P_T/V_{FI}) can be used to characterize fusion reactors. The COE is plotted against this parameter in figure 3.7 and is seen to decrease as the fusion island power density (i.e. beta) increases. The power densities corresponding to the DT reactors of this study are comparable to those for several gas-cooled fission reactors (0.8 MW/m^3 - 1.2 MW/m^3 inside the pressure vessel [3.14]). The values given for the power density inside the primary pressure vessel are somewhat higher for BWRs ($\sim 4MW/m^3$) and PWRs ($\sim 10MW/m^3$). As is indicated in the figure, there is little cost advantage in going to power densities larger than about 1.2 MW/m^3. This is in agreement with Sheffield's findings [3.4].

Figure 3.8 shows the variation of COE with net electric power per unit mass of the fusion island (P_e/M_{FI}). Little economic benefit is gained beyond 0.1 MWe/tonne (100 kWe/tonne). This also agrees with the conclusions of Sheffield [3.4]. For the 10 % beta design, the fusion island power density is 1.22 MW/m^3 and the net electric power per unit mass is 0.114 MWe/tonne. This suggests that pursuing a beta greater than 10 % for DT designs is not worthwhile.

3.2.2 The Effects of Varying Aspect Ratio and Elongation

The COE was determined for designs having a fixed beta of 10 %, an elongation of 2.5 and an aspect ratio ranging from 3 to 7. In figure 3.9, the COE is seen to be a decreasing function of aspect ratio. Beyond an aspect ratio of 4 or 5, little further improvement is seen. Thus, the apriori choice of an aspect ratio of 4 for those designs having this parameter held fixed (i.e. beta and elongation variations) has not resulted in an economic disadvantage. Sheffield [3.4] found that over a range of values of beta, the minimum cost lies in the range of $\frac{R}{a}$ between 4 and 8. From the family of curves that he presents, the minimum cost occurs at an aspect ratio which increases as beta increases. This suggests that a larger aspect ratio is more

FIGURE 3.7:
COST OF ELECTRICITY VS POWER DENSITY OF FUSION ISLAND
FOR THE DT FUEL CYCLE

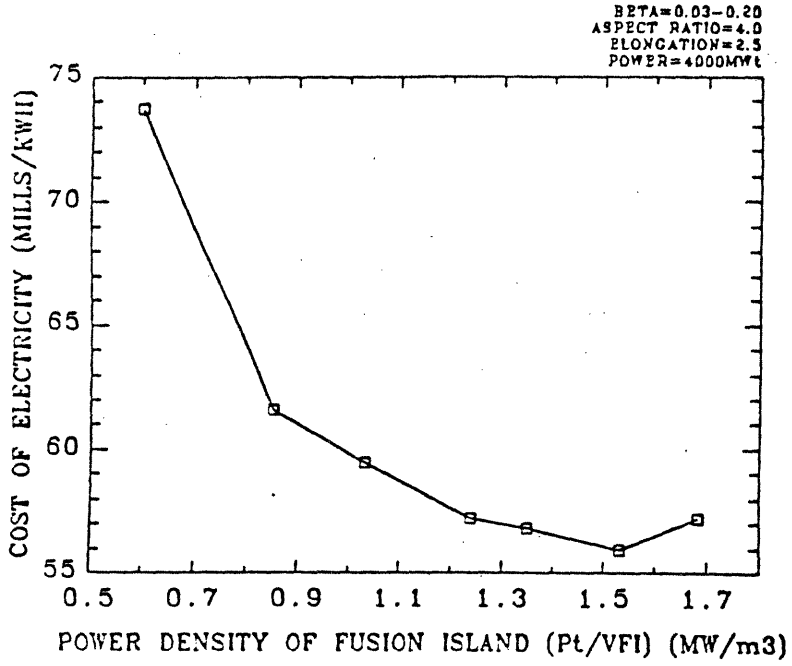

FIGURE 3.8:
COST OF ELECTRICITY VS MASS POWER DENSITY
FOR THE DT FUEL CYCLE

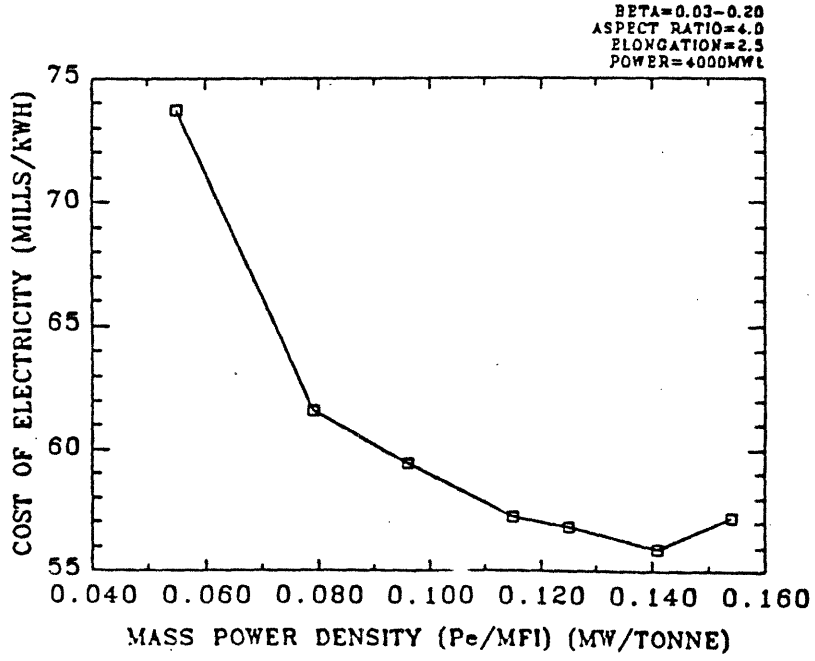

FIGURE 3.9:
COST OF ELECTRICITY VS ASPECT RATIO FOR THE DT FUEL CYCLE

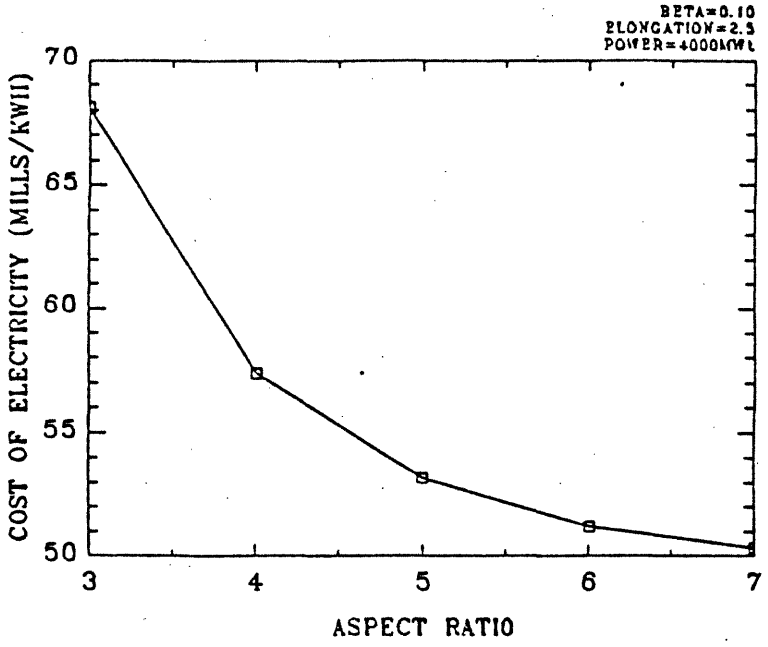

FIGURE 3.10:
DIRECT CAPITAL COST VS MASS PER UNIT THERMAL POWER
FOR THE DT FUEL CYCLE

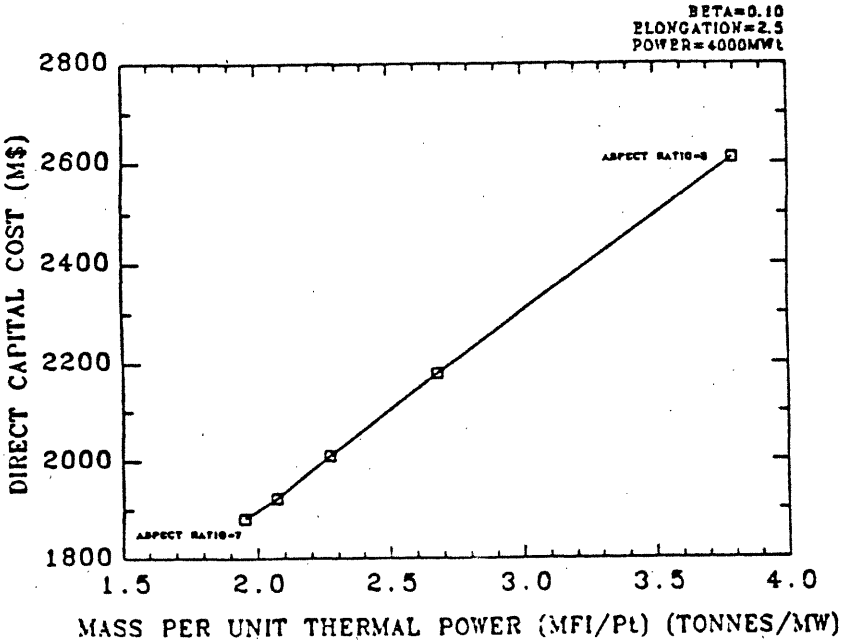

desirable at higher beta (which is in agreement with physics needs) and a lower aspect ratio is more desirable at low beta.

In figure 3.10, the direct plant cost for the series of designs having aspect ratios ranging from 3 to 7 is plotted against the mass per unit thermal power (M_{FI}/P_T), or mass utilization factor. A linear relationship is observed, given by:

$$C_{D0} = 1100 + 400\frac{M_{FI}}{P_T} \quad M\$ \tag{3.4}$$

This trend was also seen in an earlier study [3.15], where several reference fusion reactors were compared. Miley [3.16] gives a similar scaling of the direct costs with the mass utilization factor. The work here, however, indicates a stronger dependence on the mass utilization factor than the other two studies. It is evident that designers should strive to obtain improved mass utilization.

The effect of varying plasma elongation on the COE over the range of interest is shown in figure 3.11. A minimum in cost is observed for an elongation of 2.0. Decreasing the ellipticity below 2.0 requires greater triangularity to give the desired beta (see table 2.1) resulting in increased poloidal field coil and power conditioning costs. Also, wall loading is higher at low elongation due to the smaller reactor size (see table A.4), leading to more frequent replacement and greater costs. At higher elongation, the reactor size increases and costs scaling with volume increase. The wall loading and replacement frequency are lower, but this is offset by the larger volume of material to be replaced per changeout. An optimum is achieved for the DT design (with 10 % beta and an aspect ratio of 4) with an elongation of 2.0, where the combined impact of these two effects is minimized. The apriori choice of 2.5 results in a COE less than 2 mills/kWh higher than this optimum. As will be seen, this does not strongly affect the economic position of the DT fuel cycle relative to the advanced fuels.

FIGURE 3.11:
COST OF ELECTRICITY VS PLASMA ELONGATION FOR THE DT FUEL CYCLE

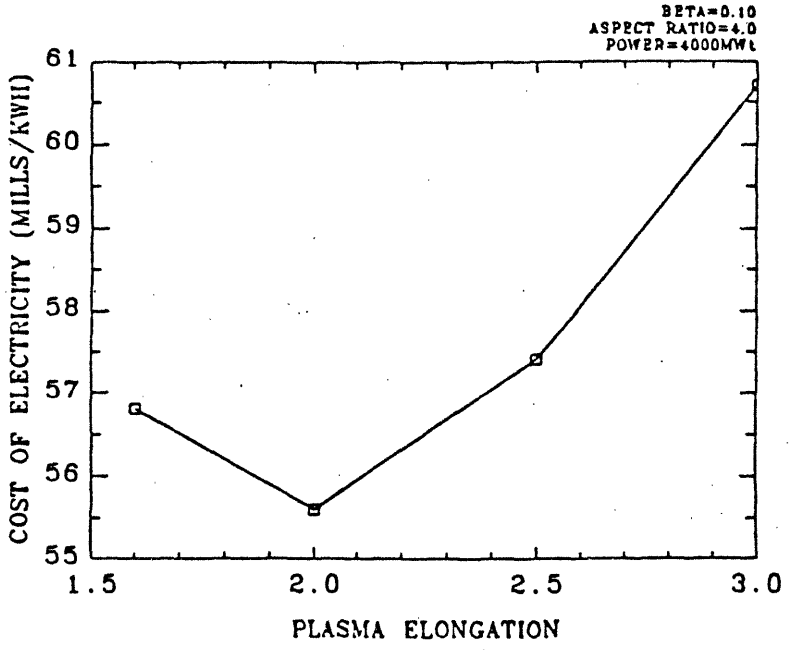

FIGURE 3.12:
COST OF ELECTRICITY VS CAPACITY FACTOR FOR THE DT FUEL CYCLE

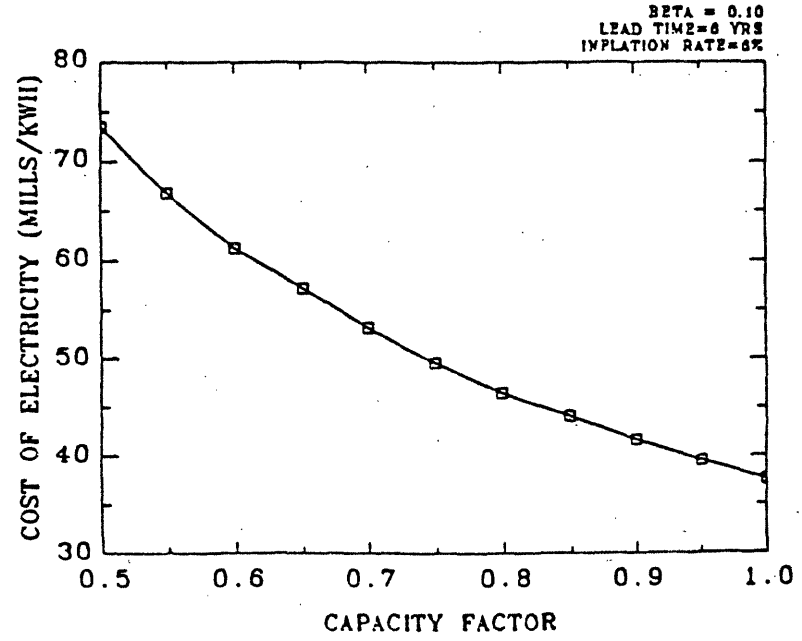

3.2.3 Other Effects

The manner in which certain assumptions regarding input to the economics code affect the COE are displayed in figures 3.12 through 3.16. The analyses were carried out for the DT reactor with 10 % beta and an Fe1422 shield. The plant capacity factor has an important influence in determining the COE. A 20 % change in capacity factor from 60 to 80 % leads to a drop of $\sim$ 14 mills/kWh in the COE. The value assumed for the DT fuel cycle was 65 %. This value does place the fusion reactors in the competitive range. For high power densities, the capacity factor may be reduced. Because of the higher wall loadings, blanket changeouts may no longer be performed during scheduled outages and additional downtime may be required. Furthermore, the reliability of plant components may decrease at higher power densities, leading to more unscheduled outages. This possibility was not taken into account and the capacity factor for all DT designs was fixed at 65 %.

Construction lead time also affects the COE, as indicated in figure 3.13. Longer plant construction times result in greater interest charges and also lead to a greater expense for supporting construction personnel. A one year reduction in construction time can lead to a 5 % improvement in the COE. A six year construction time was used for all designs.

The effect of varying the neutron fluence limit on the COE is shown in figure 3.14. There is a relatively rapid decrease in the COE up to a value of F_{wn} of about 15 MW $\cdot$ yr/m^2. At values of F_{wn} lower than this, the blanket/first wall lifetime would become quite short. This would eventually impact the plant capacity factor and lead to an even higher COE (65 % capacity factor was assumed here). The effect of the neutron fluence limit is not large as the COE decreases by less than 4 mills/kWh ($\sim$ 6 %) as the fluence limit varies from 10 to 30 MW$\cdot$yrs/m^2. Roughly half of this decrease in cost can be achieved if the fluence limit is increased from

FIGURE 3.13:
COST OF ELECTRICITY VS CONSTRUCTION TIME FOR THE DT FUEL CYCLE

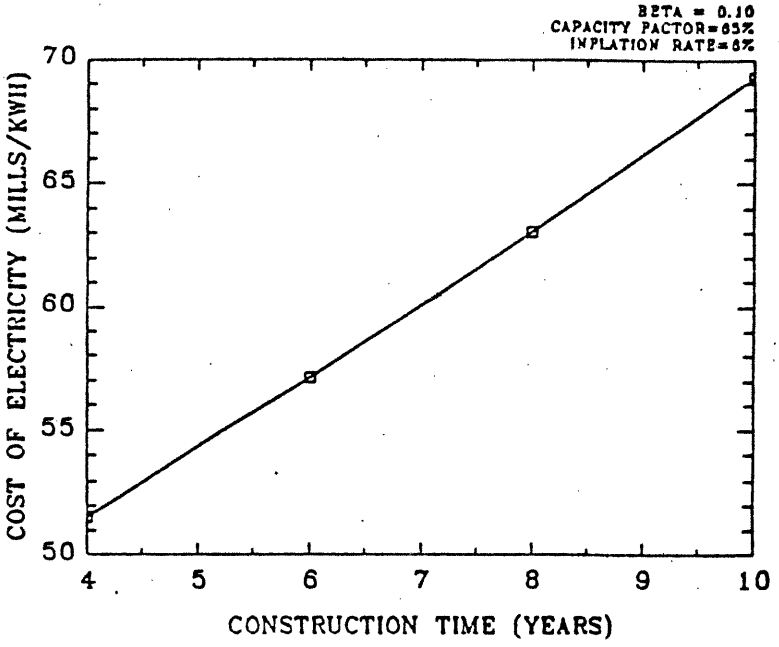

FIGURE 3.14:
COST OF ELECTRICITY VS LIFETIME NEUTRON FLUENCE LIMIT
FOR THE DT FUEL CYCLE

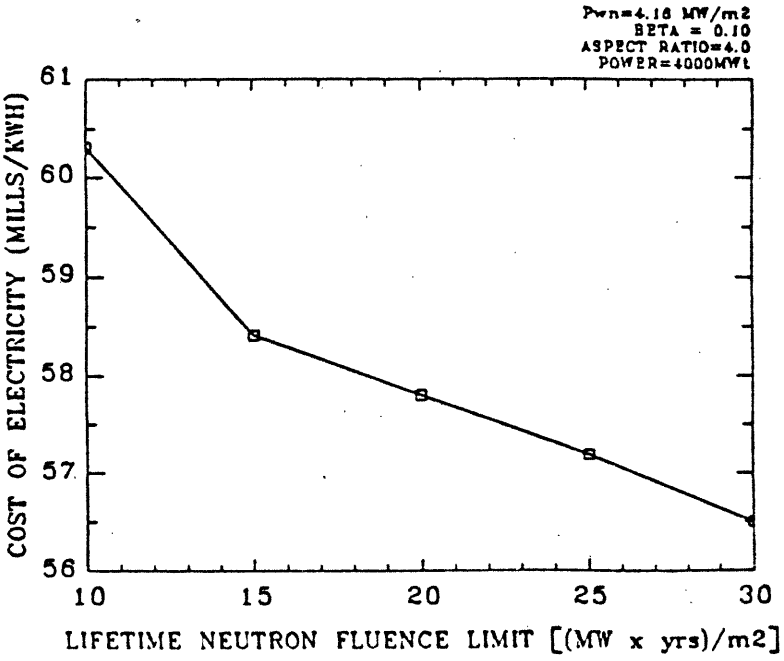

10 to 15 MW · yrs/m^2. Materials fluence limits much beyond this do not appear to have a major influence in in lowering the cost of electricity. This does not agree with Sheffield's work which indicates the need to achieve a neutron fluence limit above 20 MW · yrs/m^2.

Figure 3.15 plots the COE against blanket lifetime. Neutron wall loading was varied for a fixed lifetime neutron fluence of 25 MW · yr/m^2. This was the neutron fluence limit adopted in the Generomak study [3.17]. As the blanket lifetime lengthens (i.e. wall loading decreases), fewer changeouts are needed. Consequently, there is a reduction in the COE. A similar trend would be observed for the COE versus blanket lifetime plot if the wall loading was held constant and the allowable lifetime fluence was varied. A greater lifetime fluence would lead to longer blanket life and fewer replacements, resulting in an improved capacity factor, lower replacement component costs, and a lower COE. Blanket elements are best replaced during the scheduled maintenance period for the turbines, which occurs every two years, as discussed in the STARFIRE report [3.7]. If the blanket lifetime was six years, one-third of it could be replaced every two years during the scheduled outage. In this way, no additional downtime would be needed for replacement. Also, since only one-third of the blanket would be nearing the end of its lifetime every two years, there may be a reduction in blanket failures if this scheme is adopted (as opposed to replacing the entire blanket every six years).

Figure 3.16 indicates the effect of wall loading on the COE for two values of lifetime neutron fluence. For a lifetime fluence of 5 MW·yr/m^2, the rise of COE with wall loading is quite steep. This reflects the shorter blanket lifetime and increased replacement costs. With a lifetime fluence of 20 MW·yr/m^2, the impact of increased wall loading is not as strongly felt. Increasing the wall loading from 2 MW/m^2 to 10 MW/m^2 results in a 12 % increase in the COE. This compares to a 37 % increase with a lifetime fluence of 5 MW · yr/m^2. Operating at a wall loading of 5 MW/m^2 with a lifetime fluence of 20 MW · yr/m^2 appears to place fusion in the competitive range for the COE. Furthermore, this neutron loading is within the range of power

FIGURE 3.15:
COST OF ELECTRICITY VS BLANKET/FIRST WALL LIFETIME
FOR THE DT FUEL CYCLE

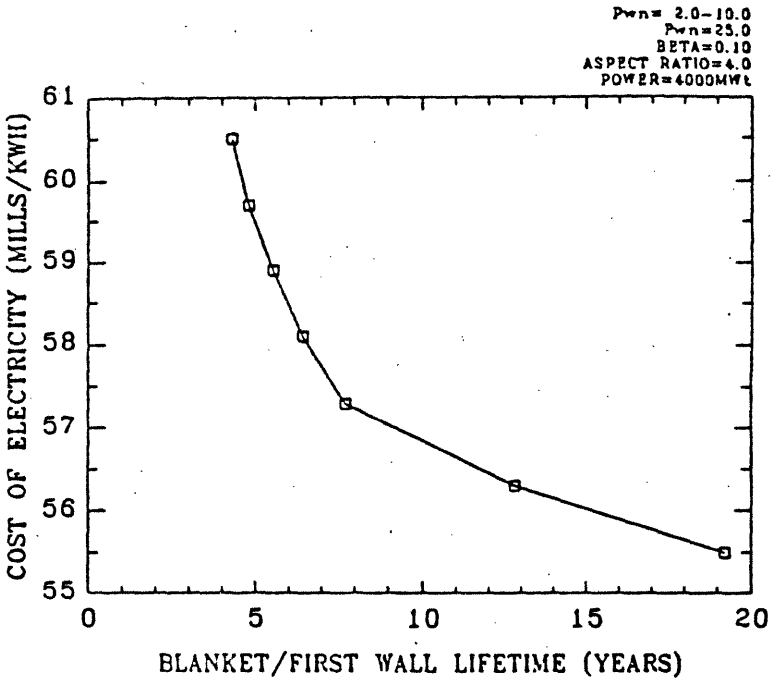

FIGURE 3.16:
COST OF ELECTRICITY VS NEUTRON WALL LOADING
FOR THE DT FUEL CYCLE

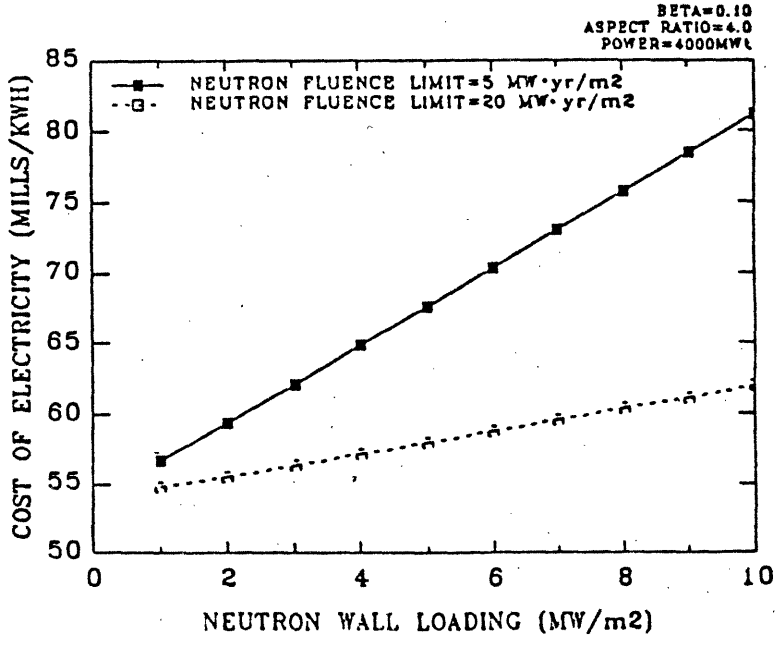

density that can be inherently safe [3.18, 3.19].

The sensitivity of the COE to the unit costs of particular items may be of importance. In this study, two shielding materials have been considered. The standard shielding material, Fe1422, is relatively inexpensive but may not perform as well as an HT-9 shield from a safety point of view ($\sim$ order of magnitude decrease in decay heat with HT-9 [3.20]). The shielding capabilities of these materials are nearly identical (compare shielding thicknesses in tables 2.2 and A.2). The cost for HT-9 shielding is 50 \$/kg, compared to 20 \$/kg for Fe1422. Figure 3.17 indicates that a linear relationship exists between the COE and the shielding cost, given by:

$$\mathrm{COE} = 0.166 \cdot \mathrm{UC_{SHLD}} + 53.8 \ \ (\mathrm{mills/kWh}) \tag{3.5}$$

where

$\mathrm{UC_{SHLD}}$ = unit cost of shielding material (\$/kg)

This relationship was obtained for a DT design with a beta of 10 %, an elongation of 2.5, an aspect ratio of 4 and an Fe1422 shield. The cost of the Fe1422 was varied from 10 \$/kg to 100 \$/kg. At 50 \$/kg, the COE found using the Fe1422 design was within 0.5 % of the COE obtained for the HT-9 design. There is an almost negligible difference in the COE for these designs assuming the same unit cost for the shielding (although the volume of shielding material is not identical and design parameters are slightly different). A difference of 5 mills/kWh is seen when the Fe1422 shielding cost changes from 20 \$/kg to 50 \$/kg. Since the relationship of the COE to shielding cost is linear, approximate costs for designs with Fe1422 shields can be obtained from those for HT-9 shields by simply subtracting 5 mills/kWh. The difference in the COE for these two shielding materials is significant. This indicates the importance of selecting low cost materials for reactor components where ever possible.

FIGURE 3.17:
COST OF ELECTRICITY VS COST OF SHIELDING
FOR THE DT FUEL CYCLE

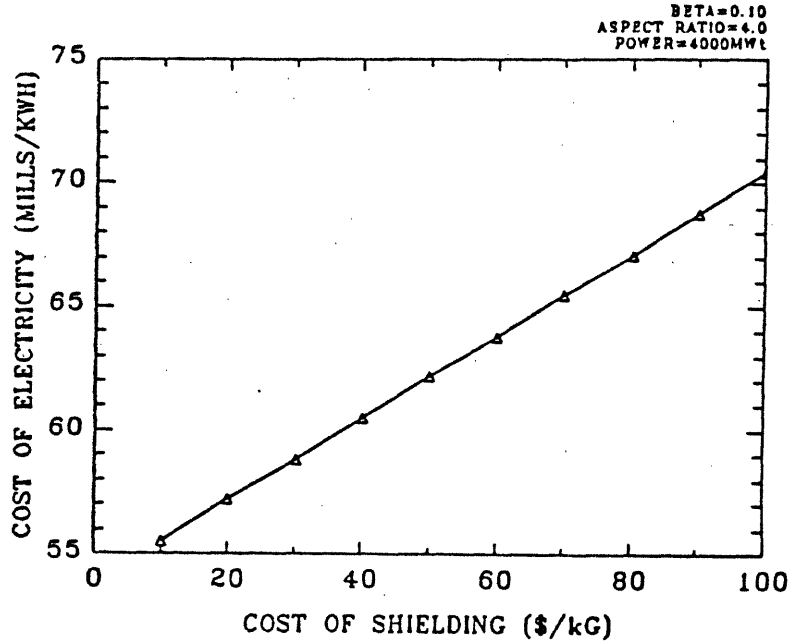

FIGURE 3.18:
COST OF ELECTRICITY VS COST OF DEUTERIUM
FOR THE DT FUEL CYCLE

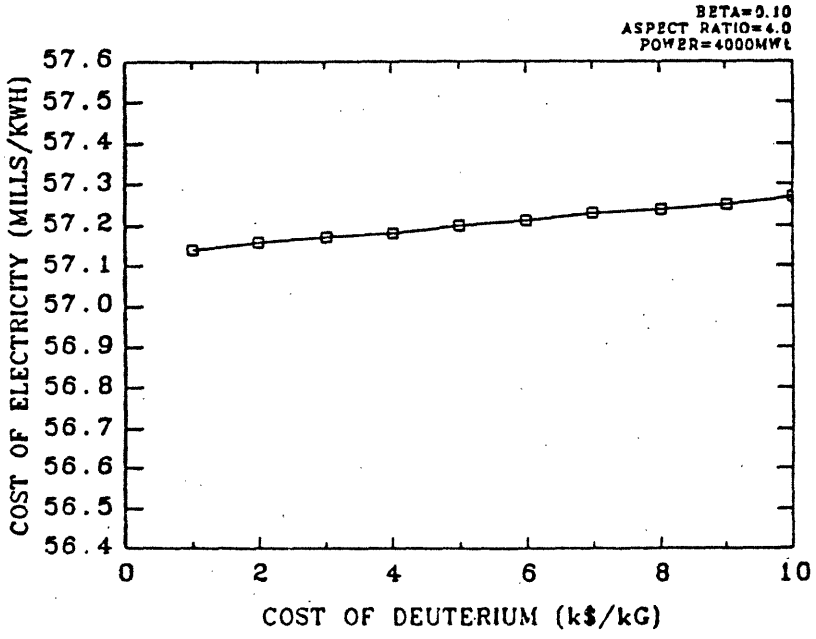

The effect of fuel costs on the COE for DT reactors is shown in figure 3.18. Since tritium is produced on site in the breeding blanket, its cost is actually reflected in the cost of the breeder. Hence, deuterium is the only fueling component which must be purchased for the DT reactors. Evidently, the effect of its cost on the COE is almost negligible (note magnification of scale). Although the COE is seen to rise with the cost of deuterium, this increase is only 0.15 mills/kWh as the price of deuterium rises from 1 k$/kg to 10 k$/kg.

3.3 Economics of DD Designs

3.3.1 The Effect of Varying Beta

For the DD reactors, a range of values for beta was also scanned. Economic information is given in table 3.3. A decrease in the cost of electricity was observed as beta was increased. An improvement of 25 % was seen with the HT-9 designs in going from beta of 5 % to 10 %, from 126 mills/kWh to 94 mills/kWh. Further increasing beta to 20 % resulted in an additional reduction of 10 % in the cost of electricity (to 85 mills/kWh). Clearly, higher values of beta are more advantageous for DD reactors than for DT reactors. (As noted in section 3.2.1, the attainment of the second stability region using high q and lower current may lead to a further improvement in the economics of the high beta design.) The major factor causing this is the great reduction in fusion island volume for DD reactors ($\sim$ 76 %) when beta is increased from 5 % to 20 %. The reduction in fusion island volume is not as large ($\sim$ 49 %) for the DT designs. This consideration is felt more strongly than the increase in wall loading at higher betas for two reasons. Firstly, the cost elements which scale with volume are major contributors to the total cost. Secondly, since volume scales with the cube of the linear dimensions of the reactor and wall loading scales with the square of the linear dimensions, a reduction in reactor size will more strongly impact costs proportional to volume (resulting in a decrease) than costs associated with wall loading (resulting in a increase). Furthermore, the wall

Table 3.3: Economics for DD Designs

Parameter	Low Beta	Medium Beta (10 %)		High Beta
	(5 %)	HT-9	RAF	(20 %)
Direct Costs (1986 M$)	5752	3982	3654	3501
Land & Land Rights	5.0	5.0	5.0	5.0
Structures & Site Facilities	849	557	552	406
Reactor Plant Equipment	4275	2793	2470	2459
Blanket & First Wall	759	461	172	296
Shielding	319	189	207	123
Structure & Support	454	183	178	83
Particle Removal/Control	5.9	4.3	4.3	3.3
Magnet Systems	1678	919	890	670
Power Injection System	69	56	54	49
Vacuum System	54	31	31	20
Power Conditioning Systems	543	603	591	889
Heat Transport System	255	208	206	187
Fuel Handling & Storage	46	46	46	46
Instrumentation & Control	30	30	30	30
Maintenance Equipment	63	63	63	63
Turbine Plant Equipment	404	404	403	404
Electric Plant Equipment	110	110	110	110
Misc. Plant Equipment	55	59	59	64
Heat Rejection System	54	54	54	54
Indirect Costs (1986 M$)	2317	1624	1495	1437
Contingency (1986 M$)	1210	841	772	741

Parameter	Low Beta (5 %)	Medium Beta (10 %) HT-9	Medium Beta (10 %) RAF	High Beta (20 %)
Total Constructed Cost (1986 M$)	9279	6447	5920	5679
Total Capital Cost (constant 1986 M$)	10291	7150	6566	6298
Total Capital Cost (current 1992 M$)	14132	9819	9018	8649
Annual Operation & Maintenance (1986 M$/yr)	52.5	52.4	52.2	52.1
Fuel Cycle (1986 M$/yr)	70.9	82.7	45.3	80.4
COE (mills (1992)/kWh)	296	218	199	197
COE (mills (1986)/kWh)	126	94	85	85
Relevant Design Information:				
Plasma Volume (m^3)	6781	2661	2595	1190
First Wall/Blanket Volume (m^3)	2440	1481	1365	951
Shield Volume (m^3)	2692	1588	1745	1031
TF Coil Volume (m^3)	3001	1322	1271	614
Fusion Island Volume (m^3)	19157	8920	8779	4671
Major Radius (m)	13.01	9.52	9.44	7.28
Minor Radius (m)	3.25	2.38	2.36	1.82
Toroidal Field (T)	8.0	7.2	7.1	6.2
Plasma Current (MA)	53.8	35.2	34.5	23.2
Triangularity	0	0.3	0.3	1.2
Plasma Density (m^{-3})	1.80×10^{20}	2.88×10^{20}	2.88×10^{20}	4.31×10^{20}
Neutron Wall Loading (MW/m^2)	0.63	1.17	1.11	1.98
Thermal Wall Loading (MW/m^2)	0.42	0.78	0.74	1.32

loadings associated with the DD fuel cycle are lower, resulting in longer lifetimes. This implies that the decrease in wall area (i.e. reactor size) would have to be larger before component lifetimes and the COE were affected.

Total fuel cycle costs for the HT-9 DD designs are seen to increase as beta is increased from 5 to 10 %, and then to decrease again as beta is increased to 20 %. For a beta of 5 %, fuel cycle costs are 70.9 M$/yr. This increases to 82.7 M$/yr (17 % increase) at beta of 10 %, and then decreases again to 80.4 M$/yr at beta of 20 %. It appears that total initial fuel cycle costs dominate for the DD reactors (see table 3.5), especially at lower beta. The more frequent blanket changeouts at higher beta result in somewhat larger replacement component and waste handling costs. However, the larger volume of material involved in reactor components drives materials and waste handling costs up for the 10 % beta case, although only one blanket changeout is required during its lifetime (compared to two changeouts for the 20 % beta case). Decommissioning costs are assumed to scale with material volume and wall loading. The combination of these factors leads to a slight decrease in the decommissioning estimate as beta increases (see table 3.6). Comparing to the DT designs, fuel cycle costs for the HT-9 DD designs are significantly larger, being 71 M$/yr at best, for a 10 % beta, compared to 21 M$/yr for the DT cycle. The larger volume of material required for components is responsible for the greater cost associated with the DD fuel cycle.

The cost of electricity for the DD fuel cycle is greater than the DT fuel cycle. The lowest COE achieved was 57.2 mills/kWh for DT and 85.0 mills/kWh for DD. The DD fuel cycle produces electricity which is 48 % more expensive despite the improved plant availability (69 % for DD, 65 % for DT - see appendix C). However, there are other attributes of the DD cycle, namely safety related, which must be examined before a conclusion on the overall attractiveness of this cycle can be reached.

The effect of varying beta on the cost of electricity is illustrated in figures 3.19 to 3.26. Figure 3.19 shows that high beta results in a lower COE. The effect is much more dramatic for the DD fuel cycle than for the DT fuel cycle. It is also apparent that going beyond a beta of 10 % for the DD fuel cycle there is not a great improvement in the COE. This reflects the increasing role of greater plasma shaping and higher wall loadings in determining the COE at high beta. Power conditioning costs, replacement component costs and waste handling costs are all seen to increase with plasma beta. Baxter et al. [3.21] found that beyond a beta of 15 %, the cost decrease per unit increase in beta for a DD tokamak becomes very small. They also state that the COE from a DD tokamak approaches that of a DT tokamak if high plasma beta can be achieved. This study shows that although the cost difference between DD and DT decreases as beta increases, the COE for the DD fuel cycle is still significantly above that for DT even at 20 % beta (DD is 2.05 times more expensive at 5 % beta compared to 1.49 times more expensive at 20 % beta).

In figure 3.20, the COE is plotted against the neutron wall loadings corresponding to the various values of beta. The neutron wall loading is seen to have a greater impact on the COE for the DD reactors. An initial sharp decrease is seen as the wall loading increases. This corresponds to a reduction in the volume of the fusion island and an increase in beta. Beyond a wall loading of 1 MW/m^2 and a beta of 10 %, the COE is not largely affected because plasma shaping and replacement components costs become more important. Although the wall loadings for the DD designs are less than for the DT designs, the lifetime neutron fluence limit was assumed to be lower (14.6 $MW \cdot yr/m^2$ for DD vs 25.0 $MW \cdot yr/m^2$ for DT, see appendix A for an explanation and section 3.3.3 for a discussion of the impact of varying this parameter on the COE). Despite this, less frequent component replacement is required at a given beta for DD than for DT. The role of component size in determining costs is much more strongly felt by the DD reactors. It is apparent from figure 3.20 that the contribution to the COE of costs for more frequent replacement of the smaller high beta DD reactor components is less than the contribution of the

FIGURE 3.19: COST OF ELECTRICITY VS BETA

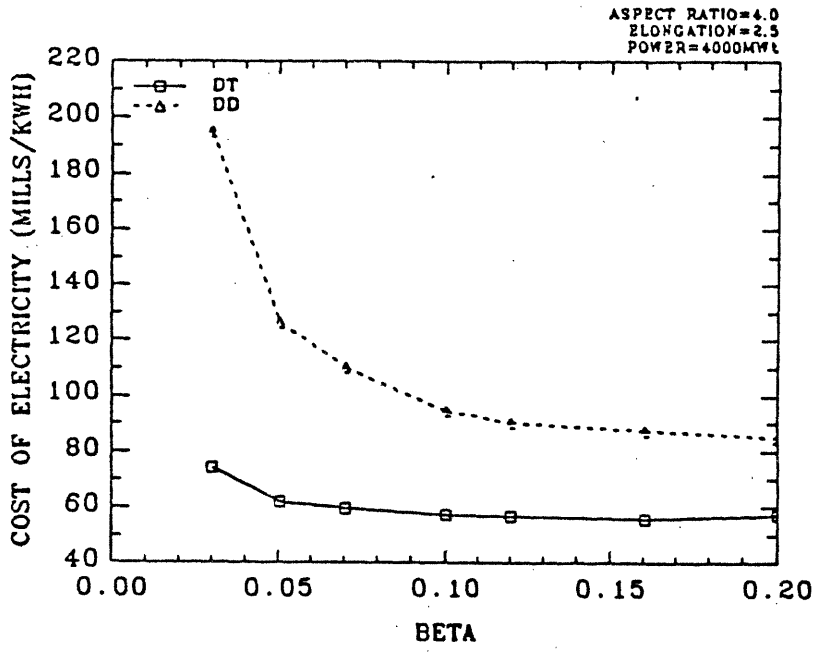

FIGURE 3.20: COST OF ELECTRICITY VS NEUTRON WALL LOADING

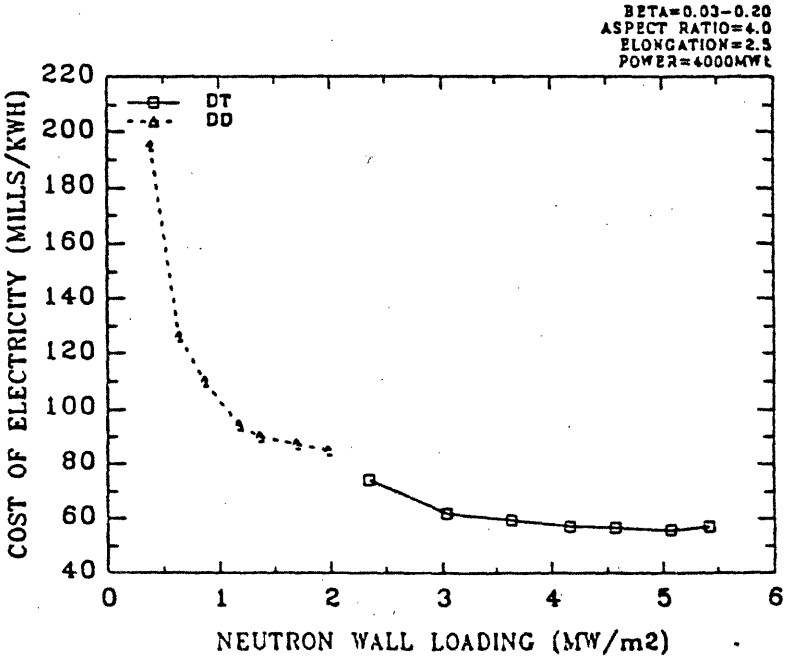

larger and less frequently replaced components of the low beta DD reactor.

High beta allows for the use of lower toroidal field magnetic fields, as shown in figure 3.21. Because of the reduced magnet size due to the smaller reactor and reduced fields required to produce the 4000 MW of thermal power, the magnet costs are significantly reduced at higher beta. This leads to a lower COE. However, the lower power density of the DD reactors compared to the DT reactors necessitates higher fields for this fuel cycle. A reduction in magnetic field and magnet costs at high beta is therefore felt more strongly by the DD designs. This contributes to the larger reduction in the COE seen with beta for the DD fuel cycle.

In figure 3.22, it is clear that a smaller reactor size reduces the cost of electricity, reflecting the scaling of costs with volume. There is a large reduction in reactor dimensions for the DD machines when beta is increased from 3 % to 10 %. At this point, the DD reactor size becomes comparable to the low beta DT reactor size. However, the DD reactors are still more costly because of the higher required magnetic field and greater plasma shaping needed to obtain the higher value of beta.

The variation of the cost of electricity and fusion island costs with the mass of the fusion island for the DD fuel cycle are shown in figure 3.23. As expected, a lower mass for the fusion island corresponds to lower costs. Fusion island costs are seen to decrease smoothly as the mass of the fusion island decreases. The minimum mass for the fusion island found in this work for the DD fuel cycle is approximately 20,000 tonnes. This is still quite large, for it was found that the DT fuel cycle would be economically competitive as a source of electricity if the fusion island mass was in the vicinity of 10,000 tonnes.

The volume of the fusion island for the DD fuel cycle can be compared to the DT fuel cycle in figure 3.24. As expected, the fusion island volume and COE for the DD reactors is greater than for the DT reactors.

FIGURE 3.21: COST OF ELECTRICITY VS TOROIDAL FIELD

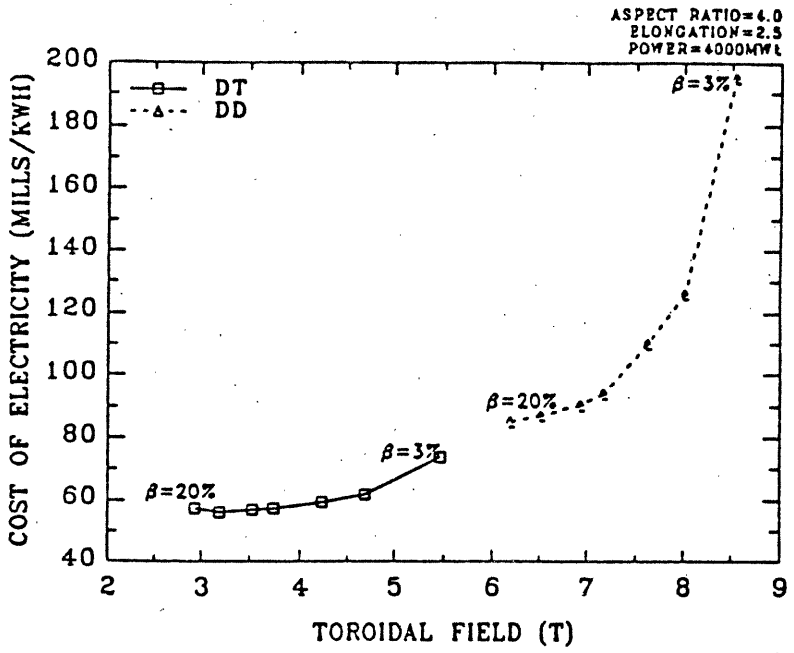

FIGURE 3.22: COST OF ELECTRICITY VS MINOR RADIUS

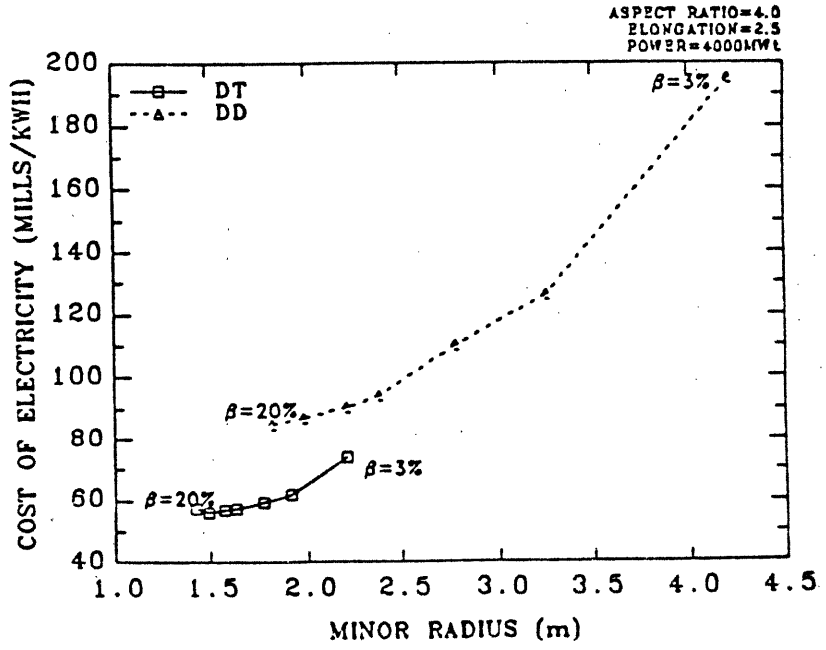

FIGURE 3.23: COST OF ELECTRICITY VS MASS OF FUSION ISLAND FOR THE DD FUEL CYCLE

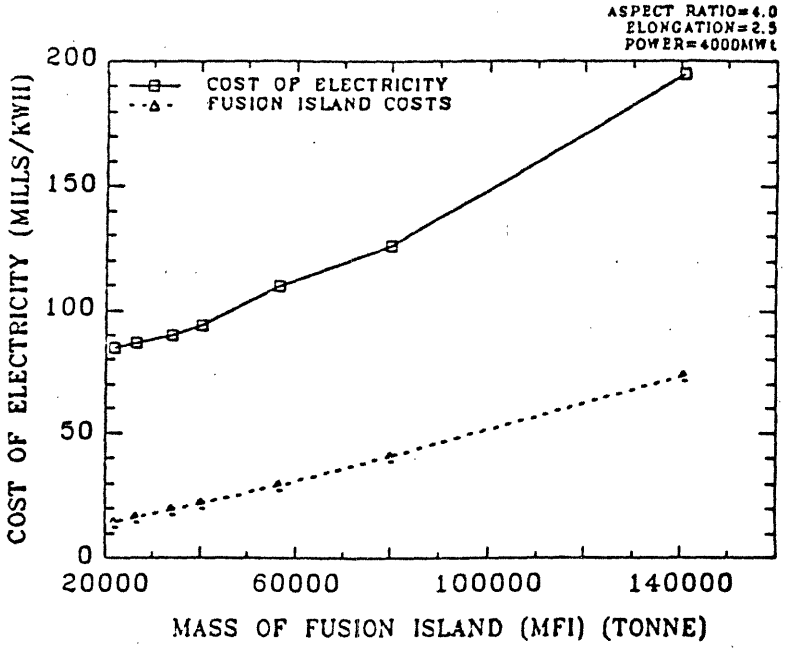

FIGURE 3.24: COST OF ELECTRICITY VS VOLUME OF FUSION ISLAND

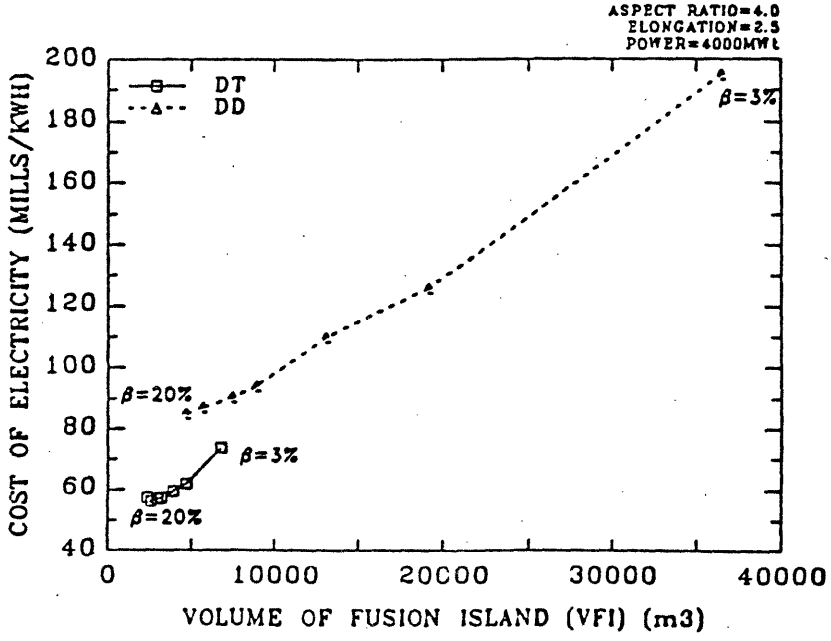

FIGURE 3.25:
COST OF ELECTRICITY VS POWER DENSITY OF FUSION ISLAND

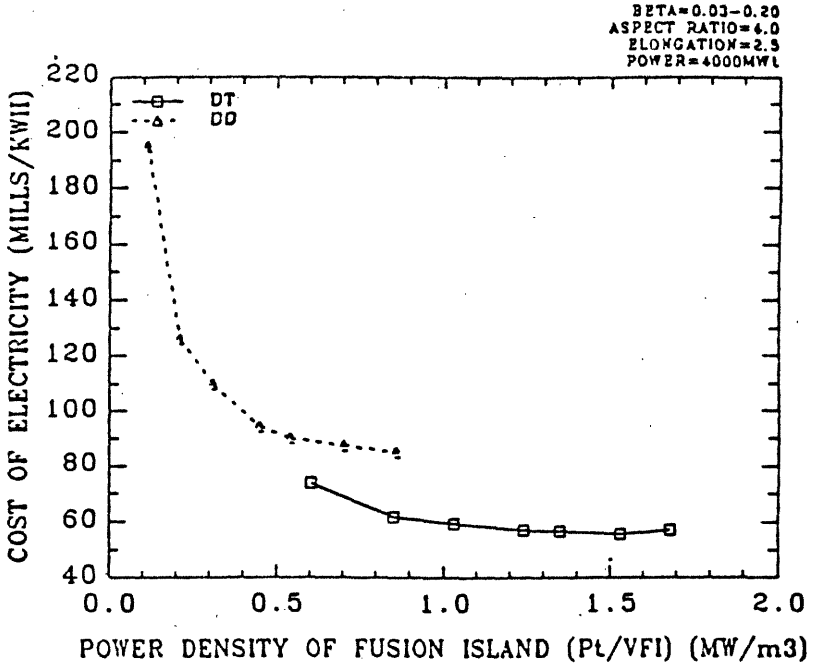

FIGURE 3.26: COST OF ELECTRICITY VS MASS POWER DENSITY

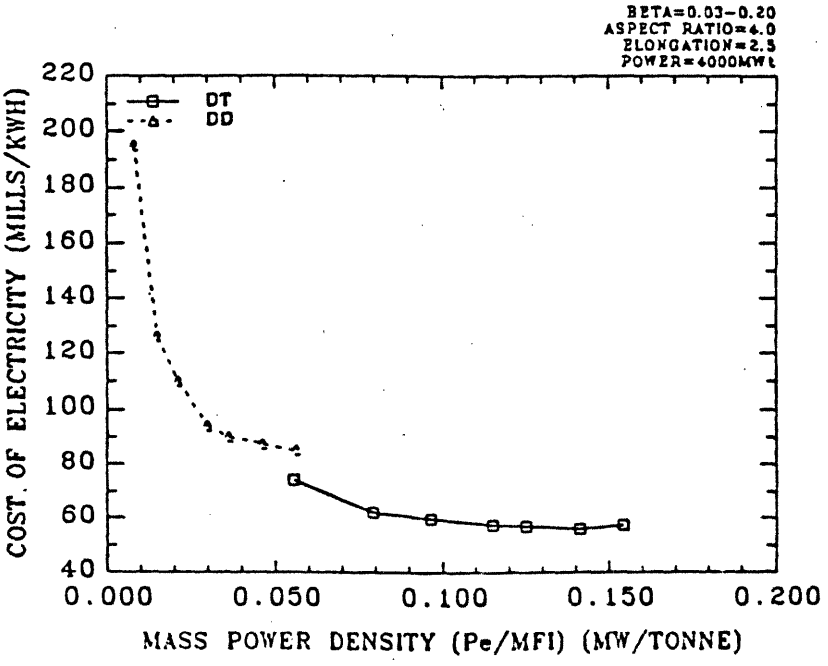

Less effective utilization of fusion island volume for the DD fuel cycle is evident in figure 3.25, as less power is produced per unit volume of the fusion island, at a more expensive rate. A further example of less effective material utilization for the DD fuel cycle is illustrated in figure 3.26, where the net electric power produced is plotted against the mass of the fusion island. DD reactors have a lower mass power density and produce more costly electricity.

3.3.2 The Effects of Varying Aspect Ratio and Elongation

The effect of varying aspect ratio is illustrated in figure 3.27 for both the DD and DT fuel cycles. The trend observed is similar for both fuel cycles. There appears to be a fairly large decrease in the COE in going from an aspect ratio of 3 to an aspect ratio of 4. Beyond a value of 4, further increasing the aspect ratio has only a small effect on the COE.

In figure 3.28, the direct capital cost is plotted against the mass per unit thermal power (mass utilization) for designs with aspect ratios varying from 3 to 7. The DD reactors appear less attractive than the DT reactors for two reasons. Firstly, the direct capital cost is greater for DD in all cases. Secondly, the mass per unit thermal power is higher for DD, indicating less effective utilization of fusion island mass for power production.

In figure 3.29, plasma elongation is varied. The DD fuel cycle appears to exhibit a very broad minimum between an elongation of 2.0 and 2.5. The DT fuel cycle exhibited a minimum at an elongation of 2.0. As the elongation is reduced below 2.0, the fusion island volume decreases, but the magnet and power supply systems become more costly. This is due to the fact that lower plasma elongation requires more elaborate plasma shaping, and hence, more costly magnet systems, to achieve the same value of beta (10 %). The wall loading is also seen to increase as the elongation is decreased, leading to more frequent blanket changeouts and increased

FIGURE 3.27: COST OF ELECTRICITY VS ASPECT RATIO

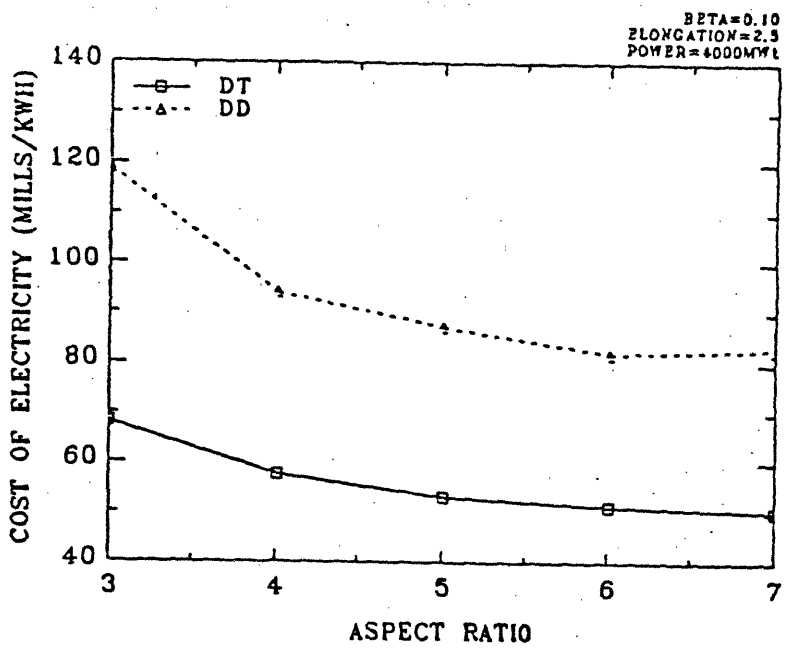

FIGURE 3.28:
DIRECT CAPITAL COST VS MASS PER UNIT THERMAL POWER

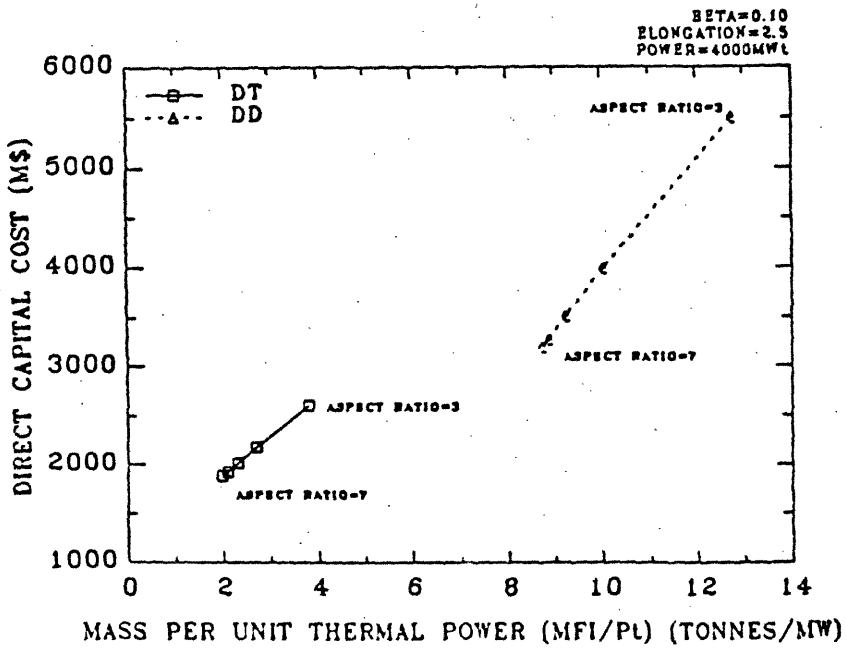

FIGURE 3.29: COST OF ELECTRICITY VS PLASMA ELONGATION

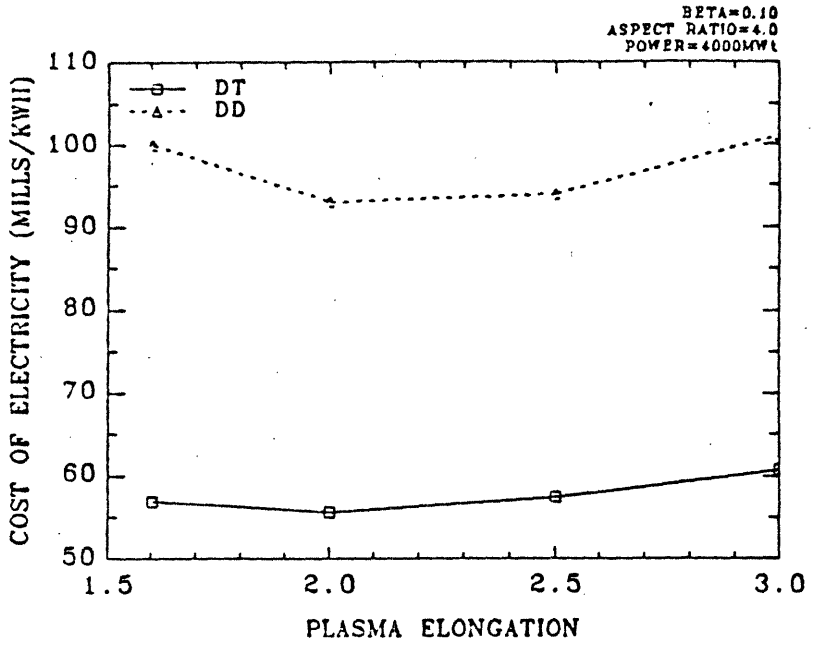

FIGURE 3.30:
COST OF ELECTRICITY VS BLANKET/FIRST WALL LIFETIME

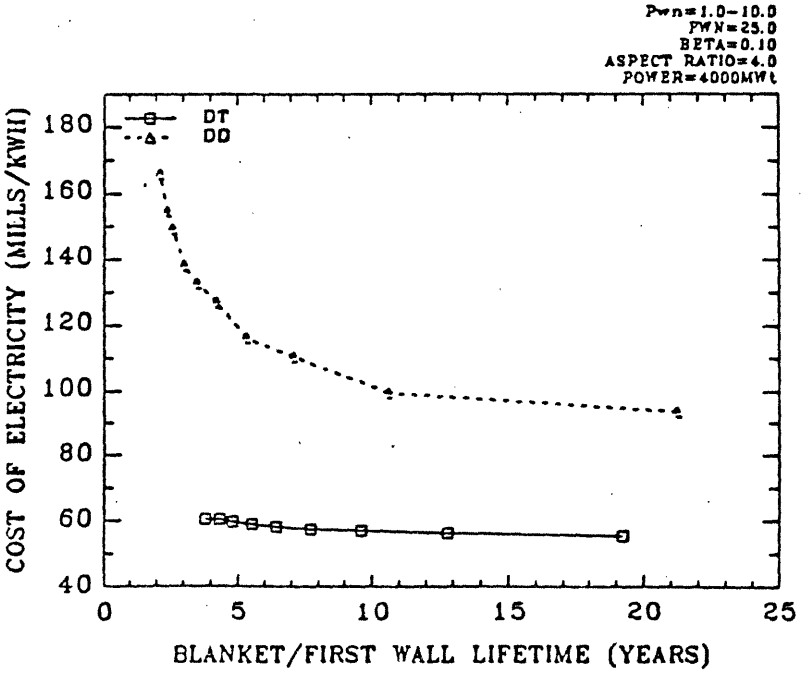

replacement component costs. At an elongation of 3.0, an increase in cost is seen because of the larger volume of the fusion island. The choice of an elongation of 2.5 in the designs where elongation is fixed (beta and aspect ratio variations) has not adversely affected the economics of the DD designs, as very little variation in the COE is seen over the range of values of elongation examined.

3.3.3 Other Effects

It is interesting to see the effect of varying the blanket lifetime on the COE for the DD reactors. Blanket lifetimes were determined for both the DT and DD fuel cycles for a fixed lifetime neutron fluence of 25 $MW \cdot yr/m^2$, for neutron wall loadings ranging from 1 to 10 MW/m^2. The COE is plotted against blanket lifetime in figure 3.30. Increasing blanket lifetime has more impact on reducing the COE for DD than for DT. This occurs because blanket changeouts are more costly for the DD reactors due to the larger volume of material involved. It should be noted that these results apply to the designs with 10 % beta. A different conclusion may be reached due to the different wall loadings at different values of beta. The effect of varying neutron fluence limit on the COE for the DD fuel cycle is shown in figure 3.31. An initial sharp decrease in the cost of electricity is seen as the fluence limit is increased up to a value of $\sim 5 \frac{MW \cdot yr}{m^2}$. Beyond this point, the impact of the fluence limit on the COE is small. The fluence limit for HT-9 used for the economic analyses for the DD fuel cycle ($14.6 \frac{MW \cdot yr}{m^2}$) was obtained from that for the DT fuel cycle by scaling with the average neutron energy. An alternate approach assumes the fluence limit to be independent of neutron energy (see appendix A), and is therefore constant for all fuel cycles ($25 \frac{MW \cdot yr}{m^2}$). The correct approach for determining the appropriate fluence limit for a different neutron energy spectrum from that for DT probably lies between these two methods. However, as indicated in figure 3.31, the impact of choosing either approach will not affect the results given here since both fluence limits lie in the range where there is little effect of this parameter on the COE.

FIGURE 3.31:
COST OF ELECTRICITY VS LIFETIME NEUTRON FLUENCE LIMIT

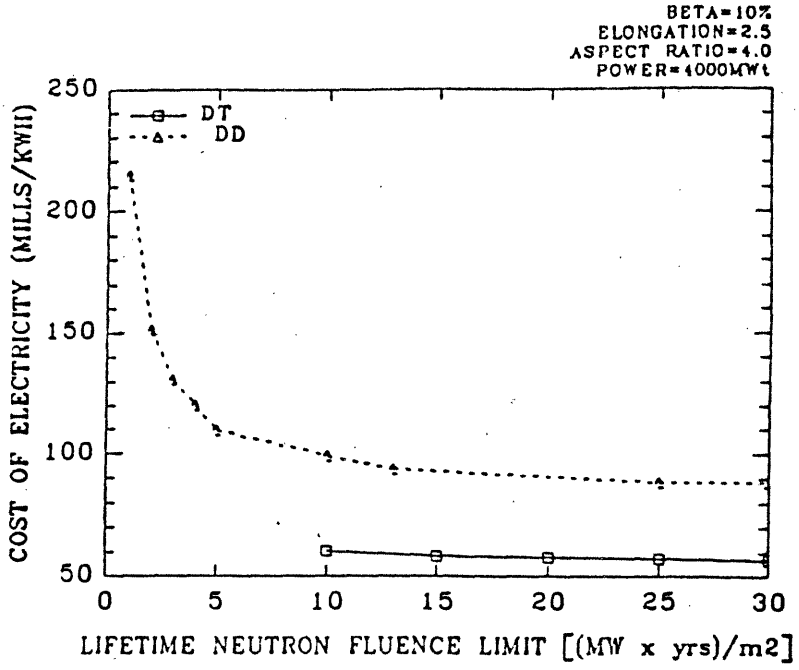

FIGURE 3.32: COST OF ELECTRICITY VS COST OF DEUTERIUM

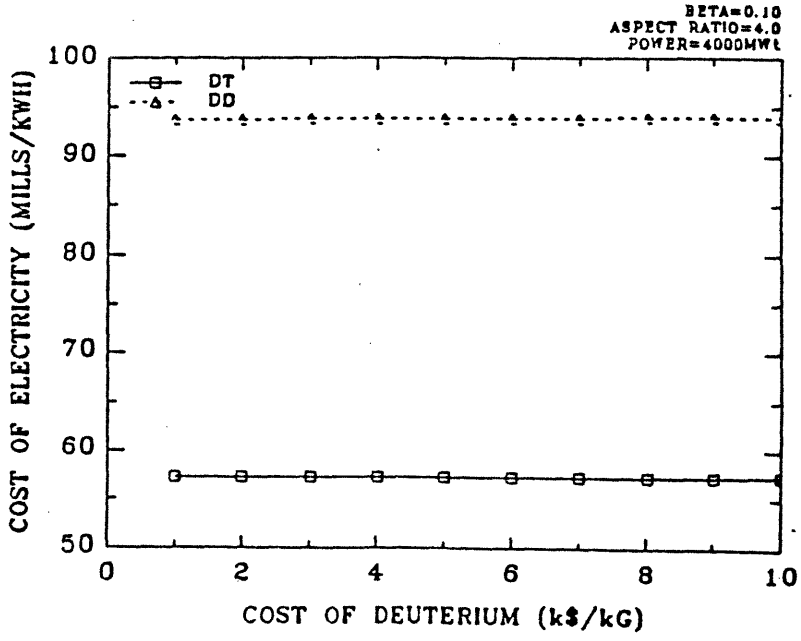

The effect of increasing the cost of deuterium on the COE for the DD fuel cycle is shown in figure 3.32. A cost for deuterium of 2.88 k$/kg (from reference [3.8], updated to current dollars) was assumed. A very small increase in the cost for this fuel cycle is observed (less than 0.3 mills/kWh) as the cost of deuterium is increased from 1 k$/kg to 10 k$/kg. In the case of the DD fuel cycle, the cost of fuel is not a significant contributor to the total costs.

The impact of using an alternate material on the economics of the DD fuel cycle is indicated in table 3.3. The RAF first wall/Fe2Cr1V blanket DD design has a higher blanket multiplication factor relative to the HT-9 design. This allows the reactor to produce less fusion power and still meet the 4000 MWt power output requirement. Consequently, a smaller, less costly reactor is needed. The COE for this alternate 10 % beta design is improved by nearly 10 %, from 94 mills/kWh for the HT-9 design, to 85 mills/kWh. In addition to the reduction in size, part of the cost savings is achieved through the use of a less expensive blanket material (cost of Fe2Cr1V is 20 $/kg, compared to 50 $/kg for HT-9). The reduction in blanket costs account for roughly 25 % of the savings in the COE. Initial and replacement blanket costs, which are major contributors to the fuel cycle costs, are greatly reduced for the alternate DD design. The balance of the reduction in the cost of electricity is a consequence of the smaller reactor size, for the costs of many other components scale with reactor dimensions. It should also be noted that the RAF first wall/Fe2Cr1V blanket design produces electricity at the same cost as the high beta HT-9 DD design, but at a lower wall load. This may result in a safety advantage with the use of this alternate material, with no accompanying economic penalty (relative to the high beta DD design).

3.4 Economics of the DHe Design

The COE was also evaluated for the DHe fuel cycle at a single intermediate value of beta (10 %). This is compared to the costs for the DT and DD fuel cycles with a 10 % beta in table 3.4. Despite the fact that the DHe reactor is slightly larger than its DD counterpart, it produces electricity at a somewhat lower cost (78.8 mills/kWh compared to 93.8 mills/kWh). Several factors contribute to lowering the COE. A large fraction of the power is produced as radiation, which can be absorbed in a much thinner blanket compared to neutrons [3.22]. The reduced neutron flux allows for a reduced total blanket/shield thickness. Savings in site facilities costs, support structures costs, maintenance equipment costs and other miscellaneous plant equipment costs result from lower activation and the use of non-nuclear grade components at certain locations. The reduced activation allows for the use of contact maintenance in certain areas for certain tasks, as opposed to time consuming and inefficient remote maintenance. Consequently, the plant capacity factor increases (a value of 72 % was found - see appendix C). Because of the reduction in dose rates throughout the plant, there is less concern about exceeding worker exposure limits. Fewer workers are needed at the plant since replacement manpower would not be a concern. Plant staffing requirements were estimated at 406 persons, compared to 426 persons for DD and 457 persons for DT (see appendix C). In comparison with the DT cycle, the electricity generated from DHe fusion is $\sim$ 38 % more expensive for reactors of the same beta, assuming a helium-3 cost of 40 k$/kg (the impact of the cost of helium-3 on the COE is discussed towards the end of this section). The 10 % beta DD design gives a value of COE $\sim$ 64 % greater than for the DT design.

Examining the costs directly associated with the fuel cycle, there is not a large difference between DT and DHe, both being significantly lower than DD. Annual costs attributable to the fuel cycle are 21.5 M$/yr for DT, 82.7 M$/yr for DD and 22.6 M$/yr for DHe. The greater cost for the DD fuel cycle is mainly due to the

Table 3.4:

Economics for DT, DD & DHe Designs with 10 % Beta

Parameter	DT	DD	DHe
Direct Costs (1986 M$)	2165	3982	3667
Land & Land Rights	5.0	5.0	5.0
Structures & Site Facilities	346	557	331†
Reactor Plant Equipment	1182	2793	2684
Blanket & First Wall	24	461	140
Shielding	168	189	212
Structure & Support	48	183	166†
Particle Removal/Control	3.0	4.3	4.6
Magnet Systems	169	919	1019
Power Injection System	131	56	62
Vacuum System	8.6	31	59
Power Conditioning Systems	221	603	672
Heat Transport System	174	208	207
Fuel Handling & Storage	143	46	73
Instrumentation & Control	30	30	30
Maintenance Equipment	63	63	38†
Turbine Plant Equipment	399	404	428
Electric Plant Equipment	110	110	110
Misc. Plant Equipment	69	59	55†
Heat Rejection System	54	54	54
Indirect Costs (1986 M$)	910	1624	1504
Contingency (1986 M$)	461	841	776
Total Constructed Cost (1986 M$)	3536	6447	5946
Total Capital Cost (constant 1986 M$)	3922	7150	6594

Parameter	DT	DD	DHe
Total Capital Cost (current 1992 M$)	5386	9819	9056
Annual Operation & Maintenance (1986 M$/yr)	57.7	52.4	47.0
Fuel Cycle (1986 M$/yr)	21.5	82.7	22.6/107.1*
COE (mills (1992)/kWh)	132	218	185/206*
COE (mills (1986)/kWh)	57.2	93.8	78.8/89.8*
Relevant Design Information:			
Plasma Volume (m^3)	854	2661	3090
First Wall/Blanket Volume (m^3)	574	1481	451
Shield Volume (m^3)	1399	1587	1825
TF Coil Volume (m^3)	111	1322	1316
Fusion Island Volume (m^3)	3225	8920	8605
Major Radius (m)	6.51	9.52	10.02
Minor Radius (m)	1.63	2.38	2.50
Toroidal Field (T)	3.73	7.16	7.61
Plasma Current (MA)	12.5	35.2	39.3
Triangularity	0.3	0.3	0.3
Plasma Density (m^{-3})	2.16×10^{20}	2.88×10^{20}	2.77×10^{20}
Neutron Wall Loading (MW/m^2)	4.16	1.17	0.18
Thermal Wall Loading (MW/m^2)	1.04	0.78	2.13

† some reduction due to low activation, inherent safety, and non-nuclear grade components

* helium-3 fuel costs are 40 k$/kg and 700 k$/kg

larger volume of materials used for initial components compared to DT, and the greater replacement frequency compared to DHe. One area in which the DHe fuel cycle is the most expensive is in fuel costs. Annual fuel costs for this fuel cycle are 5.52 M$/yr, compared to 0.59 M$/yr for DD and 0.27 M$/yr for DT (this assumes a helium-3 cost of 40 k$/kg). Waste handling costs are least for DHe. The reduction for DHe is due to the expected reduced materials, labor and overhead costs for waste handling activities resulting from dealing with less volume and lower activity waste, in addition to the reduced waste disposal costs. The waste handling cost, however, does not include the waste handling expenses incurred during decommissioning. The decommissioning costs were assumed to scale with neutron wall loading and material volume. The combination of these factors would result in these costs being least for DHe. The decommissioning allowance for the DHe fuel cycle has been estimated at 0.49 M$/yr, compared to 3.3 M$/yr for DD and 4.4 M$/yr for DT. Although the volume of the fusion island is lowest for the DT fuel cycle, the neutron wall loading is greatest and the activity of the waste at decommissioning, and therefore decommissioning costs, would be higher.

Fuel costs for the DD fuel cycle are double that for the DT fuel cycle. Deuterium is the only fuel to be purchased in both cases, since for the DT reactors, tritium is produced on site and is considered to be a non-cost item. The DHe fuel costs are nearly ten times larger than DD and twenty times larger than DT due to the high cost of helium-3. The cost of helium-3 fuel assumed for this analysis was 40 k$/kg [3.23]. Figure 3.33 illustrates how the cost of electricity is affected by the cost of helium-3 fuel. A linear relationship was found to exist, given by:

$$\mathrm{COE} = 0.0176 \cdot \mathrm{UC_{He}} + 77.6 \ \ \mathrm{mills/kWh} \tag{3.6}$$

where

$\mathrm{UC_{He}}$ = unit cost of helium-3 fuel ($/g)

FIGURE 3.33:
COST OF ELECTRICITY VS COST OF HELIUM-3
FOR THE DHe FUEL CYCLE

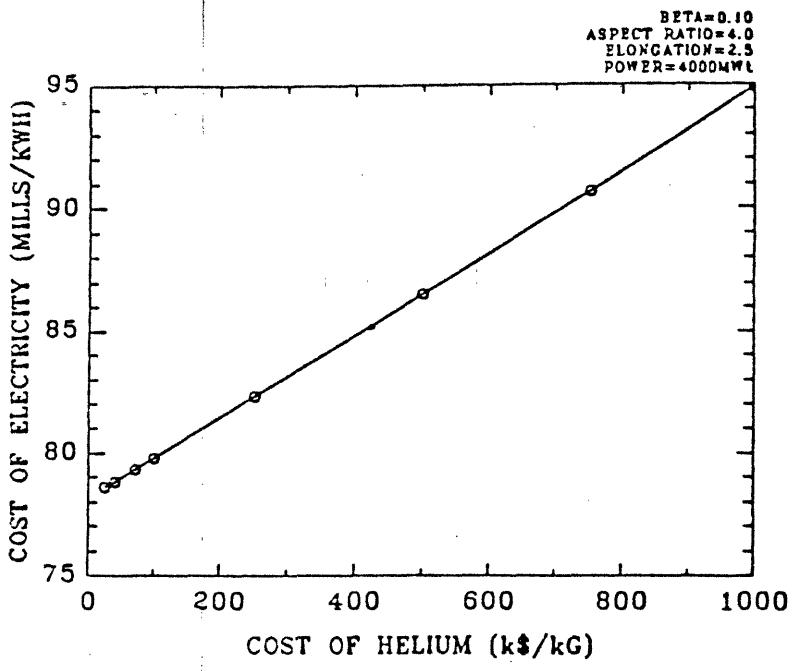

FIGURE 3.34: COST OF ELECTRICITY VS BETA FOR FUSION FUEL CYCLES

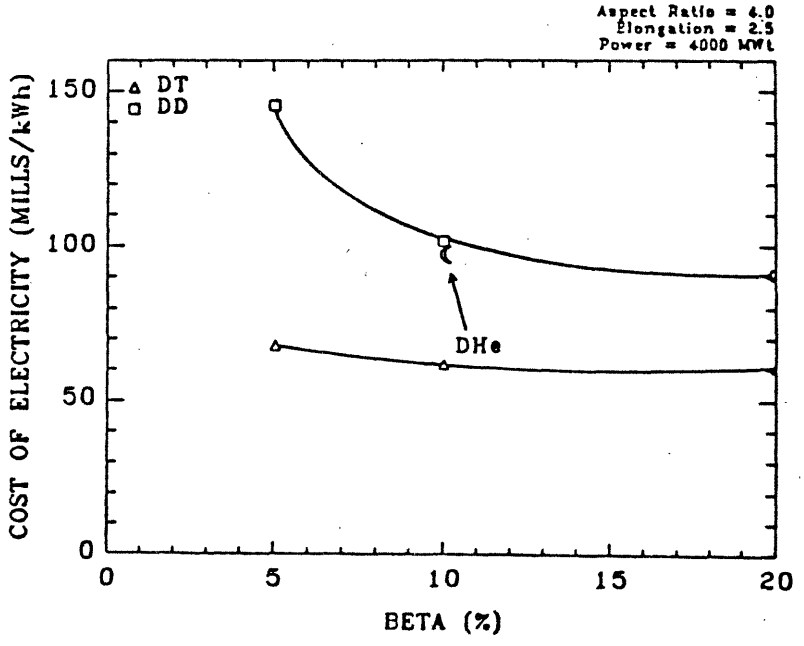

As the cost of helium-3 increases from 40 k$/kg to 100 k$/kg, the COE increases by 1 mill/kWh. A further increase in the fuel cost to 500 k$/kg would lead to an additional increase of 7 mills/kWh in the cost of electricity. Thus, a high cost for helium-3 can have significant impact on the COE. It is important to note that the cost of helium-3 is highly uncertain at this time. In fact, adequate supply of this fuel component cannot be guaranteed.

Although the electricity produced by the DHe fuel cycle is more expensive than that produced by the DT fuel cycle, the significant reduction in neutron flux and the resulting safety merits associated with this fuel cycle may justify the increased cost. Figure 3.34 illustrates the relative economic positions of all three fuel cycles.

3.5 General Discussion of Fuel Cycle Economics

The economic impact of the change in fuel cycle can be determined by examining specific direct cost accounts of the three fuel cycles. Firstly, the effect of changing the blanket material from one needed for tritium breeding (Li compound for DT reactors) to one dedicated to heat removal (ferritic steel for DD and DHe reactors) will be discussed. For the advanced fuels, the first wall/blanket costs increase significantly over the DT blanket costs (by approximately a factor of 20 for DD and a factor of 6 for DHe). This is due to the larger machine size and greater volume of material used as well as to the slightly more costly material used in the advanced fuel blankets. In the case of the DD fuel cycle, the improved neutron energy multiplication obtained with the use of HT-9 compared to lithium allows for a smaller fusion power to give the same total thermal power. This is improved even further with the Fe2Cr1V blanket. Despite having a large neutron energy multiplication factor (i.e. energy gain per neutron or total blanket power divided by fusion neutron power), there is not a large total gain in energy in the blanket for the DHe reactor because very few neutrons enter the blanket (only $\sim$ 7%). A better overall

Table 3.5: Fuel Cycle Costs

Parameter	DT (5 %)	DT (10 %)	DT (20 %)	DD (5 %)	DD (10 %) HT-9	DD (10 %) RAF	DD (20 %)	DHe (10 %)
Initial First Wall/ Blanket (M$/yr)	2.67	2.03	1.62	64.3	39.0	14.6	25.0	11.9
Replacement First Wall/ Blanket (M$/yr)	2.31	2.64	2.80	0	16.9	6.3	21.7	0
Total First Wall/ Blanket (M$/yr)	4.97	4.67	4.42	64.3	55.9	20.9	46.8	11.9
Neutron Flux (MW/m^2)	3.04	4.16	5.41	0.63	1.17	1.11	1.98	0.18
Number of Blanket Changeouts	2	3	4	0	1	1	2	0
Initial Limiter (M$/yr)	0.29	0.25	0.22	0.50	0.37	0.36	0.28	0.39
Replacement Limiter (M$/yr)	0.14	0.24	0.21	0.24	0.17	0.17	0.40	0.36
Total Limiter (M$/yr)	0.43	0.49	0.43	0.74	0.54	0.53	0.68	0.75

Parameter	DT (5 %)	DT (10 %)	DT (20 %)	DD (5 %)	DD (10 %) HT-9	DD (10 %) RAF	DD (20 %)	DHe (10 %)
Initial Auxiliary Heating (M$/yr)	4.31	3.69	3.10	1.94	1.58	1.51	1.38	1.74
Replacement Auxiliary Heating (M$/yr)	3.74	4.79	5.37	0	0.68	0.65	1.20	0
Total Auxiliary Heating (M$/yr)	8.05	8.48	8.47	1.94	2.26	2.16	2.58	1.74
Misc. Sched. Replaceable Items (M$/yr)	1.23	1.84	2.46	0	0.61	0.61	1.23	0
Fuel (M$/yr)	0.27	0.27	0.27	0.59	0.59	0.55	0.59	5.52/90.03*
Waste Handling (M$/yr)	5.28	5.80	5.86	3.33	22.8	20.6	28.6	2.65
Total Initial Components Costs (M$/yr)	7.27	5.97	4.94	66.7	40.9	16.4	26.7	14.0
Total Replacement Components Costs (M$/yr)	7.42	9.51	10.84	0.24	18.4	7.7	24.5	0.36
Total Fuel Cycle (M$/yr)	20.2	21.5	21.8	70.9	82.7	45.3	80.4	22.5/107.0*

* helium-3 fuel costs are 40 k$/kg and 700 k$/kg

indicator of this effect is given by the system multiplication factor which is the total thermal power divided by the total fusion power. The DT and DHe values are very close, but that for DD is somewhat larger (for both materials). Because of this, the DD reactor can produce less fusion power and still result in the same total thermal power. It appears, however, that despite the elimination of tritium breeding and the potential for enhanced neutron energy multiplication, the advanced fuels have more costly blankets and produce electricity more expensively.

For the DT fuel cycle, lithium handling costs must be considered. These have been included in the fuel handling and storage account which also covers blanket and coolant tritium removal, fuel preparation and injection, fuel purification, storage and atmospheric tritium recovery systems. The advanced fuels do not need to be concerned with lithium handling and blanket or coolant tritium recovery. Additionally, the fuel purification, storage and atmospheric tritium recovery systems are scaled down for the advanced fuels because of the reduced tritium inventory. These costs are, however, only a factor of three less for DD than for DT so that the savings seen here do not compensate for the greater expense associated with their blankets. Fuel handling costs are only reduced by a factor of two for DHe. This is a consequence of the additional equipment required for purification and handling of large quantities of helium isotopes.

Tritiated waste will be considerably reduced for the advanced fuels. Although there is a reduction in the number of blanket changeouts, the total volume of activated waste to be disposed of is greater. However, in the case of the DHe fuel cycle, the activity of the structure will be considerably below that for DD and DT. It may, in fact, qualify for shallow land burial as opposed to deep geological disposal. Waste handling cost information is listed in table 3.6. Calculations were based on the method used in reference [3.9].

Magnet costs are considerably affected by the fuel cycle. The DT machine requires a lower toroidal field (6.8 T at coil, 3.7 T on axis) and has a lower plasma

Table 3.6: Waste Handling Information

Fuel Cycle	DT			DD				DHe
Beta	(5 %)	(10 %)	(20 %)	(5 %)	HT-9 (10 %)	RAF (10 %)	(20 %)	(10%
Number of Complete Blanket Changeouts	2	3	4	0	1	1	2	0
Number of Complete Limiter Changeouts	1	2	2	1	1	1	2	2
Low Activity Waste Volume (m^3/yr)	550	551	551	539	546	546	549	546
Tritiated Waste Volume (m^3/yr)	31	31	31	0.3	0.3	0.3	0.3	0.3
Storage Pool Volume (m^3/yr)	102	102	102	1	1	1	1	1
Lithium Waste Volume (m^3/yr)	36	41	43	0	0	0	0	0
Lithium Waste Volume at EOL (m^3)	535	408	325	0	0	0	0	0
Structural Waste Volume (m^3/yr)	3	4	4	0	39	36	25	0

Fuel Cycle	DT			DD				D
Beta	(5 %)	(10 %)	(20 %)	(5 %)	HT-9 (10 %)	RAF (10 %)	(20 %)	(1
Structural Waste Volume at EOL (m^3)	48	36	29	1952	1185	1092	761	3
Fraction of Blanket Lifetime Consumed at EOL	0.37	0.25	0.22	0.89	0.66	0.57	0.64	0
Materials, Labor and Overhead Costs for Waste Handling Activities (M$/yr)	3.3	3.4	3.4	2.7	3.6	3.0	3.3	2
Cost for Transportation of Waste (M$/yr)	0.14	0.14	0.14	0.12	0.13	0.13	0.13	0.
Cost for Disposal of Waste† (M$/yr)	1.9	2.3	2.3	0.55	19.1	17.4	12.4	0.
Decommissioning Estimate (M$/yr)	4.6	4.4	4.2	3.8	3.3	3.1	3.0	0.
Total Cost for Waste Handling† (M$/yr)	5.3	5.8	5.9	3.3	22.8	20.6	15.7	2

† does not include disposal of waste from decommissioning

current. Thus, both TF and PF coils are smaller, and hence, less costly. The larger field, current and reactor size for the DD and DHe reactors lead to more expensive magnet systems.

Table 3.7 lists several key parameters which are good indicators of the relative economic merit of the various designs. Four relate to power density: plasma power density (MW/m^3), blanket specific power density (MWe/tonne of blanket material), neutron wall loading (MW/m^2) and thermal wall loading (MW/m^2). The DT fuel cycle is superior in terms of material and volume utilization per unit power generated. With a 5 % beta, the plasma power density of the DT machine is 6.3 times greater than the DD machine (see table 3.8). At 10 % beta, the DT power density is 4.0 times greater than that for DD, and 3.5 times greater than that for DHe. At a beta of 20 %, the DT plasma has a power density 2.7 times larger than the DD plasma. It is evident that at higher values of plasma beta, the performance gap between the DT fuel cycle and the advanced fuels is narrowing. This is also indicated by the specific blanket power density. However, the gap is much wider for this parameter because of the greater density and volume of blanket material used for the advanced fuels. There is not a large difference seen in the values of these economic scaling factors for the two materials examined for the DD fuel cycle.

In terms of neutron wall loading, the advanced fuels show a distinct advantage. It is desirable to have as low a wall loading as possible to minimize damage and the need for component replacement. At a given beta, the neutron wall loading is lower for the DD fuel cycle compared to the DT fuel cycle (see table 3.7). The DHe fuel cycle appears even more desirable from this perspective. However, the neutron wall loading for the DD machines with a 10 % beta still requires that the initial first wall/ blanket be replaced during the plant lifetime. In this respect, the DHe cycle presents an advantage because it can retain the blanket for the life of the plant. Relative to the DT cycle, which requires 3 blanket changeouts during the plant lifetime for a beta of 10 %, the improvement of the advanced fuel cycles is clear.

Table 3.7: Economic Scaling Factors

Parameter	DT (5 %)	DT (10 %)	DT (20 %)	DD (5 %)	DD (10 %) HT-9	DD (10 %) RAF	DD (20 %)	DHe (10 %)
Power Density (MW/m^3)	2.65	4.27	6.45	0.42	1.08	1.03	2.42	1.22
Blanket Specific Power Density (MWe/tonne blkt mat'l)	1.90	2.50	3.14	0.079	0.13	0.11	0.21	0.35
Neutron Wall Loading (MW/m^2)	3.04	4.16	5.41	0.63	1.17	1.11	1.98	0.18
Thermal Wall Loading (MW/m^2)	0.76	1.04	1.35	0.42	0.78	0.74	1.32	2.13
Blanket Changeouts During Lifetime	2	3	4	0	1	1	2	0
Limiter Changeouts During Lifetime	1	2	2	1	1	1	2	2
Magnet Stored Energy (MJ/MWe)	242	94	38	3565	1121	1051	368	1473
Fraction of Direct Cost due to Fusion Island	0.240	0.189	0.161	0.558	0.440	0.396	0.335	0.419
Plant Capacity Factor	0.65	0.65	0.65	0.69	0.69	0.69	0.69	0.72

Table 3.8: Relative Ranking of Economic Scaling Factors of Advanced Fuels Compared to the DT Fuel Cycle

Parameter	DT/DD (5 %)	DT/DD HT-9 (10 %)	DT/DD RAF (10 %)	DT/DD (20 %)	DT/DHe (10 %)
Power Density	6.3	4.0	4.1	2.7	3.5
Blanket Specific Power Density	24.1	19.2	22.7	15.0	7.1
Neutron Wall Loading	4.8	3.6	3.7	2.7	23.1
Thermal Wall Loading	1.8	1.3	1.4	1.0	0.5
Magnet Stored Energy	0.068	0.084	0.089	0.103	0.064
Fraction of Direct Cost due to Fusion Island	0.43	0.43	0.48	0.48	0.45

As mentioned previously, the blankets of the DD and DHe reactors have the a reduced need for replacement as a consequence of the lower neutron wall loading and the elimination of tritium breeding. Hence, there is less need for shutdown. Furthermore, unscheduled replacement of failed blanket modules may be reduced, especially for the DHe reactor, because of the reduced neutron damage and possibly more reliable performance. If replacement is required, this can be done easily and rapidly since limited direct access to the plasma chamber of the DHe reactor is possible [3.22]. Such direct access capability could be very important for handling unexpected problems. These effects lead to the possibility of enhancing the reactor capacity factor for advanced fuel reactors and improving the COE. An attempt to account for these effects resulted in a plant capacity factor of 69 % for DD and 72 % for DHe (see appendix C), compared to the assumed 65 % capacity factor for the DT fuel cycle.

The thermal wall loading (radiation and charged particles) exhibits a different trend. The DT reactors have a slightly larger wall loading than the DD reactors for all values of beta. However, at a beta of 20 %, the thermal wall loading is nearly identical for both machines. On the other hand, the thermal wall loading of the DHe reactor is almost twice that of the DT reactor and nearly three times that of the DD reactor for a beta of 10 %. A higher thermal and particle flux to the wall leads to more frequent limiter changeouts during the plant lifetime, and hence, greater replacement costs for these components. However, these costs are not a large contributor to the COE so that this consideration is not strongly felt.

An additional parameter related to the cost of the magnet system is the magnetic stored energy (MJ/MWe). Its magnitude is indicative of the cost of the magnet system. As can be seen in table 3.7, this parameter is higher for the advanced fuels, and is observed to decrease as beta increases for a given fuel cycle. It is apparent that more costly magnet systems are required for the advanced fuels. This is also true for low beta designs, which require higher magnetic fields (and larger volumes in which the magnetic energy is stored) in order to achieve a higher power density.

The fraction of the direct costs attributable to the fusion island reflects the capital cost intensity of the power producing components of the plant. This is lowest for the DT fuel cycle, and is seen to decrease as beta is increased, due to the decreasing fusion island volume. The DD fractional fusion island costs are slightly greater than for DT, but exhibit the same trend. The DHe fusion island fractional cost is nearly the same as for DD at 10 % beta. The higher fusion island capital cost for the advanced fuels is a reflection of the lower power densities associated with these fuel cycles.

The values of the COE obtained for the DT fuel cycle in this work appear somewhat high when compared to other studies. The Environmental, Safety and Economics Committee (ESECOM) [3.24] examined a range of fusion reactor designs and determined the COE's for tokamaks varying from 35.4 mills/kWh (V/Li/Li with an advanced MHD conversion system) to 55.7 mills/kWh (SiC/He/Li_2O). The COE determined for a tokamak employing HT-9 structure, helium coolant and Li_2O breeder was 49.7 mills/kWh. Their assessment assumed a beta of 10 % for the tokamak designs. The COE for the 10 % beta DT design in this work was 57.2 mills/kWh. In addition to small effects due to differences in financial parameters, the bulk of this discrepancy can be attributed to the pulsed burn cycle employed here versus the steady state burn cycle employed in the ESECOM study. A major cost contributor for the pulsed design is the thermal energy storage system which is needed to ensure a continuous flow of steam to the turbine for constant electrical output. This adds approximately 165 M$ to the capital cost of the reactor plant equipment. The pulsed nature of the reactor also results in greater poloidal field magnet costs because of the larger ohmic heating coils required, greater poloidal field power supply equipment costs and slightly greater structures and site facilities costs (since more electrical equipment must be operated, maintained and housed). It is estimated that these considerations add 8 to 10 mills/kWh to the COE.

3.6 Summary of Economic Analysis

From the results presented in the previous sections, it is evident that the advanced fuels are at a clear economic disadvantage with respect to the DT fuel cycle. At best, the DD fuel cycle employing an HT-9 blanket (20 % beta), produces electricity at a cost 48 % greater than for DD. The cost of electricity produced by the DHe fuel cycle is 38 % greater than for DT, if the cost of helium-3 is as low as 40 k$/kg. The COE may increase substantially, if the cost of helium-3 fuel is much greater than this. A cost improvement for the DD fuel cycle was seen with the use of an RAF first wall/Fe2Cr1V blanket. This resulted from the smaller sized reactor due to enhanced neutron multiplication in the blanket, in addition to the lower cost blanket material. the DD reactors is greater than for the DT reactors.the DD reactors is greater than for the DT reactors. Although a comparison amongst the fuel cycles cannot be made with this alternate material, it would be expected that a cost reduction would also be seen for the DT and DHe fuel cycles. The savings would likely not be as significant as for the DD fuel cycle. due to the smaller volume of structure in the DT and DHe blankets.

It is apparent from the parametric analyses performed for DT that there is no economic incentive for pursuing values of plasma beta above 10 %. This vvvvoptimum is a consequence of the competition between decreasing costs due to a smaller reactor and increasing costs due to more frequent component replacement as beta is increased. It was found that for 10 % beta, a high aspect ratio and an elongation of 2.0 are desirable.

From the other parametric variations carried out for the DT fuel cycle, several interesting observations can be made:

- The fusion island mass of a 4000 MWt plant must be in the area of 10,000 tonne for DT fusion to be competitive with fission.
- A fusion island volume on the order of 3,000 m^3 will result in a competitive

COE.

- Desirable values for the power density of the fusion island ($\frac{P_T}{V_{FI}}$) and the net electric power per unit mass of the fusion island ($\frac{P_e}{M_{FI}}$) are 1.2 $\frac{MW}{m^3}$ and 0.1 $\frac{MWe}{tonne}$. These values are obtained with the 10 % beta design and place DT fusion within the economically competitive range.

- The COE depends fairly strongly on the mass utilization factor ($\frac{M_{FI}}{P_T}$).

- The neutron fluence limit has a large impact on the COE up to values of $\sim$ 15 $\frac{MW\cdot yr}{m^2}$. Above this value, the decrease in the COE per unit increase in fluence limit is not large.

- The COE for DT was found to be linearly dependent on the cost of shielding, and almost unaffected by the cost of deuterium fuel.

With the DD designs, the impact of varying beta is more strongly felt. Higher beta appears to be more important in reducing the COE for this fuel cycle, although the unit reduction in cost per unit increase in beta becomes small beyond a beta of 10 - 15 %. This is again a consequence of the competing effects of decreasing costs due to smaller component sizes and increasing costs due to more frequent replacement at high beta. A high aspect ratio and elongation of 2.0 to 2.5 should be sought to minimize the COE for DD reactors. A longer blanket lifetime is more important for this fuel cycle because the larger reactor components result in more costly blanket changeouts. For the DD fuel cycle the neutron fluence limit has a significant impact on the COE up to approximately 5 $\frac{MW\cdot yr}{m^2}$. Beyond this value, the reduction in COE as the fluence limit is increased is small. Some cost savings results with the RAF first wall/Fe2Cr1V blanket DD design compared to the HT-9 DD design at 10 % beta. This is a consequence of the improved energy multiplication in the blanket (due to increased iron content), and the lower unit cost of the blanket material. The mass and volume of the least costly DD designs (20 % beta HT-9 and 10 % beta RAF first wall/Fe2Cr1V blanket) are far too large to result in a

competitive COE. The fusion island power density and mass power density of the DD designs are too low to result in economical energy production.

The cost of electricity determined for the DHe fuel cycle is somewhat reduced from the DD fuel cycle, although still significantly above that from the DT fuel cycle. An important factor in determining the COE for this fuel cycle is the cost of fuel. An increase of 7 mills/kWh in the COE was seen as the cost of helium-3 was increased from 40 kS/kg to 500 kS/kg. A major concern is the availability of fuel to supply an economy dependent on this fuel cycle.

Costs directly associated with the fuel cycle were seen to be similar for DT and DHe, both being much below the costs for DD. The greater cost for DD is mainly a consequence of the larger volume of materials use for components compared to DT, and the greater replacement frequency compared to DHe.

The contribution of fuel costs to the fuel cycle costs are greatest for DHe; the contribution of waste handling costs are least for this fuel cycle. This reflects the reduced volume and activity of the wastes to be handled.

Despite the elimination of tritium breeding and the potential for enhanced neutron energy multiplication, the advanced fuels have more costly blankets and produce energy more expensively. The absence of a lithium compound and breeder tritium extraction equipment do not lead to a great cost reduction for the DD and DHe fuel cycles. Tritium handling and hydrogen isotope separation equipment is still required, although at a smaller scale than for DT, to provide for plasma exhaust purification. Some cost savings is seen, but not enough to offset the large expense associated with the advanced fuel blankets. This suggests the use of a less costly blanket material for these fuel cycles.

As indicated by the economic scaling factors, the DT fuel cycle is superior in terms of material and volume utilization per unit power produced. It also requires much less magnetic energy for power production. The advantage of the DT fuel cycle

diminishes however, at higher values of beta. The DT fusion island is less capital intensive, but has a greater need for component replacement as reflected through the wall loading. The reduced need for component replacement, the absence of a lithium breeder, the lower tritium inventory and the reduction in activation of structural materials (especially in the case of the DHe fuel cycle) all lead to the possibility of improved plant availability for the advanced fuels. This partially offsets the increased costs for the advanced fuel cycles seen in other areas.

The DD and DHe fuel cycles are at a distinct economic disadvantage with respect to the DT fuel cycle. However, there appears to be some safety benefits to be obtained by adopting an advanced fuel cycle. In the next several chapters, safety advantages will be identified and quantified where possible. It will then be the necessary to determine if these safety advantages can justify the increased cost for electricity.

3.7 References

(3.1) K. Evans, A Tokamak Reactor Cost Model Based on STARFIRE/WILDCAT Costing, Argonne National Laboratory, ANL/FPP/TM-168, March 1983.

(3.2) S.C. Schulte et al., Fusion Reactor Design Studies - Standard Accounts for Cost Estimates, Pacific Northwest Laboratories, PNL-2648, 1979.

(3.3) S.C. Schulte et al., Fusion Reactor Studies - Standard Unit Costs and Cost Scaling Rules, Pacific Northwest Laboratories, PNL-2987, 1979.

(3.4) J. Sheffield et al., Cost Assessment of a Generic Magnetic Fusion Reactor, Oak Ridge National Laboratory, ORNL/TM-9311, March 1986.

(3.5) W.R. Hamilton et al., Cost Accounting System for Fusion Studies, Fusion Engineering Design Center, Oak Ridge National Laboratory, Draft, 1985.

(3.6) Nuclear Energy Cost Data Base, A Reference Data Base for Nuclear and Coal-fired Powerplant Power Generation Cost Analysis, U.S. Department of Energy, DOE/NE-0044/3, June 1985.

(3.7) C.C. Baker et al., STARFIRE: A Commercial Tokamak Fusion Power Plant Study, Argonne National Laboratory, ANL/FPP-80-1, September 1980.

(3.8) K. Evans et al., WILDCAT: A Catalyzed DD Tokamak Reactor, Argonne National Laboratory, ANL/FPP/TM-150, November 1981.

(3.9) S. Brereton and M. Kazimi, A Methodology for Cost/Benefit Safety Analysis for Fusion Reactors, M.I.T. Plasma Fusion Center, PFC/RR-85-3, March 1985.

(3.10) J.B Cannon, Background Information and Technical Basis for Assessment of Environmental Implications of Magnetic Fusion Energy, U.S. Department of Energy, DOE/ER-0170. August 1983.

(3.11) R.C. Grimm et al., MHD Stability Properties of Bean-Shaped Tokamaks, Nuclear Fusion, Vol. 25, No.7, 1985.

(3.12) D. Ehst, Argonne National Laboratory, private communication, February 1987.

(3.13) A.D. Rossin and T.A Rieck, Economics of Nuclear Power, Science, 201, p. 582, August 1978.

(3.14) M.M. El-Wakil, Nuclear Energy Conversion, Intext Educational Publishers, Scranton Pennsylvania, 1971.

(3.15) R.L. Miller et al., Parametric Systems Analysis of the Modular Stellarator Reactor, Los Alamos National Laboratory, LA-9344-MS, 1982.

(3.16) G. Miley, Economic Comparison of Large and Small Fusion Reactor Concepts, Nuclear Technology/Fusion, 4, p. 368, September 1983.

(3.17) R. Krakowski, Memorandum to Esecom: Parametric Results Using Generomak Model With Emphasis on Power Density Versus Inherent-Safety Tradeoffs, March 1986.

(3.18) B.G. Logan, A Rationale for Fusion Economics Based on Inherent Safety, Journal of Fusion Energy, Vol. 4, No. 4, p. 245, 1985.

(3.19) J. Massidda, private communication, September 1986.

(3.20) S. Fetter, The Radiological Hazards of Magnetic Fusion Reactors, Ph.D. Thesis, University of California - Berkeley, 1985.

(3.21) D.C. Baxter et al., DD Tokamak Reactor Assessment, Nuclear Technology/ Fusion, 4, p. 246, September 1983.

(3.22) C. Choi et al., Exploratory Studies of High-Efficiency Advanced Fuel Fusion Reactors, Electric Power Research Institute, EPRI-ER-919, December 1978.

(3.23) B.G. Logan, An Advanced-Fuel Variant for ESECOM: D^3He Fusion Using Direct Conversion of Microwave Synchrotron Radiation, Presentation to the Committee on Environmental, Safety and Economic Aspects of Magnetic Fusion Energy, Lawrence Livermore National Laboratory, April 1986.

(3.24) Report by the Committee on Environmental, Safety and Economic Aspects of Magnetic Fusion Energy, Final Report, U.S. DOE, to be issued, 1987.

Chapter 4
Fuel Cycle Systems

The fuel cycle systems consist of all the subsystems of the fusion reactor which are needed to process and handle the fuel components. These include: the plasma exhaust/vacuum system, the exhaust impurity removal system, the isotopic separation systems, fuel storage, the fuel injection system, the atmospheric tritium recovery system, the tritiated waste processing system, and the blanket tritium recovery system (DT).

Burnt gases are removed from the plasma chamber by the exhaust/vacuum system. This system must be capable of reaching and maintaining very low pressures (10^{-5} - 10^{-7} kPa) and must offer a very large pumping capacity. Compound cryopumps are well suited to this operation. Gases being evacuated from the torus will include hydrogen (H_2, HD, HT, D_2, DT and T_2), helium (^{3}He and ^{4}He), along with gaseous impurities coming from the walls. It is also possible to find oxygen, nitrogen, water vapor, carbon monoxide, carbon dioxide, ammonia, methane and other hydrocarbons.

Before isotopic separation can be performed, impurities must be extracted from the exhaust stream. Helium is initially separated from the other gases at the compound cryopumps. If it is desired to recover helium-3, the stream containing the helium isotopes is directed to the helium isotope separation system. The mixture of hydrogen isotopes and impurities is passed through several chemical process beds so that the impurities can be removed and either stored in the beds or passed out of the facility after a final processing in the tritium waste treatment system. Once the impurities are removed, a relatively pure mixture of hydrogen isotopes can be delivered to the hydrogen isotope separation system.

Separation and enrichment of the isotopes will be performed according to device specific requirements. Cryogenic distillation seems to be well suited for this task, for both hydrogen and helium isotopes. The hydrogen isotopes can be isotopically distilled at $\sim$ 20 K. In addition to the stream from the plasma exhaust, there will be an input stream from the blanket tritium recovery system, for the DT reactors, consisting primarily of tritium, with a small amount of protium. Also, there may be an input stream from the low level tritiated water processing and air processing subsystems, containing largely protium with smaller amounts of tritium and deuterium. Cryogenic distillation of helium isotopes (at $\sim$ 4 K) appears straightforward, and separation factors higher than for hydrogen isotopes have been reported [4.1].

Once separated, the fuel constituents can be stored until they are needed. Storage is required for both the short term to smooth out supply and demand transients and for the long term to provide fuel for reactor operation in the event that the upstream fuel system is non-operational. When needed, the fuel components can be combined to form the proper fueling mixture and injected into the torus.

A tritium recovery system may be needed to process tritium contaminated atmospheres. The contaminated gas is processed by being continuously pumped through a catalytic bed where tritium gas is converted to tritiated water. The cooled gas is directed to a molecular sieve or cold trap where the tritiated water is captured, reducing tritium in these streams to acceptable levels for discharge.

The blanket tritium recovery system is needed for the DT reactors to recover the tritium bred in the blanket. For the liquid lithium breeder used in the designs considered in this work, a molten salt extraction process is most attractive for removing the tritium.

In the following sections, each of the fuel cycle subsystems will be described in more detail. An attempt to characterize particular aspects (i.e. equipment size and system capacities) of some of the components of the fuel handling systems for the

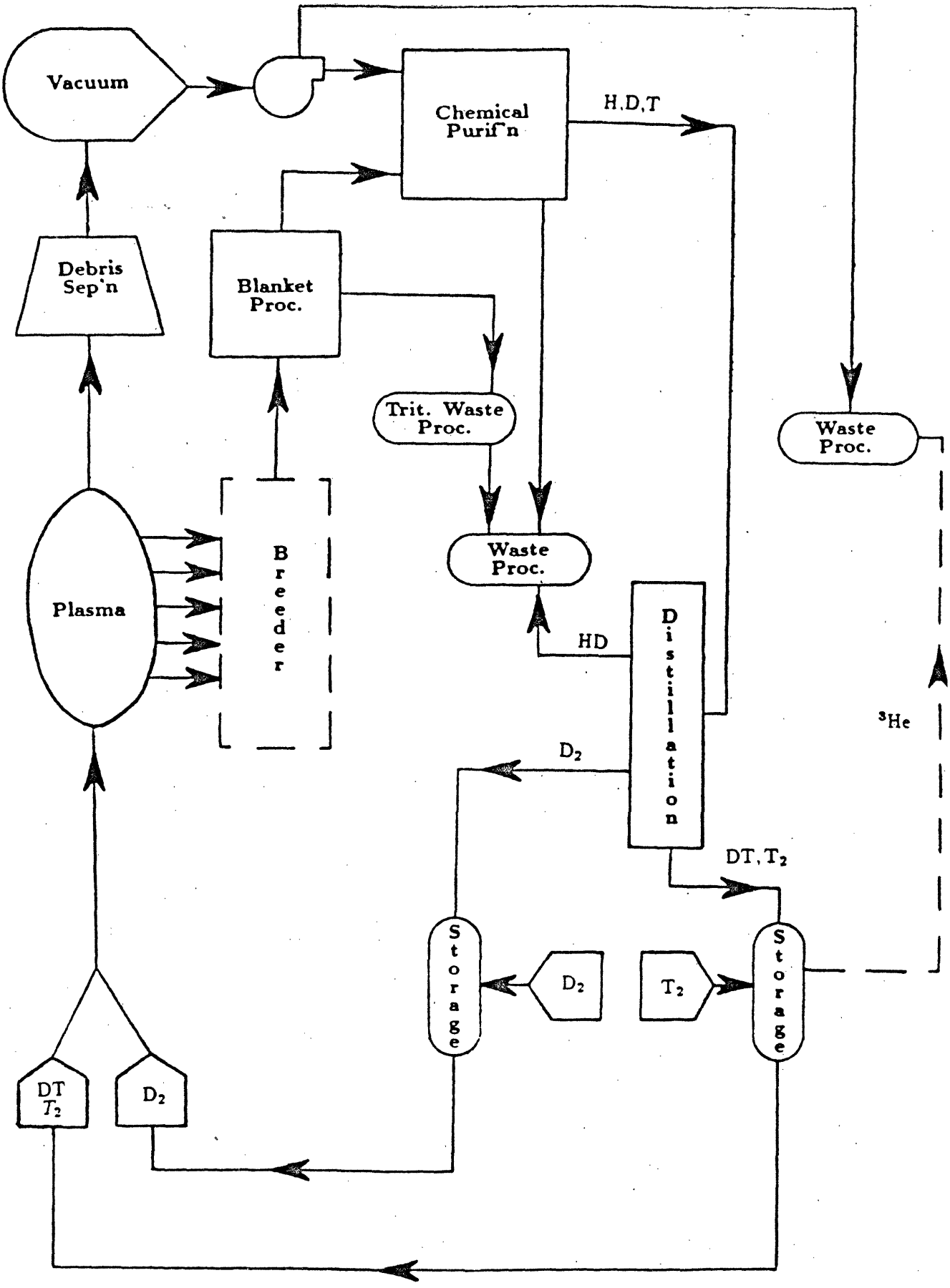

Figure 4.1: Schematic of DT Fuel Processing System

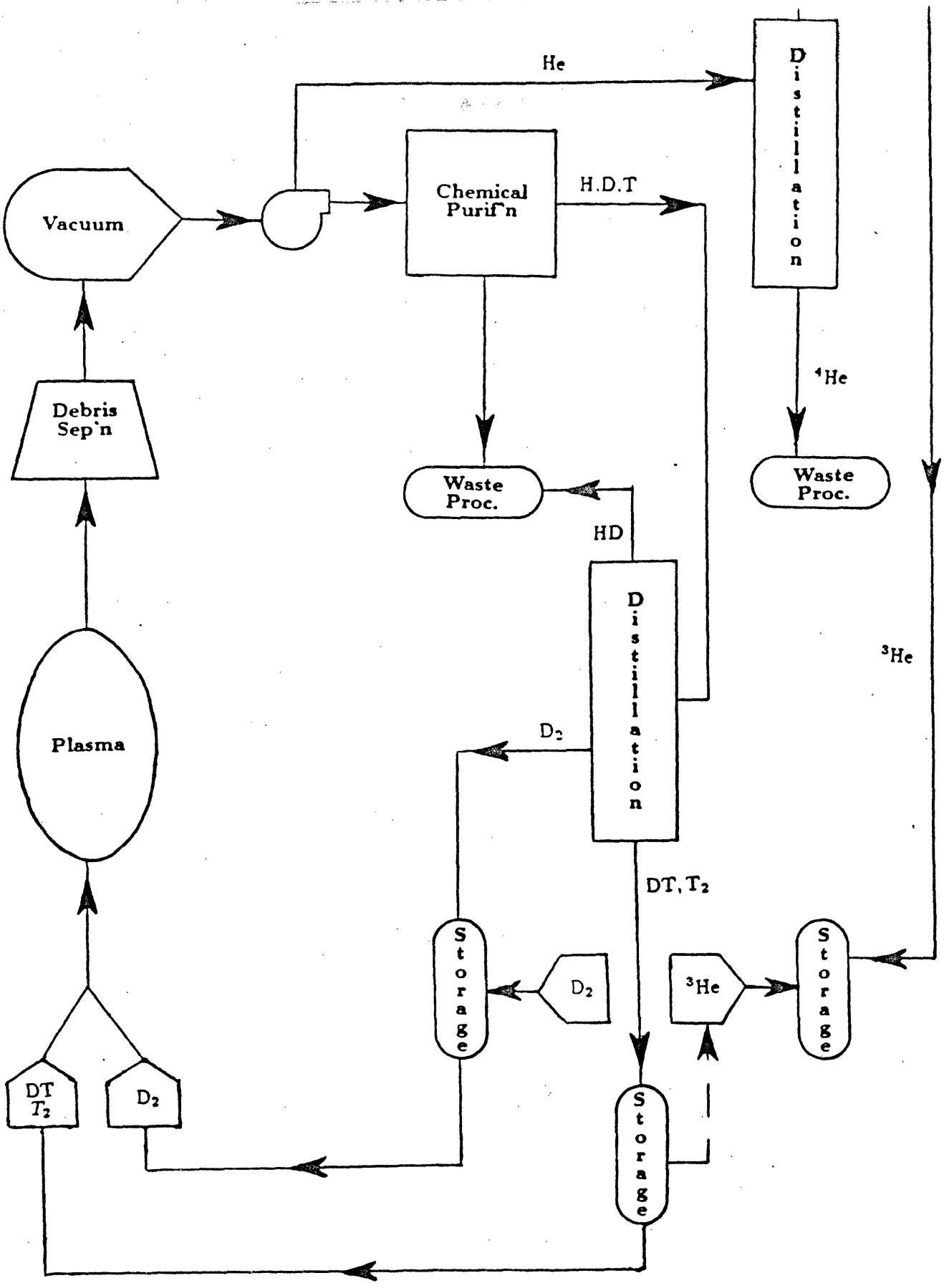

Figure 4.2: Schematic of DD Fuel Processing System

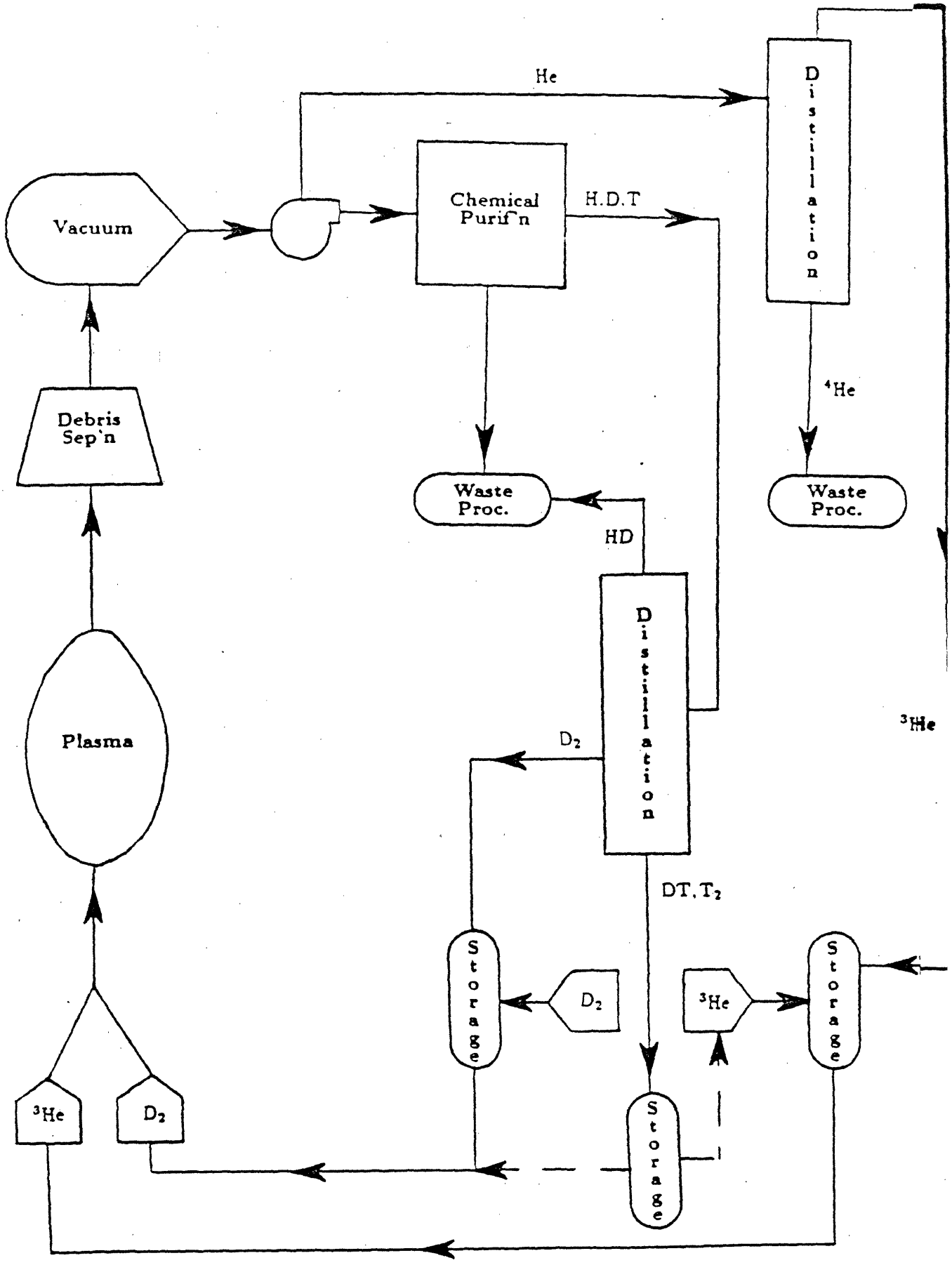

Figure 4.3: Schematic of DHe Fuel Processing System

designs considered in this work has been made. The design differences amongst the DT, DD and DHe fuel cycles will be discussed. Schematics of the fuel processing systems for each of the fuel cycles are shown in figures 4.1, 4.2 and 4.3. There is very little difference in the fuel handling systems for the different values of beta for a given fuel cycle.

4.1 Vacuum System

The primary requirement of the vacuum system is to remove non-fusing plasma ash particles, such as protons, alpha particles and impurities formed from interactions with wall materials, from the torus. It is desirable for this system to achieve good reliability and maintainability, and to have minimum tritium inventory, minimal neutron streaming and minimum number of vacuum ducts within the system. Tradeoffs between these design objectives are necessary since they tend to conflict with one another. Maximizing helium pumping would maximize plasma purity, but it would require more and/or larger vacuum ducts leading to excessive neutron and gamma streaming. It would also remove large amounts of unburnt tritium leading to large tritium inventories in the vacuum pumps and the fuel recycle systems. In the STARFIRE report [4.2], a number of analyses were performed to determine how to best satisfy these conflicting design objectives. The recommendations provided there were followed in designing the vacuum systems here to ensure a minimum amount of neutron streaming and adequate ash removal.

A pumped limiter has been used for the vacuum system consisting of a toroidal "belt" located at the outboard midplane. The components of this system include the limiter slots, the limiter duct, the plenum, the vacuum ducts and the cryopumps (see figure 4.4). There are two limiter slots located between the back of the limiter and the first wall, above and below the reactor midplane. The orifice extending from the limiter slots through the blanket to the plenum region is the limiter duct. The plenum is the open region behind the blanket and serves to provide a high

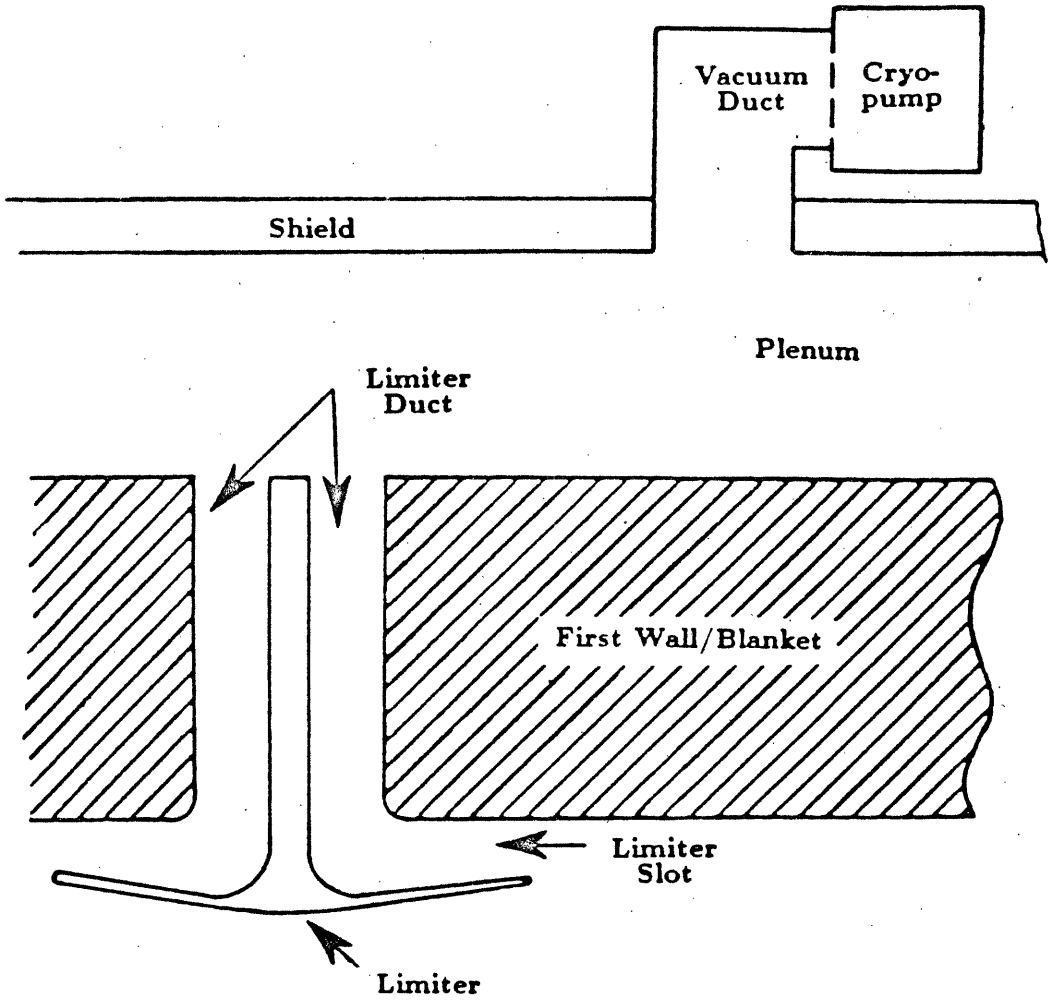

Figure 4.4: Geometric Representation of Limiter/Vacuum System

conductance † pathway to the vacuum ducts while hindering neutron streaming. The limiter slots, the limiter ducts and the plenum region extend around the torus circumference and are symmetric about the reactor midplane. The circular vacuum ducts connect the vacuum pumps to the plenum region. The pumps are located below the reactor.

As in STARFIRE [4.2], evacuation is achieved using compound cryopumps. They provide high pumping speeds, cleanliness, reliability/maintainability, tritium compatibility and have no moving parts. However, the cryopumps are batch pumping devices, and undesirable holdup of tritium within the pumps is unavoidable. The pumps remove hydrogen isotopes and any impurities by cryocondensation on a 4 K panel; helium is removed by cryosorption on a separate refrigerated panel. Tritiated water vapor and ammonia can be separated from the stream within the pump if a liquid nitrogen baffle is incorporated. These impurities can then be easily routed to the most advantageous process beds. Helium is separated from the bulk of the plasma exhaust within the cryopumps. The cryocondensing panel yields the hydrogen isotopes plus some hydrocarbons and argon; pure helium is found on the cryosorbing panel. Most cryosorbers capable of pumping pure helium are quickly inactivated by hydrogens, which condense and freeze on their surfaces. If the condensing chevrons are located in front of the cryosorbers, the fouling species can be intercepted before reaching the cryosorbers, circumventing the problem. This type of pump is one of three candidates being employed at the Tritium Systems Test Assembly (TSTA) for long term tritium pumping experiments [4.3].

The vacuum pumps must be regenerated on a regular basis. Frequent regeneration will minimize the tritium inventory. However, this may have a deleterious effect on the valve lifetime. A two hour regeneration period for the DT reactor was

† Conductance refers to the ease with which the gas flows through a given component of the vacuum system; it depends on whether molecular-wall interactions (molecular flow) or molecule-molecule interactions (viscous flow) are dominant.

thought to be suitable, giving a valve life of two years [4.2, 4.4]. The regeneration time can be extended for the advanced fuels because of the greatly reduced quantities of tritium in the plasma exhaust. A regeneration time of 32 hours was selected, as in the WILDCAT study [4.5]. With this scenario, the valves would last for the entire plant lifetime. For regeneration of the cryopumps, a series of hermetic, tritium compatible mechanical pumps can be employed. Such a series, consisting of a magnetic-bearing turbopump, a moving spiral pump and a two-stage metal bellows pump, has performed satisfactorily and was not degraded by a tritium environment [4.6].

The vacuum systems for the fusion reactors examined in this work have been designed. The conductance analysis followed the procedure outlined in the DEMO report [4.4] and is summarized in appendix D. Vacuum system parameters for the three fuel cycles are listed in tables 4.1, 4.2 and 4.3. There is not a great variation amongst the designs having different values of beta since the vacuum system parameters depend largely on the exhaust rates from the vacuum chamber, which are constant for a given fuel cycle.

The DT reactors utilize 28 cryopumps, 1.2 m in diameter, on 14 vacuum ducts. Two pumps are provided on each duct so that regeneration of one of them can be accomplished during plasma operation. The 14 operating pumps provide sufficient pumping capacity to remove the helium ash at its production rate, and the tritium inventory in each is kept to below 10 g. Because of the need for higher plasma purity to maintain the burn, the advanced fuel reactors have greater pumping requirements. The DD reactors employ 32 cyropumps on 16 vacuum ducts and the DHe reactor uses 48 pumps on 24 ducts. The fact that the helium production rate in the DHe plasma is greater than in the DD plasma combined with the need for a high purity plasma requires this system to have the greatest pumping capacity. Because of the high exhaust rate, large quantities of all species will be recirculated. To accommodate the greater gas load, a larger plenum and larger vacuum ducts as well as more pumps must be incorporated into the vacuum system. The alpha pro-

Table 4.1: Vacuum System Parameters for DT Reactors

Parameter	Low Beta (5 %)	Medium Beta (10 %)	High Beta (20 %)
Number of pumps	14	14	14
Regeneration time (h)	2	2	2
Helium pressure in limiter slot (Pa)	0.042	0.053	0.065
Hydrogen pressure in limiter slot (Pa)	0.598	0.762	0.936
Total limiter gas load ($Pa \cdot m^3/sec$)	32.76	32.76	32.76
Helium limiter gas load ($Pa \cdot m^3/sec$)	4.89	4.89	4.89
Hydrogen limiter gas load ($Pa \cdot m^3/sec$)	27.87	27.87	27.87
Limiter slot helium conductance (m^3/sec)	1511	1290	1127
Limiter duct helium conductance (m^3/sec)	2776	2381	2080
Plenum helium conductance (m^3/sec)	5326	4617	4097
Vacuum duct helium conductance (m^3/sec)	81	81	81
Pump conductance for helium (m^3/sec)	70	70	70
Effective conductance for helium (m^3/sec)	320	311	303
Required helium pumping speed (m^3/sec)	236	186	152
Limiter slot hydrogen conductance (m^3/sec)	1906	1627	1422
Limiter duct hydrogen conductance (m^3/sec)	3502	3003	2624
Plenum hydrogen conductance (m^3/sec)	6718	5823	5168
Vacuum duct hydrogen conductance (m^3/sec)	102	102	102
Pump conductance for hydrogen (m^3/sec)	127	127	127
Effective conductance for hydrogen (m^3/sec)	448	434	421
Required hydrogen pumping speed (m^3/sec)	69	54	47
Tritium Exhausted (g/day)	1598	1598	1598
Deuterium Exhausted (g/day)	1067	1067	1067
Protium Exhausted (g/day)	0.5	0.5	0.6
Helium-3 Exhausted (g/day)	1.6	1.6	1.6
Helium-4 Exhausted (g/day)	742	742	742
Tritium inventory per pump (g)	9.5	9.5	9.5
Total Tritium in pumps (g)	133	133	133

Table 4.2: Vacuum System Parameters for DD Reactors

Parameter	Low Beta (5 %)	Medium Beta (10 %)	High Beta (20 %)
Number of pumps	16	16	16
Regeneration time (h)	32	32	32
Helium pressure (Pa)	0.027	0.044	0.065
Hydrogen pressure (Pa)	0.652	1.043	1.559
Total gas load ($Pa \cdot m^3/sec$)	41.37	41.37	41.38
Helium gas load ($Pa \cdot m^3/sec$)	3.92	3.92	3.92
Hydrogen gas load ($Pa \cdot m^3/sec$)	37.45	37.45	37.46
Limiter slot helium conductance (m^3/sec)	2712	1989	1525
Limiter duct helium conductance (m^3/sec)	4474	3281	2516
Plenum helium conductance (m^3/sec)	9316	7009	5528
Vacuum duct helium conductance (m^3/sec)	86	85	86
Pump conductance for helium (m^3/sec)	75	75	75
Effective conductance for helium (m^3/sec)	407	388	369
Required helium pumping speed (m^3/sec)	287	180	120
Limiter slot hydrogen conductance (m^3/sec)	3661	2686	2059
Limiter duct hydrogen conductance (m^3/sec)	6040	4430	3397
Plenum hydrogen conductance (m^3/sec)	12578	9463	7464
Vacuum duct hydrogen conductance (m^3/sec)	116	116	116
Pump conductance for hydrogen (m^3/sec)	144	144	144
Effective conductance for hydrogen (m^3/sec)	612	581	550
Required hydrogen pumping speed (m^3/sec)	86	54	36
Tritium Exhausted (g/day)	16	16	16
Deuterium Exhausted (g/day)	2687	2687	2687
Protium Exhausted (g/day)	86	86	86
Helium-3 Exhausted (g/day)	198	198	198
Helium-4 Exhausted (g/day)	334	334	334
Tritium inventory per pump (g)	1.3	1.3	1.3
Total Tritium in pumps (g)	21	21	21

Table 4.3: Vacuum System Parameters for DT, DD and DHe Reactors

Parameter	DT	DD	DHe
Number of pumps	14	16	24
Regeneration time (h)	2	32	32
Helium pressure (Pa)	0.053	0.044	0.533
Hydrogen pressure (Pa)	0.762	1.043	0.510
Total gas load ($Pa \cdot m^3/sec$)	32.76	41.37	253.48
Helium gas load ($Pa \cdot m^3/sec$)	4.89	3.92	184.50
Hydrogen gas load ($Pa \cdot m^3/sec$)	27.87	37.45	68.98
Limiter slot helium conductance (m^3/sec)	1290	1989	2266
Limiter duct helium conductance (m^3/sec)	2381	3281	5069
Plenum helium conductance (m^3/sec)	4617	7009	8978
Vacuum duct helium conductance (m^3/sec)	81	86	145
Pump conductance for helium (m^3/sec)	70	75	126
Effective conductance for helium (m^3/sec)	311	388	872
Required helium pumping speed (m^3/sec)	186	180	684
Limiter slot hydrogen conductance (m^3/sec)	1627	2686	2830
Limiter duct hydrogen conductance (m^3/sec)	3003	4430	6330
Plenum hydrogen conductance (m^3/sec)	5823	9463	11211
Vacuum duct hydrogen conductance (m^3/sec)	102	116	181
Pump conductance for hydrogen (m^3/sec)	127	144	225
Effective conductance for hydrogen (m^3/sec)	434	581	1192
Required hydrogen pumping speed (m^3/sec)	54	54	201
Tritium Exhausted (g/day)	1598	16	20
Deuterium Exhausted (g/day)	1067	2687	4920
Protium Exhausted (g/day)	0.5	86	176
Helium-3 Exhausted (g/day)	1.6	198	20663
Helium-4 Exhausted (g/day)	742	334	672
Tritium inventory per pump (g)	9.5	1.3	1.1
Total Tritium in pumps (g)	133	21	26

duction rate is lower in the DD plasma due to fewer DHe reactions. Consequently, the pumping capacity need not be as large for the DD reactors as for the DHe reactor. However, the total gas load for DD is greater than for DT. The tolerable level of impurities is lower for DD so that a somewhat greater removal rate of plasma exhaust is required to offset the production rate of impurities and maintain a lower steady state density of ash.

The tritium inventory in the DT pumps is 9.5 g. This is substantially larger than either of the advanced fuels despite the shorter regeneration period because of the much higher tritium content of the plasma exhaust. Although the total tritium held up in the cryopumps of the DHe system exceeds that of the DD system, the tritium inventory per pump is almost the same as for the DD system. This is a consequence of the greater number of pumps needed to handle the higher recirculation rate of species in the DHe system.

4.2 Impurity Removal System

The primary function of this system is to remove impurities in the form of argon, tritiated methane, water, and ammonia from the reactor exhaust stream and to recover the tritium for reuse from the tritiated impurities. This step is crucial since if the other molecular species were present in the feed to the hydrogen isotope separation system, they would freeze and plug the low temperature distillation columns. Helium is separated from the impure reactor exhaust gases by operation of the compound cryopump at the reactor (helium is collected on one adsorbent surface and all other species are collected on another surface). This separation is easily maintained during regeneration of the cryopumps [4.7]. An analysis to determine the impurities other than alpha and protium ash was not performed as part of this work. This should not have an effect on the outcome of this study. Consequently, the required impurity removal capacity for the present designs was not evaluated at this time. Nevertheless, a brief account of candidate impurity

removal schemes will be given here.

Hot metal catalyst beds can be used to achieve separation of the impurities [4.3, 4.8]. The impurity stream can first be passed over a uranium bed at 1170 K to remove any free oxygen, nitrogen and carbon, forming oxides, nitrides and carbides (see figure 4.5). Cryogenic adsorption on a molecular sieve bed at 77 K will remove all other impurities (DTO, N_2O, NO_2. CO_2, CO, Ar, methane), leaving a stream of hydrogen isotopes suitable as feed for the isotope separation system. Upon regeneration of the molecular sieve beds, the stream is directed to a titanium getter bed at 500 K, where hydrides are formed and argon is eliminated from the system. Subsequently, the hydrogens are regenerated from the titanium bed by heating to 1170 K and rerouted to the isotope separation system. Upon further heating of the molecular sieve bed, other adsorbed species are evolved. At this time, the stream is directed to a CuO/MnO_2 catalyst recombiner where hydrocarbons are oxidized to DTO and CO_2 at 800 K. The water is condensed in a cold trap at 77 K while the impurities (CO, CO_2, N_2O, NO_2, Ar) are exhausted. Vaporized water from the cold trap is reacted with uranium at 750 K to liberate hydrogen isotopes and form uranium oxides. The use of a ceramic electrolysis cell may be used as an alternative to decompose tritiated water [4.9]. This stream is then passed over a catalyst bed at 450 K where any free oxygen can be removed. The stream then meets the outflow of the initial feed from the uranium bed at 1170 K (which removes O, C, and N from the feed coming from the cryopumps) and both enter the molecular sieve bed at 77 K as described above.

Another approach to exhaust impurity removal utilizes a Pd-Ag permeation membrane assembly to extract pure hydrogen isotopes from the plasma exhaust stream, leaving a mixture of carbon monoxide, carbon dioxide, tritiated methane, water vapor, ammonia and residual hydrogen for subsequent processing [4.9, 4.10]. Elements of the Pd-Ag diffuser would be operated at 300 °C to minimize permeation through the surrounding structure. Hydrogen isotopes are drawn through the membrane by a backing pressure of less than 100 Pa to minimize the carryover of

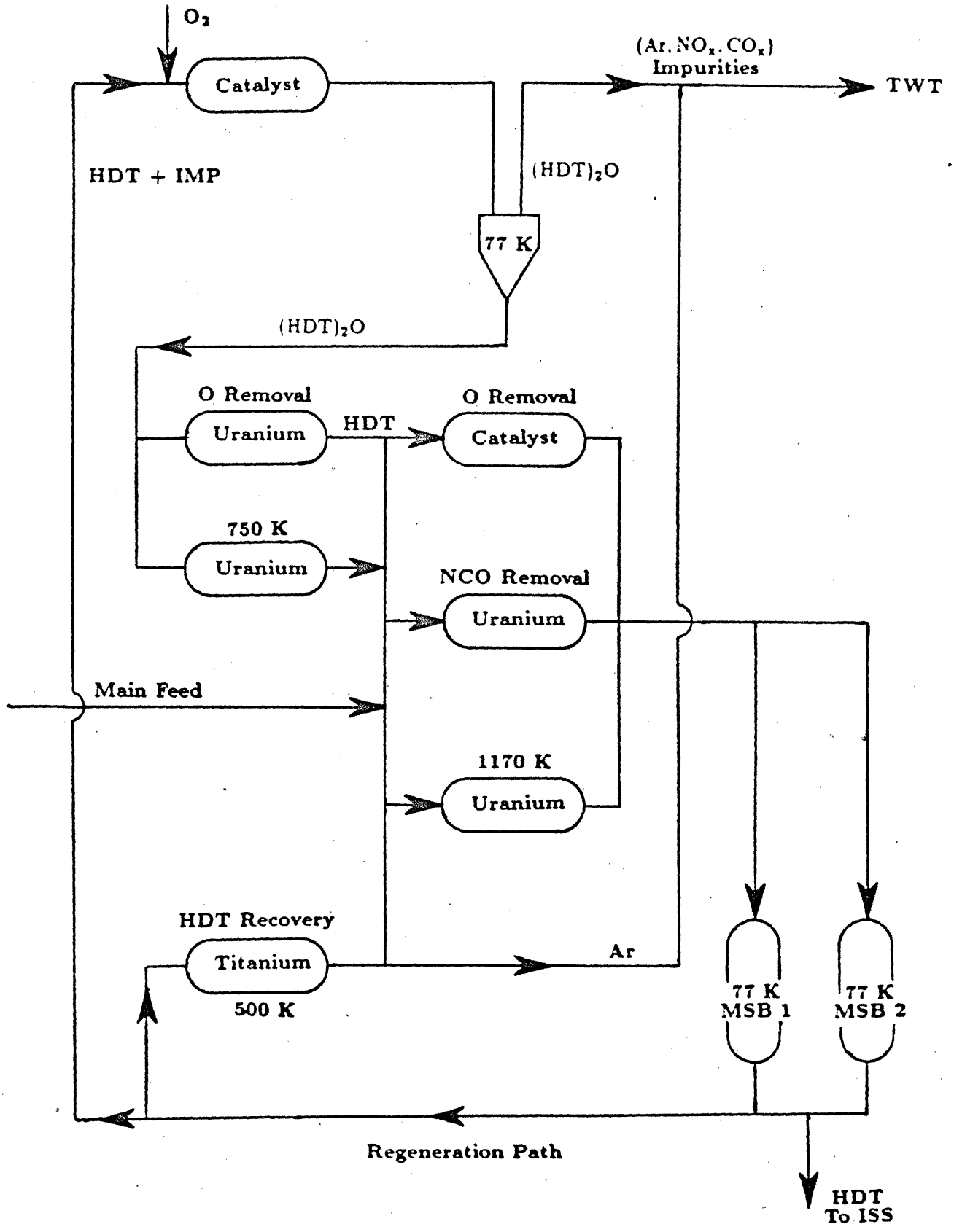

Figure 4.5: Schematic of Impurity Removal System [4.3]

DT with the impurities. The stream which does not pass through the permeator membrane would be passed over hot metal beds to react the impurities forming carbides, nitrides and oxides, liberating hydrogen isotopes. The later could be passed through another Pd-Ag diffuser or be adsorbed on a low temperature uranium bed. Although the palladium diffuser can produce a hydrogen isotope stream free of impurities, it cannot produce an impurity stream free of hydrogen isotopes. Other disadvantages include the need for elevated pressures, potential for brittle failure during temperature recycling, and poisoning by methane and ammonia.

4.3 Isotope Separation Systems

The plasma exhaust contains a mixture of hydrogen isotopes, helium isotopes and various impurities. Helium isotopes are separated from the mixture in the cryopumps; the outflow from the impurity removal system provides a pure stream of hydrogen isotopes. The hydrogen isotopes must be separated so that the appropriate constituents for fueling are available. High purity deuterium is needed for all of the fuel cycles. A stream of relatively high tritium concentration is required for the DT system. A mixed D/T stream is required for achieving ignition of the plasma for the advanced fuels. This fueling mixture would be altered once the operating temperature for the advanced fuel cycles was achieved. Separation of helium isotopes is required for the DHe fuel cycle. This is also likely for the DD system since the plasma exhaust contains significant quantities of ^{3}He. The very low quantity of ^{3}He in the DT exhaust does not warrant separation.

The systems required to achieve the separation of the hydrogen and helium isotopes are described below. Cryogenic distillation is the preferred approach in both cases.

4.3.1 Hydrogen Isotope Separation

Many possible methods exist for the separation of mixtures of H_2, HD, HT, D_2, DT and T_2 which exit the fusion reactor chamber. These include cryogenic distillation, thermal diffusion, palladium diffusion, gas chromatography, differential hydriding and laser activated separation processes [4.11]. Cryogenic distillation is probably the best understood and has been successfully employed on a large scale in industry for H-D-T separation. For fusion reactor applications, the system must be capable of providing deuterium and tritium streams for fueling and a waste stream of H_2 with trace amounts of HD suitable for discharge to the environment.

Cryogenic distillation provides relatively large separation factors, high throughput, short start-up times and a large degree of design flexibility. Steady state operation allows for good control. The operating pressure is approximately one atmosphere and there are no large pressure gradients within the system. Although there are large temperature gradients there is no thermal cycling during operation, resulting in fewer mechanical strains to the system. There are some drawbacks to this process, however. A relatively large inventory of tritium is held up as surface film on the column packing and walls or as bulk liquid in the reboiler. Refrigeration power requirements for maintaining the low temperature ($\sim$ 25 K) are large.

Some basic principles must be considered in the design of an isotope separation system based on distillation. The most volatile of the hydrogenic molecules is H_2, followed by the others in order of increasing molecular weight (HD, HT, D_2, DT and T_2). The columns are generally designed to provide a specified separation between any two species, called the light and heavy keys, which are usually adjacent on the volatility scale. The lighter and more volatile key is recovered in the distillate or top product, while the heavier and less volatile key is recovered in the reboiler as the bottoms product. At least one column is required for each pure product.

Because it is undesirable to inject protium back into the torus, and because it is unacceptable to release tritium to the environment, the HT form of molecular hydrogen must somehow be eliminated. Half of the protium in the system will be in this form [4.11]. Removal of this undesirable species can be accomplished by promoting the equilibrium:

$$HT + D_2 \Longleftrightarrow HD + DT \tag{4.1}$$

This liberates HD which can be removed as an innocuous distillate product and be discharged directly from the plant in a stream free of tritium. The DT can be recovered for recycling into the fuel stream. This operation can be carried out in room temperature catalytic equilibrators fed with a stream of pure D_2, strategically located between distillation columns.

The radioactive nature of tritium cannot be ignored. Its decay heat of 0.326 W/g manifests itself as a heat leak to the column or reboiler. To prevent liquid streams in the stripping sections of the columns from decreasing to dryness as a result of the decay heat, cooling matched to remove this heat must be provided stage by stage.

Because cryogenic distillation involves tritium in a condensed state, a disadvantage of the process is its relatively large tritium inventory within the system. This results from liquid holdup on the column packing or on the column walls and from the bulk liquid contained in the reboiler. However, if no high purity tritium stream is needed, this inventory could be reduced. This is the case for advanced fuel reactors, and also for DT reactors if high purity tritium is not needed for neutral beam injections. If another mode of fueling is employed (i.e. gas puffing), the required fueling mixtures can be prepared by varying the flows of a pure D_2 stream and a mixed DT/D_2 stream.

The feed stream to the isotope separation system comes directly from the impurity removal system. It will consist of the various hydrogenic molecules in their equilibrium concentrations and containing on the order of 1 ppm of total noncondensible impurities [4.12].

Since six species are being separated in the hydrogen isotope separation system, calculations to evaluate flow rates and compositions are quite involved. Large computer codes are available to perform these calculations [4.13, 4.14]. However, it was felt that such an elaborate model would not enhance the understanding the systems required for this study. Furthermore, as indicated in section 4.8, the fuel cycle systems contribute at most 7 % (for the DT fuel cycle) to the total direct cost of the plant. Thus, economic uncertainties due to lack of design detail will not have a significant impact. A general description of the expected requirements for hydrogen isotope separation for each of the fuel cycles is given below. A summary of the isotope separations system parameters is given in table 4.4.

For the DT reactors considered in this study, the feed to the hydrogen isotope separation system consists of an equimolar mixture of deuterium and tritium, with a small amount of protium. A three column cascade is needed to produce the desired product streams: pure D_2, mixed DT/T_2 and a waste stream of HD and H_2. In column 1 (see figure 4.6), the principal separation between recycled fuel and waste is made. The distillate will contain some HT along with HD and H_2. By passing this stream through a chemical equilibrator fed with a large amount of D_2, the formation of HD will be strongly favored. Any unreacted D_2 and the DT formed in the equilibrator will be passed out of the bottom of column 2 and fed back into column 1 at the appropriate location. The distillate from column 2 can be directly eluted to the environment since it is essentially free of tritium. The bottoms from column 1 are fed into column 3. The distillate of column 3 consists of nearly pure deuterium; the reboiler product is a mixture of DT and T_2. From these two streams, it is possible to prepare a wide range of torus fueling mixtures by varying the flow rates. If pure tritium is required, another column would be needed to separate it

Table 4.4: Isotope Separation System Parameters

Parameter	DT	DD	DHe
Flow Rate to Hydrogen Isotope Separation System (mole/d)	1060	1425	2424
Composition of Feed to Hydrogen Isotope Separation System◇ (mole %):			
T	49.95	0.37	0.27
D	49.95	93.64	95.53
H	0.1	5.99	7.20
Number of Columns required for Hydrogen Isotope Separation System	3	2 (3*)	2 (3*)
Flow Rate to Helium Isotope Separation System (mole/d)	-	149	7019
Composition of Feed to Helium Isotope Separation System (mole %):			
^{3}He	-	56	97
^{4}He	-	44	3
Number of Columns required for Helium Isotope Separation System	-	1	10

◇ The feed would actually consist of an equilibrium mixture of H_2, HD, HT, D_2, DT and T_2, but the atomic fractions would be as listed here.

* The third column is needed only during the initial phase of the burn, when large quantities of tritium are supplied to the reactor in order to achieve ignition.

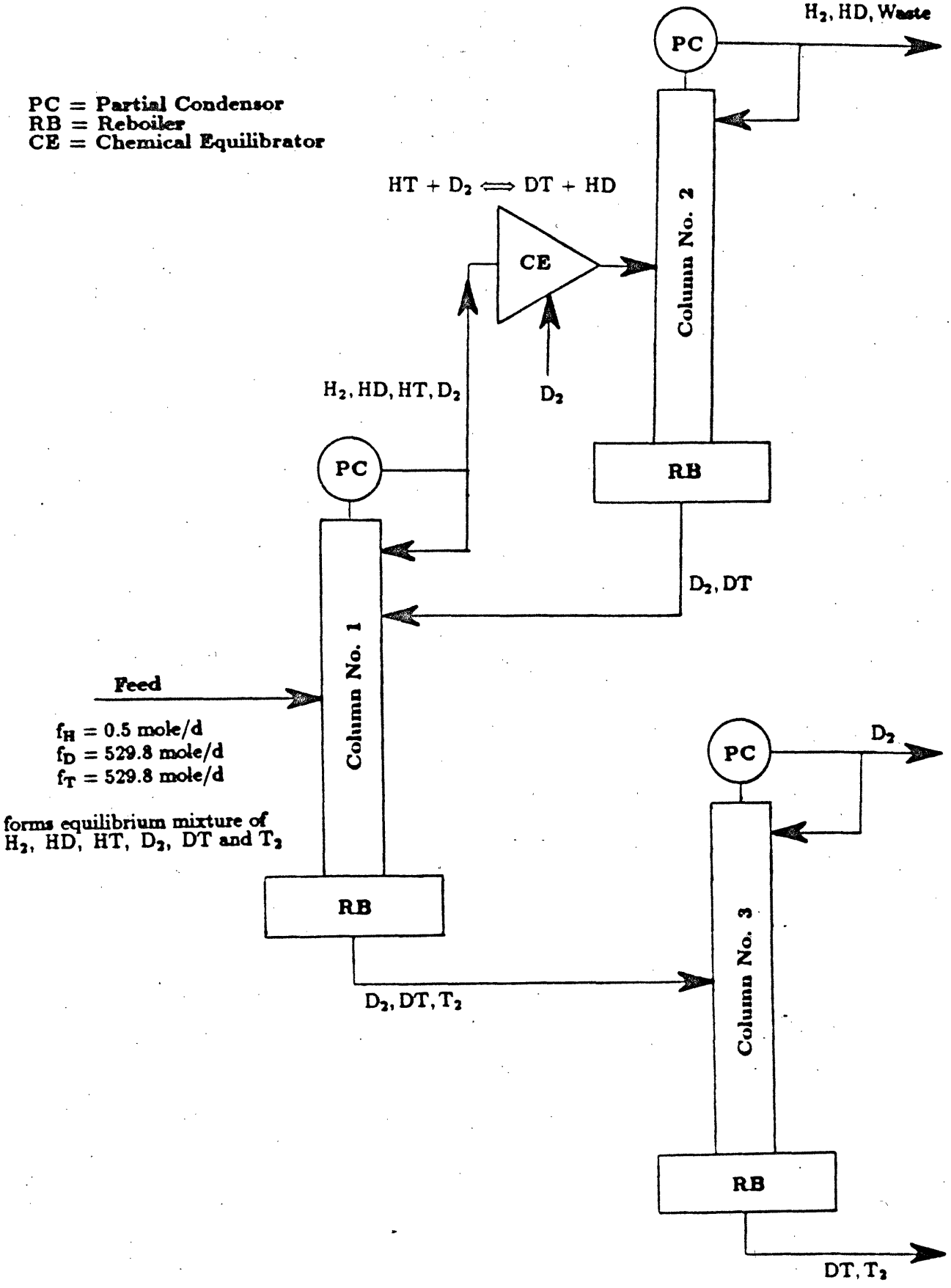

Figure 4.6: DT Hydrogen Isotope Separation System

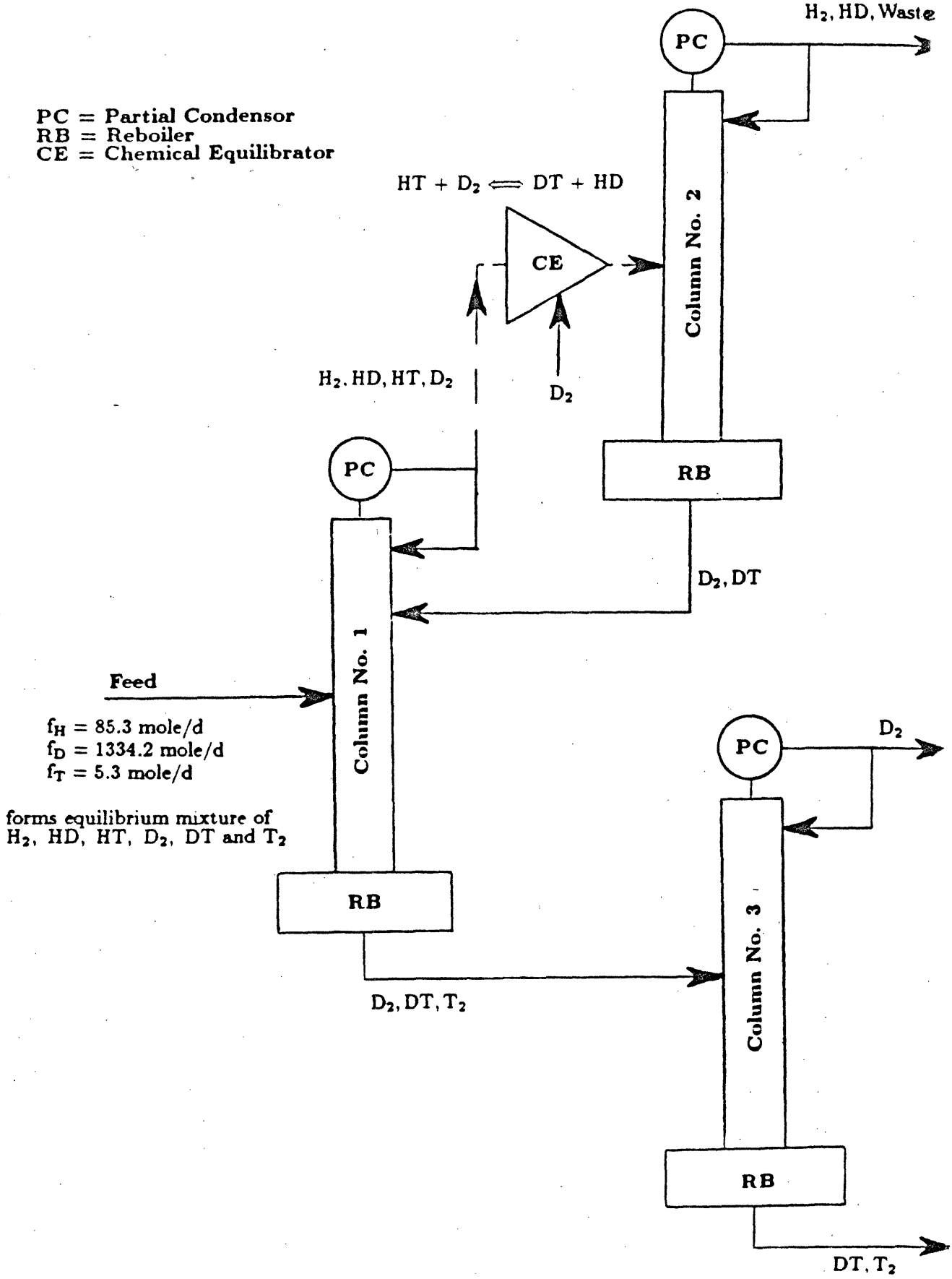

Figure 4.7: DD Hydrogen Isotope Separation System

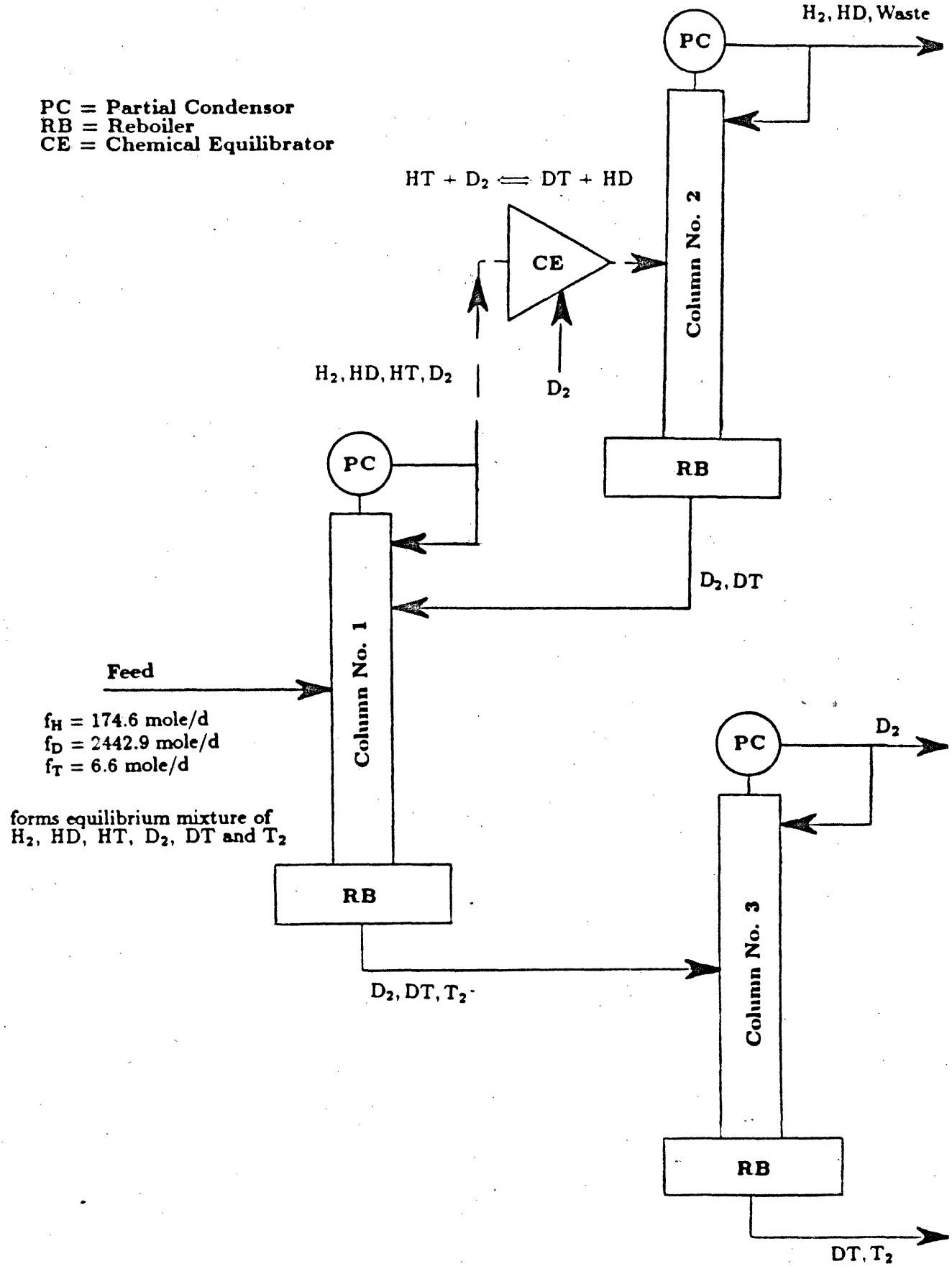

Figure 4.8: DHe Hydrogen Isotope Separation System

from the DT. This, however, would significantly increase the tritium inventory in the isotope separation system [4.11].

The hydrogen isotope separation systems for the DD and DHe fuel cycles are essentially the same (see figures 4.7 and 4.8). The first column separates the three lighter hydrogens from the three heavier hydrogens. To initiate the plasma burn, each of the advanced fuel reactors will require some tritium fueling in order to reach ignition. Consequently, the feed to the isotope separation system shortly after initiating the pulse will contain more tritium than throughout the rest of the burn. Thus, the distillate from column 1 will contain more HT at this time. This must be removed before discharge to the environment. The chemical equilibrator fed with D_2 and column 2 will remove this species from the effluent. Throughout the rest of the burn cycle, the tritium exhausted from the torus (and hence, the HT content of the exhaust) will be substantially lower. As a result, the distillate from column 1 may be safe for immediate discharge without further processing, if the total annual tritium emissions from this system do not exceed 20 Ci [4.12]. Column 2 can then be put on standby. The reboiler product from column 1 is fed to column 3 where the D_2 for fueling is separated. The bottoms from this column (DT/T_2) is sent to storage until it is needed at the start of the next pulse. In the case of steady state systems, this column would not be needed since the primary function of the isotope separation system would be to remove the protium waste from the spent fuel. Start-up tritium could be supplied from a separate source since it would not be needed on a regular basis.

4.3.2 Helium Isotope Separation

The purification of stable rare gas isotopes has generally been performed by thermal diffusion. The separation factor is proportional to the square root of the mass ratio for the species being separated. For helium isotopes, this is 1.15. In order to accomplish separation, the diffusion columns may be many meters tall,

and several of these may be needed in a cascade to obtain the desired product quality. This, in addition to the large electrical power requirements, render this method of separation inefficient.

Cryogenic distillation has also been used effectively to separate helium isotopes. The main advantage of this means of separation over thermal diffusion is the much larger separation factor. For distillation, the separation factor is proportional to the ratio of the vapor pressure of the two species being separated. The minimum value of this for helium isotope separation is 3 at the critical temperature of ^{3}He, 3.2 K. It rises rapidly as the temperature decreases. Other advantages of cryogenic distillation include high throughput, short start-up times and a high degree of design flexibility. Although radioactivity is not a concern for the separation of helium isotopes as it is with hydrogen isotopes, refrigeration requirements are more severe since the separation is performed at a temperature below 4.2 K.

Because only two isotopes of helium must be separated in helium isotope separation system, standard analytical techniques for assessing the separation of a binary mixture by distillation can be applied. A M^{c}Cabe – Thiele analysis [4.15] was employed here to assess the needs of the helium isotope separation systems for the various fuel cycles. A summary of the isotope separation system parameters is given in table 4.4.

Continuous production of 99.95 % ^{3}He has been achieved using cryogenic distillation with a packed column employing a closed cycle ^{3}He refrigerator [4.16, 4.17]. The bottoms product concentration obtained was 99.92 % ^{4}He. A M^{c}Cabe – Thiele analysis of this separation, assuming a saturated vapor feed, indicated that the column provided 15 theoretical stages of separation. With the column height of 30 cm, the height equivalent of a theoretical plate (HETP) was determined as 2 cm. In other work, HETP's ranging from 1 to 8 cm have been reported [4.18]. The fact that only a few centimeters of column length are required for each stage is a reflection of the large separation factor occurring in helium isotope separation.

Helium isotope separation is not included as part of the fuel cycle for the DT fusion reactors. The quantities of ^{3}He being handled are not large enough to warrant recovery. It was assumed that the helium recovered from the cryopumps was directly passed to the waste processing facility with no attempt made to separate the species.

In the case of the DD fuel cycle, however, recovery of ^{3}He appears worthwhile. The quantity of ^{3}He being exhausted from the plasma is $\sim$ 66 mole/d, compared to $\sim$ 0.5 mole/d for DT. A single packed column, 2.1 cm in diameter should accomplish the separation (see figure 4.9). A M^{c}Cabe – Thiele analysis [4.15] indicated that 13 theoretical stages should accomplish the separation. This gives a column height of 26 cm, assuming an HETP of 2 cm. Further details of the design calculations are given in appendix D.

The much greater flow rates for the DHe reactor demand several distillation columns operated in parallel to perform the helium isotope separation. The higher flow rates in the columns necessitate larger diameters to prevent flooding. For columns 9.5 cm in diameter, 5 columns would adequately perform the separation. If 10 columns are operated in parallel, their diameter could be reduced to 6.7 cm for the same product quality. Since the bulk of the flow passes through the enriching or upper part of the column, the column sizing calculations were based on the flow rates here. The lower flow rates of the stripping section would allow for a smaller diameter. The columns could be designed with the larger diameter in the upper section, and be tapered to the smaller diameter below the feed inlet. A M^{c}Cabe – Thiele analysis estimates 14 theoretical stages are needed for the separation. This corresponds to a column height of 28 cm, assuming an HETP of 2 cm. The flows anticipated for a single column (assuming 10 parallel columns will be used to handle the total feed to the helium isotope separation system) are shown in figure 4.10.

The number of stages required for helium isotope separation (as determined by the M^{c}Cabe – Thiele approach) for both the DD and DHe fuel cycles

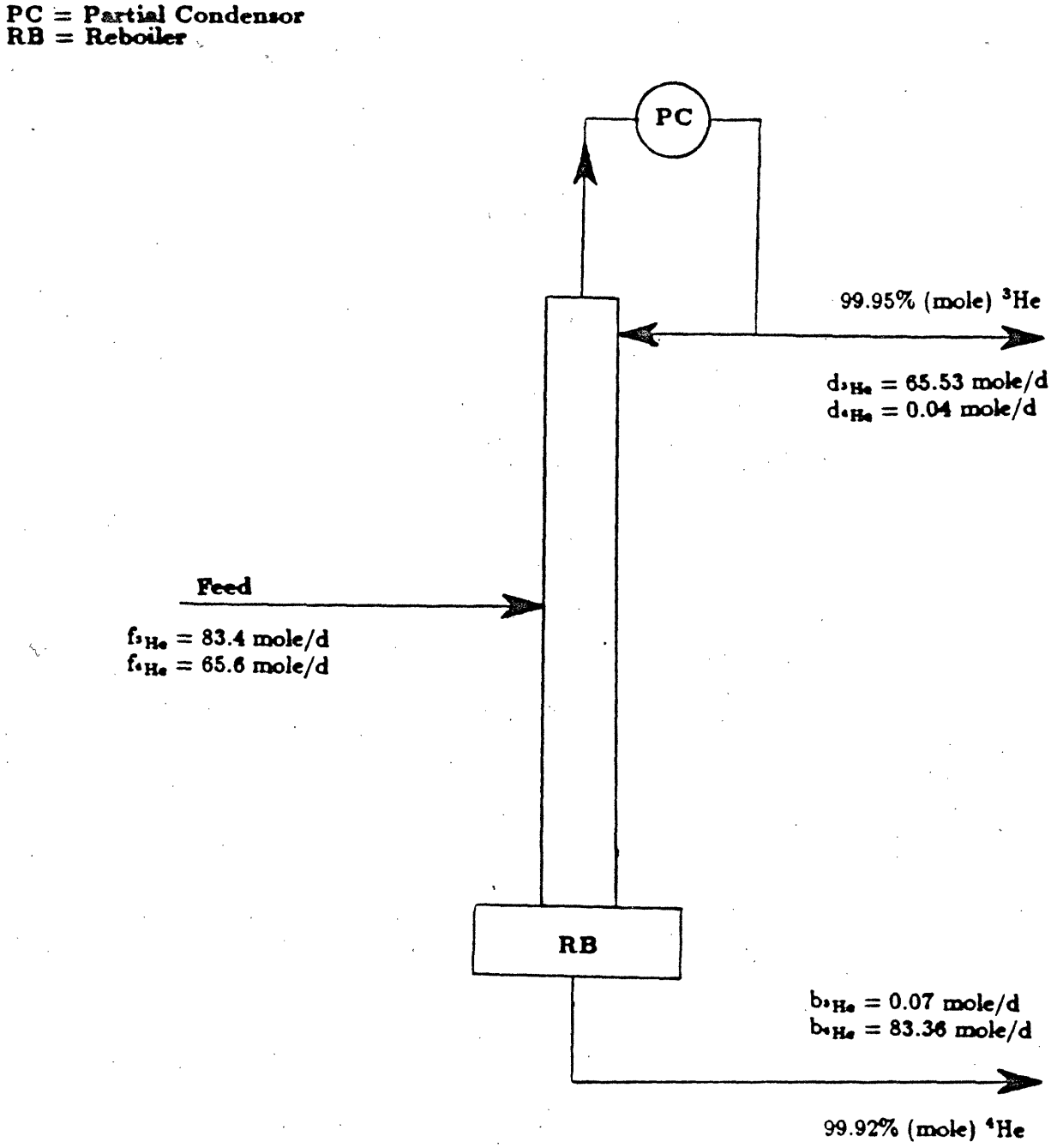

Figure 4.9: DD Helium Isotope Separation System

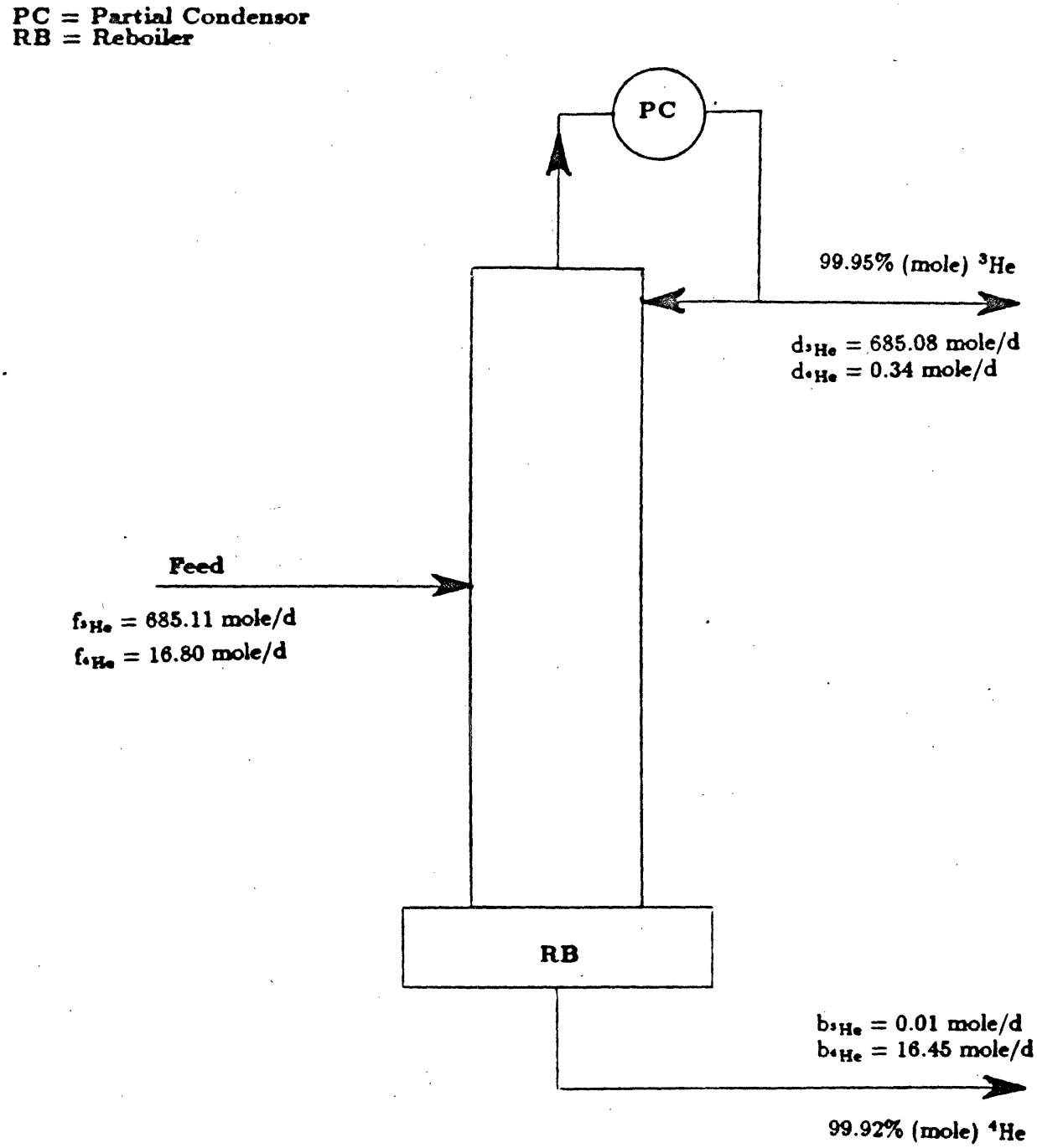

Figure 4.10: DHe Helium Isotope Separation System

agree well with results obtained from an analytical expression (the Fenske equation - see appendix D). It must be pointed out, however, that both M^{c}Cabe – Thiele analysis and use of the Fenske equation assume that the latent heats of the components are nearly equal, that the boiling temperatures are close together, that the relative volatility is roughly constant and that the feed quality is known. Since these conditions are not met in the current problem, the number of stages obtained here is just a rough estimate.

4.4 Fuel Storage and Delivery System

The fuel storage and delivery system must be capable of supplying the fusion reactor with a fuel mixture of very high purity, at the required flowrate and in the correct isotopic proportion of fuel components. Storage of fuel constituents is required for both the short term to smooth out supply and demand transients and for the long term to provide fuel for reactor operation in the event that the upstream fuel system is non-operational. The fuel must be stored in a safe and stable form; the potential for a tritium release to the environment in the event of an accidental system failure must be minimized. The system must also maintain the particulate and molecular impurities in the fuel stream to values below the tolerable limits for efficient operation of the torus. Finally, the injection system must deliver accurate quantities of the fuel mixture into the torus in the given time sequence.

Storage of hydrogen isotopes as a metal matrix has received attention as being an attractive option for this purpose. Uranium forms a stable hydride ($U(H, D, T)_3$) which can accommodate tritium, deuterium or protium in large quantities in a very small space. As much as 10^4 Ci of tritium (1.04 g or 0.34 mole) can be stored on as little as 26.4 g of uranium, although approximately five times this is used in practice. The uranium getter bed is in the form of a metal sponge and is placed in a stainless steel vessel. Although operating conditions should never exceed pressures of 30 psig or temperatures of 550 °C, vessels are designed to withstand the pressure of the

entire tritium inventory in gaseous form [4.19]. The equilibrium partial pressure of hydrogen over the uranium hydride at room temperature is about 0.3 mPa. Even at 400 °C, the dissociation pressure of the hydride is only 40 Pa. Because of this, uranium is an excellent material on which to store the hydrogens, particularly in the case of tritium where immobilization is an important safety concern. The hydrogen isotopes will rapidly desorb when heated to about 700 K, where the equilibrium partial pressure is around 100 kPa. Except in the case of tritium with its ^{3}He decay product, the hydrogen evolved from the getter bed is very pure. Most of the ^{3}He from tritium decay can be pumped off using an auxiliary vacuum system, but there will still be some residual ^{3}He which is released from the UT_3 lattice as the bed is heated to drive off the tritium. Any other impurities which may be evolved during heating can be separated from the hydrogen isotope by passage over a Pd/Ag diffusor and particulates can be removed by passage through a filter.

Due to the hazardous nature of tritium, it is proposed to immobilize this fuel component at the fusion plant as uranium tritide, as described above [4.2, 4.19]. Although it would also be possible to store the deuterium needed for fuel as uranium deuteride, this is not actually necessary since this species is not hazardous and immobilization is not essential. However, some streams coming from the isotopic separation system may contain a mixture of deuterium and tritium (D_2 and DT). For the DD and DHe fuel cycles, storage of this mixture is necessary so that a supply of fuel for start-up of the advanced fuel cycles (by DT ignition followed by thermal runaway) is on hand. Storage of the D_2/DT mixture on uranium beds would be required. High purity D_2 and ^{3}He can be stored in standard pressurized containers according to the same criteria as the industrial storage of hydrogen and helium [4.20].

The fuel is prepared for injection in the fuel blending units or mixing tanks. These vessels are of stainless steel construction, insulated and thermostated for precise control of the content's temperature. The hydrogens may first pass through a Pd/Ag membrane for final purification before entering the tank. Mass spectrometry

can be used to determine the exact composition of the gas in the mixing tank. This can then be adjusted by adding the appropriate component until the desired ratio is achieved. The mixture can subsequently be transferred to the torus injection system. As for STARFIRE [4.2], two blending units are assumed to be adequate for fueling the DT reactors. For the advanced fuels, two units would be used during the burn phase of the pulse and one additional unit would be required for preparing the initial fueling mixture needed for igniting the plasma.

Fuel delivery to the plasma can be performed by either gas puffing or pellet injection. Gas puffing is the simplest fueling technique and has been used effectively to maintain and increase the plasma density over several particle confinement times [4.21]. It consists of injecting cold gas at the plasma boundary. The mechanism by which the center of the tokamak plasma is fueled, however, is not well understood. Repetitive injection of frozen pellets at high speed is also a promising means of carrying fresh fuel across confining magnetic fields to the central plasma core [4.22]. With this method of fueling come the advantages of lower particle losses compared to cold gas inlet at the plasma edge and greater flexibility in tailoring plasma parameter profiles. Both centrifugal and pneumatic injectors are being developed [4.10, 4.23], the latter being preferred for higher injection velocities. Very high injection velocities are required in order to fuel the center of the plasma without large pellets, which can cause excessive plasma density perturbations. Individual D_2 and T_2 pellets 4 mm in diameter, injected once per second at a velocity of 5000 m/s may result in density perturbations of less than 10 % [4.10].

Fuel is injected by through several injector sets spaced at equal intervals around the torus. For pellet fueling, each of these is secondarily contained in a cryogenic injector volume which is filled with the appropriate fuel mixture. The liquid fuel is admitted to the pellet former for injection at at rate determined by the plant needs. Fast acting flow regulating valves can be programmed to admit the gas to the torus at the appropriate rate. The FED will inject 4 mm pellets at a velocity of 2000 m/s at a rate of 20 per second during operation [4.23]. STARFIRE [4.2]

proposes the use of gas puffing for its fueling system. This choice was based on the fairly low refueling rate and the simplicity of the engineering.

Both systems of fueling may be utilized to meet fueling requirements during start-up, burn and shutdown phases of the operating cycle. Gas puffing may be used to backfill the torus prior to start-up and to fuel the torus until a 1 keV plasma is established [4.23]. Frozen deuterium and/or tritium pellets can then be injected to control the plasma density. For fueling of ^{3}He, gas puffing [4.24] or the injection of a ^{3}He neutral beam [4.25] may be envisioned. In the designs considered here, only the gas puffing mode was assumed for fueling the torus. Four puffers were thought to be adequate for the DT and DD reactors; 14 puffers were assumed to be adequate to handle the greater fueling needs of the DHe reactor.

4.5 Atmospheric Tritium Recovery Systems

The atmospheric tritium recovery system is required to treat under normal and/or accident conditions, the atmospheres and exhausts from the reactor building and the rooms housing all the tritium related systems. The atmospheric processing system must be capable of removing airborne tritium, either in the molecular or oxide form, from the reactor building, the fuel processing building and all secondary enclosures internal to these buildings. During normal operation, small amounts of tritium may be routinely released to the reactor building from various components. Expected sources of tritium release include leakage and permeation from the plasma chamber and associated components, leakage from the coolant/heat transfer system and leakage and permeation from fuel handling components. Because of the much greater tritium inventory associated with the DT fuel cycle, the capacity of this system will be greater. The DD and DHe fuel cycles will not require continuous atmospheric processing (see chapter 5). However, some provision for

atmospheric tritium removal in the event of an accident must be available.

A widely used method for tritium removal from air streams is oxidation of tritium in a recombiner containing Pt/Pd catalyst, followed by adsorption of the tritiated water vapor together with water vapor in the air, on molecular sieve driers. Operation of the Pt/Pd catalyst at temperatures around 180 °C avoids the problem of catalyst deactivation by condensed water vapor and increases the tritium conversion rate. The cooled gas is passed to the molecular sieve driers where adsorption occurs. The tritiated water can be recovered from the beds by regeneration, or the molecular sieves can be removed for disposal. Critical features of the system for ensuring effective tritium removal include the efficiency of the recombiner, the efficiency of the driers and the leak tightness of the reactor hall. Drier efficiency can be enhanced by partially pre-loading the molecular sieve with clean water to promote isotopic exchange with tritiated water molecules.

The availability of an atmospheric cleanup system does not alleviate the need for effective tritium containment. Large atmospheric cleanup systems can be expensive to operate, and efforts should be made to minimize both the capital and operating costs. To minimize releases of airborne tritium, different levels of containment can be used in tritium-related systems. Primary containment within the fuel handling and processing systems consists of the equipment itself. More effective containment is achieved through the use of all metal components. Secondary containment is accomplished through the use of gloveboxes, vacuum jackets, jacketed tubing and nested containers. Routine leakage and permeation of tritium into the environment can be minimized by applying secondary containment. Major maintenance activities, such as replacement of blanket segments, vacuum pumps, impurity control devices and fueling equipment may result in some tritium release due to component offgassing. An atmospheric tritium recovery system may be needed during these times to maintain the tritium concentration at an acceptable level. Operation of these areas at a reduced atmospheric pressure will minimize tritium outleakage from the reactor building.

Personnel access for maintenance is the dominant factor in sizing the required atmosphere detritiation system. For unprotected workers, the tritium concentration must be below $5\mu Ci/m^3$. Bubble suits with an independent air supply are required if a worker spends extended periods at levels above $5\mu Ci/m^3$. These suits provide a safety factor of at least 100 against tritium so that suited workers are permitted in areas with tritium levels up to $500\mu Ci/m^3$. The degree of protection affects worker productivity, and the tritium concentration level to be maintained also significantly affects the capital and operating costs associated with the air detritiation system. The productivity of a worker in a bubble suit is reduced by a factor of two [4.26, 4.27] (see table 4.5). It has been suggested [4.26, 4.27] that the best strategy for a DT reactor with tritium leakage rates between 15 and 30 Ci/d is a combination of a detritiation system and a bubble suit, where the tritium concentration could be maintained between 5 and $500\mu Ci/m^3$. A study performed to determine the impact of maintenance strategy (i.e. remote vs suited contact vs unsuited contact) [4.27] concluded that maintenance of levels below $50\mu Ci/m^3$ does not appear justified. Also, they concluded that the use of bubble suits at $50\mu Ci/m^3$ does not adversely affect reactor availability. The MARS report [4.20] affirmed that maintaining a building atmosphere of $5\mu Ci/m^3$ would be extremely expensive. They selected an airborne concentration of $50\mu Ci/m^3$ for the MARS reactor hall since this level can be maintained at a reasonable cost, provides a reasonable level for maintenance workers using bubble suits and allows only a minimal release to the environment.

If tritium releases to the reactor hall and inactive auxiliaries during normal operation are below 10 Ci/day, direct emission to the environment without treatment may be possible if the room concentration is kept below $5\mu Ci/m^3$. [4.10, 4.26]. This is the case for the advanced fuel reactors (see chapter 5), where tritium leakage rates are well below 10 Ci/d and the tritium level in the reactor room is less than $5\mu Ci/m^3$. A ventilation system may be used with direct release of reactor room

Table 4.5: Working Environment and Protective Clothing Requirements [4.26]

Room Concentration	Surface Concentration	Clothing Required	Worker Efficiency
~ 0 (uncontrolled areas)	~ 0	None	100%
$< 5\mu Ci/m^3$	$< 50 \frac{counts}{min}$ ($< 2.3 \times 10^{-5}\mu Ci$)	smock and shoecovers	71 %
$< 5\mu Ci/m^3$	$< 50 - 10,000 \frac{counts}{min}$ ($2.3 \times 10^{-5}\mu Ci - 4.5 \times 10^{-3}\mu Ci$)	2 pc. blues and gloves	56 %
$5 - 500\mu Ci/m^3$	No water $> 1 \frac{Ci}{L}$	bubble suit and supplied air	50 %

air to the environment. This is not the case for the DT fuel cycle. Sizing of the atmospheric tritium removal system for this fuel cycle is performed in chapter 5.

Emergency tritium cleanup capabilities must be available for all fuel cycles in the event of an accidental release of tritium into the reactor hall. Even in accident situations, the tritium concentration must be maintained below $500\mu Ci/m^3$ or personnel access is not possible. In the MARS design, a two day clean up time subsequent to an accident was thought to be acceptable after consideration of the costs involved for quicker clean up capability [4.20]. The emergency detritiation systems for the reactors considered in this work were sized based on a 48 hour clean up period after an accidental release of the maximum vulnerable tritium inventory. Smaller tritium releases will take less time for the $500\mu Ci/m^3$ level to be reached. Shielding of components from decay gamma rays was designed to achieve a 2.5 mrem/h dose equivalent in the reactor hall one day after shutdown. The use of robotic units during the cool down time is proposed to improve device availability. Once the 2.5 mrem/h level has been reached, hands on operation is permitted to maintain external reactor components if the tritium level is below $500\mu Ci/m^3$ (this level may be reached within 24 hours for smaller tritium releases). Sorption of tritium and subsequent release from the surfaces of equipment within the containment volume can delay the arrival of tritium to the detritiation system. Appropriate choices of materials to minimize surface adsorption of tritium will mitigate this concern [4.28, 4.29].

An air detritiation system is comprised of the following major components: a blower, an air pre-heater, a catalytic reactor, an aftercooler and a drier (molecular sieve). A schematic is shown in figure 4.11. The air entering the system first passes through a filter to remove particulates. It is then preheated to 180 °C before entering the catalyst oxidizer. After exiting the catalyst bed, the molecular hydrogen content would essentially be reduced to zero. The gas is then cooled to near its dew point and routed to the molecular sieve drier. Clean water can be added to promote adsorption. The air leaving the driers can be either sent to the stack or recirculated

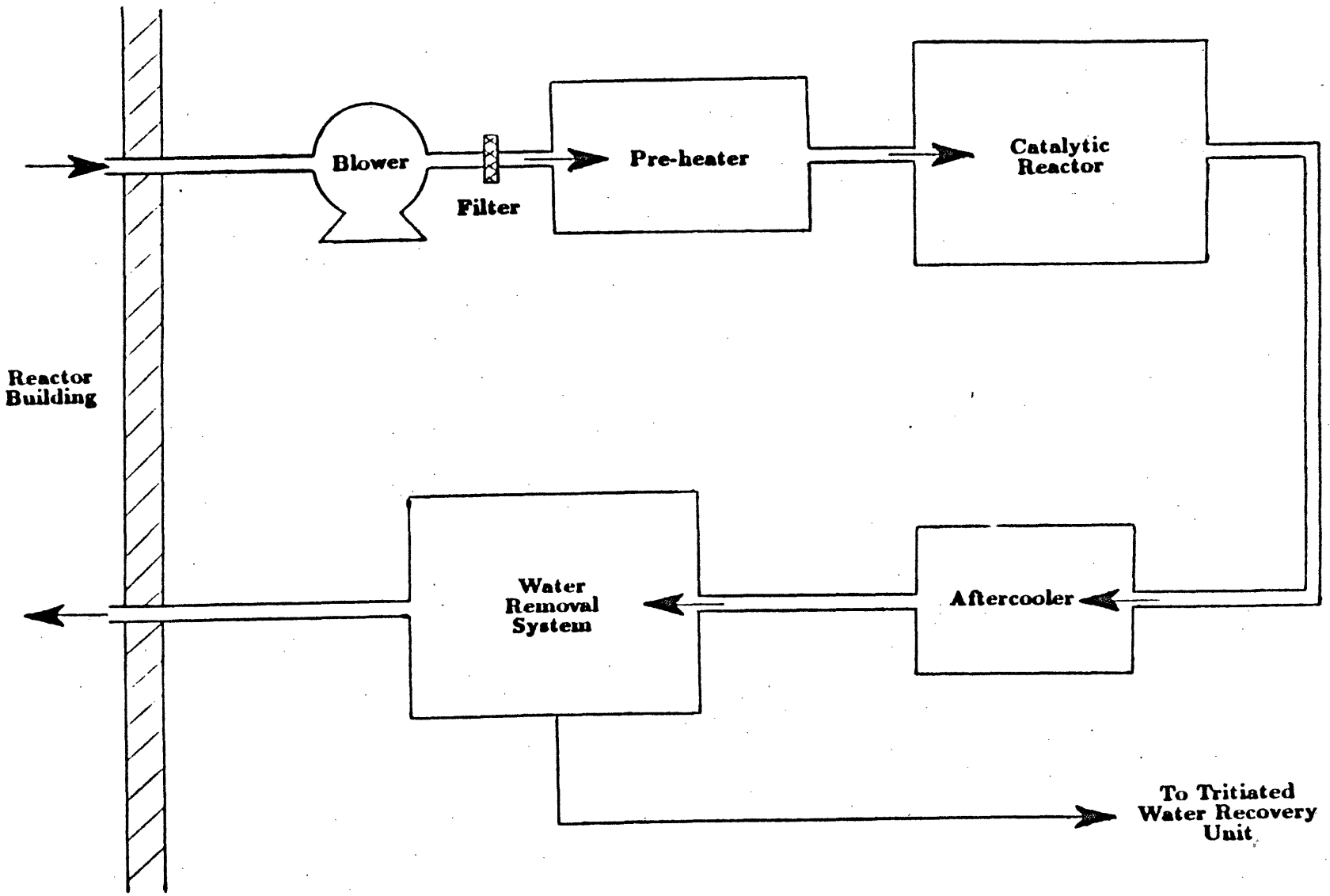

Figure 4.11: Reactor Building Detritiation System

to the room. To regenerate the beds, the cycle would be operated as a closed to supply the energy necessary to remove the water from the molecular sieve [4.30]. The steam leaving the dryer is cooled to near its dew point and then routed to a refrigerated condenser, where most of the water would be condensed and collected in tritiated water storage tanks. This water may later be processed so that the tritium can be recovered and returned to the fuel cycle.

In order to evaluate the capacity of the routine and emergency atmospheric processing equipment, vulnerable tritium inventories and chronic tritium releases to the reactor building must be known. Tritium inventories and release rates are estimated in the following chapter and an attempt to determine the equipment needs is made at that point.

4.6 Tritiated Waste Treatment System

Effluents from various systems may retain quantities of tritium which are uneconomical to recover, but are too high to release directly to the environment. A system is needed to provide routine processing of these gases generated within the plant to reduce tritium to acceptable levels before discharge to the environment. Tritium is removed from all waste gases exhausted from the fuel handling loop, the glovebox atmosphere purge systems or the vacuum systems before release to the environment. Such a system is operated at the TSTA [4.31] and involves catalytic conversion of all hydrogen isotopes in the input stream to water, and organic materials to water and carbon dioxide. Oxygen is maintained at a level to ensure catalytic conversion of all hydrogen isotopes to water. The water formed from this process is adsorbed on a molecular sieve; the remaini .g gaseous effluent can be discharged to the atmosphere after determining that the tritium level is low as practicable. A process flow diagram is given in figure 4.12. Required system capacities for this system were not evaluated.

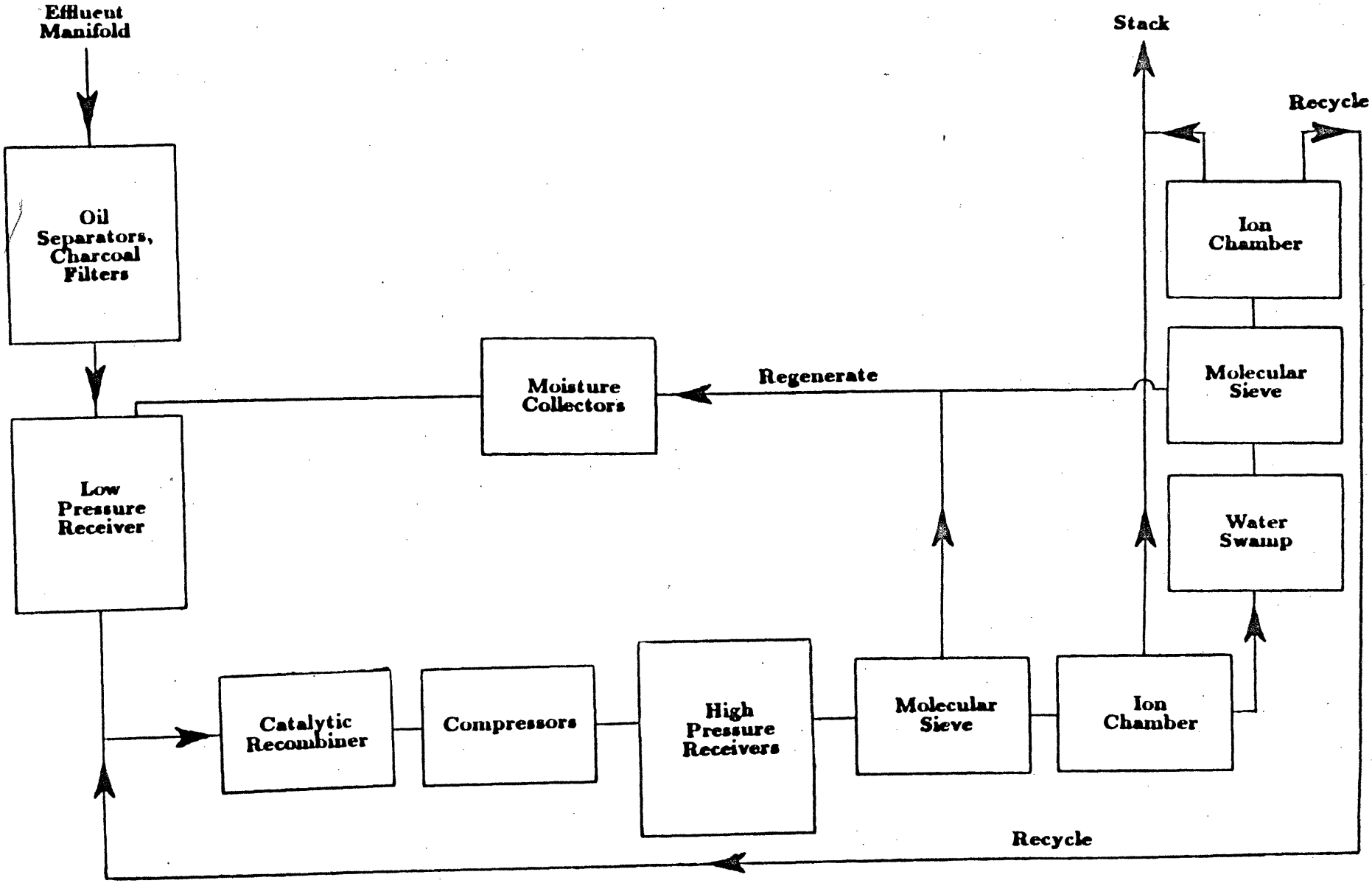

Figure 4.12: Schematic of the Tritium Waste Treatment System [4.20]

4.7 Blanket Tritium Recovery System

The blanket tritium recovery system is needed to recover the tritium bred in the blanket. This system is, of course, only required for the DT fuel cycle. The breeding material chosen for this study was liquid lithium metal. An effective way to remove tritium from liquid lithium is by extraction with a molten salt. This requires the use of a centrifugal contactor, an electrolysis unit and a tritium purification system to remove gamma and other impurities [4.32]. The tritium produced in the breeder can be recovered by slow circulation of the lithium to the tritium recovery system where the tritium is extracted by the molten salt. Technology exists to reduce the tritium content of the breeder to the 1.0 wppm level (see figure 4.13). In the BCSS [4.33, 4.34], the tritium inventory in the breeder was kept to an acceptable level by circulating the lithium at a rate of 0.092 m^3/s. The associated MHD pressure drop was 1.01 MPa. Circulation of the lithium at a faster rate increases the pressure drop but the tritium inventory does not drop appreciably. This is due to the minimum achievable tritium concentration after the extraction process of 1.0 wppm. Once the tritium is removed from the breeder, the lithium must be chemically purified. It may then be stored in dump tanks or recirculated to the blanket module. A tank heating system and tritium control measures must be provided for the lithium storage. Detailed design calculations of this system were not undertaken. It is expected that the system size would be very near to that described in the BCSS [4.33] for the Li/HT-9/He blanket since both are part of a 4000 MWt fusion plant.

By maintaining a sufficiently low tritium partial pressure in the lithium tubes, tritium entering the helium coolant via the first wall will permeate into the lithium and be recovered with the bred tritium. If necessary, additional tritium in the primary coolant can be recovered by passing a slip stream over an oxidizing catalyst followed by cryocondensation of the water produced.

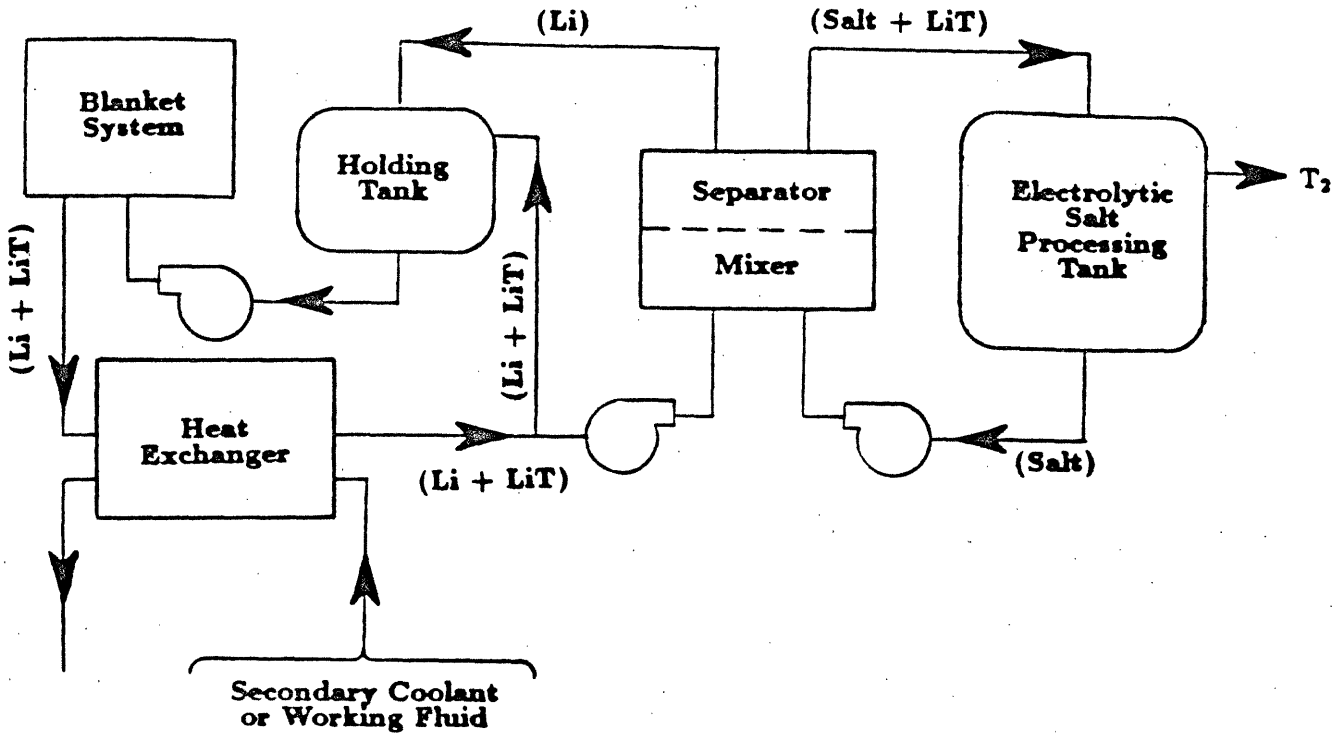

Figure 4.13: Schematic of Molten Salt Tritium Extraction Method for Fusion Reactors with Liquid Lithium Blankets [4.31]

4.8 Economic Evaluation of Fuel Cycle Systems

An assessment of the economics of the fuel handling systems for each fuel cycle has been made. Estimates of the costs of the various components were made using information given in references [4.2], [4.5] and [4.32], and are listed in table 4.6. Little cost variation is seen for the different values of beta for a given fuel cycle. These costs are small relative to other capital costs associated with the fusion plant ($\sim$ 6 % for DT, $\sim$ 2 % for DD and DHe) so that the overall impact of the fuel handling systems costs on the cost of electricity is not large. The effect is smallest for the advanced fuels, where equipment needs are less and the costs associated with the fusion island (blanket, shield, coils, structure) are much higher.

The fuel handling systems are most costly for the DT fuel cycle, followed by the DHe fuel cycle and then by the DD fuel cycle. Major contributors to the cost for the DT reactors include the blanket tritium removal and purification systems, and the helium coolant tritium removal equipment, which are not needed for the other fuel cycles, and the atmospheric tritium recovery system, which has a larger capacity than for DD or DHe. The operating cost for the atmospheric tritium recovery system indicated in the table is for the continual processing of the air in the DT reactor hall. The estimate was obtained from information given in reference [4.26]. A single detritiation unit was found to be capable of maintaining the tritium concentration in the DT reactor building at an acceptable level. Storage costs are also higher for the DT fuel cycle because of the need to store large quantities of tritium. Major contributors to the cost for the DHe fuel cycle are the fuel preparation and injection systems and the vacuum system, which must be capable of handling the greater gas load, and the plasma exhaust purification systems which must be capable of separating large quantities of both hydrogen and helium isotopes.

Annual operating and maintenance costs were estimated based on expected staffing levels for the fuel handling systems. From projected staff requirements for

the tritium plant at JET [4.35], it was anticipated that six workers will be needed for the operation and maintenance of the fuel handling systems for the DD and DHe fuel cycles, and eight workers will be needed to perform these activities for the DT fuel cycle (two additional workers will be employed for operation and maintenance of the breeder systems). Annual operation and maintenance costs, consisting of salaries, outside personnel support services and miscellaneous costs were scaled from the total estimate for the plant using the fraction of the total plant staff involved in fuel handling systems activities (see appendix B for algorithms). Annual operation and maintenance costs, consisting of process materials and miscellaneous supplies and equipment, were obtained in a similar way, except that the costs were scaled using the fraction of the plant operation and maintenance staff (as opposed to the total plant staff) involved in fuel handling systems activities. The estimated annual operation and maintenance costs are given in table 4.6.

An independent cost estimate was made for the fuel handling systems using information from TSTA [4.36]. The goal of the Tritium Systems Test Assembly was to develop and demonstrate the processes for handling the fuel and exhaust from a magnetic fusion reactor. Cost data for the TSTA subsystems required to separate, purify and circulate the gas recovered from the vacuum vessel have been used to make a second estimate of the costs for the reactors of concern here. No blanket or coolant tritium removal and purification systems exist at TSTA. Hence, cost data for these systems were not available from this source. However, it is possible to compare cost estimates for the other systems. Values extracted from table 4.6, based largely on estimates made at Argonne National Laboratory [4.2, 4.5], are compared with the TSTA based estimates in table 4.7. The agreement is fairly good, lending some confidence to these estimates.

Table 4.6: Economics of Fuel Cycle Systems

Component	DT			DD			DHe
	5 %	10 %	20 %	5 %	10 %	20 %	10 %
Vacuum System (M$)	3.5	3.5	3.5	4.0	4.0	4.0	6.0
Cryopumps (M$)	2.0	2.0	2.0	2.3	2.3	2.3	3.5
Valves (M$)	1.4	1.4	1.4	1.6	1.6	1.6	2.4
Regeneration System (M$)	0.1	0.1	0.1	0.1	0.1	0.1	0.2
Fuel Preparation & Injection (M$)	2.2	2.2	2.2	2.4	2.4	2.4	6.9
Blending Units & Piping (M$)	0.4	0.4	0.4	0.6	0.6	0.6	0.6
Gas Puffers & Piping (M$)	1.8	1.8	1.8	1.8	1.8	1.8	6.4
Fuel & Coolant Processing & Purification (M$)	103.1	103.1	103.2	26.4	26.4	26.4	48.6
Blanket Tritium Removal & Purification (M$)	50.6	50.7	50.7	-	-	-	-
Centrifugal Contactor (M$)	11.9	11.9	11.9	-	-	-	-
Electrolysis Unit (M$)	11.9	11.9	11.9	-	-	-	-
Blanket Tritium Purification System(M$)	10.7	10.7	10.7	-	-	-	-
Lithium Chemical Purification (M$)	10.7	10.7	10.7	-	-	-	-
Lithium Dump Tank & Heating System(M$)	5.4	5.4	5.4	-	-	-	-
Plasma Exhaust Purification (M$)	9.5	9.5	9.5	13.3	13.3	13.3	35.4
H Isotope Separation System (M$)	4.7	4.7	4.7	6.1	6.1	6.1	6.1
He Isotope Separation System (M$)	-	-	-	2.0	2.0	2.0	20.4
Fuel Cleanup Units (M$)	2.6	2.6	2.6	1.7	1.7	1.7	1.7
Pumps & Piping (M$)	2.6	2.6	2.6	3.4	3.4	3.4	7.2
Coolant Tritium Removal & Purification (M$)	41.0	41.1	41.1	10.7	10.7	10.7	10.7
Helium Coolant Tritium Removal (M$)	30.3	30.3	30.4	-	-	-	-
Helium Coolant Chemical Purification (M$)	10.7	10.7	10.7	10.7	10.7	10.7	10.7
Storage (M$)	2.6	2.6	2.6	0.9	0.9	0.9	1.8
Tritium Storage (M$)	2.1	2.1	2.1	-	-	-	-
Deuterium Storage (M$)	0.1	0.1	0.1	0.3	0.3	0.3	0.3
Helium-3 Storage (M$)	-	-	-	-	-	-	1.0
Storage System Pumps & Piping (M$)	0.4	0.4	0.4	0.5	0.5	0.5	0.5
Atmospheric Tritium Recovery System (M$)	36.8	36.8	36.8	18.4	18.4	18.4	18.4
Total (M$)	148.2	148.2	148.3	52.1	52.1	52.1	81.7
Fraction of Total Direct Cost (%)	6.1	6.7	6.8	0.9	1.2	1.4	2.2
Spare Parts Allowance (2 %) (M$)	2.9	2.9	2.9	1.0	1.0	1.0	1.6
Annual O & M Costs (M$/yr)	1.83	1.83	1.83	0.87	0.87	0.87	0.88

Table 4.7: Comparison of Fuel Handling Systems Cost Estimates

Source of Estimate	Fuel Cycle DT	DD	DHe
TSTA Cost Data [4.36]	44.1	39.9	66.1
Argonne Studies† [4.2, 4.5]	56.4	41.4	71.0
Difference (%)	21	4	7

† not including blanket and coolant tritium removal systems costs

4.9 Summary of Fuel Cycle Systems

The major difference between the fuel handling systems of the advanced fuels and that for DT fuel is the need for a blanket tritium recovery system and tritium removal from the coolant for the DT fuel cycle. Although tritium is not bred in the advanced fuel blankets, all other components of the fuel handling systems needed for DT are also required for these fuel cycles. Most of these components, however, are scaled down in size from the DT components because of the lower tritium throughput. This is not the case for the vacuum systems which are larger for the advanced fuels because of the more severe plasma purity requirements. The hydrogen isotope separation systems are not largely different, although a third column for the advanced fuels is only needed during and shortly after pulse initiation. The additional capacity is needed at this time because the plasma exhaust will contain a higher tritium concentration (since tritium is being fueled to ignite the plasma) which must be reduced before discharge to the environment. Helium isotope separation capabilities are greatest for the DHe fuel cycle. No helium isotope separation equipment is used for the DT plants because the ^{3}He is the plasma exhaust is not worth recovering. Other components of the fuel cycle systems are not expected to be largely different amongst the fuel cycles. No difference in equipment needs is seen for the different values of beta for a given fuel cycle.

The economic evaluation of the fuel cycle systems indicated that the largest costs will occur for the DT fuel cycle. This is mainly a consequence of blanket and coolant tritium removal and purification needs. For the DT and DD fuel cycles, little cost variation is seen for the different values of beta. The total economic impact of the fuel cycle systems is small. The effect is least for the advanced fuels, where the fuel cycle equipment needs are less and where the costs are overshadowed by the much greater costs associated with the fusion island.

4.10 References

(4.1) C.C. Baker et al., Fusion Reactor Technology Impact of Alternate Fuels, Proceedings of the Eighth Symposium on the Engineering Problems of Fusion Research, p. 861, San Francisco California, November 1979.

(4.2) C.C. Baker et al., STARFIRE - A Commercial Tokamak Fusion Power Plant, Argonne National Laboratory, ANL/FPP-80-1, September 1980.

(4.3) J.L. Anderson, D.O. Coffin and C.R. Walthers, Vacuum Applications for the Tritium Systems Test Assembly, Journal of Vacuum Science and Technology, A 1 (2), April - June 1983.

(4.4) M. Abdou et al., A Demonstration Tokamak Power Plant Study (DEMO), Argonne National Laboratory, ANL/FPP/82-1, September 1982.

(4.5) K. Evans et al., WILDCAT: A Catalyzed DD Tokamak Reactor, Argonne National Laboratory, ANL/FPP/TM-150, November 1981.

(4.6) D.O.Coffin, A Tritium Compatible High Vacuum Pumping System, Journal of Vacuum Science and Technology, , 20 (4), April 1982.

(4.7) E.C. Kerr et al., Fuel Cleanup for the Tritium Systems Test Assembly: Design and Experiments, Proceedings of the ANS Topical Meeting on Tritium Technology in Fission, Fusion and Isotopic Applications, CONF-800427, Dayton Ohio, May 1980.

(4.8) A.H. Dombra, A Review of Fusion Fuel Cleanup System Options for the Frascati Tokamak Upgrade, Canadian Fusion Fuels Technology Project, F84005P, June 1984.

(4.9) S. Konishi et al., Experiments on a Ceramic Electrolysis Cell and a Palladium Diffuser at the Tritium Systems Test Assembly, Proceedings of the Second ANS

National Topical Meeting on Tritium Technology in Fission, Fusion and Isotopic Applications, Dayton Ohio, May 1985, printed is special issue of Fusion Technology, 8, September 1985.

(4.10) P.J. Dinner et al., Tritium System Concepts for the Next European Torus Project, Proceedings of the Second ANS National Topical Meeting on Tritium Technology in Fission, Fusion and Isotopic Applications, Dayton Ohio, May 1985, printed is special issue of Fusion Technology, 8, September 1985.

(4.11) R.H Sherman, Cryogenic Hydrogen Isotope Distillation for the Fusion Fuel Cycle, Proceedings of the Second ANS National Topical Meeting on Tritium Technology in Fission, Fusion and Isotopic Applications, Dayton Ohio, May 1985, printed in special issue of Fusion Technology, 8, September 1985.

(4.12) J.R Bartlit et al., Hydrogen Isotope Distillation for the Tritium Systems Test Assembly, Proceedings of the Third Topical Meeting on The Technology of Controlled Nuclear Fusion, CONF-780508, Sante Fe New Mexico, May 1978.

(4.13) J.R. Bartlit et al., Hydrogen Isotope Distillation for Fusion Power Reactors, Cryogenics, 19, p. 275, 1979.

(4.14) M. Kinoshita, An Efficient Simulation Procedure Especially Developed for Hydrogen Isotope Distillation Columns, Fusion Technology, 6, p. 574, November 1984.

(4.15) R.E. Treybal, Mass Transfer Operations, M^{c}Graw – Hill Company, 1980.

(4.16) W.R. Wilkes, Distillation of Helium Isotopes, Proceedings of ICEC – 4, Eindhoven, p. 119, IPC Science and Technology Press, 1972.

(4.17) W.R. Wilkes, ^{3}He $-^{4}$ He Distillation Apparatus, Mound Laboratory, MLM-2005, March 1973.

(4.18) V.M. Kuznetsov, Soviet Physics J.E.T.P., 5, p. 819, 1957.

(4.19) K.Y. Wong et al., Canadian Tritium Experience, Canadian Fusion Fuels Technology Project, Ontario Hydro, 1984.

(4.20) B.G Logan et al., MARS - Mirror Advanced Reactor Study, Lawrence Livermore National Laboratory, UCRL-53480, July 1984.

(4.21) INTOR - International Tokamak Reactor, US Contribution, International Atomic Energy Agency, Vienna, 1979.

(4.22) D. Dobrott et al., Catalyzed Deuterium Fueled Tandem Mirror Reactor Assessment, Science Applications International Corp., SAI02383-476LJ/ APPAT-13, January 1985.

(4.23) C.A. Flanagan et al., Fusion Engineering Device (FED) Design Description, Volumes 1 & 2, Oak Ridge National Laboratory, ORNL/TM-7948, December 1981.

(4.24) F.H. Southworth, D$-^3$He Fueled Tokamak Reactors, Proceedings of the Review Meeting on Advanced Fuel Fusion, EPRI ER-536-SR, p. 365, June 1977.

(4.25) J.A. Fillo et al., Exploratory Studies of High-Efficiency Advanced Fuel Fusion Reactors, Electric Power Research Institute, EPRI-ER-919, December 1978.

(4.26) INTOR - International Tokamak Reactor, Phase Two A, Part I, International Atomic Energy Agency, Vienna, 1983.

(4.27) P.A. Finn and M.L. Rogers, The Effects of Tritium Contamination in the FED/INTOR Reactor Hall, Nuclear Technology/Fusion, 4, p. 99, September 1983.

(4.28) INTOR - International Tokamak Reactor, US Contribution - Conceptual Design, USA INTOR/81-2, 1981.

(4.29) R. Jalbert et al., Contamination of Aluminium and Painted Surfaces Exposed to Tritium, Proceedings of the ANS Annual Meeting, Reno Nevada, June 1986.

(4.30) M.E. Muller, Conceptual Desiign of an Emergency Tritium Clean-up System, Proceedings of the Third Topical Meeting on the Technology of Controlled Nuclear Fusion,
Sante Fe New Mexico, May 1978.

(4.31) J.L. Anderson, Design and Construction of the Tritium Systems Test Assembly, Proceedings of the ANS Topical Meeting on Tritium Technology in Fission, Fusion and Isotopic Applications, CONF-800427, Dayton Ohio, May 1980.

(4.32) P.A. Finn, A Systematic Methodology for Estimating Direct Capital Costs for Blanket Tritium Processing Systems, Fusion/Technology, 8, p. 904, July 1985.

(4.33) D.C. Smith et al., Blanket Comparison and Selection Study (BCSS) - Final Report, Argonne National Laboratory, ANL/FPP-84-1, September 1984.

(4.34) C.P.C. Wong et al., Helium-Cooled Blanket Designs, Fusion Technology, 8, p. 114, July 1985.

(4.35) C.W. Gordon, private communication, JET Joint Undertaking, November 1986.

(4.36) J.R. Bartlit et al., Subsystem Cost Data for the Tritium Systems Test Assembly, Proceedings of the Tenth Symposium on Fusion Engineering, Philadelphia Pennsylvania, December 1983.

(4.37) INTOR - International Tokamak Reactor, Phase Two A, Part II, International Atomic Energy Agency, Vienna, 1986.

(4.38) J.B. Cannon, Background Information and Technical Basis for Assessment of Environmental Implications of Magnetic Fusion Energy, U.S. Department of Energy, DOE/ER-0170, August 1983.

Chapter 5
Radiological Hazards of Fusion Fuel Cycles

During operation of fusion power plants, the potential for exposure of workers to radioactive hazards will exist. Ionizing radiation is anticipated to be the most prevalent hazard within a reactor station because it is associated with all parts of the on-site fuel cycle. Sources of ionizing radiation include tritium, neutrons and beta-gamma radiation resulting from the decay of neutron activation products. The degree of hazard associated with each of these sources depends on which of the fuel cycles is being considered.

Tritium is associated with many of the reactor station operations: fueling, fuel processing and breeding. Some of the plant wastes, especially in the case of the DT fuel cycle, will contain tritium. It can be found in the coolant streams and on the surfaces of components. The degree of concern over exposure to the tritium hazard is greatest for the DT fuel cycle.

Neutrons are of potential concern only during operation of the reactor because they are produced in the DT reaction and the neutron branch of the DD reaction, which take place only while there is a burning plasma. Because of radioactivity levels resulting from neutron activation of structural materials and potential neutron leakage through penetrations of the reactor structure, personnel entry to the reactor hall during operation is precluded. Some neutrons may escape from the reactor building via penetrations through the reactor room but the reactor building walls will capture nearly all neutrons that escape the reactor structure. Exposure of workers to neutrons is not expected for any of the fuel cycles.

All parts of the reactor structure and impurities in the primary coolant will become radioactive during neutron bombardment. Activation products in the reactor structure are not expected to be a significant radioactive hazard during reactor operation. During maintenance outages, a 24 h cool down period will allow gamma dose rates to be reduced to 2.5 mrem/h so that personnel access is possible. Radioactivity levels may still be high (especially for the DT fuel cycle) so that proper procedures and protective measures may be needed. Subsequent storage, decontamination, disassembly and disposal of activated components may also involve potential exposure of personnel to radioactive material so that appropriated safety measures may be needed. The primary coolant loop will circulate an inventory of activation products from the reactor to other components of the power cycle, such as the steam generator, pumps, valves and piping. This is not foreseen to be a major hazard with helium cooled systems [5.1, 5.2]. Appropriate procedures to minimize personnel exposure in areas of high radioactivity will be needed. These concerns are greatest for the DT fuel cycle, and least for the DHe fuel cycle.

In this chapter, the radiological hazards associated with the different fuel cycles are identified. Most of the effort has been focused on occupational hazards. An attempt to quantify activity levels and rates of release at various locations in the plant has been made. Some attention was given to release rates to the environment and hazards posed to the public.

5.1 Tritium Hazards

The reactors considered in this work burn various fuels. Since it does not exist in useful concentrations in nature, tritium for fueling the DT reactors must be generated by neutron transmutation of lithium contained in a blanket surrounding the reactor plasma. For the DD and DHe fuel cycles, tritium is generated as a reaction product from the proton branch of the DD reaction. Some of this tritium

will be burned in the plasma. However, not all of the fuel will be burned during a single pass through the reactor. Thus, some tritium will be present in the plasma exhaust for all fuel cycles. For the DT and semi-catalyzed DD fuel cycles, the tritium is recycled and reinjected into the torus. For the DHe fuel cycle, the tritium produced in the plasma which does not burn during its residence in the torus is separated from the reusable fuel components of the plasma exhaust. The circulation of tritium throughout the fusion plant will lead to an accumulation of this species at various locations and will also lead to routine releases. Accurate determination of tritium inventories and release rates requires precise knowledge of tritium implantation, diffusion and permeation rates. This, in turn, requires that first wall surface conditions, and temperatures and pressures throughout the plant be well known. Information to this level of detail has not been determined for the designs presented in chapter 2. However, estimates of tritium inventories and release rates can be made via scaling and extension of previous studies. An attempt to quantify tritium activity levels and release rates for the three fuel cycles using this approach has been made here.

5.1.1 Tritium Inventory

The flow of tritium throughout the fusion plant will result in an inventory of this species being established at various locations. Knowledge of the magnitude of the tritium retained at a given location is needed so that appropriate tritium containment measures can be instituted. Components which will establish a tritium inventory include the fuel preparation and injection system, the plasma chamber, the vacuum pumps, the fuel purification and processing systems, the blanket structure, the coolant system and the storage units. For the DT fuel cycle, a steady state inventory of tritium in the breeding blanket and associated processing systems will also exist. The tritium inventory in the plant is classified as either vulnerable or non-vulnerable depending on the extent of mobilization of tritium during poten-

tial transients. This is useful for initial evaluation of accident hazard. It refers to the likelihood for release from the primary containment and does not always mean that the material will reach the environment. The quantities of tritium found and their classification as to vulnerability are discussed below. Estimates were generally scaled from previous detailed reactor design studies [5.3, 5.4] using tritium throughput.

5.1.1.1 Tritium Inventory in Fuel Handling Systems

The fuel handling systems include the fuel preparation and injection systems, the plasma chamber, the vacuum system, the impurity removal system, the hydrogen isotope separation system, and the storage equipment. In short, the path of tritium in the fuel loop can be summarized as follows (see figures 4.1, 4.2 and 4.3). The plasma exhaust consisting of unburned fuel, helium-4 ash and impurities is routed from the torus to the compound cryopumps. The helium is separated at this point and the remaining mixture enters an impurity removal unit. Tritiated methane, water and ammonia are decomposed; gaseous CO_2, O_2 and N_2 are discharged to the environment and the hydrogens are directed to the isotope separation system. The required streams for fueling leave the isotope separation system and enter the fuel preparation system or are passed into storage. Additional fuel requirements to yield the appropriate mixture for fueling can be drawn from the onsite supply in storage. From the fuel preparation system, the mixture is injected into the torus. These systems have been discussed in more detail in the preceeding chapter. Here, an estimate of the tritium inventory found in these components will be made.

Fuel may be provided to the plasma chamber by gas puffing, pellet injection or a combination of these. The STARFIRE and WILDCAT designs use gas puffing to fuel the torus [5.3, 5.4]. This method of fueling has also been assumed for the

designs considered in this work. The fuel injection system will contain a tritium inventory. In the STARFIRE report [5.3], it was assumed that the gas puffers would hold one hour's supply of tritium. This assumption was adopted here and the resulting tritium inventory in the fuelers is given in table 5.1. Two tritium fuelers will be used for the DT reactors, each containing 45 g of tritium; only one fueler, holding 0.4 g of tritium, will be needed for each of the DD reactors. This inventory is considered vulnerable since the fuelers are closely coupled to the torus and therefore subject to accidents or component failures in the torus.

The quantity of tritium found in the plasma chamber during operation of the reactor is simply the product of the triton density and the plasma volume. These values are indicated in table 5.1 for each of the fuel cycles. The amount of tritium contained in the torus at a given time is not large, even for the DT reactors. This is classified as vulnerable since breach of containment would allow for the immediate release of the tritium inventory.

Compound cryopumps were selected to accomplish torus evacuation and pumping of the plasma exhaust. The helium can be separated from the impure exhaust gases and hydrogen isotopes by careful temperature and pressure control during regeneration of the pumps. The tritium inventory in the cryopumps depends on the tritium exhaust rate from the torus and the regeneration period. The cycle time for pump regeneration should be short so that the tritium inventory is kept to a minimum; on the other hand, it should be long enough so not to have a deleterious effect on the pump valve lifetime. For the DT reactor a 2 hour regeneration time is used; a 32 hour regeneration time is used for the advanced fuels. The maximum tritium inventory in the cryopumps will exist just before regeneration. The quantity of tritium found in each pump at this time will be 9.5 g for DT, 1.3 g for DD and 1.1 g for DHe (same inventory for all values of beta for a given fuel cycle). The total inventory held up in all of the cryopumps will be 133 g for DT (in 14 pumps), 20.8 g for DD (in 16 pumps) and 26.4 g for DHe (in 24 pumps). The relatively large tritium inventory held up in the

cryopumps of the DHe system is a consequence of the high plasma exhaust rate. The vulnerability of tritium in the vacuum pumps has not been established with any degree of certainty [5.4]. However, because of their proximity to the torus, they could be affected by accidents and failures of other components. The ingress of air into the torus, and hence into the vacuum system, or loss of liquid-helium cooling to the pumps, would cause tritium to be released from the pumping surfaces. If this occurred, tritium could be released to the reactor hall if the integrity of the vacuum seals was not maintained. Because of this possibility, the tritium inventory in the cryopumps is designated as vulnerable.

The mixture of hydrogen isotopes and gaseous impurities separated from the helium at the cryopumps is routed to the impurity removal system. Here, $(H, D, T)_2$ is separated from reactor off-gas contaminants and hydrogen isotopes chemically combined with oxygen, nitrogen and carbon are recovered. It is proposed that hot uranium beds be used to accomplish the removal of impurities from the hydrogen isotopes. Calculations to determine the tritium inventory in the impurity removal system were not performed. This inventory would be classified as non-vulnerable since multiple containment would be used. For the purposes of evaluating the tritium inventory, the tritium which would be retained in the impurity removal system was assumed to be passed into the hydrogen isotope separation system and is included in the inventory estimate for this system.

The stream of pure hydrogen isotopes flows from the impurity removal system to the isotope separation system where cryogenic distillation will be used to separate the tritium, deuterium and protium. This system requires little maintenance and is relatively self contained. The hydrogen isotope separation system was described in the previous chapter. As discussed there, a large computer code would be required to assess the tritium inventory and flow rates in this system because of the complexity introduced when many components are to be separated. It was felt that this elaborate approach would not increase the understanding required for this work. Hence, the tritium hold up in the distillation columns was assessed by scaling from

STARFIRE and WILDCAT, using the tritium throughput. The total quantity of tritium retained in this system during steady state was found to be 322 g, 21.1 g and 26.4 g for the DT, DD and DHe fuel cycles respectively. Since the tritium exhaust rates are the same for all values of beta for a given fuel cycle, the amount of tritium in the columns is independent of this variable. The tritium inventory in the isotope separation system is in the unoxidized form. Because the units have a high reliability, the tritium located here is considered to be non-vulnerable [5.3].

Some supply of fuel must be kept on hand to smooth out fluctuations in operation, disruptions in fuel shipments and possible non-operational periods in fuel recycle or blanket process operations. It was assumed that two days fuel supply would be kept onsite. For the DT fuel cycle, this requires that 4.3 kg of tritium must be stored (2.15 kg of tritium fueled per day, see table 2.2) For the semi- catalyzed DD fuel cycle, some tritium is fueled to the torus on a regular basis. Two days supply implies that 19 g of tritium must be stored (9.5 g of tritium fueled per day, see table 2.3). Also, the advanced fuels require additional tritium to be fueled in order to reach ignition at the beginning of each pulse. A further 10 g of tritium was assumed to be kept on hand for this purpose. During normal operation, tritium for ignition for each pulse can be supplied from the isotope separation system. The supply in storage may be needed in the event of operational interruption of the upstream processing system. The tritium stored on site will be in the form a uranium tritide (UT_x), placed within storage vessels, located inside a barricaded vault with an inert cover gas for fire protection. This inventory is considered to be non-vulnerable to accidents. In addition to tritium, a supply of the other fuel components must be available. Assuming two days fuel supply of these species will also be kept onsite, the DT reactors will require 2.89 kg of deuterium, the DD reactors will require 6.93 kg of deuterium, and the DHe reactor will require 10.9 kg of deuterium and 41.1 kg of helium-3. The storage of these fuel constituents presents no radioactive hazard.

5.1.1.2 Tritium Inventory in the Blanket and Breeder Processing Systems

The greatest contribution to the vulnerable tritium inventory for the DT fuel cycle will be found in the blanket and the blanket processing systems. The elimination of the need to breed tritium for the advanced fuels removes this source from consideration and is a major advantage in terms of reducing the tritium hazard.

The tritium inventory in the breeding blanket is established from neutron interactions with lithium. The liquid lithium containing the tritium flows from the blanket module to the processing systems. It was assumed that the same ratio of tritium in the processing system to tritium in the blanket would exist as in reference [5.5]. Molten salt extraction was the breeder tritium removal technique assumed to be employed. The tritium inventory in the breeding blanket for the DT designs was estimated from the information given in the Blanket Comparison and Selection Study [5.6, 5.7, 5.8] for the Li/He/HT-9 tokamak design. The tritium inventory in the blanket was scaled from that given in the BCSS using the blanket tritium production rate. The inventories determined are summarized in table 5.1. The inventory in the blanket and blanket processing systems is considered as vulnerable since the possibility for the liquid metal to drain from the reactor and release its tritium inventory after some accident scenarios exists.

5.1.1.3 Tritium Inventory in Blanket Structure and Coolant System

A steady state inventory of tritium will be found in the blanket structure and coolant. The blankets of the advanced fuel reactors are composed entirely of structure (HT-9). Their purpose is to provide a pathway for heat removal, either by neutron interaction/conduction or radiation/conduction. Some tritium will be present in the blanket structure of all reactors because of tritium implantation and

permeation. Tritium implantation is dependent upon the tritium flux impinging on the first wall and the first wall conditions. Tritium permeation is a function of the permeability and thickness of the metal involved. It occurs more rapidly through high temperature surfaces and for higher tritium pressures in the torus or blanket. Actual permeation rates are strongly dependent on the surface conditions of the material. Rates may be lower than calculated values because of surface barriers, such as oxide films, that could impede surface dissolution of tritium [5.9, 5.10]. Permeation rates may also be higher than anticipated. High concentrations of tritium in the near surface depths of the first wall can result from implantation of energetic charge-exchange neutrals. The depth of penetration can impede the recombination rate of the implanted atoms into molecules at the surface. These effects translate into a higher effective tritium pressure in the metal near the surface. The resultant concentration gradient through the wall causes the tritium to diffuse into the bulk and into the coolant at a considerably higher rate [5.5, 5.10, 5.11]. This consideration is especially important for the limiter. Estimates of the tritium inventories in the first wall and blanket structure were based on information given in the BCSS [5.6, 5.7, 5.8]. First wall inventories were scaled from the value given in the BCSS by the triton flux and the first wall area. For the inventory in the blanket structure of the DT designs, the BCSS value was scaled with triton flux and structure volume. The advanced fuel inventories were found in a similar way, but an additional factor was applied to account for the elimination of the breeding blanket as a source of tritium for permeation into the structure (i.e. source is only due to implantation so that the first wall area is a factor, and that fraction of the structural tritium inventory due to tritium permeation from the breeder is removed from the base scaling value). Because of the fairly high diffusion rates of tritium in metals, possible thermal transients could "bake-out" the tritium in a short period of time. Thus, tritium contained in the structure is designated as vulnerable.

A tritium inventory in the blanket coolant will also be established due to permeation from the plasma. Helium cooled designs have been considered in this work.

Table 5.1: Tritium Inventory in Various Plant Components

Location	DT			DD			DHe	
	5 %	10 %	20 %	5 %	10 %	20 %	10 %	Classificati
Individual Fueler (g)	45	45	45	0.4	0.4	0.4	0	vulnerabl
Total in Fuelers (g)	90	90	90	0.4	0.4	0.4	0	
Plasma Chamber (g)	0.55	0.43	0.35	0.022	0.014	0.009	0.005	vulnerable
Individual Cryopumps (g)	9.5	9.5	9.5	1.3	1.3	1.3	1.1	vulnerable
Total in Cryopumps (g)	133	133	133	20.8	20.8	20.8	26.4	
Breeder (g)	242	242	242	-	-	-	-	vulnerable
Blanket Processing (g)	68.5	68.5	68.5	-	-	-	-	vulnerable
First Wall (g)	13.4	13.3	13.1	0.133	0.134	0.134	0.167	vulnerable
Blanket Structure (g)	5.02×10^{-2}	5.20×10^{-2}	5.33×10^{-2}	1.82×10^{-5}	2.05×10^{-5}	2.23×10^{-5}	7.08×10^{-6}	vulnerable
Coolant (g)	4.30×10^{-7}	4.29×10^{-7}	4.22×10^{-7}	4.26×10^{-9}	4.29×10^{-9}	4.30×10^{-9}	5.36×10^{-9}	vulnerable
Total Vulnerable Inventory (g)	547	547	547	21.3	21.3	21.3	26.6	
Total Vulnerable Inventory (MCi)	5.25	5.25	5.25	0.204	0.204	0.204	0.255	
Hydrogen Isotope Separation System (g)	322	322	322	21.1	21.1	21.1	26.4	non-vulnerabl
Storage (g)	4300	4300	4300	30	30	30	10	non-vulnerabl
Total Non-vulnerable Inventory (g)	4634	4634	4634	49.8	49.8	49.8	36.4	
Total Non-vulnerable Inventory (MCi)	44.5	44.5	44.5	0.48	0.48	0.48	0.35	
Total Inventory (g)	5170	5170	5170	72.5	72.5	72.5	63.0	
Total Inventory (MCi)	49.7	49.7	49.7	0.68	0.68	0.68	0.61	

Tritium losses from the helium circuit through the steam generator to the steam loop may result from permeation and leakage. Tritium management in this regard is of greatest concern for the DT designs. The source of the tritium in the coolant is the plasma, and not the breeding material [5.10]. Thus, tritium enters the coolant stream by the same pathway (i.e. via the first wall) for all fuel cycles, regardless of the presence of a tritium breeding material in the blanket. For the DT design, tritium which has entered the coolant can be recovered by maintaining a sufficiently low tritium partial pressure in the lithium tubes so that the tritium will permeate from the helium into the lithium and be recovered with the tritium from the breeder. The source of tritium (i.e. tritium implanted in the first wall from the plasma) will be significantly lower for the advanced fuels. The tritium entering the coolant can be recovered through oxidation of tritium followed by adsorption on molecular sieves [5.6]. Coolant inventories were simply found by scaling the value given in the BCSS with tritium flux to the first wall and first wall area. No account for tritium entering the coolant from the breeder was taken. Inventories of tritium in the coolant are indicated in table 5.1. This is classified as vulnerable.

5.1.2 Tritium Releases

Fuel cycle activities and handling of tritium contaminated materials could result in release of tritium to the environment. The potential for this occurring is directly related to the tritium inventory and tritium flow rates throughout the plant. Components of the fuel cycle systems from which tritium may be released include the fuel preparation and injection equipment, the vacuum ducts and pumps, the fuel purification and processing systems, the blanket and blanket processing equipment, the coolant system, and the tritium storage units. Mechanisms for tritium release from these systems have been identified as steady state leaks from imperfect fluid system connections, valves and pumps, permeation through pipes and vessel walls, and occasional leaks during routine maintenance and accidents. These pathways

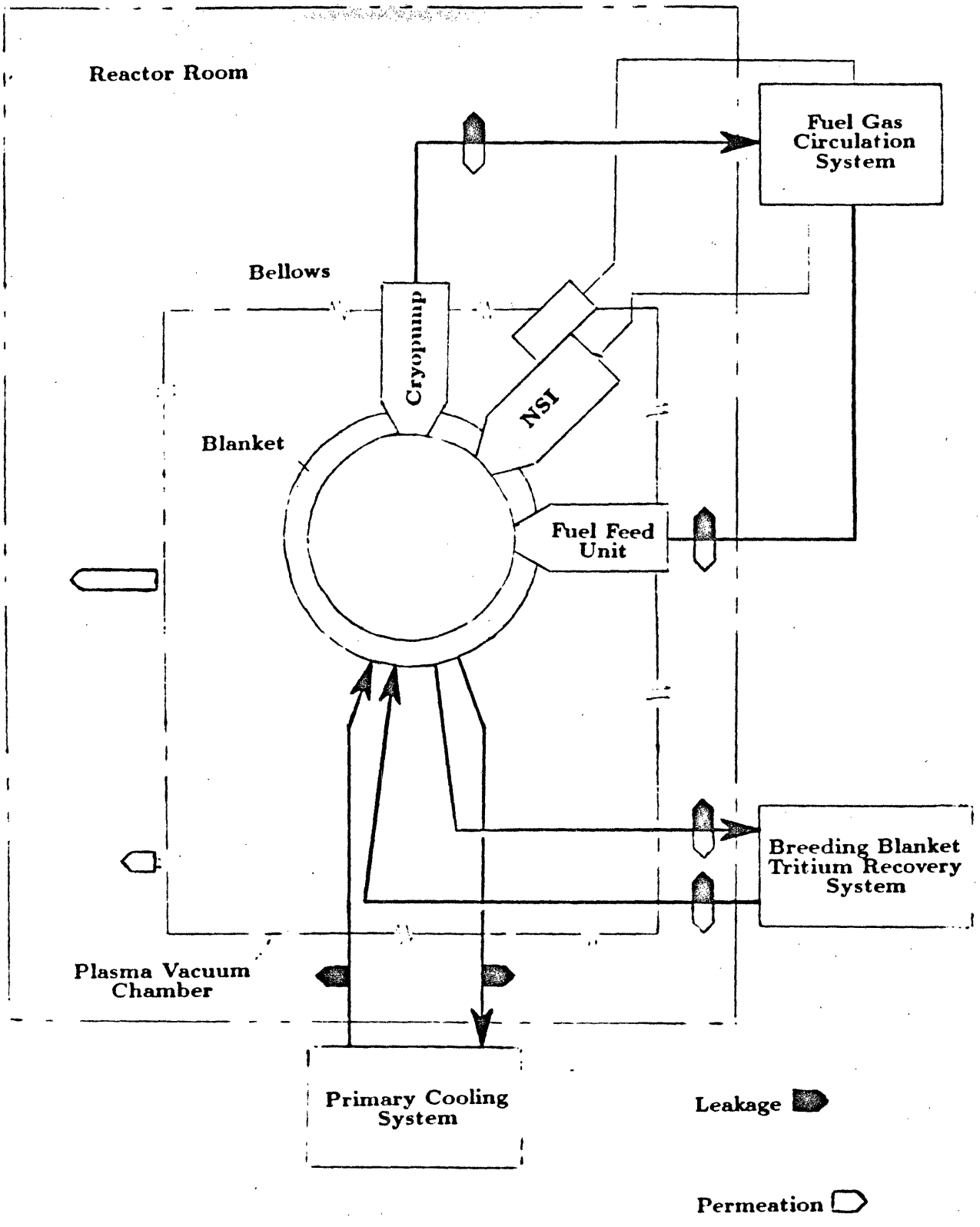

Figure 5.1: Schematic Pathways of Tritium Release During Normal Operation

for tritium release are summarized in figure 5.1. Only the routine releases will be examined here.

In table 5.2, the major design parameters affecting the tritium release rates for the three fuel cycles (with 10 % beta) being evaluated are listed. An important difference from the standpoint of tritium containment is the absence of the tritium breeding material in the advanced fuel designs. Also of interest is the tritium fractional burnup. For the DT fuel cycle, only 26 % of the tritium injected into the plasma is consumed in fusion reactions. For the DD fuel cycle, 93 % of the tritium in the plasma is burned. For the plasma conditions associated with this fuel cycle, tritium producing reactions become important (proton branch of the DD reaction). Because of the high temperature of the plasma and the relatively long residence time of particles in the torus, most of the tritium produced, and most of the tritium injected into the torus is consumed, giving the high tritium burnup. For the DHe fuel cycle, no tritium is fueled, but a significant amount is produced due to DD side reactions in the plasma. Almost 67 % of this tritium is burned before being exhausted from the torus. One reason for the fractional burnup of the DHe fuel cycle being lower than the DD fuel cycle, despite operating at the same temperature, is the shorter particle confinement time for the DHe system. Determination of this confinement time was based on tolerable alpha ash levels in the plasma. Alpha particles are produced from reactions of deuterons with tritons and with helium-3 nuclei. Compared to the DD fuel cycle, the production rate of alphas in the DHe fuel cycle is much greater. Consequently, the exhaust rate from the DHe reactor must be much greater than from the DD reactor to maintain the same degree of plasma purity. Thus, any tritium produced in the DHe plasma has a much shorter time to react, resulting in a lower fractional burnup than for the DD reactor. The tritium inventories throughout the plants are significantly lower for the advanced fuels than for the DT case, as would be expected. Despite the lower steady state triton density in the DHe plasma (3.49×10^{17} for DHe, 1.04×10^{18} for DD and 1.01×10^{20} for DT at 10 % beta), tritium inventories throughout the plant

Table 5.2: Design Parameters That Affect Tritium Releases

Parameter	Fuel Cycle (10 % beta)		
	DT	DD	DHe
Breeding Material	Li	-	-
Breeding Temperature (°C)	500 - 560	-	-
Coolant	He	He	He
Coolant Temperature (°C)	275 - 510	275 - 510	275 - 510
Structural Material	HT-9	HT-9	HT-9
Fusion Power (MW)	3650	2875	3765
Net Electric Power (MW)	1225	1213	1213
Plant Availability	0.65	0.69	0.72
Burntime (s)	5000	5000	5000
Particle Confinement Time (s)	2.3	7.4	2.3
Tritium Fractional Burn-up	0.259	0.932	0.674
Tritium Burned (g/d)	559	221	42
Tritium Exhausted (g/d)	1600	16	20
Tritium Fueled (g/d)	2160	9.4	0
Tritium Bred (g/d)	633	-	-
Tritium Inventory (g)			
Vacuum Pumps	133	20.8	26.4
Fuelers	90	0.4	0
Fuel Purification	322	21.1	26.4
Storage	4300	30	10
Blanket	242	-	-
Blanket Processing	68.5	-	-
Structure	13.3	0.13	0.17
Coolant	4.3×10^{-7}	4.3×10^{-9}	5.4×10^{-9}
Total	5170	72.5	63.0

are comparable to the DD plant. This is a consequence of the higher processing rate.

The tritium release rates for each tritium containing subsystem have been estimated, based on the methodology given in reference [5.5]. These are listed in table 5.3. The most significant releases occur from the fuel handling and blanket processing systems of the DT reactors. There is not a large variation in these release rates with plasma beta for a given fuel cycle. This is due to the fact that the amount of tritium circulating in the system depends on the fusion power, which is constant for each fuel cycle. Although the tritium release rates during operation of the DT fuel processing systems may be significant, secondary enclosure and continuously operating the routine atmosphere cleanup system is expected to remove over 99 % of the tritium. This will significantly reduce the potential for tritium release from these sources to the environment.

It is important to note that the quantities of tritium released during routine maintenance depend upon the design of components (to permit outgassing before maintenance), the maintenance procedures and rapid resealing of components after maintenance. Some attention to these considerations would result in releases to the environment lower than those indicated in table 5.3. Temporary secondary containment during maintenance work could also reduce the releases. However, utilizing continuous secondary containment around components adjacent to the reactor would be difficult and possibly expensive due to geometrical complexities. Remote maintenance and removal of these components would be hindered by secondary enclosures and may encumber maintenance or replacement of other large pieces of equipment. In any case, the atmospheric cleanup system would process the tritium released to the reactor building during maintenance if tritium levels approached the maximum permissible concentration.

5.1.2.1 Tritium Releases From the Fuel Handling Systems

Fuel handling system components from which tritium may be released include fueling devices, the vacuum system, the impurity removal system, the hydrogen isotope separation system and tritium storage. In this section, the tritium source terms associated with the fuel handling systems, for each fuel cycle, will be estimated. They are largely be based on release estimates from TSTA (Tritium Systems Test Assembly) given in reference [5.5].

The fueling approach used for the designs considered in this work is gas puffing. It was assumed that one hour's supply of fuel would be held in the fueling devices at any one time. The piping to and from the fuelers will be operated at high vacuum and with vacuum quality seals. It is expected that tritium leakage from the fuelers during operation will not be significant. Some release, however, may occur during maintenance. Scheduled maintenance or repair of the fueling devices is estimated to be necessary twice a year [5.5]. For STARFIRE, the maximum release to the reactor building per replacement has been estimated by Cannon as 200 Ci [5.5]. The release rate for the DT designs considered in this work can be scaled from this value, based on the tritium inventory in the fuelers (see table 5.1). This results in a release rate during fueler maintenance of 1440 Ci/year. The expected release is the same for all values of beta since the required amount of tritium for fueling is the same in each case. For the DD designs, only one tritium fueler is needed, containing a much smaller quantity of tritium. The expected release rate is somewhat reduced, and was estimated at 3.2 Ci/year (for maintenance of a single fueler, twice per year). For the DHe fuel cycle, no tritium is fueled, and hence, no release will occur during fueler maintenance or repair. It should be noted that any possible tritium release from the fuelers during the initial phase of the pulse, when some tritium must be injected into the advanced fuel reactors to achieve ignition, is not considered. The DT mixture would reside in the fuelers for a short time during the initial phase of reactor operation, when releases are expected to be insignificant. Subsequent use

of the fueler with either deuterium or helium-3 should remove any residual tritium so that a negligible quantity would remain and be vulnerable to release during maintenance.

The ash removal system used in the present work is a pumped limiter. This is composed of the limiter and limiter ducts, a plenum region, vacuum ducts and the cryopumps. During plant operation, no significant tritium out leakage is expected since a high vacuum will be maintained and vacuum quality seals will be used. Some repair or maintenance of this system will take place during the scheduled outage period. The maximum tritium release to the reactor building per maintenance event (once per year) has been estimated at 500 Ci for STARFIRE [5.5]. This was based on tritium contamination and available surface area of the components. An estimate of the tritium release for the different fuel cycles can be made, assuming that the tritium contamination is proportional to the tritium exhausted through the vacuum system and the surface area of components. The available area in the vacuum system was calculated for each fuel cycle. These are listed in table 5.3, along with the tritium exhaust rates and the release estimate.

Estimates of tritium release rates from the cryopumps can be obtained from estimates from TSTA. During normal operation, the TSTA vacuum pumps will contain anywhere from very small amounts up to 6 g of tritium on the cryopanels just before regeneration. The estimated release to the reactor hall is 80 to 150 Ci/year [5.5]. Tritium release rates for the designs considered here can be scaled from these estimates using either the total vacuum pump inventory (0 to 6 g for TSTA) or the tritium exhaust rate (188 g/d for TSTA) [5.5]. The exhaust rate approach is probably more appropriate because the inventory can be affected by relatively minor changes in design and may have little or no effect on tritium release rates. Estimates of release rates using both approaches are given in table 5.3.

From the cryopumps, the mixture of hydrogen isotopes enters the impurity removal system where chemical impurities are removed. It is expected that the impurity removal system will be contained in inert atmosphere glove boxes with a routine atmospheric cleanup system for secondary protection [5.5]. It is anticipated that little or none of the release will reach the environment [5.5].

An inventory of tritium may be held up in the hydrogen isotope separation system, where tritium, deuterium and protium are separated by cryogenic distillation. All of the components of the isotope separation system are under double containment provided by the vacuum jacket. Also, the vacuum jacket is designed to hold the entire contents of all of the columns. Surge tanks for storing evolved gas from vaporization of the hydrogen liquids are provided in the event of refrigeration loss. Additionally, vessels filled with uranium powder are available for storing gaseous hydrogen isotopes as solids. Any releases to the vacuum jacket and the distillate waste stream (containing mostly H_2, HD, with very little HT) are directed to the tritiated waste processing system before discharge to the environment. The release rates from this system can be estimated by linear scaling from TSTA using the tritium plasma exhaust rate [5.5]. They were found to be 45.7 Ci/year for the DT reactors, 0.46 Ci/year for the DD reactors and 0.57 Ci/year for the DHe reactor.

The tritium waste treatment system will routinely remove tritium from all gaseous effluents generated in the various subsystems, such as the isotope separation system, purge streams, the impurity removal system, effluent streams, secondary containment and exhaust from primary and secondary vacuum pumps. Catalytic conversion of molecular tritium to tritiated water, and of organic materials to water and carbon dioxide will be performed by this system. The water is adsorbed on molecular sieves in drying towers and if the remaining gaseous effluents have a tritium level low enough, they will be discharged to the atmosphere. The release rates estimated for the cases considered here were obtained by linear scaling with tritium exhaust rates from TSTA values. These values are listed in table 5.3.

Table 5.3: Tritium Release Estimates from the Fuel Handling Systems

Fuel Handling System	Fuel Cycle							Classification
	DT			DD			DHe	
	5 %	10 %	20 %	5 %	10 %	20 %	10 %	
Fueling Devices:								
Total Tritium Inventory (g)	90	90	90	0.4	0.4	0.4	0	
Tritium Release (Ci/year)	1440	1440	1440	3.2	3.2	3.2	0	maintenance
Vacuum System:								
Vacuum Duct Surface Area (m^2)	1742	1543	1400	2840	2210	1805	2219	
Tritium Exhaust Rate (g/d)	1598	1598	1598	16	16	16	20	
Tritium Release Rate From Vacuum Ducts (Ci/year)	1046	927	841	17.1	13.3	10.9	16.7	maintenance
Total Pump Tritium Inventory (g)	133	133	133	20.8	20.8	20.8	26.4	
Vacuum Pump Release Rate (Ci/year) (scaled by inventory)	1773 - 3325	1773 - 3325	1773 - 3325	277 - 520	277 - 520	277 - 520	352 - 660	chronic
Vacuum Pump Release Rate (Ci/year) (scaled by exhaust rate)	680 - 1275	680 - 1275	680 - 1275	7 - 13	7 - 13	7 - 13	9 - 16	chronic
Release From Impurity Removal System	-	-	-	-	-	-	-	

Fuel Handling System	Fuel Cycle							Classification
	DT			DD			DHe	
	5 %	10 %	20 %	5 %	10 %	20 %	10 %	
Release From Isotope Separation System (Ci/year)	45.7	45.7	45.7	0.46	0.46	0.46	0.57	chronic
Release From Tritium Waste Treatment System (Ci/year)	45.7	45.7	45.7	0.46	0.46	0.46	0.57	chronic
Total Release Rate (Ci/year):								
Scaled by Inventory	4352 - 4856	4233 - 5783	4147 - 5697	296 - 541	292 - 537	290 - 535	368 - 693	
Scaled by Exhaust Rate	3257 - 3852	3138 - 3733	3052 - 3647	231 - 421	227 - 417	225 - 415	283 - 518	

Provision for tritium storage must be furnished, both for fueling needs and to provide surge capacity between several items of process equipment. It is assumed that the tritium will be stored as uranium tritide. The uranium beds would be stored in gloveboxes located within a vault containing an inert gas (to reduce the fire hazard). Tritium losses to the containment system from storage would be processed by the tritium waste treatment system. Only minor quantities escaping from the waste treatment facility could be attributed to on-site tritium storage. Thus, releases from storage have been assumed to be included in the releases from the tritium waste treatment system.

5.1.2.2 Tritium Releases From the Blanket and the Breeder Processing Systems

For the DT fuel cycle, the blanket processing systems provide another pathway for the release of tritium to the environment. As described in the previous chapter, a molten salt extraction process can be used to remove tritium from the lithium breeder. Tritium can escape from the blanket by permeation, leaks and release during maintenance. Tritium released from annual blanket module replacement is due to outgassing of dissolved tritium. This has been estimated for a helium cooled tokamak using a lithium breeder in reference [5.5]. Their estimate for the annual quantity of tritium released was 1200 Ci/year. Scaling this by the first wall area and tritium flux (to account for the contribution to the release from tritium adsorbed on the surface or implanted a short distance below the surface) and by blanket volume and tritium inventory (to account for the contribution to the release from tritium diffusing out of the module) gives the appropriate value for the DT designs used in this study. These are given in table 5.4. Some variation with beta is seen and is a consequence of the geometric scalings. Tritium releases from the blanket recovery system were also estimated in reference [5.5] to be a maximum of 1 Ci/d. This value was scaled by the recovery system tritium inventory to give a tritium release rate

for the DT designs in this work of 56 Ci/year.

Because of the extremely small tritium inventory in the advanced fuel blankets, no significant release of tritium from the blanket structure is expected.

5.1.2.3 Tritium Releases From The Coolant System

The coolant system presents another potential source for tritium releases. Tritium can permeate or leak from the plasma through the first wall or from the blanket into the coolant stream. Once in the primary loop, the tritium can reach the steam system from which removal is especially difficult. Tritium can escape from the coolant system by permeation, leaks and releases during maintenance.

For the DT design, tritium transport rates into the coolant and loss rates from water leakage from the steam generator can be estimated from the work done for the BCSS [5.6, 5.7, 5.8, 5.9]. To obtain the appropriate values for the designs considered here, the BCSS values were scaled with tritium flux to the first wall and the first wall area. The tritium found in the helium stream was assumed to be entirely in the T_2 form. The tritium loss rates from the steam generator given in the BCSS are for the case without any slipstream processing of the main helium flow for tritium removal. However, the loss rate corresponds to the addition of hydrogen for isotopic dilution at a rate of 100 times the first wall tritium influx rate. This creates a reducing atmosphere on the helium side of the blanket and heat exchanger tubes, inhibiting the formation of an oxide layer. A permeation barrier factor of only 2 was assumed in the calculations. However, the isotopic dilution is effective in reducing the tritium losses to a large degree. The release rates for the advanced fuels were obtained in the same way as for the DT case. The resultant values for tritium lost rates from the plasma to the coolant and from tritium losses due to leakage of steam generator water are given in table 5.4. The values for the advanced fuels are roughly two orders of magnitude lower than for the DT case.

5.1.2.4 Tritium Releases From Waste Handling

Tritiated wastes will be in both solid and liquid forms. Tritiated water, cleaning solvents and oil will comprise the bulk of the tritiated liquid wastes. Solid wastes will be generated from the blanket sectors, replaced auxiliary equipment, depleted catalysts, molecular sieve beds and miscellaneous contaminated wastes such as paper, rags, tools and clothes. Contaminated equipment components removed from the reactor must be decontaminated, probably by heating or gas flushing, before being disposed of. Effluent from decontamination operations must be processed to remove tritium prior to exhaust to the atmosphere. Subsequent to tritium removal, components having a large inventory of activation products will be stored under water in a waste handling pool. Some residual tritium may still remain on the equipment placed in the storage pool so that contamination of the pool water may result. This water can later be processed with other aqueous wastes from the plant if it contains a high enough tritium content that recovery is worthwhile. Unrecovered tritiated wastes can be solidified and stored in concrete form or adsorbed on vermiculite or molecular sieves. These solidified wastes along with other miscellaneous wastes can be packaged in a nested series of watertight drums. Blanket modules and other large pieces of equipment contaminated with tritium may be outgassed in a chamber with good containment before being compacted and stored [5.5].

Tritiated wastes generated at the fusion plant will be greatest for the DT fuel cycle. The volume and activity of tritiated wastes will be reduced for the advanced fuels. In Cannon's work [5.5], he estimated that tritium releases to the environment from handling tritiated wastes at a DT plant would be approximately 1 Ci/d. Release rates for these activities at the advanced fuel fusion plants were estimated by scaling with the total tritium inventory in the plant. Release rates are found to be 1.03×10^{-2} Ci/d for the DD fuel cycle and 7.53×10^{-3} Ci/d for the DHe fuel cycle.

Table 5.4: Tritium Release Estimates from Various Plant Locations

Location	Fuel Cycle							Classification
	DT			DD			DHe	
	5 %	10 %	20 %	5 %	10 %	20 %	10 %	
Fuel Handling Systems (Ci/year)	2486	2367	2281	20.3	16.5	14.1	16.7	maintenance
(scaled by tritium exhaust)	771 - 1366	771 - 1366	771 - 1366	8 - 14	8 - 14	8 - 14	10 - 17	chronic
Blanket (Ci/year)	421	319	251	7.04×10^{-3}	4.32×10^{-3}	2.79×10^{-3}	2.05×10^{-3}	maintenance
Blanket Processing (Ci/year)	56	56	56	-	-	-	-	chronic
Plasma to coolant (g/d)	0.16	0.16	0.16	1.59×10^{-3}	1.59×10^{-3}	1.59×10^{-3}	1.99×10^{-3}	chronic
Plasma to coolant (Ci/d)	1536	1536	1536	15.3	15.3	15.3	19.1	
Steam Generator Leakage (Ci/d)	12.2	12.1	12.0	0.12	0.12	0.12	0.15	chronic
Steam Generator Leakage (Ci/year)	4456	4420	4383	44	44	44	55	
Waste Handling (Ci/year)	1.0	1.0	1.0	1.03×10^{-2}	1.03×10^{-2}	1.03×10^{-2}	7.53×10^{-3}	chronic
Average Tritium Source Term (Ci/year)	8839	8583	8401	79	75	73	85	
Average Tritium Source Term (Ci/d)	24.2	23.5	23.0	0.216	0.205	0.199	0.233	

5.1.2.5 Atmospheric Tritium Releases From The Plant

It is desirable to contain all tritium releases, whether from normal leakage or from an accidental release, within the confines of the plant. Different levels of containment can be used in tritium related systems to minimize releases of airborne tritium to the environment. Effective primary containment is provided by the use of all metal components in fuel handling equipment. Gloveboxes, vacuum jackets, jacketed tubing and nested containers provide secondary containment and are of special need for high temperature components. The walls of potential tritium containing areas can be lined with a tritium barrier such as stainless steel or aluminium. Equipment used within a tritium area can be constructed of materials to minimize surface adsorption. Operating tritium areas at reduced atmospheric pressure will reduce tritium out-leakage. The number and length of lines used for tritium transport between buildings should be minimized. These measures in addition to operation of an atmospheric cleanup system can minimize routine leakage and permeation to the environment. Major maintenance activities, including replacement of blanket modules, vacuum pumps, impurity control devices and fueling equipment are the principal sources of tritium releases to the reactor building. Other miscellaneous tritium releases in areas without secondary containment may also occur on a regular basis [5.5].

The need for effective tritium containment is not eliminated by the availability of an atmospheric cleanup system. These systems are expensive to operate and also produce tritium contaminated waste water which must be appropriately dealt with. The system can be activated during maintenance activities if the tritium level in the reactor hall exceeds the $5\mu Ci/m^3$ limit for unprotected personnel access. The normal tritium release rates into the reactor hall are not large, even for DT reactors. Because the reactor buildings can be made very leak tight and have low leakage rates if maintained at a slightly negative pressure, tritium discharges to the environment from the plant should not present a significant hazard. The STARFIRE report [5.3]

estimated a tritium loss due to building leakage of less than 1μCi/d assuming a leakage rate of 3 x 10^{-5} vol%/d and a tritium concentration of 5μCi/m^3 in the 4 x 10^5 m^3 of tritium containing volume.

The quantity of tritium released from a fusion plant to the environment depends upon the tritium level within the reactor building. A steady state tritium concentration will be reached after commencing reactor operation, where leakage rates from system components are balanced by stack emissions, building leakage and removal by the atmospheric tritium recovery system. If the tritium release to the reactor hall is below 10 Ci/d and the room concentration is below 5μCi/m^3, direct ventilation to the environment is possible [5.12]. Leakage rates from plant components have been determined in the previous sections and an average tritium source term was estimated for each fuel cycle (see table 5.4). Assuming a leakage rate of 3 x 10^{-5} % per day [5.3] and one atmospheric changeout per day (vented through the stack)†, the steady state tritium concentration without the use of an atmospheric tritium removal system was evaluated. As discussed in chapter 4, it appears unjustified to maintain the reactor hall tritium level below 50μCi/m^3 [5.13]. From table 5.5, it appears that the DT reactor buildings will require continual processing to maintain the atmosphere at the 50μCi/m^3 level. The largest atmospheric detritiation system processes air at a rate of 140 m^3/min (2.3 m^3/s), at an estimated cost of 4.6 M$ (from reference [5.14], updated to current dollars). A single unit would be capable of maintaining the acceptable tritium level for the DT reactors. The tritium level was recalculated assuming this unit would operate at full capacity. The steady state tritium concentration, the stack emissions and the tritium leakage from the building resulting when a single detritiation unit is used for the DT reactors

† With an assumed reactor building volume of 4 x 10^5 m^3 [5.3], one atmospheric changeout per day would release 20 Ci per day to the environment if the reactor building steady state tritium concentration was 50μCi/m^3. This was the recommended design goal for tritium release to the environment under routine operation for INTOR [5.12].

are listed in table 5.5. For the advanced fuels, where the tritium release rates from plant components are far below 10 Ci/d and the steady state tritium concentration is much less than $5\mu Ci/m^3$, direct venting of the reactor building atmosphere to the environment is permitted. Tritium releases to the environment for the DD and DHe fuel cycles are also listed in table 5.5. Further details related to the sizing of the atmospheric tritium removal system are given in appendix D.

The projected tritium release rates for the fusion reactors examined here are compared to releases from other nuclear installations in table 5.6. As can be seen, the anticipated releases from the DT fusion plants exceed those from Light Water Reactors (LWRs), but are less than those from Heavy Water Reactors (HWRs). The projected releases from the DT fusion plants are also higher than those expected from High Temperature Gas Reactors (HTGRs) and Liquid Metal Fast Breeder Reactors (LMFBRs). However, the DT plant releases 3 % of the amount produced naturally as a consequence of cosmic ray interactions with N_2 and O_2 in the upper atmosphere and from the accretion of tritons emitted during solar flares. Tritium is also produced through the fission of natural uranium ores. However, this is a much smaller source and leads to tritium that is bound in the earth's crust. The advanced fuel reactors release much less tritium than any other of the nuclear facilities and a negligible amount compared to that produced naturally in the environment.

Some provision for atmospheric clean up in the event of an accident must be available. Emergency tritium removal capabilities were determined based on a 48 hour clean up period subsequent to the release of the maximum vulnerable tritium inventory. The maximum vulnerable tritium inventory is located in the blanket processing system for the DT reactors and in the cryopumps for the advanced fuels. Eight units could reduce the tritium concentration to the level where suited personnel access is allowed ($500\mu Ci/m^3$) within 48 hours for the DT designs. Four units could accomplish the job for the advanced fuels. Because these units are expensive to operate, they would only be used in the event of an accident. For normal conditions, the DT reactor buildings will have continuous atmospheric processing using

one detritiation unit; the advanced fuel reactor buildings will not require continuous atmospheric processing.

A further evaluation was performed where the effect of tritium soaking into materials was considered. Initially clean surfaces, or surfaces exposed to high room air tritium concentrations act as sinks for tritium. If the room air concentration is substantially lowered, outgassing of absorbed tritium may occur. This phenomenon will prolong the duration of clean up after maintenance or accidental releases, and may result in greater clean up capacity requirements. A computer code has been developed, based on diffusion theory, which takes this effect into account. A discussion of the theory and method of solution, along with a listing of the code are given in appendix D.

Application of the code to normal conditions verified the results previously obtained using the simpler model. As would be expected, the steady state concentration for all fuel cycles were found to agree with the earlier predictions. Thus, the use of a single clean up unit during normal operation for the DT fuel cycle was confirmed. Also, the advanced fuel cycles were found not to require continual atmospheric processing during normal operation. Assuming an initially tritium free room, the steady state room air tritium concentration in the reactor hall would be reached $\sim$ 6 days after initiating the source term for the DT fuel cycle; $\sim$ 12.5 days would be required for steady state to be achieved for the advanced fuels. The diffusion model would predict slightly longer times to achieve steady state than the simple model because some tritium would continue to be lost from the room to the walls until the surfaces were saturated.

Emergency clean up capabilities were also evaluated using the code. The criterion of achieving a tritium concentration of 500 μCi/m^3 within 48 hours of the release of the most vulnerable tritium inventory was applied. Consideration of diffusion of tritium into solid surfaces had the effect of prolonging clean up so that the 500 μCi/m^3 level was not achieved within 48 hours with the previously determined

Table 5.5: Atmospheric Tritium Releases

	Fuel Cycle						
	DT			DD			DHe
	5 %	10 %	20 %	5 %	10 %	20 %	10 %
Tritium Source Term (Ci/d)	24.2	23.5	23.0	0.216	0.205	0.199	0.233
Tritium Conc Without ATRS† (μCi/m^3)	60.5	58.8	57.5	0.54	0.51	0.49	0.58
Tritium Stack Release Without ATRS (Ci/d)	24.2	23.5	23.0	0.216	0.205	0.199	0.233
Tritium Leakage Without ATRS (μCi/d)	7.3	7.1	6.9	6.50×10^{-2}	6.1×10^{-2}	5.9×10^{-2}	7.0×10^{-2}
ATRS Capacity to maintain 50μCi/m^3 (m^3/min)	58.3	48.6	41.7	0	0	0	0
No. Units Operative Under Normal Conditions	1	1	1	0	0	0	0
Steady State Tritium Conc Using full ATRS capacity (μCi/m^3)	40.2	39.1	38.2	N/A	N/A	N/A	N/A
Tritium Stack Release Using full ATRS capacity (Ci/d)	16.1	15.6	15.3	N/A	N/A	N/A	N/A
Tritium Leakage Using full ATRS capacity (μCi/d)	4.8	4.7	4.6	N/A	N/A	N/A	N/A
Maximum Vulnerable Tritium Release (g)	68.5	68.5	68.5	1.3	1.3	1.3	1.1
ATRS Capacity for 48 h Clean up (m^3/min)	1120	1120	1120	560	560	560	560
No. Units Operative Under Accident Conditions	8	8	8	4	4	4	4
Cost of ATRS (M$)	36.8	36.8	36.8	18.4	18.4	18.4	18.4

† Atmospheric Tritium Removal System

Table 5.6: Comparison of Tritium Releases to the Environment From Fusion and Fission Plants

Source	Tritium Release (Ci/yr)
DT Plant[a]	5720
DD Plant[a]	75
DHe Plant[a]	85
STARFIRE [5.3]	7135[b]
LWR[d] [5.19]	778
HWR [d]	18,000[c]
HTGR[d] [5.19]	714
LMFBR[d] [5.19]	649
Natural [5.19]	1.95×10^6

[a] Average release rate for designs of 5 %, 10 % and 20 % beta

[b] Note that this is a water cooled plant which will likely have greater losses than a helium cooled plant.

[c] Emissions to air from Pickering-NGSA in 1982 [5.20]

[d] This does not account for releases due to any fuel reprocessing activity.

clean up capacities. One additional unit was required in each case, giving a total of 9 units for the DT fuel cycle and 5 units for the advanced fuel cycles.

The capital and operating costs indicated in table 4.6 refer to the results obtained using the simple model. Capital costs would increase by 4.6 M$, or 12.5 % for the DT fuel cycle and 25 % for the DD and DHe fuel cycles, if diffusion theory results were used. Operating costs would not be affected since they refer to normal plant conditions.

5.1.3 Doses Due to Tritium Exposure

Tritium will be encountered in the fusion plant wherever it is conveyed by pumping, air flow or liquid flow, or wherever the diffusion process could result in significant concentrations. Leakage of tritium into the reactor hall will occur from the vacuum system, the blanket, coolant lines and tritium processing equipment. The consequences of tritium exposure have been investigated over many years. Tritium decays with a half-life of 12.35 years, emitting a low energy beta particle (18 keV peak energy, 5.7 keV average energy). As an isotope of hydrogen, it pervades the environment in the same chemical form as other hydrogen isotopes. Tritium in its water form is much more hazardous than in its elemental form; the potential hazard from inhalation is 25,000 times greater for HTO than for HT [5.15]. Submersion in a cloud of HT gas will result in direct exposure to the lung tissue and internal exposure due to HT gas absorbed in the lung tissue. External exposure is not a serious concern because the low energy beta particle is unable to penetrate to the basal layer of the skin. Tritiated water vapor can be inhaled or absorbed through the skin. Both of th se modes of uptake are very efficient. Once within the body, the HTO is readily distributed with the rest of the body water. Through chemical exchange processes, the tritium can be incorporated into organic molecules within the body where it may remain for some time. In the water form, it will remain in

the body for a nominal 9 to 12 day half-life for body water turnover. A further mode for tritium uptake is through contact with contaminated surfaces. However, highly contaminated metal surfaces are needed for percutaneous absorption of tritium to become significant when compared to submersion.

Worker exposures to tritium will depend on the tritium release rates and on the amount of time workers spend in the reactor hall. These exposures can be kept to a minimum by processing the building air, by having the workers wear protective clothing and by controlling exposure time. Tritium inventories and major sources of tritium releases have been identified and estimated in the previous sections. Due to the uncertainty with the actual operation and maintenance scenarios (i.e. when activities which will be releasing tritium in addition to the steady state losses will be performed), the tritium source term included both chronic and maintenance releases and was averaged over the entire year. Tritium losses to building areas resulting from accidents were not included in the tritium release estimates. All contact maintenance activities were assumed to be performed at the perfectly mixed steady state tritium concentration given in table 5.5 (operation of a single detritiation unit was assumed for DT). This approach may underestimate doses for activities which cause localized releases of tritium; doses for activities which release no tritium (such as routine operation tasks) may be overestimated.

Occupational tritium exposures for the most exposed work group were obtained using an estimate of the total man-hours of contact maintenance (see appendix E). Various maintenance modes were identified allowing for different amounts of contact maintenance, depending on the actual task and anticipated radiation levels. Assuming all of the tritium in the reactor hall to be in the oxide form, dose rates due to tritium exposure were found to be 10.1 mrem/h for DT, 0.13 mrem/h for DD and 0.15 mrem/h for DHe. Cumulative doses for unsuited workers of the most

exposed group† were found to be 32.2 man-rem for DT, 0.40 man-rem for DD and 0.64 man-rem for DHe. Protective bubble suits would reduce these doses to 0.65 man-rem for DT, 0.008 man-rem for DD and 0.013 man-rem for DHe (a reduction in dose by a factor of 50 results from a protection factor of 100 from the suits and a work efficiency reduction by 50 %). It is very likely that protective clothing will be worn at the DT reactors; this practice may also be instituted at the advanced fuel reactors as a precaution against accidental release (the release of the inventory of a single cryopump would result in a concentration of 0.031 Ci/m^3 and a dose rate of 8.05 rem/h in the DD reactor building; a concentration of 0.026 Ci/m^3 and a dose rate of 6.81 rem/h would exist in the DHe reactor building). It is apparent that the occupational tritium exposures are reduced by $\sim$ 80 times for the DD fuel cycle over the DT fuel cycle; a reduction of $\sim$ 50 times results for the DHe fuel cycle. The higher cumulative dose incurred for the DHe fuel cycle compared to the DD fuel cycle is a consequence of the increased amount of contact maintenance permitted due reduced structural activation.

An estimate of individual doses to workers in the most exposed group and to the total number of exposed workers in the plant can be found. The number of workers comprising each of these groups is estimated in appendix C. Dividing the expected cumulative dose for the most exposed group by the estimate of the number of workers in this group gives the individual exposure indicated in table 5.7. For the DT plants, the average individual dose due to tritium to a member of the most exposed group was found to be $\sim$ 200 mrem/year. This is slightly lower that the estimate of 250 mrem/year given by Stasko and Wong [5.16] for the average annual occupational tritium dose for a worker in the most exposed group. Stasko and Wong

† These doses are given for the 10 % beta designs. Because of the differing requirements for blanket changeouts (and hence entry of workers into a tritium contaminated environment), the dose incurred for the 20 % beta designs will be slightly greater and that incurred for the 5 % beta designs will be slightly less. A variation of $\sim$ 5% about the 10 % beta design results.

Table 5.7: Doses Incurrred Due To Routine Tritium Releases

	Fuel Cycle (10 % beta)		
	DT	DD	DHe
Average Dose Rate in Reactor Hall (mrem/h)	10.1	0.13	0.15
Annual Cumulative Dose for Most Exposed Group (man-rem/yr)	32.2	0.396	0.671
Annual Individual Exposure to Member of Most Exposed Group (mrem/yr)	195	2.59	4.70
Annual Cumulative Dose for Total Plant Exposed Work Force (man-rem/yr)	34.8	0.426	0.728
Annual Individual Exposure to Member of Total Plant Exposed Work Force (mrem/yr)	98	1.30	2.37
Offsite Dose (mrem/yr)	< 4.7	< 0.041	< 0.047

[5.16] also indicate that the total exposed work force averages an individual dose which is 50 % lower than the most exposed group. Knowing this and an estimate of the total number of exposed workers (see appendix C), the average individual tritium exposure and the cumulative exposure for all exposed plant personnel can be evaluated. This information is given in table 5.7.

A very rough estimate of offsite doses to the public during normal operating conditions has been made at this time. In the Minimars study [5.17], a design target for chronic tritium emissions of 25 Ci/d of tritium oxide to the building atmosphere was adopted since it would not result in doses exceeding the NRC public dose limit of 5 mrem/year. Release rates to the building atmosphere given in table 5.4 are below 25 Ci/d. Thus, none of the designs in this study result in unacceptable routine offsite doses. Rough estimates of the maximum expected dose to the public were obtained by scaling with the chronic tritium release rate to the building atmosphere. These are indicated in table 5.7. The relative improvement of the advanced fuels over the DT plant is roughly 100 fold.

5.1.4 Tritium Hazard Summary

The advanced fuels have a clear advantage over the DT fuel cycle in terms of tritium hazard. The tritium circulating throughout the plant, tritium inventories in plant components, tritium release rates from these components and tritium exposures incurred during maintenance activities are all significantly reduced for the DD and DHe fuel cycles.

The tritium fueled to the DD torus is over two orders of magnitude lower than for the DT torus; no tritium is fueled to the DHe torus. The steady state tritium concentration in the plasma chamber is one to two orders of magnitude lower for DD and DHe. The higher fractional burnup of tritium for the advanced fuels contributes to the tritium exhausted from the plasma being two orders of magnitude lower. This

is important because the tritium inventories established throughout the plant are strongly dependent on the tritium exhaust rate from the plasma.

Concerns associated with tritium in the breeding blanket and blanket processing systems are completely eliminated for the advanced fuels. First wall tritium inventory is reduced by two orders of magnitude; tritium retained in the blanket structure is reduced by three orders of magnitude. Although the quantity of tritium found in the coolant is small for all fuel cycles, the two orders of magnitude reduction for the DD and DHe fuel cycles is significant because permeation of tritium into the steam cycle and subsequent leakage from this system is a major tritium pathway to the environment. There is a large reduction in the quantity of tritium found in the cryopumps for the advanced fuels. The inventory in the fuelers for the DD fuel cycle is reduced by two orders of magnitude over the DT fuel cycle; the DHe fuel cycle requires no tritium fueling so that this hazard is completely eliminated. As indicated in table 5.5, the total vulnerable tritium inventory is reduced by over a factor of twenty for the DD and DHe fuel cycles. The presence of any radioactive species, in any form, may be judged undesirable (the public will likely not distinguish between vulnerable and non-vulnerable inventories). Thus, in the public's eye, it would be the total inventory at the site which would be of concern. This places the advanced fuel reactors in a more favorable position because the total inventory is reduced by nearly two orders of magnitude over the inventory associated with a DT reactor.

The impact of eliminating the tritium breeding blanket should be examined more closely. The relative contribution of the tritium inventory in the blanket to the total DT plant inventory is depicted in figure 5.2a. The tritium inventory in the blanket and blanket processing system is somewhat less than that in the exhaust processing system and much smaller than that in storage. For the advanced fuels, as shown in figures 5.2b and 5.2c, the bulk of the inventory is also located in the exhaust processing systems. From a tritium handling viewpoint, the advanced fuels are much more desirable because of the reduced quantities of tritium passed

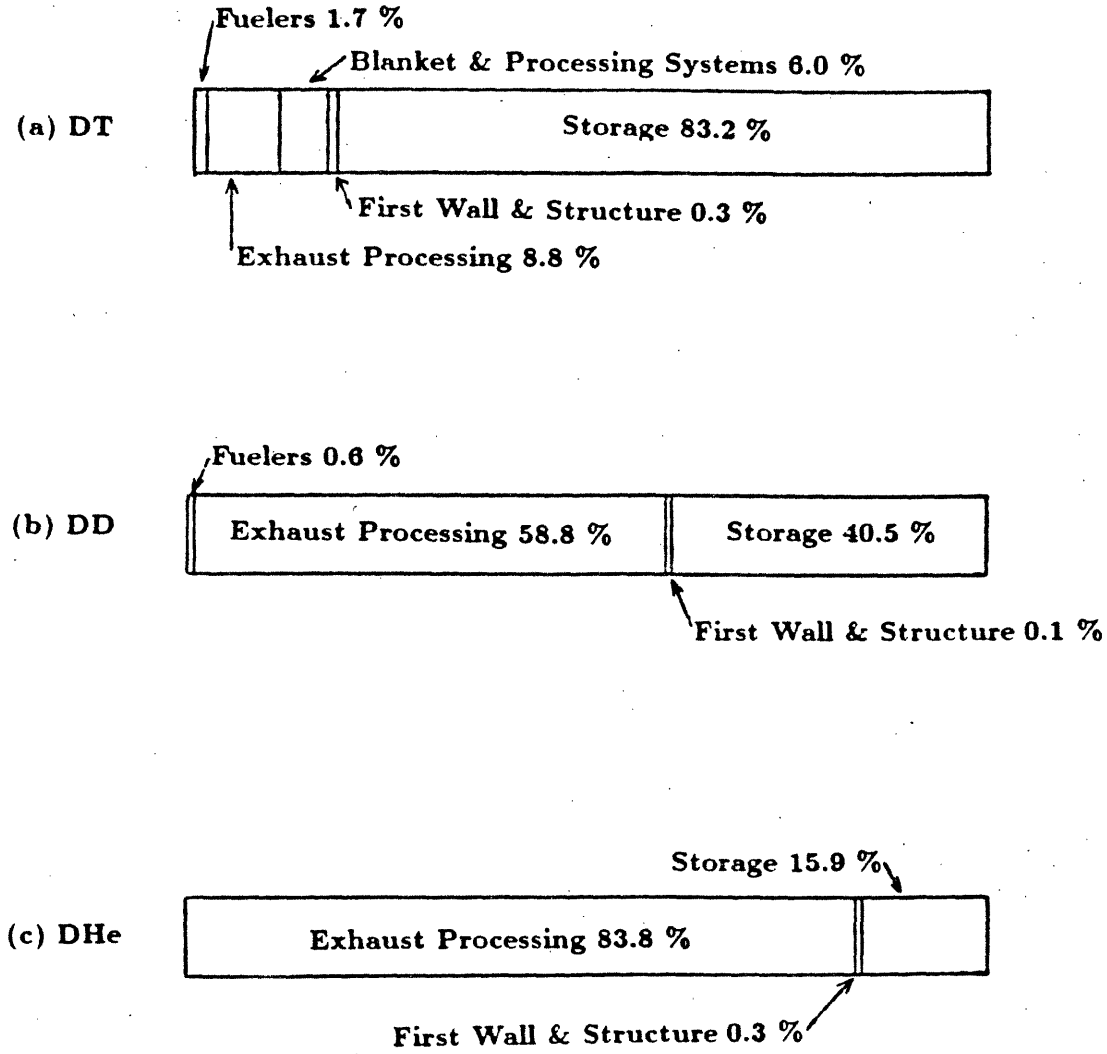

Figure 5.2: Relative Contributions to Total Tritium Inventory

through the exhaust system. The quantity of tritium bred in the DT reactors is 634 g/day. The tritium flow rate out of the reactor is significantly higher than this being 1598 g/day. This compares to 16 g/day for DD and 20 g/day for DHe. Thus, the reduction in tritium handling by the elimination of tritium breeding is not as significant as may have been expected. Tritium breeding and processing are not the major contributors to the plant tritium inventory, making up only 6 % of the total. The elimination of the tritium breeding function with the advanced fuels does not eliminate the need for tritium extraction systems from the coolant or the need for cryopumps, molecular sieves, cryogenic distillation columns and fuelers. These components are required whether or not tritium is bred. However, the quantity of tritium handled by these components for the DT fuel cycle is much greater than for the advanced fuels. With regards to the DT fuel cycle, it is the fuel handling systems and not the breeder and breeder processing systems which have the greatest tritium throughput and inventory.

The occupational tritium hazard and tritium releases to the environment are dependent upon the releases to the reactor building during normal operation and maintenance. As can be seen in tables 5.3 and 5.4, a significant improvement in this respect is evident for the advanced fuels. The average tritium source term is two orders of magnitude lower than for DT. Because of this, the steady state tritium concentration in the reactor hall is low enough that unprotected personnel access is permitted, and the building atmosphere can be directly vented to the environment without processing. It is also evident that for the DT fuel cycle, the greatest tritium hazard is associated with the fuel handling systems due to the large tritium throughput. Release rates from the fuel handling systems total $\sim$ 2400 Ci/year, compared to $\sim$ 400 Ci/year from the blanket and blanket processing systems. The release rate from the fuel handling systems for each of DD and DHe is $\sim$ 17 Ci/year, a considerable reduction from the DT fuel cycle.

An earlier study concluded that the tritium throughput for a catalyzed DD machine would be a factor of 100 less than for a DT machine, and that the throughput

for a DHe machine would be reduced by a factor of 1000 [5.18]. For the semi-catalyzed DD reactors studied here, a reduction by a factor of 100 in tritium throughput is indeed seen. However, the tritium throughput for the DHe reactor is very near to that for the DD reactor. A reduction in tritium throughput by 100 times from DT is seen, not by 1000 times as indicated in the previous work. The details on which this earlier conclusion is based were not given. In the present work, the plasma exhaust rate is based on the tolerable level of alpha ash in the plasma. Since alpha particles are produced from D$-^3$He reactions and from D-T reactions, their formation rate is high in the plasma of a DHe reactor. A large plasma exhaust rate is needed to maintain the alpha ash concentration in the plasma at an acceptable level. This results in relatively high recirculation rates of all species and a relatively high tritium inventory throughout the plant.

5.2 Induced Radioactivity Hazards

Although the fusion reactions considered in this study do not produce any non-fusable radioactive products, the neutrons released can activate the materials surrounding the plasma chamber. This results in an inventory of radioactive by-products in the reactor materials. In this section, estimates of the inventory of activation products that will result from the operation of fusion reactors employing the various fuel cycles is provided. These estimates have been made using one-dimensional neutron transport calculations. Dose rates in the fusion reactor environment and their potential impact on the occupational work force are also estimated. Routine offsite releases are also discussed.

5.2.1 Activation Product Inventories

The level of activation that occurs in a fusion reactor depends on the neutron wall loading, the neutron flux spectrum, the operating history of the reactor and the elements that are activated. The neutron wall loading is dependent on the fuel cycle. For the DT fuel cycle, 80 % of the fusion energy is released in the form of neutrons; for the semi-catalyzed DD fuel cycle, this fraction is reduced to 60 %. Although no neutrons are produced directly from the fusion of deuterium and helium-3, unavoidable DD and DT side reactions result in some neutron production. In the present study, 7.7 % of the fusion energy resides with the neutrons for the DHe fuel cycle. The lower energy carried by the neutrons coupled with the fact that the advanced fuel reactors must be larger than their DT counterparts for the same thermal power production results in a much lower neutron wall loading for the DD and DHe fuel cycles. The neutron flux energy spectrum is also dependent on the fuel cycle. For the DT fuel cycle, the fusion neutrons are essentially all released at an energy of 14.1 MeV. For the advanced fuels, a large fraction of the neutrons have substantially lower energy: for the DD fuel cycle, $\sim$ 51 % are released at 2.45 MeV, the balance being released at 14.1 MeV. For DHe, the fraction released at 2.45 MeV is $\sim$ 60 %. The interaction of the neutrons of different energies and different flux levels with the materials surrounding the plasma chamber will lead to different activation products, activation levels and decay times. These will also be affected by the operating history of the plant. Different fluence limits and reactor availabilities lead to a characteristic operating history for each fuel cycle. The use of the same structural material (HT-9) for all fuel cycles will expose the same elements to the neutron flux (except for the additional exposure of a lithium bearing material for the DT fuel cycle for the purpose of breeding tritium). Thus, the radioactive inventories will be a direct reflection of the fuel cycle. The use of an alternate blanket material for the DD fuel cycle (reduced activation ferritic (RAF) first wall/Fe2Cr1V blanket) will provide additional information on the impact of changing the structural material

on activation product inventories.

The neutrons escaping from the plasma will migrate through the reactor. The majority will be absorbed in the blanket region surrounding the plasma chamber, where their kinetic energy will be recovered and converted to usable power. Some reaction of neutrons with the structural material of the blanket will result in the transmutation of stable nuclei into radioactive nuclei. Neutrons leaking out of the blanket will also react in the shield, TF coils and other reactor components, producing additional radionuclides. The production of any radionuclides is a major consideration for designers who aspire to achieve favorable safety and environmental features. Maintenance procedures, waste management operations and plant effluents will be affected by activation product levels. These, in turn, will determine the degree of occupational and public exposure. Hence, it is important that these inventories be quantified.

Activation product inventories have been evaluated for the three fuel cycles using neutron fluxes from ONEDANT† [5.21] and the activation code REAC‡ [5.22]. The concentration of major activation products in the first wall at the end of the blanket life for the different fuel cycles are given in table 5.8. The blanket lifetime depends on the total neutron fluence to which it has been exposed. This is determined by the energy of the impinging neutrons and the displacement limit of the material. Fluence limits corresponding to 250 dpa for HT-9 are 25.0 MW $\cdot$ yr/m^2 for DT, 14.6 MW $\cdot$ yr/m^2 for DD and 12.7 MW $\cdot$ yr/m^2 for DHe. For a given fuel cycle, the total activity at shutdown is seen to increase with beta and wall loading (wall

† The **O**ne-dimensional **D**iffusion **A**ccelerated **N**eutron **T**ransport code solves the linear Boltzman transport equation using the method of discrete ordinates with the diffusion approximation to accelerate convergence, in order to obtain the neutron fluxes as a function of position and energy.

‡ The **REAC** code folds the multi-group cross sections for the materials of interest with the multi-group fluxes to obtain transmutation rates and activation product inventories at various exposure times.

Table 5.8: Major Contributors to First Wall* Radioactive Inventory at End of Blanket Lifetime † (Ci/cm^3)

	DT			DD				DHe
Isotope	5 %	10 %	20 %	5 %	10 % (HT-9)	10 % (RAF)	20 %	10 %
Short Term Concerns:								
^{55}Fe	21.8	27.2	30.5	4.8	8.0	7.9	12.6	1.2
^{56}Mn	7.2	9.8	12.7	1.6	3.0	3.3	5.3	0.40
^{54}Mn	2.9	3.5	4.7	0.54	0.77	1.0	1.7	0.13
^{51}Cr	2.6	3.5	4.6	0.51	0.90	0.90	1.5	0.11
^{99}Mo	0.13	0.22	0.23	9.2×10^{-2}	0.21	4.9×10^{-5}	0.28	3.4×10^{-2}
^{188}Re	3.3×10^{-3}	4.2×10^{-3}	6.2×10^{-3}	0.11	0.17	0.19	0.26	2.2×10^{-2}
Long Term Concerns:								
^{93}Mo	7.8×10^{-5}	8.1×10^{-5}	9.1×10^{-5}	1.7×10^{-4}	1.7×10^{-4}	3.0×10^{-8}	1.7×10^{-4}	5.0×10^{-5}
^{93m}Nb	4.1×10^{-4}	4.2×10^{-4}	4.4×10^{-4}	1.1×10^{-4}	2.8×10^{-4}	9.0×10^{-8}	4.7×10^{-4}	5.5×10^{-5}
^{63}Ni	2.3×10^{-4}	2.3×10^{-4}	2.4×10^{-4}	3.8×10^{-4}	4.0×10^{-4}	7.8×10^{-6}	4.7×10^{-4}	1.0×10^{-4}
Very Long Term Concerns:								
^{99}Tc	1.2×10^{-6}	1.2×10^{-6}	1.4×10^{-6}	1.4×10^{-6}	2.3×10^{-6}	4.2×10^{-10}	2.6×10^{-6}	8.0×10^{-7}
^{59}Ni	2.8×10^{-6}	2.8×10^{-6}	2.8×10^{-6}	3.8×10^{-6}	4.5×10^{-6}	4.3×10^{-8}	4.6×10^{-6}	1.2×10^{-6}
Total Activity	37.1	47.4	57.0	8.5	14.5	15.5	24.4	2.2

* The first wall is 12 % HT-9, 88 % He by volume.

† The blanket attains the end of its life when the fluence limit is reached. Fluence limits used were 25.0 MW · yr/m^2 for DT, 14.6 MW · yr/m^2 for DD and 12.7 MW · yr/m^2 for DHe.

loadings are given in table 2.2). The high beta DT case presents the greatest hazard in terms of activity concentration in the first wall of all the cases examined. This is a consequence of the higher neutron flux to the first wall for this design. As is apparent in the table, the advanced fuel designs do result in a non-negligible level of activity in their first walls. This may not have been expected, especially in the DHe case. The relative improvement of the HT-9 DD first wall activity concentration over the DT levels is best at lower beta. This is due to the greater relative increase in wall area for DD than for DT in going from 20 % beta to 5 % beta. Thus, the flux at low beta is reduced by a larger factor from that at high beta for DD than for DT. With 5 % beta, the DD total activity is reduced by a factor of ~ 4 over DT; with 10 % beta it is reduced by and factor of ~ 3, and with 20 % beta it is reduced by a factor of ~ 2. The DHe activity at 10 % beta is ~ 4 % of that of DT, and ~ 15 % of that of DD.

Table 5.8 lists the major contributors to the first wall activity, categorized as to whether they present a short term, long term or very long term hazard. Short lived isotopes dominate the activity at shutdown. In all cases ^{55}Fe is the isotope of highest concentration in the first wall at the end of the blanket lifetime. Two isotopes of manganese, ^{56}Mn and ^{54}Mn, are the next major contributors. For the advanced fuels, the fractional contribution to the activity of isotopes such as ^{55}Fe, ^{54}Mn and ^{51}Cr is reduced from that of DT. As indicated in table 5.9, the production rates* of such isotopes due to (n,2n), (n,α) and (n,p) reactions are somewhat reduced in the softer DD spectrum. Isotopes produced from molybdenum and tungsten contribute a greater fraction of the activity for DD (HT-9 blanket) than for DT. In fact, levels of ^{188}Re, produced from tungsten, are over an order of magnitude greater for the HT-9 DD designs than for the DT designs. The quantities of isotopes such as ^{99}Mo produced in the HT-9 DD reactors are nearly the same as the quantities produced in the DT reactors, at the same value of beta, despite the reduction in total flux. This effect is due to the softer neutron spectrum associated with the DD fuel cycle.

* obtained from REAC

Table 5.9: Relative Reaction Rates[a] Producing Major Short Lived Isotopes

	DT		DD		DHe	
Reaction	First Wall[b]	Blanket[c]	First Wall	Blanket[d]	First Wall	Blanket[d]
^{56}Fe (n,2n) ^{55}Fe	1.0	0.36	0.22	1.0	0.032	0.14
^{56}Fe (n,p) ^{56}Mn	1.0	0.39	0.20	1.0	0.030	0.12
^{55}Mn (n,2n) ^{54}Mn	1.0	0.36	0.22	1.0	0.032	0.14
^{54}Fe (n,α) ^{51}Cr	1.0	0.38	0.21	1.0	0.030	0.14
^{94}Mo (n,2n) ^{93}Mo	1.0	0.36	0.22	1.0	0.031	0.14

[a] information pertains to 10 % beta designs

[b] all first walls are 12 % HT-9

[c] DT blanket is 6.3 % HT-9

[d] DD and DHe blankets are 80 % HT-9

The isotopes ^{93}Mo and ^{93m}Nb, produced from molybdenum, are important when considering long term hazards. Although these isotopes represent a small fraction of the shutdown activity, they are dominant in the long term and hence, present a waste management concern. Production of ^{93}Mo in the HT-9 blanket through radiative capture in ^{92}Mo is enhanced in the softer DD neutron spectrum (see table 5.9). Of concern in the very long term are ^{99}Tc and ^{59}Ni, which are produced at similar, although small, levels in the DT and HT-9 DD reactors. This is partially a result of the longer blanket lifetime for the DD machines. The build up of these long lived isotopes increases linearly with operating time [5.23], whereas the shorter lived species reach saturation within a few years of commencing operation. The DHe reactor shows a reduced level of activity of the long lived species. Thus, it appears that the first wall activity concentration of the shorter lived radionuclides, which constitute most of the activity at shutdown, are reduced for the advanced fuels. The softer spectrum of the DD and DHe fuel cycles appears to enhance neutron capture in isotopes producing longer lived nuclides. The DHe fuel cycle results in a lower concentration of both short and long lived species in the first wall, and hence presents the least hazard.

When comparing activity levels for the two first wall materials for the 10 % beta DD designs, similar levels of the short lived species are seen. This would be expected from the similar levels of parent nuclides (iron and manganese) and the similar wall loads. A significant reduction in the inventory of the longer lived species, is seen for the RAF first wall. Species resulting from molybdenum, which is greatly reduced in RAF, (^{99}Mo, ^{93}Mo, ^{93m}Nb, ^{99}Tc) are reduced by roughly four orders of magnitude. Nickel produced isotopes (^{63}Ni, ^{59}Ni are roughly two orders of magnitude less concentrated in the RAF first wall as a result of the reduction in the nickel content. This will have a major impact on long term waste disposal concerns.

Decay heating levels in the first wall at the end of blanket lifetime are indicated in table 5.10. The greatest heating occurs in the DT first walls, and is seen to

Table 5.10: Major Contributors to First Wall* Decay Heat Levels at End of Blanket Lifetime † (W/cm³)

		DT			DD				DHe
Isotope	Halflife	5 %	10 %	20 %	5 %	10 % (HT-9)	10 % (RAF)	20 %	10 %
^{54}Mn	313 d	144	172	234	25.4	38.3	52.1	86.1	5.57
^{56}Mn	2.58 h	1070	1450	1890	243	448	490	792	59.2
^{58}Co	70.8 d	6.96	9.52	12.5	1.54	2.38	0.071	4.92	0.383
^{51}Cr	27.7 d	5.37	7.34	9.52	1.05	1.86	1.86	3.21	0.277
^{49}V	331 d	4.60	6.20	7.97	0.748	1.32	0.0066	2.34	0.193
^{55}Fe	2.7 y	2.58	3.22	3.61	0.565	0.949	0.935	1.49	0.146
^{99}Mo	66.0 h	4.16	7.09	7.39	2.94	6.61	0.0016	9.05	1.09
^{185}W	75.1 d	2.11	2.96	3.87	1.50	2.96	16.5	5.17	0.415
Total Heating		1560	1970	2570	347	620	688	1100	87

* first wall region is 12 % HT-9, 88 % He by volume

† all values have been multiplied by 10^4

increase with beta. An improvement by a factor of $\sim$ 4 occurs for the DD design at 5 % beta; at 10 % beta the HT-9 DD decay heating is reduced by roughly a factor of 3 (for both materials). At 20 % beta, the decay heating in the DT first wall is twice that in the DD first wall. The greater improvement at low beta is again a result of the larger relative increase in the DD first wall area in going from 20 % to 5 % beta compared to DT, resulting in a larger decrease in the flux. For DHe, the first wall decay heat level is $\sim$ 25 times below that for DT at 10 % beta.

The main contributors to decay heating at shutdown for all fuel cycles are two isotopes of manganese. Initially, ^{56}Mn produces the greatest amount of heat. However, because of its relatively short half life (2.56 h), it soon decays away and the main isotope responsible for heating would be ^{54}Mn. The enhanced production of ^{99}Mo in the softer DD spectrum results in its fractional contribution to the shutdown decay heating being larger than for DT for the HT-9 first wall. The heating due to the decay of tungsten produced isotopes is greater in the RAF first wall compared to the HT-9 first wall for the 10 % beta DD designs. This is a consequence of the greater quantitiy of tungsten in RAF steel compared to HT-9.

As noted above, the local decay heat level at the first wall is largest for DT. This would appear to present the greatest hazard in the event of a Loss of Flow Accident (LOFA) or Loss of Coolant Accident (LOCA), when cooling of the first wall would not take place. However, one needs to consider the effect of the adjacent blanket material before arriving at any conclusions in this regard. The relatively high thermal conductivity of the lithium in the DT blanket material may assist in the heat removal, mitigating the consequences of such an event. For DD, the absence of such a highly conductive material and the greater fraction of steel in the blanket (and therefore activated material) may lead to more severe consequences from a LOFA or LOCA than expected.

The radioactivity decreases in components behind the first wall as the neutron flux is attenuated through the blanket. Activation levels towards the rear of the

blanket are much lower than those at the front of the blanket. The average value for the activity concentration in the inboard blanket region and the total inboard blanket activity are given in table 5.11. Information is given for the inboard region only, where the activity will be most concentrated (due to the smaller volume of material). The sum of the average activity concentrations of the isotopes of short term, long term and very long term concern are also given. For the DT fuel cycle, the average blanket activity concentration is lower than for the first wall. This would be expected, as the flux attenuates through the blanket. For the advanced fuels, this is not the case. The activity concentration is larger in the blanket than in the first wall due to the increased fraction of the region occupied by structure. For the HT-9 designs, the first wall is only 12 % HT-9, while the blanket is 80 % HT-9. Thus, despite the attenuation of the flux, the increased atomic density in the blanket results in higher activation levels. The blanket for the DT designs is 6.3 % HT-9 (compared to 12 % in the first wall). Since the lithium does not highly activate, compared to the steel, this reduction in the amount of steel (in addition to the flux attenuation) contributes to the decreased activation in the blanket compared to the first wall for this fuel cycle. The effect of the larger structural volume fraction of steel in the DD machine is significant; the average concentration of the inboard blanket activity is greatest for DD. As indicated in table 5.9, the larger number of reactive target nuclei per unit volume in the DD blanket leads to a higher production rate of certain species. Once again, the short lived isotopes dominate the total activity. The major contributors to the blanket activity are ^{55}Fe, ^{54}Mn and ^{56}Mn. Isotopes produced from molybdenum and tungsten contribute a greater fraction of the total activity in the HT-9 blanket for the advanced fuels than for DT. The concentration of long lived isotopes is greater for the advanced fuels than for DT. This is true even in the case of DHe. After considering the total volume of blanket material, the DD blankets appear even less attractive (DD blankets are larger). Although most of the activity is due to short lived isotopes, there is a significantly larger quantity of longer lived species in the DD blanket. This is also true for the DHe fuel cycle, whose blanket will contain more longer lived radionuclides at the end of its life than

Table 5.11: Average Inboard[a] Blanket Activity and Decay Heat Levels at End of Blanket Lifetime

	DT			DD				DHe
	5 %	10 %	20 %	5 %	10 % (HT-9)	10 % (RAF)	20 %	10 %
Average Activity Concentration (Ci/cm^3)	10.4	13.5	16.5	19.0	33.7	38.5	53.5	6.1
short lived isotopes[b]	8.6	11.0	13.2	17.3	30.9	34.3	48.8	5.5
long lived isotopes[b]	$1.4x10^{-4}$	$1.4x10^{-4}$	$1.4x10^{-4}$	$2.7x10^{-3}$	$2.9x10^{-3}$	$1.2x10^{-3}$	$3.0x10^{-3}$	$1.0x10^{-3}$
very long lived isotopes[b]	$1.7x10^{-6}$	$1.7x10^{-6}$	$1.7x10^{-6}$	$2.8x10^{-5}$	$3.0x10^{-5}$	$2.4x10^{-6}$	$3.2x10^{-5}$	$1.1x10^{-5}$
Total Inboard Activity (MCi)	2,360	2,324	2,262	13,891	14,959	15,774	15,261	828
short lived isotopes[b] (MCi)	1,945	1,893	1.819	12,638	13,710	14,060	13,919	738
long lived isotopes[b] (MCi)	0.032	0.024	0.019	1.95	1.32	0.50	0.86	0.14
very long lived isotopes[b] (MCi)	0.00038	0.00029	0.00023	0.021	0.014	0.0010	0.0091	0.0015
Average Decay Heat Density (W/cm^3)	0.049	0.067	0.087	0.087	0.15	0.18	0.26	0.026
Total Inboard Decay Heat (MW)	11.1	11.5	11.9	63.9	68.5	73.8	73.9	3.6
Fraction of Operational Blanket Power[c] (%)	3.1	3.2	3.3	5.1	5.5	5.6	6.1	1.4

[a] The inboard blanket was taken to be 30 % of the total blanket volume.

[b] sum of average activity of isotopes listed in table 5.8

[c] power due to blanket multiplication of neutron energy only

its DT counterpart. It should be noted, however, that the DT blankets must be replaced more frequently. Hence, handling and storage of more radioactive material is associated with this fuel cycle. This will be reflected in the average annual dose incurred during blanket changeouts and during waste handling activities.

Upon examining the two blankets for the 10 % beta DD designs, a slightly higher concentration of short lived species is seen in the Fe2Cr1V blanket compared to HT-9. This is largely a result of the higher iron content of the alternate material. A major difference between these materials is in the production of long lived isotopes. Over an order of magnitude reduction in long lived species is seen with the Fe2Cr1V blanket. This will have important implications for long term waste disposal hazards.

Although radionuclides will be produced in the shield, TF coils and other components, time constraints limited the scope of this study to activity levels in the blanket. This region, however, represents a greater concentration of activation products and is therefore of greater concern. Some activation of materials in the shield will take place. Activation levels here are expected to be several orders of magnitude below that in the blanket region [5.5]. An even lower level of activity will be produced in the TF coils. Thus, the contribution of the activation products in these regions to the total inventory should not be significant.

The average and total blanket decay heat levels at shutdown are also given in table 5.11. The greater fraction of structure in the DD blanket leads to higher levels of decay heat compared to DT. Although the fraction of structure is still large (80 %) for DHe, the reduction in neutron flux leads to lower decay heat density for this fuel cycle. The shutdown decay heat level in the Fe2Cr1V DD blanket is slightly higher than for the HT-9 DD blanket. This may be important in the event of a loss of coolant accident. Also given in the table is the magnitude of the decay heat relative to that produced by neutron multiplication in the blanket. The DD blankets produce the most heat in their blankets via neutron energy multiplication (largest

blanket multiplication factor due to many (n,γ) reactions). The fact that the decay heat represents a larger fraction of this power compared to the other fuel cycles makes the DD fuel cycle appear more hazardous. The total decay heat available in the blanket at shutdown is much larger in the DD blanket that the other fuel cycles. The DD blanket thus presents a greater hazard in this respect since it has the potential of providing a greater amount of energy for mobilization of activated species.

5.2.2 Releases of Activated Material

Routine releases of radioactive effluents will occur during the normal operation of commercial fusion power reactors. These effluents will consist of activated corrosion products and tritium. Tritium effluents have been treated in an earlier section. An estimate of the source term for routine releases of activated products is the object of this section.

Releases of activation products during routine operation of a helium-cooled device are expected to be much less than their water-cooled counterparts [5.5]. The dominant source of radioactive effluents is activated material carried in the primary coolant loop. The degree of this hazard is greatly reduced by the use of helium as the coolant, where sputtering is the significant mechanism by which activated materials enter the coolant stream (as opposed to the much greater levels which would occur due to corrosion if water was the coolant). Leakage of the primary coolant to the secondary side of the steam generators provides a release pathway for small quantities of radionuclides. Based on studies of the primary coolant circuit of High Temperature Gas-Cooled Reactors (HTGR), no routine releases of radioactive materials from the primary circuit of a helium cooled fusion reactor are expected [5.24]. Some releases may occur from purification systems which are designed to maintain acceptable levels of coolant purity and remove activated materials from

the coolant loop. Other releases will occur from the ventilation systems of buildings where various radioactive waste management operations are performed.

The activated species in the helium coolant take the form of erosion/sputtered particles. Bickford [5.25] discussed direct-daughter recoil and bulk neutron sputtering mechanisms for transfer of radionuclides from coolant channels into a pressurized helium coolant. This material may adhere to the interior surface of the primary coolant piping or be transported to and trapped in the primary side of the steam generator. Waste processing systems are provided to remove activated suspended material which may be entrained in the coolant. Studies performed for High Temperature Gas Reactors have led to the expectation that there will be essentially no routine releases of radioactive materials from the primary circuit of a helium cooled fusion reactor [5.24]. Some leakage of the primary coolant through steam generator components into the secondary loop may occur before cleanup. A separate processing system is provided for the secondary loop to limit the possibility of further radioactive releases. It is anticipated that the only routine releases from a helium cooled fusion plant, excluding tritium and gaseous activation products, will be aqueous streams from decontaminating equipment. Leaks through valve stems, pumpshaft seals, and other equipment may also contribute to releases. Auxiliary cooling systems include continuous systems used for cooling highly radioactive components (such as limiters and plasma heating devices) and low-activity components (such as magnets and power supplies). Radioactive material may also be entrained in these auxiliary cooling systems and may contribute to releases through leakage. Further routine releases may result from laundry water, ion exchange regenerant solutions and other minor sources of contaminated water. The activity levels of these sources cannot be specified as accurately as they are for a water-cooled tokamak, but it is expected that the aqueous released from a helium-cooled tokamak will be less than 10 % of the corresponding releases from a water-cooled tokamak [5.5]. Cannon [5.5] has estimated an upper limit of 15 mCi/yr for the release in aqueous streams from a DT plant. Based on activity levels in the blanket, an upper limit

for aqueous releases from a DD plant would be ~ 100 mCi/yr. Aqueous releases from the DHe plant should not exceed ~ 5 mCi/yr.

Blanket segments removed from a fusion reactor during routine maintenance or as the result of equipment failure will produce large quantities of heat from radioactive decay. In order to remove this heat, blanket segments will probably be stored in a water pool for several years. Some transfer of radionuclides to the pool water by corrosion and erosion during the temporary storage period will take place. Removal of the radioactivity from this water before discharge will lead to the production of radwastes. It is expected that the quantities of radioactivity transferred from the metals to water and then to demineralizers will not be large. Furthermore, experience indicates that pools designed to cool radioactive materials can be operated without regular loss of radioactivity [5.5]. Thus, this source of radioactive releases was not evaluated.

Releases of radioactivity may occur from the reactor containment atmosphere. The extent of activation of the containment atmosphere will depend on whether the containment is evacuated or filled with air, or an inert cover gas (such as CO_2, N_2 or Ar). Concern regarding ^{14}C is derived from its long half life; ^{16}N and ^{41}Ar are of concern because of the energetic decay products. Maintaining the reactor building at a slight negative pressure will decrease the possibility of the accidental release of activated gases to the environment. Under normal conditions, a system will be in operation for clean up of the building atmosphere prior to venting to the surroundings. High-efficiency particulate air (HEPA) and sand filters can effectively remove particles from the effluent streams. Reaction of CO_2 with other materials forming calcium or barium carbonate may be necessary to retain ^{14}C. Release of short-lived nuclides including ^{15}C, ^{13}N, ^{16}N, and possibly ^{41}Ar can be controlled by use of a holdup tank.

The concentrations of gaseous radioactivity can be evaluated if the information on the spatial and energy dependence of the neutron flux within the reactor hall is

available. The total flux at any point should be small. Thus, the activity in the reactor hall due to direct activation of the atmosphere will not be large. Occupational doses will be dominated by tritium exposures and gamma exposures from activities such as steam generator maintenance. The probability of a release of radioactive cover gas from the reactor building is quite low [5.5]. If such a release does occur, public doses will be insignificant [5.26], especially after considering dispersion effects in the environment. Hence, doses due to activation of the reactor hall should not have a significant effect on the outcome of this study, and were not considered.

5.2.3 Occupational Doses

During operation of the fusion reactor, neutron bombardment of the reactor structure and impurities in the primary coolant will result in the production of radioactive species. Activated products in the structure will not present a hazard during normal operation of the plant. However, during maintenance of blanket sectors or fueling, heating, pumping and instrumentation components, personnel may be exposed to high levels of radioactivity. Proper procedures and protective measures must be instituted to minimize doses. Circulation of material in the primary coolant will result in activation products being transported from the reactor and deposited in other components of the power cycle, such as the steam generator, pumps, valves and piping. Procedures to minimize personnel exposure during maintenance in these areas are required. In this section, worker exposure to activation products during plant maintenance will be examined. It should be pointed out that a large fraction of the radiation dose accumulated by fusion facility staff will not be the result of exposure in high field areas. Experience in the fission industry indicates that the greater proportion of the dose is the result of integrated exposure to lower radiation field areas such as those encountered in heat exchanger and circulating equipment rooms, auxiliary equipment rooms and waste handling/clean up system rooms [5.16]. Activated corrosion products are transported outside the

primary reactor shield leading to radiation fields in these locations which, while not high enough to justify the cost of remote systems for maintenance, are significant enough to require radiological work planning and dose control.

During normal maintenance at a typical PWR, more than 75 % of the exposures occur during maintenance of the reactor coolant loop, due to the radiation fields produced by activated corrosion products [5.27]. Radioactive material may enter the coolant channels by three basic mechanisms: corrosion of activation products in the channel walls, activation of coolant impurities and neutron sputtering of channel walls. With the use of helium as the coolant, as in the present work, neutron sputtering of wall material has been identified as the primary source of activation products in the coolant channels [5.25]. The other two source terms are relatively unimportant because helium is an inert gas with a very low corrosion rate, and purification techniques are capable of maintaining impurity levels very low. Neutron sputtering occurs as a result of two processes: lattice dynamic sputtering or bulk sputtering of atoms, and fast neutron induced recoil sputtering of radioactive daughter nuclei near the surface of the coolant tubes. High energy neutrons have a greater impact on sputtering yield [5.25] (since the displacement cross section scales roughly linearly with energy [5.28]). Bickford [5.2] has modeled the transport and deposition of sputtered activation products in a helium cooled fusion power plant. He found that about 17 % of the inventory deposited out in the blanket modules themselves, 8 % deposited in the larger pipe runs of the hot leg, and the remaining 75 % deposited in the steam generator. Negligible quantities were found to be deposited in the circulator and cold return leg. Contact dose rates on hot pipes coming from the blanket were as high as 10 rem/h. Contact doses at the steam generator were estimated at 100 mrem/h, despite the much larger fraction of the radioactive inventory which is deposited here. This can be attributed to the large self shielding of the steam generator. Although Bickford's calculated values of radioactivity at the steam generator for the helium-cooled fusion reactor are slightly lower than those found at a PWR, they are of the same order. It is expected that,

without special clean up procedure, occupational doses at a helium cooled fusion plant would only be slightly less than those experienced at PWR stations.

Dose rates to which workers are exposed during maintenance on the coolant system and steam generator have been estimated using the information given by Bickford [5.2]. The design used in his analysis is similar to the 5 % beta DT design of this work. Thus, in lieu of repeating Bickford's involved analysis, a contact dose rate of 100 mrem/h was adopted for the 5 % beta DT design. Contact dose rates for the other designs were estimated from this value by scaling with the Remote Maintenance Rating (RMR) of the blanket structure one day after shutdown. The RMR is defined as the radiation dose rate at the surface of a uniformly activated, infinite slab with the same composition and density as the specific machine component. The values used for scaling are those at one day after shutdown, and are given in table 5.12. Scaling in this manner was thought to be appropriate since the sputtered material originates from the structure. The RMR of the structure should then also reflect the health hazard of sputtered material in the coolant. Estimates of coolant/steam generator maintenance dose rates are given in table 5.12.

As discussed in section 5.1.3, doses incurred by the most exposed work group can be evaluated using an estimate of the total man-hours of contact maintenance (see appendix E). Time estimates for maintenance and doses incurred during these activities are listed in table 5.13. As indicated here, steam generator/coolant system maintenance doses are greatest for the DT fuel cycle. The reduced dose rate encountered during steam generator/ coolant system maintenance for the advanced fuels allows for an increased amount of contact activity. Despite this fact, the lower dose rate results in the total cumulative dose for the DD and DHe fuel cycles being much lower than for DT. Because of the slightly higher concentration of short lived isotopes in the DD RAF first wall/Fe2Cr1V blanket compared to the DD HT-9 blanket, it is expected that the sputtered material from the coolant tubes of the alternate design will also have slightly higher levels of these species. Thus, the dose rate and total exposure during coolant/steam generator maintenance will be higher

Table 5.12: Gamma Dose Rates at Various Plant Locations

	DT			DD				DHe
Location	5 %	10 %	20 %	5 %	10 % (HT-9)	10 % (RAF)	20 %	10 %
RMR of Blanket Structure (mrem/h)	1.1×10^{9}	1.4×10^{9}	1.8×10^{9}	9.2×10^{7}	1.6×10^{8}	2.0×10^{8}	2.6×10^{8}	3.2×10^{7}
Steam Generator/ Coolant System Dose Rate (mrem/h)	100	127	164	8	15	18	24	3
Near Reactor Dose Rate (mrem/h)	1.5×10^{-2}	1.5×10^{-2}	1.5×10^{-2}	1.5×10^{-2}	1.5×10^{-2}	1.5×10^{-2}	1.5×10^{-2}	1.5×10^{-2}
Dose Rate During Blanket Changeouts (mrem/h)	26	33	43	2.2	3.8	4.7	6.1	0.76
RMR of Breeder (mrem/h)	4.5×10^{5}	6.0×10^{5}	7.7×10^{5}	-	-	-	-	-
Dose Rate During Breeder Processing (mrem/h)	1.9	2.5	3.2	-	-	-	-	-

Table 5.13: Maintenance Time Estimates and Annual Cumulative Doses Incurred During Maintenance Activities

	DT			DD				DHe
Location	5 %	10 %	20 %	5 %	10 % (HT-9)	10 % (RAF)	20 %	10 %
Coolant/Steam Generator System:								
Maintenance Time (man-hours)	595	595	595	654	654	654	654	733
Cumulative Dose (man-rem)	59.5	75.6	97.6	5.23	9.81	11.8	15.7	2.20
Near Reactor:								
Maintenance Time (man-hours)	868	868	868	926	926	926	926	2,266
Cumulative Dose (man-rem)	0.013	0.013	0.013	0.014	0.014	0.014	0.014	0.034
Blanket System:								
Maintenance Time (man-hours)	75	75	75	-	-	-	-	-
Cumulative Dose (man-rem)	0.141	0.188	0.241	-	-	-	-	-
Blanket Changeouts:								
Maintenance Time (man-hours)	313	417	556	132	218	205	363	233
Cumulative Dose (man-rem)	8.14	13.8	23.9	0.290	0.828	0.964	2.21	0.177
Waste Handling:								
Exposure Time (man-hours)	616	834	1,112	274	436	411	726	108
Cumulative Dose (man-rem)	0.308	0.515	0.806	0.274	0.497	0.748	1.23	0.108
Total Gamma Dose (man-rem):	68.1	90.0	123	5.81	11.1	13.5	19.2	2.52
Tritium Areas:								
Maintenance Time (man-hours)	3,089	3,193	3,332	2,960	3,046	3,046	3,191	4,473
Cumulative Dose (man-rem)	31.2	32.2	33.7	0.385	0.396	0.396	0.415	0.671
Total Dose (man-rem):	99.3	122	156	6.20	11.5	13.9	19.6	3.19
Fraction of Dose Due to Tritium	0.31	0.26	0.22	0.06	0.04	0.03	0.02	0.21
Fraction of Dose Due to Gammas	0.69	0.74	0.78	0.94	0.96	0.97	0.98	0.79

for this design, compared to the HT-9 design.

Some degree of personnel exposure will result from contact maintenance carried out in the vicinity of the plasma chamber. Extensive diagnostic and other support equipment will be located adjacent to the reactor, and it is unlikely that all maintenance on this equipment can be carried out remotely. The reactors were designed with shielding capable of reducing the radiation dose level to the level of a few millirem per hour or less, one day after shutdown. At these levels, plant personnel could work up to 40 hours per week within the reactor containment during an outage period. Tasks performed would not include any work within the outboard shield or on components with penetrations (e.g. fueling devices) since these would be more highly activated than the components protected by the outboard shield due to the higher neutron fluxes to which they are exposed. Nevertheless, access to the toroidal field coils, cryogenic systems and other components external to the outboard shield appears feasible. Values for the gamma dose rate at this location were obtained from the REAC output. The dose rate midway through the outage was chosen as the representative dose rate during these activities at this location. In all cases, the dose rate beyond the shield at this time was found to be below 1.0×10^{-2} mrem/h. This value is below the mean background radiation level of 1.5×10^{-2} mrem/h [5.29]. It was therefore thought appropriate to use the higher background value of 1.5×10^{-2} mrem/h for the dose rate encountered during maintenance near the plasma chamber. The greatest dose, although not large itself, is incurred for the DHe fuel cycle, as a consequence of the increased amount of contact maintenance permitted.

A major operation carried out during fusion plant outages will be that of first wall and blanket replacement. Some contribution to the total cumulative dose incurred at the plant is expected as a result of these procedures. Operations associated with this activity include disconnecting coolant lines and support equipment, disconnecting first and second walls, preparation and installation of new blanket assemblies and reconnecting coolant and support equipment. An estimate of 75 mrem/h

for the dose rate during these activities was given for STARFIRE in reference [5.30]. Scaling this by the RMR of the structural materials (PCA for STARFIRE vs HT-9 for the designs here) as given in the BCSS [5.8] (where STARFIRE is the reference tokamak design) gave an estimate of 26 mrem/h as the dose rate during blanket changeouts. This value was taken to represent the 5 % DT design. Estimates of the dose rate encountered during blanket changeouts for the other designs were obtained by scaling this value with the RMR of the blanket structure. Table 5.12 lists the anticipated dose rates. Estimates of exposure times and cumulative doses incurred for all designs are given in table 5.13. Despite the greater concentration of activity in the DD blanket, a lower dose rate is expected during blanket changeouts than for DT due to the self shielding effect of the blanket material. This effect will not be observed for the DT blanket module since the breeder will be drained prior to changeout and there is much less steel present to act as shielding. Once again, a slightly higher dose rate is expected during these operations for the DD RAF first wall/Fe2Cr1V blanket design compared to the DD HT-9 design, due to the higher activity levels of short lived species. As indicated in table 5.13, a shorter blanket changeout time is expected for the advanced fuels because of the elimination of procedures dealing with the breeder. More contact maintenance will be permitted for the DHe fuel cycle, due to the lower dose rate encountered during blanket changeouts.

An additional area for exposure exists for the DT plants. Workers may be exposed to radiation fields during maintenance activities on blanket processing and tritium extraction equipment. It was assumed that shielding would be provided to reduce the dose rate during these operations for the 10 % beta DT design to 2.5 mrem/h. Values for the 5 % and 20 % beta designs were estimated by scaling with the RMR of the breeder at shutdown. Table 5.12 gives the RMR of the breeder and dose rate expected during maintenance activities of breeder processing equipment. Estimates of the exposure time and cumulative doses incurred during these procedures for these designs are given in table 5.13. As expected, a greater

dose rate and cumulative dose results for the high beta design.

The total occupational dose incurred and the fractions attributed to tritium exposure and gamma exposure are summarized in table 5.13. The design presenting the greatest hazard is the high beta DT; the DHe design is the least hazardous. Gamma exposures account for 69 - 78 % of the total dose for DT; this increases to 94 - 98 % of the total dose for DD. For DHe 21 % of the dose is due to tritium and 79 % due to structural activity. Even in the worst case, however, the dose incurred at the fusion plant ($\sim$ 150 man-rem) is significantly lower than current doses at fission plants. In 1986, the total annual radiation dose at the Pickering Nuclear Station in Canada was 900 man-rem [5.31]. According to Ontario Hydro statistics, the average collective dose over the five year period from 1979 to 1983 for U.S. LWR's was about four times that incurred at Ontario Hydro units. Thus, when compared to fission, even the worst case fusion plant considered here appears attractive.

5.2.4 Waste Management

During the operating life of a reactor, radioactive materials requiring disposal will be removed from the plant at regular intervals. Primary wastes will be derived from disassembly of the torus sectors. These operations are expected to dominate waste handling activities, essentially because of the large volume, large weight, high activity level, and processing requirements associated with these items. Secondary wastes will be generated from processing of the torus sectors and from clean up of the coolant and other circulating streams. These low level wastes, which may include tritiated wastes, will consist of contaminated work clothes and tools, resin beds, solidified concentrates of ion exchange regenerant solutions, pumps, pump oils, filters, sludges and suspect trash. Additional waste materials will become available at the end of the plant's operating life when decommissioning takes place.

The non-tritiated low level wastes produced at a water cooled fusion plant are expected to be very similar in quality and quantity to that produced at an LWR [5.5, 5.32, 5.33]. More than 90 % of the radioactivity in the waste processing streams is expected to originate from the primary coolant [5.5]. For a helium cooled system, the radioactivity in the primary coolant loop is generated and transported by different mechanisms. It is anticipated that when using helium as the coolant, significantly less solidified concentrates, filter sludges and resins will be produced. Cannon [5.5] suggests that the total volume of low activity wastes from a helium cooled fusion reactor will be about half of that from a water cooled reactor. Furthermore, he expects that the radionuclide concentration will be about two orders of magnitude less. Thus, the need for handling, storage and transportation of these wastes will also be less than for a water cooled plant.

As a result of the low level waste handling activities, some occupational exposure will occur. Easterly [5.33] states that waste management operations of this type at a fission plant give rise to a relatively small occupational exposure, resulting in $\sim$ 5 to 7 % of the total dose. A similar dose would be expected due to these activities at a water cooled fusion plant. The anticipated reduction in volume and activity level of the low level wastes generated at a helium cooled fusion plant will result in an even lower dose. It was thus assumed that the dose attributable to the handling of these wastes at the plants considered in this work will be of no major consequence and no attempt was made to evaluate it.

A unique waste management task for fusion will be the regular partial replacement of the first wall/blanket structure of the reactor. This operation will occur at several times at predetermined intervals during the lifetime of the plant. Activities involved will include removal of the blanket sector to the processing cell, disassembly, bakeout, cutting, compacting, packaging and temporary storage. These procedures will be undertaken routinely during the normal operation of the fusion facility. At the end of the reactor lifetime, removal and processing of all the blanket sectors will be necessary. Structural members and magnets must be dismantled

and stored for reuse or packaged for disposal. After completion of the dismantling actions, decommissioning of the reactor site can take place.

Radioactive wastes produced by operating fusion plants will require disposal at sites licensed for this purpose. Low level wastes from fission power plants are currently being disposed of in shallow pits at designated locations. Much of the low level waste generated at a fusion plant will be of the same character. Hence, it can be envisioned that these sites will also be used for the disposal of low level fusion plant radioactive wastes. Much of the blanket sector wastes will be unsuitable for near-surface burial. The regulations governing land disposal of radioactive wastes, are given in 10CFR61. Four categories of waste are defined: Class A is the least hazardous, followed by classes B and C as the radiation hazard increases. If radioactivity levels exceed those allowable for class C, the waste is not acceptable for near surface burial. These regulations were designed with fission reactors in mind. Hence, the properties of fusion reactor wastes have not been explicitly considered. Inappropriate application of the standard to fusion wastes may lead to faulty guidance. Inadequacies in the current regulations include the omission of several important fusion specific isotopes and the lack of attention given to activated metal wastes. Some effort has been given to formulating limits for isotopes such as ^{53}Mn ^{93}Zr and ^{93}Mo , which are not currently included in the regulations [5.34]. Other recommendations for making these regulations more suitable to fusion include reevaluation of the scenarios for inadvertent intrusion into the disposal facility after closure (since a large fraction of the wastes are activated solids) and establishment of a separate waste class for activated metals and ceramics [5.32].

Nuclides of concern for which 10CFR61 regulations exist are listed in table 5.14, along with the limiting concentration for shallow land burial and the expected average concentrations in the inboard first wall/blanket structure of reactors being examined in this study. The additional nuclides of ^{53}Mn, ^{93}Zr and ^{93}Mo are also included. Concentrations of these nuclides at one year after shutdown exceed the limiting values for all fuel cycles with HT-9 blankets for ^{94}Nb and ^{93}Mo. For the

Table 5.14: Concentrations of Important Nuclides in the Blanket* One Year after Shutdown and 10CFR61 Class C Shallow Land Burial Limits (Ci/m^3)

		Fuel Cycle							
	Class C	DT			DD				DHe
	Limit	5 %	10 %	20 %	5 %	10 % (HT-9)	10 % (RAF)	20 %	10 %
^{59}Ni	220	1.1	1.1	1.1	18.5	20.9	2.24	20.5	7.8
^{94}Nb†	0.2	0.3	0.3	0.3	0.5	0.5	0.005	0.5	0.2
^{99}Tc	3	0.6	0.6	0.6	9.5	9.6	0.13	11.3	3.5
^{63}Ni	700	104	107	106	1956	2244	1198	2334	759
^{53}Mn	22*	1.0	1.0	1.0	2.0	2.2	1.6	2.3	0.7
^{93}Zr	0.02*	0.002	0.002	0.002	0.006	0.006	0.00006	0.006	0.0004
^{93}Mo	22*	33	34	35	619	623	10	658	232
Maximum intruder dose at 500 years after disposal*,‡ (rem)		5.8	5.9	6.0	66	69	0.36	73	54
Intruder Hazard Potential (m^3) (individual blanket)		2,624	2,032	1,649	96,624	61,313	295	41,654	14,612
Intruder Hazard Potential (m^3) (lifetime)		6,219	6,604	6,959	96,624	101,780	463	109,967	14,612

⋆ not specifically covered in 10 CFR61, estimate given in ref [5.31]

‡ although the present form does not qualify for shallow land disposal, this gives a measure of the relative hazard

* refers to inboard blanket only

HT-9 DD blanket wastes, class C disposal limits are also exceeded for ^{99}Tc and ^{63}Ni; the DHe blanket wastes just exceed these limits as well. A considerable improvement is seen for the alternate material DD design in terms of activity levels of several of the long lived species. The concentrations of ^{94}Nb, ^{99}Tc and ^{93}Mo are reduced below the class C disposal limits. The level of ^{63}Ni is still slightly above the disposal limit after 30 years. Thus, none of the blanket wastes qualify for shallow land burial. An alternative disposal method, such as deep geologic disposal, which would afford greater and longer term isolation is required.

In lieu of disposal of all wastes, recycling of material is being considered. The decision to recycle components will hinge upon the value of the raw material, disposal costs, costs of separation processes and fabrication under conditions hindered by radioactivity, rates of decay of important radionuclides to manageable, levels and the magnitude of the resource depletion by the fusion reactor system in the absence of recycle. Significant amounts of potentially strategic metals are contained in the structure and equipment of a fusion reactor. Conservation of raw materials will become increasingly important in the future. The rejected components from fusion power reactors may be regarded as a valuable reserve; recovery of these materials may be important. Knowledge of the rate of decay of major species is needed to determine if safe, hands on refabrication can be accomplished within a reasonable time after shutdown (e.g. contact dose rate < 2.5 mrem/h at 30 years or less after shutdown). An economic evaluation must also play a role in the decision to recycle. This would examine the relative costs of separation and refabrication versus those for disposal, procurement of new raw materials and fabrication of new components.

After the useful life of a fusion reactor, it will be necessary to dismantle many components and prepare them for recycle or disposal. The degree of dismantlement will depend on the future use intended for the site and the degree of modifications required if a new fusion reactor is to be constructed on the site. Decommissioning alternatives to immediate dismantlement include mothballing and entombment. Mothballing will leave the facility virtually intact; the nuclear island will be sealed

and the site will be maintained. After a given period of time, dismantling may then be undertaken. This approach provides a time delay, allowing for the decay of radionuclides. Doses incurred will be reduced compared to immediate dismantlement and greater freedom of movement of workers around the plant will be allowed in subsequent dismantlement procedures. Entombment involves encasement of contaminated material and equipment, and provision of shielding of sufficient durability to allow radioactive decay to innocuous levels before failure. The final decision as to which decommissioning approach to take will largely be based on an economic comparison of the alternatives.

The level of radioactivity and the specific radionuclides generated by neutron activation can be significantly affected by the selection of materials and the design of the blanket [5.34]. This was evidenced by the comparison between the Fe2Cr1V and HT-9 DD blankets. The level of activation will determine remote handling needs for waste handling procedures, disposal methods for the waste and accident severity. It is clear that several materials may provide a lower induced activity of specific nuclides than the HT-9 structure used here, most notably modified ferritic steels (RAF or Fe2Cr1V), vanadium alloys and ceramics such as silicon carbide. If steel is to be used, elemental and isotopic tailoring have been proposed as means of reducing the activation [5.35]. Elemental tailoring refers to the elimination of a particular element which leads to high levels of radioactivity and replacing it with another element which will reduce the activation and not significantly alter the properties of the original material. This has been partially undertaken with RAF and Fe2Cr1V, where the levels of Mo and Ni have been largely reduced. Isotopic tailoring involves the removal of only particular isotopes of an element which give rise to the daughter products of concern in the waste. Conn and Okula [5.35] have investigated the contribution of specific isotopes of molybdenum and nickel (the two major elements preventing near surface burial) to blanket activity and suggest that isotopic tailoring of steels to include only ^{61}Ni, ^{96}Mo and ^{97}Mo will minimize the induced activity. Once again, it must be determined how the cost of tailoring the

material compares with radwaste disposal costs. If it is more costly to tailor the material, then it must be determined if the additional expense can be justified by the consequent reduction in waste hazards.

The risk from radioactive wastes depends on the activity level of the waste, the biological hazard of the radioisotopes involved, the pathways available for transport of the radioactivity to the environment, the rate at which radioisotopes enter the public domain and the time elapsed before public exposure occurs. The last three concerns depend on the particular mode of waste handling and are not easily incorporated into simple hazard indices. The activity level and hazard associated with waste materials can be compared on the basis of the Remote Maintenance Rating (RMR) and the Waste Disposal Rating (WDR). The RMR gives a measure of the gamma ray contact dose at the surface of a thick infinite slab of activated material. The units of this index are mrem/h. If the RMR is less than 2.5 mrem/h, workers can be in contact with the material without having any special protection for gamma radiation. The WDR gives a measure for classifying wastes in accordance with 10CFR61 regulations for land disposal of radioactive wastes. These regulations were intended to protect an inadvertent intruder at a disposal site from incurring a radiation dose greater than 500 mrem/yr. The WDR is defined as the sum of the ratios of the actual concentration of each nuclide in the waste divided by its allowable concentration limit for a given waste class. Near surface land disposal is possible if the WDR is less than one. Since the concentrations of many of the isotopes listed in table 5.14 exceed the class C disposal limit, the WDR of the blanket wastes for all of the fuel cycles exceeds one. Thus, processing (e.g. dilution) is required to reduce the specific activity before near surface burial will be permitted. Otherwise, another disposal option must be employed. It should be noted that dilution may not always be an attractive solution for it increases the total volume of waste to be disposed of. This may be a problem if the capacity of the burial site is limited.

Another alternative would be to temporarily store the wastes onsite, allowing for some decay before disposal. Table 5.15 gives the activity concentrations of the

Table 5.15: Concentrations of Important Nuclides in the Blanket* Thirty Years after Shutdown and 10CFR61 Class C Shallow Land Burial Limits (Ci/m^3)

		Fuel Cycle							
	Class C	DT			DD				DHe
	Limit	5 %	10 %	20 %	5 %	10 % (HT-9)	10 % (RAF)	20 %	10 %
^{59}Ni	220	1.1	1.1	1.1	18.5	20.9	2.24	20.5	7.8
^{94}Nb†	0.2	0.3	0.3	0.3	0.5	0.5	0.005	0.5	0.2
^{99}Tc	3	0.6	0.6	0.6	9.5	9.6	0.13	11.3	3.5
^{63}Ni	700	85	88	87	1600	1835	979	1909	621
^{53}Mn	22*	1.0	1.0	1.0	2.0	2.2	1.6	2.3	0.7
^{93}Zr	0.02*	0.002	0.002	0.002	0.006	0.006	0.00006	0.006	0.0004
^{93}Mo	22*	33	34	35	616	619	10	654	231

* not specifically covered in 10 CFR61, estimate given in ref [5.31]

* refers to inboard blanket only

nuclides of interest 30 years after shutdown. It is evident that there is no benefit to delaying disposal, for some nuclides still exceed the limit, disqualifying the waste for shallow land burial.

Upon removal from the reactor, blanket sectors will be placed in the cool down region of the blanket disposal area. As indicated in table 5.11, average decay heat levels in the blanket modules at shutdown may range from 4 to 74 MW. Looking at the worst case of the 20 % beta DD design, a rough calculation indicates that the average temperature of the module could rise $\sim$ 210 C due to the decay heat generated within the first two days subsequent to removal (this considers only the isotopes contributing more than 0.1 % to the shutdown decay heat, and assumes no cooling). This temperature rise may be tolerable if the sector is not to be reused. However, if a sector removed due to operational problems is to be reused after correcting the difficulty, special provisions for cooling may be needed to avoid distortion of the blanket assembly. The expected temperature rise in the other blankets will be lower than for the 20 % beta DD design, and cooling is not as important a concern. In any case, a cool down period of one year was assumed for all designs. At this time, the contact dose rates of the blanket modules will be 5 % or less of the shutdown values (due to decay of many short lived species). The module can than be moved to the disassembly region of the blanket disposal area, allowing for a newly removed module to be placed in the cooldown region. After cooling, the spent blanket sectors are separated into their various components. Some cutting may be involved to reduce the size of some of the pieces. Because the contact dose rates are still relatively high (as given by the RMR at one year, see table 5.16), most of this will be performed remotely, although some contact assistance is possible with adequate shielding. Compacting of pieces of the steel structure may be accomplished by pressing. The waste can then be placed in sealed steel canisters for storage under water until they are ready for shipment to a final disposal site. It is expected that very little radioactivity will enter the cooling water of the storage pool [5.5]. The DT blankets also contain lithium. The breeder will be drained as

Table 5.16: Wastes Generated from Fusion Plant Operation

	DT			DD				DHe
	5 %	10 %	20 %	5 %	10 % (HT-9)	10 % (RAF)	20 %	10 %
Number of complete blanket changeouts	2	3	4	0	1	1	2	0
Number of complete limiter changeouts	1	2	2	1	1	1	2	2
Annual volume of lithium waste (m^3/yr)	36	41	43	-	-	-	-	-
Volume of Lithium waste at EOL (m^3)	535	408	325	-	-	-	-	-
Annual volume of Structural waste (m^3/yr)	3	4	4	0.6*	39	36	25	0.6*
Volume of Structural waste at EOL (m^3)	48	36	29	1952	1185	1092	761	361
Fraction of Lifetime consumed at EOL	0.37	0.25	0.22	0.89	0.66	0.57	0.64	0.31
Total volume of Blanket wastes during plant life (m^3)	1,753	1,794	2,124	1,970	2,355	2,172	1,511	379
Volume of low level and tritiated wastes (m^3/yr)	581	582	582	539	546	546	549	546
Blanket RMR† at 1 year (mrem/h)	4.2×10^{8}	5.5×10^{8}	6.9×10^{8}	2.8×10^{7}	5.0×10^{7}	7.7×10^{7}	8.0×10^{7}	8.6×10^{6}
Blanket RMR† at 30 years (mrem/h)	2.3×10^{5}	2.6×10^{5}	2.8×10^{5}	1.1×10^{5}	1.7×10^{5}	2.8×10^{5}	2.2×10^{5}	2.4×10^{4}
Breeder RMR† at 1 year (mrem/h)	9.9×10^{4}	1.2×10^{5}	1.4×10^{5}	-	-	-	-	-
Breeder RMR† at 30 years (mrem/h)	45	56	63	-	-	-	-	-

* limiter waste

† evaluated using FUSEDOSE package, created by S. Fetter [5.33, 5.34]

part of the blanket changeout procedure. It may then be processed for immediate disposal or recycled to remove activated impurities and to reestablish the desired ^{6}Li content. As indicated in table 5.16, the breeder contact dose rates are lower than those for steel, but still to high to permit unprotected contact maintenance.

The volumes of the blanket materials scheduled to be discharged at regular annual intervals (some fraction of the blanket is removed during each shutdown), the quantities discharged at final plant shutdown and the accumulated volume removed over the plant lifetime are given in table 5.16. In addition to the blanket sectors, a large volume of much less radioactive material from shielding, magnets, dewars and coils will also be removed at shutdown. It is expected that the total activity associated with these components is much less than that associated with the blanket [5.5]. These levels have not been quantified at this time.

Inspection of table 5.16 reveals several things. The total volume of waste removed from the DT and DD plants is nearly the same. The volume of blanket waste ejected from the DHe plant is significantly smaller. The contact dose rates for the DT structure are highest, increasing with beta. After a one year cooldown period, the DD blanket RMR's are an order of magnitude less; the DHe blanket RMR is two orders of magnitude less than DT. However, a large majority of the waste from the DT plants will be lithium, which has a contact dose rate two orders of magnitude below the blanket RMR for DD. Thus, the hazard encountered during handling of DT blanket wastes may actually be less than that encountered during DD blanket waste handling. The contact dose rates at 30 years for the blanket structure and breeder are also given in table 5.16. These are seen to decrease by about three orders of magnitude from the one year value for the DT structural waste, and by about two orders of magnitude for the DD and DHe blanket wastes. The larger decrease for DT is a reflection of the greater fraction of activity due to shorter lived species produced from exposure to the DT neutron spectrum. This is also seen in the breeder RMR, which decreases by about three orders of magnitude over 30 years. For all blanket materials, the RMR at 30 years exceeds 2.5 mrem/h

so that recycle of the materials at this time would likely not be considered.

A problem encountered in assessing the hazards associated with waste disposal is the fact that the maximum hazard to society may occur hundreds or thousands of years after disposal of the waste. It is difficult to postulate the use of disposal site at this time in the future or to predict the condition of the waste. To overcome this problem, the NRC has proposed that at no time in the future should any individual receive a dose greater than the maximum permissible dose (MPD) for public exposure (0.5 rem). This should include contributions from the possible construction and occupation of a house on the waste disposal site and the consumption of meat, milk, and vegetables produced on the site. An index indicating the magnitude of this hazard is the maximum dose to an inadvertent intruder constructing and occupying a house on a waste disposal site after institutional controls have collapsed. Values for the maximum dose to an inadvertent intruder at 500 years after disposal of the waste are given in table 5.14. The intruder dose is highest for the DD HT-9 designs. This is a consequence of the greater quantity of longer lived species in this waste, specifically ^{94}Nb, ^{63}Ni and ^{99}Tc. The intruder dose is significantly reduced with the use of the Fe2Cr1V DD blanket due to the large reduction in the quantity of the previously mentioned isotopes in the waste. The intruder dose is based on the specific activity of the waste. The probability of an exposure occurring is proportional to the surface area covered by the waste. For a constant disposal depth, this is proportional to the waste volume. Fetter [5.36] suggests that a more appropriate index of hazard which would also reflect the probability of exposure is the Intruder Hazard Potential (IHP). He defines this as the intruder dose multiplied by the waste volume divided by the MPD. Values are given in table 5.14. The IHP is seen to decrease with beta for a given fuel cycle, reflecting the volume consideration. The hazard posed by the advanced fuels, as indicated by this index, is still greater than for DT for the HT-9 blankets. The hazard is greatly reduced for the DD design with the Fe2Cr1V blanket. Some reduction in this index would also be expected for the other fuel cycles if this material was used in their blankets. However, a thorough

investigation of the materials impact was beyond the scope of the present work.

An attempt to roughly estimate the doses incurred during handling of blanket wastes was made. Dose rates were determined by scaling dose rates encountered during maintenance by the ratio of RMR at one year to RMR at shutdown. For the advanced fuels, the maintenance dose rate used for scaling was that expected during blanket changeouts (see table 5.12). For DT, both the dose rate during blanket changeouts and during breeder processing were used. The scaled dose rates were then weighted by the relative volumes of breeder and structure (which should roughly reflect the time spent on processing) to be handled to give an overall estimate for the dose rate during handling of DT blanket wastes. The dose rates are listed in table 5.17. To evaluate the cumulative dose incurred during waste handling activities, it was assumed that the amount of contact maintenance involved was equivalent to twice the annual amount estimated for blanket changeouts. The time estimates and doses incurred are also given in table 5.17. The DD blanket waste handling appears to give the greatest range of expected doses. This is largely a consequence of the greater increase in the blanket lifetime as beta decreases from 20 % (11 year lifetime) to 5 % (30 year lifetime) for DD (HT-9 designs), compared to the increase for DT (7 year lifetime at 20 % beta, 12 year lifetime at 5 % beta). A larger dose is incurred during waste handling for the RAF first wall/Fe2Cr1V blanket DD design than for the HT-9 DD design, due to the greater quantity of short lived isotopes found in the alternate material blanket. Although more time is expected to be spent on blanket changeouts for DT, the fact that a large portion of the waste is lithium as opposed to activated structure, results in lower doses than one might anticipate for waste handling activities. The low dose expected for handling of DHe blanket wastes is a combination of the lower volume and lower specific activity of the waste.

Table 5.17: Doses Incurred During Handling of Blanket Wastes

	DT			DD				DHe
	5 %	10 %	20 %	5 %	10 % (HT-9)	10 % (RAF)	20 %	10 %
Anticipated Dose Rate (mrem/h)	0.50	0.62	0.72	0.66	1.14	1.82	1.69	0.23
Estimated Exposure Time (man-hours)	616	834	1,112	274	436	411	726	466
Dose Incurred (man-mrem)	308	515	806	174	497	748	1,230	108

5.2.5 Induced Radioactivity Hazard Summary

The results of this section indicate that for the HT-9 designs considered in this work, there is no distinct advantage in terms of induced radioactivity hazard of the advanced fuels over the DT fuel cycle. This conclusion may not apply to optimized designs where different materials and/or energy conversion schemes are employed. In fact, the use of a reduced activation ferritic (RAF) steel first wall and a Fe2Cr1V alloy blanket for the DD fuel cycle indicated that a major reduction in long term hazards would result. This, however, is accompanied by a modest increase in the short term hazards.

The level of activation resulting in the the first wall is dependent on the neutron energy spectrum and the magnitude of the flux. The higher energy neutrons and greater flux intensity associated with the DT designs lead to a greater concentration of radionuclides in their first walls. As would be anticipated with the reduction in reactor size, and consequent increase in flux, activity concentrations are greatest at high beta. The design presenting the most concentrated first wall activity level is the 20 % DT design. Despite the reduction in flux and average neutron energy, significant activity levels are still seen in the first walls of the DD and DHe designs. In all cases, short lived species dominate at shutdown. The relative contribution of these isotopes to the total shutdown activity is greatest for DT. Isotopes dominating long term activity concerns are present in equal or greater amounts in the HT-9 DD first walls compared to the DT first walls. The quantities of these species are largely reduced for the RAF DD first wall. The DHe first wall (HT-9) also contains a non-negligible amount of long lived species. This is both a consequence of the softer neutron spectrum characteristic of the advanced fuels and of the longer blanket lifetime. As would be expected from the higher level of activity associated with the DT designs, decay heating levels at shutdown are greatest for this fuel cycle.

A different situation exists in the bulk of the blanket as opposed to the first wall. The DT blanket is composed largely of lithium, with smaller amounts of helium coolant and structure. The advanced fuels employ a solid structure for their blankets, with some helium provided for cooling. The average blanket activity is lower than the first wall activity for the DT designs because of the reduced amount of HT-9 structure located here. The case is reversed for the advanced fuels, where the volume fraction of steel is much greater in the blanket than the first wall. As with the first wall, short lived species dominate the shutdown activity of the blanket. Both short and long lived species are present in greater quantities for the DD fuel cycle when an HT-9 blanket is used. Thus, the DD HT-9 blankets present a greater concern for both short term (i.e. maintenance and other onsite activities dealing with blanket modules) and long term (i.e. waste management) issues. A considerable reduction in long lived isotopes, and therefore waste disposal hazards, is seen with the use of the Fe2Cr1V blanket. Long term species may present a concern for the DHe fuel cycle. The activity concentrations and decay heat levels in the blanket are greatest for the 20 % beta DD design. The contribution of the blanket decay heat will play an important role in determining consequences of offnormal events, such as loss of coolant or loss of flow accidents. The advanced fuels appear to be at a disadvantage in this regard for the materials used in this study.

The most accurate indicators of radiological hazard during normal operation are dose rates encountered by plant workers. These were found to be highest for the DT fuel cycle. Steam generator dose rates were found to be higher because of the greater hazard associated with the sputtered, activated material expected to be entrained in the coolant. Dose rates encountered during blanket changeouts were estimated to be higher for the DT fuel cycle, mainly because of the lack of self shielding provided by the blanket. A slightly higher dose rate is expected during these activities for the Fe2Cr1V DD design, compared to the HT-9 design, due to the slightly higher level of short lived species present. The DT fuel cycle also

presents an additional hazard during processing of the breeder material, although the dose incurred during these activities contributes a small amount to the total dose. Steam generator doses, followed by those incurred during blanket changeouts, dominate occupational exposures in all cases.

Examination of the wastes produced from the fusion plants indicates that none qualifies for shallow land burial. This is true even after a 30 year cool down period. The total volume of waste removed from the DT and DD plants is nearly the same, while that removed from the DHe plant is significantly less. The activity concentration of these wastes is greatest for the DD fuel cycle when an HT-9 blanket is employed. Considerable reduction is observed with the use of the Fe2Cr1V alloy in the blanket. Because the quantities of long lived species are greater for the HT-9 DD designs, they pose a greater waste disposal hazard than does DT. The use of an alternate material (RAF first wall/Fe2Cr1V blanket) significantly reduces the waste disposal hazard. The activity concentrations of nuclides in the wastes ejected from the DHe plant are equal to or slightly greater than that for DT for an HT-9 blanket. This may not be the case if the alternate material had also been examined for this fuel cycle. However, the much reduced volume of waste produced over the plant lifetime results in the DHe fuel cycle with an HT-9 blanket presenting the least hazard in terms of waste disposal.

Offsite impacts of induced radioactivity are expected to be negligible for all fuel cycles. Routine releases of aqueous effluents are expected to be less than 100 mCi/yr. Releases of activated atmospheric gases should also be low. The hazard presented to the public from induced activity under normal conditions was not evaluated,but is expected to be small for all fuel cycles.

It must be emphasized that the conclusions reached in this section are dependent on the specific designs used in this analysis. These were not optimized designs; they were based on a consistent set of design criteria. As has been illustrated with the RAF first wall/Fe2Cr1V blanket DD design, the conclusions regarding activation

and afterheat levels are strongly dependent on the materials used. This material resulted in higher levels of short lived species and decay heat levels at shutdown, but also led to a significant reduction in long lived isotopes and long term hazards. Short term hazards could be reduced by employing a different blanket material (e.g. SiC), but this would compromise some of the blanket neutron energy multiplication advantage seen with the DD designs. Blanket energy multiplication is less of a factor for the DHe design. Use of a lower activation material in this design may have significantly reduced the hazard, without losing much in terms of blanket energy gain. For all fuel cycles, the use of a different low activation material may have resulted in wastes qualifying for shallow land burial. In addition to the less hazardous wastes, there would be a cost savings if shallow land burial was in fact possible. Finally, the use of a low activation material with lower short term hazards for the advanced fuels has the potential of significantly reducing occupational exposures. Most of the maintenance doses for the advanced fuel reactors are a result of gamma exposures, as opposed to tritium exposures. Thus, utilizing a low activation material, resulting in lower gamma radiation fields, would have a greater impact on reducing total doses for the advanced fuels compared to DT. This would improve the position of the advanced fuel designs relative to DT with regards to safety.

5.3 References

(5.1) Low Activation Materials Safety Studies Project Staff, Annual Report for Fiscal Year 1981, General Atomic Technologies, GA-A16425, September 1981.

(5.2) W.E. Bickford, Transport and Deposition of Activation Products in Helium Cooled Fusion Power Plant, Pacific Northwest Laboratories, PNL-3487, September 1980.

(5.3) C.C. Baker et al., STARFIRE - A Commercial Tokamak Fusion Power Plant Study, Argonne National Laboratory, ANL/FPP-80-1, September 1980.

(5.4) K. Evans et al., WILDCAT: A Catalyzed DD Tokamak Reactor, Argonne National Laboratory, ANL/FPP/TM-150, November 1981.

(5.5) J.B Cannon, Background Information and Technical Basis for Assessment of Environmental Implications of Magnetic Fusion Energy, U.S Department of Energy, DOE/ER-0170, August 1983.

(5.6) P.A. Finn and D.K. Sze, Tritium Technology Review, Fusion Technology, 8, p. 693, July 1985.

(5.7) C.P.C. Wong et al., Helium-Cooled Blanket Designs, Fusion Technology, 8, p. 114, July 1985.

(5.8) D. Smith et al., Blanket Comparison and Selection Study (BCSS) - Final Report, Argonne National Laboratory, ANL/FPP-84-1, September 1984.

(5.9) W.M. Stacey, Jr., Fusion : An Introduction to the Physics and Technology of Magnetic Confinement Fusion, John Wiley & Sons, 1984.

(5.10) D.K. Sze et al., An Assessment of Problems Associated with Tritium Containment, Fusion Technology, 8, p. 1985, September 1985.

(5.11) Weinhold et al., Calculation of Tritium Inventory and Permeation in an INTOR-Like Tokamak Device, European Contribution to INTOR Phase I, Chap. 6, Sect. 3, International Atomic Energy Agency, Vienna.

(5.12) INTOR - International Tokamak Reactor, Phase Two A, Part I, International Atomic Energy Agency, Vienna, 1983.

(5.13) P.A Finn and M.L. Rogers, The Effects of Tritium Contamination in the FED/INTOR Reactor Hall, Nuclear Technology/Fusion, 4, p. 99, September 1983.

(5.14) B.G. Logan et al., MARS - Mirror Advanced Reactor Study, Lawrence Livermore National Laboratory, UCRL-53480, July 1984.

(5.15) International Commission on Radiological Protection, Limits for Intakes of Radionuclides by Workers, Pt. 1, ICRP Publication No. 30, Pergamon Press, Oxford, 1979.

(5.16) R.R. Stasko and K.Y. Wong, Safety Issues Relating to the Design of Fusion Power Facilities, Proceedings of the CNS Annual Meeting, Toronto, Ontario, 1986.

(5.17) J.D. Lee, Editor, Minimars Conceptual Design: Report I, Interim Report, UCID-20559, Lawrence Livermore National Laboratory, 1985.

(5.18) C.C. Baker at al., Fusion Reactor Technology Impact of Alternate Fusion Fuels, Proceedings of the Eighth IEEE Symposium on Engineering Problems of Fusion Research, San Francisco California, November 1979.

(5.19) J.E. Phillips and C.E. Easterly, Sources of Tritium, Nuclear Safety, 22, No. 5, p. 612, September-October 1981.

(5.20) K.Y. Wong et al., Canadian Tritium Experience, Canadian Fusion Fuels Technology Project, Ontario Hydro, 1984.

(5.21) R.D. O'Dell et al., User's Manual for ONEDANT: A Code Package for ONE–Dimensional, Diffusion-Accelerated, Neutral- Particle Transport, Los Alamos National Laboratory, LA-9184-M, February 1982.

(5.22) F.M. Mann, Transmutation of Alloys in MFE Facilities as Calculated by REAC (A Computer Code System for Activation and Transmutation), Hanford Engineering Development Laboratory, HEDL-TME-81-37, August 1982.

(5.23) M.Z. Youssef and R.W. Conn, Induced Radioactivity and Influence of Materials Selection in Deuterium-Deuterium and Deuterium-Tritium Fusion Reactors, Nuclear Technology/Fusion, 3, p. 361, May 1983.

(5.24) General Atomics Standard Safety Analysis Report, GA-A13200, February 1975.

(5.25) W.E. Bickford, Coolant Channel Sputtering Source Terms in a Compact Tokamak Fusion Power Plant, Pacific Northwest Laboratory, PNL-2942, March 1979.

(5.26) Fusion Safety Status Report, IAEA-TECDOC-388, International Atomic Energy Agency, Vienna, 1986.

(5.27) T.D. Murphy, An Overview of the Activated Corrosion Product Reduction Program for U.S. Power Reactors, Proceedings of the Fifth International Conference on Reactor Shielding, Knoxville Tennessee, April 1977.

(5.28) D.R. Olander, Fundamentals Aspects of Nuclear Reactor Fuel Elements, Technical Information Center - ERDA, TID-26711-PI, 1976.

(5.29) G.F. Knoll, Radiation Detection and Measurement, John Wiley and Sons, New York, 1979.

(5.30) S.J. Brereton, A Methodology For Cost/Benefit Safety Analyses For Fusion Reactors, M.I.T Plasma Fusion Center, PFC/RR-85-3, March 1985.

(5.31) G.M. Taylor, The Evolution of Radiation Protection at Ontario Hydro, Nuclear News, Vol. 29, No. 15, p. 45, December 1986.

(5.32) J.S. Herring, The Applicability of Present Near-Surface Waste Management Regulations to Fusion, INEL Annual Report, 1986.

(5.33) C.E. Easterly, Occupational Radiation Exposures at a Fusion Power Station, Nuclear Technology/Fusion, 2, p. 723, October 1982.

(5.34) R.C. Maninger and D.W. Dorn, Issues in Radioactive Waste Management for Fusion Power, IEEE Transactions on Nuclear Science, Vol. NS-30, No. 1, February 1983.

(5.35) R.W. Conn and K. Okula, Minimizing Radioactivity and Other Features of Elemental and Isotopic Tailoring of Materials for Fusion Reactors, Nuclear Technology, 41, p. 389, December 1978.

(5.36) S. Fetter, A Calculational Methodology for Comparing the Accident, Occupational and Waste Disposal Hazards of Fusion Reactor Designs, Fusion Technology, 8, p. 1359, July 1985.

(5.37) S. Fetter, Radiological Hazards of Fusion Reactors: Models and Comparisons, Doctoral Dissertation, University of California, Berkeley, May 1985.

(5.38) R.C. Maninger, Qualitative Comparisons of Fusion Reactor Materials for Waste Handling and Disposal, Fusion Technology, 8, p. 1367, July 1985.

(5.39) M.S. Ortman et al., Characteristics of Unburned Tritium Exhaust, Recovery and Reprocessing Systems in Magnetic and Inertial Confinement Reactors, Proceedings of the American Nuclear Society National Topical Meeting on Tritium Technology in Fission, Fusion and Isotopic Applications, p. 137, CONF-800427, April 1980.

(5.40) E.T. Cheng, Radioactivation Characteristics for Deuterium-Tritium Fusion Reactors, Nuclear Technology/Fusion, 4, p. 545, November 1983.

(5.41) J.A. Blink and G.P. Lasche, The Influence of Steel Type on the Activation and Decay of Fusion Reactor First Walls, Nuclear Technology/Fusion, 4, p. 1146, September 1983.

(5.42) R.W. Conn and A.W. Johnson, Minimizing Radioactivity and Other Features of Elemental and Isotopic Tailoring of Materials for Fusion Reactors, Nuclear Technology, 41, p. 1146, December 1978.

(5.43) M.Z. Youssef and R.W. Conn, On Isotopic Tailoring For Fusion Reactor Radioactivity Reduction, Nuclear Technology/Fusion, 4, p. 1177, September 1983.

Chapter 6
Accident Hazards of Fusion Fuel Cycles

As part of any safety evaluation, an investigation into potential accident hazards must be performed. This involves quantifying sources of radioactivity, identifying sources of stored energy, postulating accident scenarios that could liberate the energy and mobilize the radioactivity and assessing the consequences of the most credible accident scenarios. Inventories of radioactive species have been estimated in the previous chapter. In this chapter, sources of stored energy will be identified and their magnitude will be evaluated. A brief discussion of possible mechanisms for the release of the stored energy will be given. A loss of coolant accident will be examined in detail. The safety and economic consequences of this event will be compared amongst the fuel cycles.

6.1 Sources of Stored Energy

In order for the public to be seriously affected by a reactor accident, dispersal of volatile radioactive substances or airborne radioactive particulates outside the containment must occur. A plume containing these materials can be formed by the escape of materials through a breached containment followed by the release of these effluents from the containment building into the atmosphere. The requirements for a hazardous accident include: mobilization of radioactive species, breach of containment structures, and transport of radioactive materials out of the ruptured containment. Any scenario in which these requirements are fulfilled will involve the release of stored energy in an uncontrolled and destructive manner. It is of interest to identify and quantify what the sources of stored energy are, and the mechanisms capable of freeing this energy.

The sources of stored energy have been identified for the various fuel cycles and are summarized in table 6.1. The stored energy is in several forms including radiological, thermal, electromagnetic and chemical forms. The fusion power generated by each device during operation is also included in the table. The DD fuel cycle presents the greatest decay heat source. As discussed in section 5.2.1, this is a consequence of the larger amount of structural material relative to DT, and a higher neutron flux relative to DHe. If released in an uncontrolled manner, the subsequent temperature rise could result in component damage and volatilization of radioactive species. The plasma kinetic ($\frac{3}{2}$kT) and magnetic ($\frac{1}{2}$LI^2) stored energies are greater for the advanced fuels than for DT because of the higher operating temperature and magnetic fields associated with these designs. This energy, if deposited in a sufficiently localized area, could melt or vaporize a small portion of the first wall. The higher fields of the advanced fuels also result in a greater amount of energy being stored in the magnetic field ($\int \frac{B^2}{2\mu_o} dV$). This is a larger source of stored energy for all of the fuel cycles. It could possibly melt or vaporize a significant fraction of activated structure if a localized energy dump were to occur. Additionally, large

Table 6.1: Sources of Stored Energy

	DT			DD				DHe
Energy Source	5 %	10 %	20 %	5 %	HT-9 (10 %)	RAF (10 %)	20 %	10 %
Fusion Power (GW)	3.6	3.6	3.6	2.9	2.9	2.7	2.9	3.8
Inboard Blanket Shutdown Decay Power (GW)	0.011	0.012	0.012	0.064	0.069	0.074	0.074	0.004
Plasma Kinetic Energy (GJ)	0.63	0.50	0.41	9.8	6.1	5.8	4.1	6.8
Plasma Magnetic Energy (GJ)	4.47	1.76	0.727	65.1	20.4	19.4	6.78	26.8
Energy in Toroidal Magnetic Field (GJ)	290	113	45	4278	1345	1275	441	1768
Chemical Energy of Lithium In Blanket† (GJ)	8.62	6.56	5.23	-	-	-	-	

† 0.001 MW · yr/Mg [6.7] for spill of all liquid lithium in blanket into air

forces could be produced if this energy were released and the integrity of the first wall could be threatened. However, an event such as this would be improbable. The chemical energy stored in the lithium in the breeder blanket of the DT reactors is a source of energy not present for the advanced fuels. It is of significant magnitude (note that it is larger than the thermal and magnetic energy contained in the DT plasma) that it could possibly cause structural damage and mobilization of induced activity.

In addition to the magnitude and form of stored energy, the time constant for the release phenomenon is important. With this additional information available, an attempt to predict and understand possible abnormal events can be made. Actions to protect against the energy release can be taken and designs can be chosen to mitigate the effects of such a release. A detailed assessment of the events which may occur subsequent to the release of all of the sources of energy identified in table 6.1 has not been made. However, the information given does reveal the relative potential for mobilization of radioactivity for the fuel cycles.

6.2 Mechanisms for the Release of Stored Energy

Given the sources of energy which could mobilize the radioactivity held within the fusion plant, a mechanism for the release of this energy must be available before any harm results. It is possible to postulate scenarios in which the stored energy of the system is directly liberated or converted to thermal or mechanical energy as a result of system or component failures. These accidents may include plasma disruptions, magnet system accidents, breeder system failures leading to lithium fires, cryogenic depressurization, auxiliary system failures, hydrogen explosions and coolant system failures. The first six scenarios are discussed briefly in this section. Coolant system failures, in particular a loss of coolant accident (LOCA), are discussed in the next section.

6.2.1 Plasma Disruptions

Of major concern in tokamak devices is an event in which there is a very rapid and often very violent loss of plasma confinement due to the collective behavior of the particles. Disruptions may occur due to plasma instabilities including ballooning modes, kink instabilities and tearing modes. External events, such as a first wall LOCA, a TF magnet failure or other event modifying the plasma operating conditions could initiate a disruption within the plasma. This process results in almost all of the plasma kinetic energy and some of the associated magnetic energy being dumped in a short time on part of the first wall or limiter. It should be emphasized that neither the causes of disruptions nor their effects are well understood at this time. It is thought, however, that the thermal and magnetic energy of the plasma is deposited onto the first wall in two distinct phases [6.1]. During the thermal quench phase, most of the plasma kinetic energy is deposited and the plasma temperature rapidly decreases. This is followed by the current quench phase during which the plasma current decays and the remainder of the plasma thermal energy and all of the stored magnetic energy are released. Surface heating of the first wall as a result of this deposition may result in partial melting or vaporization. Also, induced currents will lead to volumetric heating of the first wall. The resultant non-uniform temperature rise may cause excessive structural strains. Additionally, the perturbed magnetic field may interact with currents producing magnetic forces on structural members which could lead to breach of containment and release of radioactivity.

Of critical importance in determining the effects of a plasma disruption is the disruption time. The thermal and electromechanical effects of the disruption are dependent on the disruption time scales [6.2]. Current devices have disruption times less than one millisecond, increasing with reactor size and particle density [6.3]. A longer disruption time would lead to less severe consequences for the event.

Selcow [6.4] has examined the effects of plasma disruptions in high beta DD tokamak reactors. She indicated that disruptions should be minimized in these reactors; some means of control must be found for the operation of high beta DD tokamaks to be feasible. Such an analysis was not performed as part of this study. However, it can be implied that the larger amount of stored energy in the DD and DHe plasmas relative to that stored in the DT plasmas will result in more severe consequences after a disruption.

6.2.2 Magnet System Accidents

Magnetic fusion reactors require large magnetic fields for operation. The reactors being examined in this work employed superconducting magnets. The magnets present a safety hazard in that the liberation of their stored energy could initiate an accident sequence that would release toxic or radioactive materials. Of concern for a safety analysis, are abnormal operation of the magnets which could lead to disruption of the magnetic field, and accident situations which could result in damage to the magnet and/or other reactor systems.

The principal abnormal operating event is the 'quench', where the conductor suddenly transforms from the superconducting to the normal state. A quench can be triggered by cryogenic instabilities resulting from either loss of adequate cooling or sudden localized heating exceeding the cooling capabilities. Subsequent to a quench, rapid heating of the coil can occur resulting in unacceptable thermal stresses, conductor damage and helium boiling leading to cryostat overpressurization. Systems can be designed to protect against cryogenic instabilities by providing adequate cooling to remove all the Joule heating of the conductor when the magnet operates in the normal state. Other consequences of quenching, such as current discharge, asymmetric mechanical forces and inductive current increases, can be minimized by proper design. Thus, quenches are not considered to be accidents

that could result in mechanical damage to other parts of the fusion reactor or lead to release of radioactivity. However, they are costly in that they result in reactor downtime, and a high frequency of occurrence must be avoided.

The release of the energy in the magnets could be coupled to other systems through major structural failure. A magnet accident sequence which could lead to moderate damage is the arcing across current leads or the rupture of a single conductor. Multiple-current arcs can occur if one or more of the adjacent conductors rupture due to the heat produced by the first arc. The major consequence envisioned for these events is vaporization of the conductor material, probably requiring complete replacement of the entire magnet. Additionally, adjacent cables and piping could be damaged, and coolant lines or tritium processing lines may be disturbed, resulting in the release of potentially hazardous material. Simultaneous ruptures of the entire winding and casing at two different locations would result in more severe damage and consequences. Loosened broken sections could be accelerated, generating missiles. Arendt and Komarek [6.5] estimated that if the distance between the ruptured ends of the winding and casing is greater than 1 m, missile generation will occur. Although the energy carried by the missile will be less than that assumed for airplane crashes into containment structures, it would be large enough to cause significant damage to peripheral equipment and cause breaks in coolant and tritium processing lines.

Selcow [6.4] investigated two possible magnet accidents in a superconducting TF coil of a high beta DD tokamak to determine their dependence on field strength. She found that it is the lower field magnets which have the greater probability of failure for either event (i.e. a greater heating rate in the copper stabilizer occurred for the lower field magnets subsequent to the accident). A strong dependence of the time for magnet failure to occur, as measured by the heating rate, was found for a magnet loss of coolant accident. Magnet failure was found to be only weakly dependent on field for a shorted turn accident. An investigation of possible magnet system accidents was not undertaken as part of this study. However, in light of

Selcow's findings, it would appear that the lower field DT designs pose a greater threat.

6.2.3 Lithium Fires

The material chosen for tritium breeding in the DT designs was liquid lithium metal. Although lithium has both good breeding and thermal properties, a major drawback of this material is its high reactivity with water, air and concrete. Exothermic reactions also occur with nitrogen, carbon dioxide and hydrogen. A peak theoretical flame temperature of $\sim$ 2400 K has been calculated [6.6]. At such high temperatures, melting and possibly volatilization of the activated first wall materials could occur. More realistic assumptions lead to a maximum flame temperature of 1200 °C [6.7]. This flame temperature was confirmed by tests performed on lithium pools at the Hanford Engineering Development Laboratory (HEDL) [6.8]. It has been shown that this temperature would result in the volatilization of less than 0.014% of the mass of a reduced activation ferrutic steel first wall [6.9]. Aerosol formation and release was observed during the HEDL lithium pool reaction tests. Aerosols generated from a spill at a reactor may contain activated impurities or corrosion products. It is felt, however, that collection and control of these lithium aerosols is possible [6.8].

Calculations by LITFIRE have shown that a spill of $\sim$ 22 Mg of lithium onto the floor of a plant containment the size of UWMAK III can raise the air temperature from ambient to about 300 °C within a half hour after the accident occurrence [6.10]. The maximum lithium pool temperature observed was 950 °C. The results were shown to be somewhat dependent on the containment volume and strongly dependent on the amount of lithium spilled. Barnett also assessed the consequences of a lithium spill and fire inside the vacuum torus [6.10]. He found that the effects of the fire were relatively minor because the large heat capacity of the blanket and

shield were able to absorb most of the heat conducted through the lithium pool and first wall. His results, however, did not include the effects of decay heating. This consideration may alter the conclusions somewhat.

If lithium in a reactive form is used in reactors, engineering design can probably eliminate or mitigate lithium fire accidents. Some design strategies include: using steel liners for concrete, having independent breeder modules, reducing the lithium inventory per breeding loop, reducing the oxygen concentration in the reactor building, using a structural material with a high heat removal potential, installing a containment atmosphere cooling system, using a larger containment volume and employing a dump tank below likely spill areas. Because helium is used as the primary coolant in the DT designs considered in this study, lithium-water reactions are less of a concern than they would be for a water cooled plant. However, the shield is water cooled and the potential for lithium and water coming in contact does exist. An investigation of the consequences of lithium reactions with water, air or concrete at the DT fusion plants considered in this study was not performed. However, it is important to keep in mind that a relatively large source of energy which is present at the DT plants is not present at the DD or DHe plants.

6.2.4 Cryogenic Depressurization

Liquid helium will be used in the cryopumps for the vacuum and fuel handling systems and for maintaining the cryogenic temperatures of the superconducting magnet coils. Subsequent to a coil or helium pipe break, the liquid helium could be spilled into the reactor building. The liquid will flash into a vapor, extracting heat from reactor structures, causing thermal strains. A certain degree of pressurization of the reactor building will result from the production of the helium vapor. An analysis performed for the Fusion Engineering Device (FED) to determine the consequences of a toroidal magnet inlet helium header break indicated

that the containment atmosphere pressure would rise by 0.08 MPa [6.11]. Containment buildings should be designed to withstand overpressures of this magnitude. The loss of helium coolant to the magnets will lead to the dissipation of the magnet energy, causing the temperature of the conductor to rise. This may lead to melting of the coils thereby aggravating the effects of the helium spill. A further concern for helium cooled reactors is that loss of helium may imply a loss of coolant if all helium is drawn from the same reservoir.

6.2.5 Auxiliary System Accidents

There are a number of other sources of energy that were not quantified in section 6.1 which could serve as initiators for radioactive releases. These include plasma heating equipment, fueling equipment, vacuum pumps and vacuum chamber, high voltages and eddy currents. The energy associated with these auxiliary systems present a hazard in themselves in addition to the fact that they could mobilize radioactive species.

As a consequence of current passage through the plasma, some ohmic heating of the plasma particles will take place. As indicated in table 2.2, the temperature achieved by ohmic heating of the DT plasmas falls short of that required for ignition. Radiofrequency heating was assumed to be employed to supplement the ohmic heating to achieve ignition. Because of the larger fields and reactor sizes of the advanced fuel designs, the temperature achievable by ohmic heating is higher. Ignition of a DT plasma followed by thermal runaway will heat the plasma close to the ignition temperature of the advanced fuel. As the temperature is rising, some supplemental heating will be applied and the fueling mixture will gradually be changed to that of the advanced fuel. Although the quantities of rf heating actually required were not evaluated, the power of the rf sources required for this purpose will be much larger than that of contemporary rf broadcast transmitters.

Thus, special precautions must be taken.

Several mechanical safety issues are presented by the vacuum pumps and vacuum chamber in addition to cryogenic concerns. The cryopumps will be backed by turbomolecular pumps which contain high speed rotors that could fracture and generate missiles. In the event of a vacuum chamber failure, the cryopumps could heat up and release their inventory of deuterium, tritium and helium. This could lead to a potentially flammable mixture being present in the reactor, depending on the concentration and the infiltration of air into the vacuum chamber.

6.2.6 Hydrogen Explosions

Hydrogen can combine explosively with oxygen under certain conditions. This is of concern at at fusion plant because large quantities of the hydrogen isotopes, deuterium and tritium, will be found on site. Explosive mixtures in air result with hydrogen concentrations in the range of 4 to 59 %. The consequences of a hydrogen explosion are strongly dependent on the total amount of hydrogen available, the building geometry and volume, and the cover gas used in the reactor building. It is possible to design fusion reactor containments to accommodate these accidents [6.12]. For the reactors of concern here, the room air concentration of hydrogen (D_2 and T_2) would be far below the lower explosive limit assuming release of the entire tritium inventory and the deuterium in storage into the reactor building volume. Hence, it is not expected that this issue will present a safety problem.

6.3 Consequences of a Loss of Coolant Accident

It was not possible to carefully examine and assess the consequences of the entire spectrum of accidents envisioned at a fusion plant. It was felt, however, that at least one accident scenario should be investigated to give an indication of the

relative consequences of an off-normal event for the various fuel cycles. A loss of coolant accident was selected for this comparison. In this section, the consequences of such an event for the different fuel cycles are examined. Results for both the economic and health impacts, onsite and offsite, are given. The analysis was performed only for those designs employing an HT-9 blanket. However, the impact of this accident for the RAF first wall/Fe2Cr1V blanket DD design can be inferred knowing the decay heat and activation levels.

6.3.1 Discussion of the Problem

The function of the primary coolant system of a fusion reactor is to remove the heat energy deposited in the first wall/blanket region surrounding the plasma. Energy enters the blanket region through the first wall either in the form of neutrons or direct radiation. The neutrons transfer their kinetic energy into thermal energy through collisions and nuclear reactions with the blanket material. Incident radiation is conducted away from the first wall by the blanket medium. Conduits within the blanket structure contain the primary coolant to which the energy deposited in the blanket is transferred. The primary coolant, being helium in this case, then passes to a steam generator where the energy is transferred to steam. This can then be utilized to produce electricity.

A loss of coolant accident (LOCA) may result from an individual tube plugging or the rupture of a coolant line. For an individual plugged tube, the effects of the LOCA in the blanket would be localized in the vicinity of the inactive cooling tube. A temperature rise would be expected in this area, but removal of heat by adjacent, operative cooling tubes would assist in the heat removal and limit the extent of the transient. In the event of a ruptured or leaking coolant line, loss of the coolant serving an entire module could result. The other modules would still operate normally, providing cooling. A worst case, wherein the entire coolant

inventory to all modules is lost, can be envisioned. This event is much more serious in that there is no buffer to remove the heat load. All modules would experience the same transient. The potential for damage and loss of structural integrity exists.

Subsequent to a loss of coolant accident, there are two heat sources of concern. If the plasma is not extinguished, it will continue to deposit energy in the blanket by neutron and surface heating until it is terminated by either entry of impurities into the plasma (e.g. volatilized first wall material, blanket coolant or breeder), the cause of the accident itself (e.g. magnet quench) or an active shutdown mechanism. Prompt and reliable shutdown of the plasma within a short time would minimize the impact of the LOCA. Regardless of whether or not the plasma is terminated, the decay afterheat due to induced structural activity will exist as a heat source in the blanket. In both cases, the consequences at the first wall are the major concern, for it receives the highest surface heating and it is located in the region of highest decay heat density. Large temperature excursions leading to first wall/blanket structural failure and possible radioactive releases can occur if an auxiliary cooling system is not provided, or if an emergency cooling system becomes inoperative.

The magnitude of the first wall temperature increase subsequent to a LOCA is dependent on the length of time of continued plasma burn, and the decay heat density in the blanket and first wall. It is expected that the plasma will terminate within seconds after the accident has been initiated. The decay afterheat source, however, will be present over many hours to years, so that the transient may extend over a long period of time. The first wall temperature may rise high enough to result in melting or volatilization. If the vacuum vessel is breached, oxygen may enter and oxides may form. These are generally more volatile than the elements from which they are formed, so that they may become mobilized at a lower temperature. With a breached vacuum vessel, there is a direct pathway to the reactor hall. If the reactor building has not maintained its integrity, the released activity can enter the environment and reach the public domain.

6.3.2 Assumptions Involved and Method of Analysis of the Loss of Coolant Accident

The investigation was performed to assess the response of the first wall/blanket of the various fuel cycles to a loss of coolant accident and to examine the potential consequences of the ensuing transient. The scenario envisioned is a complete loss of coolant to all modules. This is the simplest approach since all modules will experience the same transient. The accident took place at the end of blanket life in all cases, representing a worst case scenario (note that the end of blanket life does not occur at the same point in the operating life of the plant for each design). It was further assumed that there was an immediate loss of cooling capacity; no time was allowed for drainage of the coolant from the modules. This is not being overly conservative as Piet [6.2] indicated that the loss rates of coolants (particularly pressurized coolants like helium) under severe LOCA's are sufficiently high that there will be no direct effect on cooling of the blanket for time scales of interest in afterheat calculations. Concurrent with the loss of coolant, the vacuum boundary was assumed to lose integrity (perhaps due to failure of some penetration e.g. vacuum pump duct, auxiliary heating duct) and the building atmosphere was assumed to stream into the torus. The possible release of radioactive sputtered material entrained in the coolant into the reactor hall was not considered. Tritium releases from the structure were not assessed. It was assumed that pressurization of the vacuum vessel occurred rapidly so that the torus back pressure was high enough to maintain the tritium permeation rate out of the structure at a negligible level. Furthermore, during the pressure equilibration period, when any tritium release would occur, temperatures would actually be lower than indicated here as some heat would be removed during coolant drainage. The lower temperatures would result in lower tritium permeation rates. After consideration of these two effects, it was assumed that an insignificant amount of tritium was released as a consequence of this accident. Termination of the accident occurred after 10 hours. At this time,

Table 6.2: Assumptions Made for the Loss of Coolant Accident

Accident Assumptions:

- accident occurs at the end of blanket life
- loss of coolant to all modules with continued plasma burn for equivalent of three full power seconds (one second at full power, followed by a four second linear ramp down)
- coolant is lost immediately; no allowance for drain time is given
- breach of the vacuum vessel with entry of air into the torus
- oxidation of the first wall and the release of radionuclides (see table 6.3) at a rate given by EG&G data
- worker entry (crew of 3) at t=9:45 for 10 minutes to reestablish cooling
- 45 minutes of remote activity prior to initial entry to perform preparatory tasks
- the accident terminates after 10 hours
- clean up based on Three Mile Island decontamination effort
- degree of damage to components based on thermal creep during the transient
- release of any radioactive material entrained in the coolant is not considered

Scenarios Considered:

(1) radioactivity is contained until 10 hours after accident initiation when release to the environment begins at the normal ventilation rate (over 100 h)

(2) all radioactivity is contained within the reactor building; no release to the environment

(3) all radioactivity is released immediately to the environment (over 10 h)

some form of intervention was assumed to occur such that cooling of the first wall was reestablished and releases of radionuclides ceased. The assumptions involved in the accident assessment are given in table 6.2.

6.3.2.1 First Wall Temperature Response

The first wall temperature response to the loss of coolant was obtained using HEAT1D◇ [6.13]. The basic geometry for the analysis was the same as that used for the ONEDANT analysis (see figure A.1), in determining the spatial variation of neutron fluxes. Subsequent to the accident occurrence, plasma operation continued for an equivalent of three full power seconds. The decay of the plasma was assumed to occur over five seconds, with full power for the first second followed by four seconds of a linear ramp down. Values of the operational surface heat flux corresponding to each design were used as input to the code. An initial first wall temperature of 530 °C was assumed in all cases. Cooling of the magnets continued during this event so that the magnet assemblies served as a constant temperature heat sink (373 °C). Because the blanket model used smeared materials' properties, and the coolant tube locations were not specified, heat transfer throughout the blanket region was via conduction only. In regions where there were gaps (e.g. between the blanket and shield, and from the back of the shield to the heat sink), radiation heat transfer played a vital role. Convection was not included in the model for this analysis. Temperature dependent conductivities, heat capacities and densities were used. Properties for lithium and HT-9 were taken from the BCSS (see table G.1, appendix G). For radiation heat transfer in the gap regions, an emissivity of 0.5 was assumed, representative of a partially oxidized surface. The analysis was performed in one-dimensional slab geometry, so that view factors were equal to one. The volumetric heat generation rate was specified both during operation, when the neutron

◇ HEAT1D is a one-dimensional finite difference heat transfer code developed at M.I.T.

flux is still present, and after plasma termination, when nuclear decay is the only heat source. The operating nuclear heating rate was obtained from the ONEDANT (the neutronics code) output; the decay heat source was obtained from the REAC (the activation analysis code) output. The decay heat levels for the inboard region were used in the analysis. Information from the first and last nodes within each region was employed to obtain the spatial variation of the heating rate, using an exponential attenuation of nuclide concentration. The time dependence of the heat generation rate is a function of the quantities of the specific nuclides present and their decay constants, both of which are known at the onset of the accident.

6.3.2.2 Mobility of Oxides

Once the temperature history of the first wall subsequent to the LOCA has been determined, an assessment of the quantities of radionuclides mobilized must be made. If the vacuum vessel is breached, ingress of air into the vacuum region will occur. The presence of an oxidant in combination with the high wall temperature may result in rapid oxidation and volatilization. Piet et al. [6.14] give an estimate of the oxidation rate for SS 316 in dry air at 1000 °C as $\sim 10^{-3}$ mm·h^{-1}. They indicate that oxidation of TZM alloy and vanadium alloy proceed at a much faster rate and at much lower temperatures. Piet [6.2] assumed an oxidation rate of ~ 0.1 mm·h^{-1} at 1300 °C for both SS 316 and HT-9 in his analysis. The oxidation of wall material may cause severe reactor damage and loss of structural integrity. Furthermore, the oxidation takes place in the region of highest specific radioactivity. Thus, volatile chemical species produced by this process could serve as a carrier of radioactivity to the environment.

The quantities of neutron induced activation products that can be mobilized under potential accident conditions are largely uncertain. To gain some insight into this problem, experiments have recently been conducted at EG&G at the Idaho

National Engineering Laboratory (INEL) [6.15]. The volatilization of constituents resulting from oxidation of PCA and HT-9 in air was investigated. Tests were conducted at temperatures of 600 to 1300 °C for 1 to 20 hours. The results showed that molybdenum, manganese, copper, phosphorus, titanium and chromium are most readily volatilized. In terms of radiological hazard, the most important of these are molybdenum and manganese.

In the tests performed at EG&G, the variation of the volatilization rate with temperature was studied. Although there was a large degree of scatter in the data, an Arrhenius type temperature trend was observed. This type of temperature dependence of the rate is very often exhibited by chemical reactions [6.16]. Assuming this relationship to be valid, the volatilization rate can be expressed as:

$$Q = A \cdot \exp\left(\frac{B}{R \cdot T}\right) \tag{6.1}$$

where

Q = rate of volatilization of a particular element in the steel $\left(\frac{\text{atoms}}{\text{h}\cdot\text{m}^2 \text{ of first wall}}\right)$

A = curve fit constant $\left(\frac{\text{atoms}}{\text{h}\cdot\text{m}^2 \text{ of first wall}}\right)$

B = curve fit constant $\left(\frac{\text{J}}{\text{mole}}\right)$

R = ideal gas constant

$= 8.314 \left(\frac{\text{J}}{\text{mole}\cdot\text{K}}\right)$

T = temperature (K)

The constant B represents the activation energy for the reaction of interest. Most reactions proceeding at reasonable rates (i.e. the time required for half of the limiting reactant to be consumed, as measured by the half life of the reaction, is

on the order of minutes or hours) have values of B in the range of 50 to 100 $\frac{kJ}{mole}$ [6.16]. The pre-exponential factor A has been shown to have some temperature dependence for certain chemical reactions, although no common relationship has been found to exist.

Curve fit constants for the elements of interest in the HT-9 first walls used in this study are given in table 6.3. These were obtained using the average mobilization rates from the EG&G data at 800 °C and 1000 °C (since this was the temperature range of interest for this accident scenario - see section 6.3.3). Because of the wide scatter in the data and the uncertainty in the form of the temperature dependence of A, the pre-exponential factor was taken to be a constant for the present purposes. The isotopes of each element to which these rates were applied are also given in table 6.3. These isotopes were selected from the inventory in the first wall based on concentration and half life. The fraction of the total release of each element for a specific isotope was obtained from the isotopic compositions given in the REAC output.

Isotopes of other elements formed during irradiation which were not originally found in the HT-9 (e.g. magnesium, scandium) were not included in the release because mobilization rates were not available. However, it is expected that they would be responsible for only a small amount to the radiological hazard, since they are not major contributors to the first wall activity (see table 5.8). Thus, their neglect should not largely affect the outcome of this analysis. In the case of rhenium, which is a product of tungsten, the quantities formed in the softer spectrum of the advanced fuels are much larger than for DT. Neglect of this element in the releases can be justified on the basis of it being a refractory material with a melting point higher than that of tantalum, whose oxides were shown to have a low mobilization rate in tests run for PCA.

In the EG&G experiments, the volatilization rate was also studied to determine the variation with the gas flow rate past the sample and the time of exposure of the

Table 6.3: Mobilization Rates of HT-9 First Wall Elements

Mobilization Rates of the Form : $Q = A \cdot \exp\left(\frac{-B}{R \cdot T}\right)$

Element	A ($\frac{atoms}{m^2 \cdot h}$)	B ($\frac{kJ}{mole}$)	Radioisotopes Included
Phosphorus	3.81×10^{21}	14.9	^{32}P, ^{33}P
Titanium	1.47×10^{19}	14.5	^{51}Ti
Chromium	1.55×10^{22}	60.7	^{49}Cr, ^{51}Cr, ^{55}Cr
Manganese	2.86×10^{18}	4.72	$^{52*}Mn$, ^{52}Mn, ^{54}Mn, ^{56}Mn, ^{57}Mn
Iron	3.86×10^{22}	58.8	^{53}Fe, ^{55}Fe, ^{59}Fe
Nickel	2.62×10^{20}	59.9	^{57}Ni, ^{59}Ni, ^{63}Ni, ^{65}Ni
Molybdenum	1.32×10^{30}	286	^{91}Mo, $^{93*}Mo$, ^{93}Mo, ^{99}Mo, ^{101}Mo
Tungsten	1.50×10^{20}	23.4	^{181}W, ^{185}W, ^{187}W
Vanadium	3.73×10^{21}	62.8	^{48}V, ^{49}V, ^{52}V, ^{53}V

sample to air. Since the temperature is the primary parameter of concern in the LOCA analysis, these effects were not considered in the present study.

6.3.2.3 Structural Creep Considerations

Structural temperatures during operation will be as high as practical because good thermal efficiency is desired. During the accident, the temperature will rise from the operating level and the strength of the metal structure will decrease. At the same time, thermal stresses due to non-uniform heating will be generated. A general weakening of alloys, as measured by the yield strength and ultimate tensile strength, will occur with increasing temperature. A further alteration will occur with the microstructure. Alloys are typically subjected to heat treatment prior to use, to obtain a particular microstructure. A degradation of the material performance concurrent with microstructure alteration may occur during the temperature transient. This degradation could have serious consequences at a later time during the accident, or prevent future operation of the reactor. The onset of melting represents a higher temperature rise than for the onset of structural damage. It is clear that if the melting point is reached, severe consequences are imminent.

The degree of structural damage resulting from the temperature transient cannot be precisely known. Since the exact condition of the torus after the accident is not available, a detailed structural analysis to determine loads and resulting deformations and fractures could not be performed. For the purposes of this study, a very simple analysis, based on thermal creep effects (see appendix G) was carried out. This analysis followed a methodology proposed by Massidda [6.13]. During operation, both pressure and thermal stresses will exist in the first wall. The magnitude of the thermal stress will decrease from its initial value at the beginning of operation as a result of relaxation. With the loss of coolant at the onset of the accident, the pressure stress will be eliminated. Due to the relatively rapid ther-

mal response time of the first wall (< 1 sec), the front and back faces of the first wall will experience nearly the same rapid rise in temperature at the beginning of the accident. From this point on, however, the first wall temperature gradient will decrease in magnitude, as no heat is being removed from the back face, and the front and back face temperatures equilibrate. This alters the temperature gradient and a new stress results which will be opposite to that which initially existed in the first wall. Its magnitude will not exceed the initial first wall thermal stress at the beginning of operation since the maximum change in temperature gradient possible is from the operational value to zero, which would occur if the front and back face temperatures became equal. Thus, it is expected that the thermal stress due to the change in temperature gradient will be tolerable. What is of concern then, is thermal creep which will result from the presence of a stress at an elevated temperature for an extended period of time. If the stress and temperature are high enough, and are present over a long enough period of time, damage to the first wall may occur due to creep rupture. The basis for this damage assessment for the first wall subsequent to the LOCA is discussed in more detail in appendix G. Given an expression for the creep rate as a function of temperature and knowing the first wall temperature throughout the transient, the degree of elongation and stress relaxation can be followed as a function of time. Using relations for time to creep rupture as a function of temperature and stress, and progressing in a series of time steps over the transient, the fraction of the rupture lifetime consumed over each time interval can be determined. If at any point during the transient, the fraction of the rupture lifetime consumed exceeds one, then failure will result. It was therefore assumed that the torus underwent structural damage due to the initial breach of the vessel, followed by any damage due to thermal creep effects.

The immediate consequences of the accident include the quantities of radionuclides mobilized and the degree of structural damage. These are discussed in the next section.

6.3.3 Immediate Consequences of the Coolant System Accident

The primary issue subsequent to a LOCA is the rise in temperatures due to inadequate cooling. Concern arises in two areas: (1) volatilization of radioactive species, and (2) damage due to thermal stresses and weakening material strength at elevated temperatures. It is the radiological aspect which is of most concern here, although some attention was given to the structural damage for estimation of economic consequences.

Of major importance with regards to volatilization is the mobilization of material which may be radioactive. Loss of structure may further aggravate the situation if it results in significant weakening. Volatilization can occur over a range of temperatures. The resulting first wall temperature responses to the transient being considered here are shown in figures 6.1 to 6.6. During the plasma heat phase (figures 6.1 to 6.3), the initial temperature response is dominated by the surface heat flux. Most of the heat goes into raising the temperature of the first wall, resulting in a temperature spike. The height of the spike is seen to increas with the first wall thermal heat flux. After plasma termination (5 seconds), the first wall temperature gradient relaxes, lowering the first wall temperature. Once this has occurred, the wall temperature again begins to rise (see figures 6.4 to 6.6), at a rate determined by the decay heat generated in the first wall/blanket region and the thermal properties of the materials. The consequence of continued plasma operation, since it occurs over a relatively short time range, is effectively to raise the initial first wall temperature at which the afterheat response begins. The peak temperatures experienced in the first wall during the plasma heat phase and over the entire transient are summarized in table 6.4. The maximum temperature reached is seen to increase with beta for a given fuel cycle, as would be expected from the increased specific activity (see table 5.8). The temperature rise in the DT first walls is lower than would be expected from the shutdown decay heating levels (see table 5.10). This reflects the good thermal sink performance of lithium in conducting the heat away

FIGURE 6.1:
INITIAL FIRST WALL TEMPERATURE RESPONSE DURING LOCA DT DESIGNS

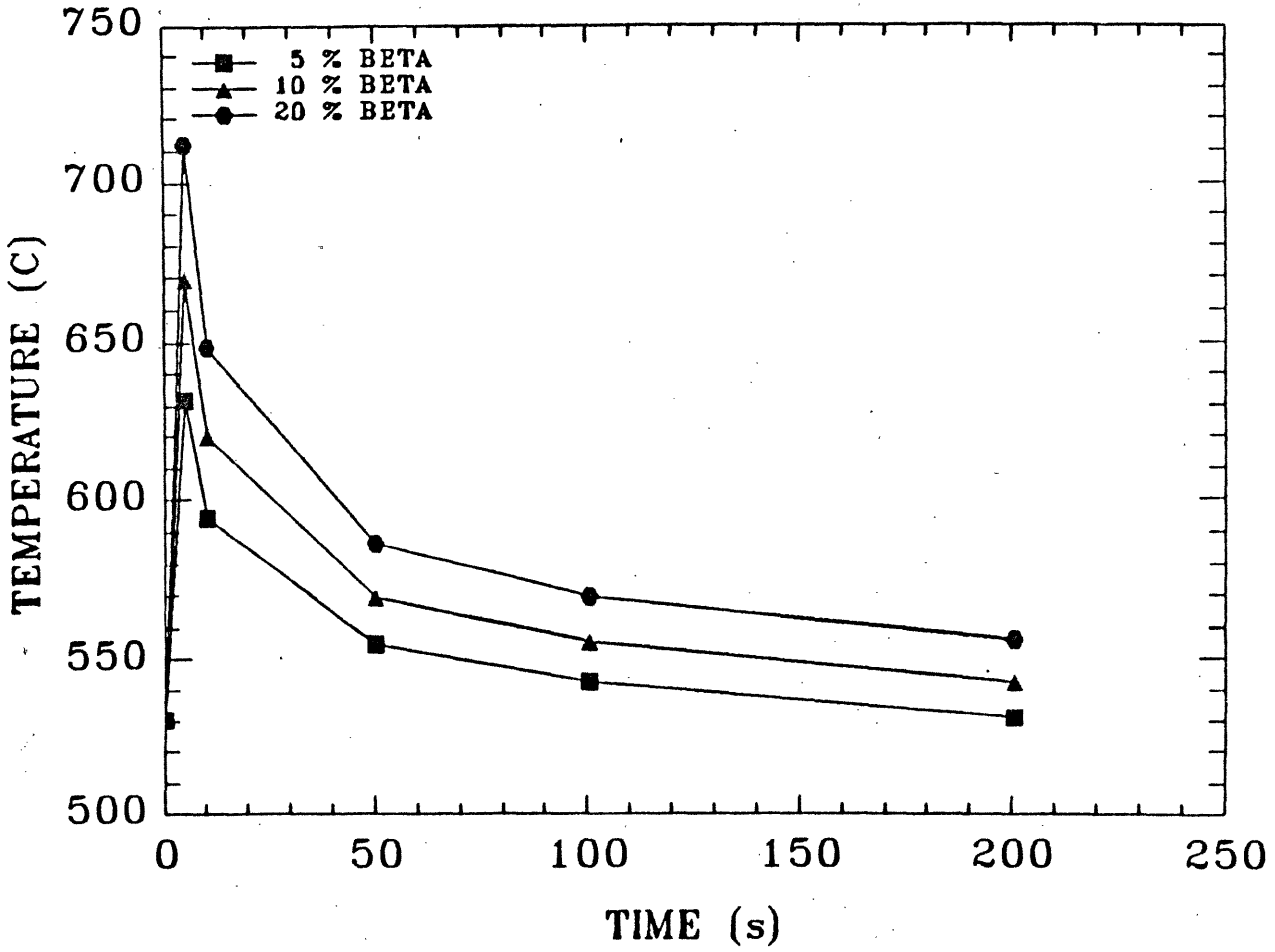

FIGURE 6.2:
INITIAL FIRST WALL TEMPERATURE RESPONSE DURING LOCA DD DESIGNS

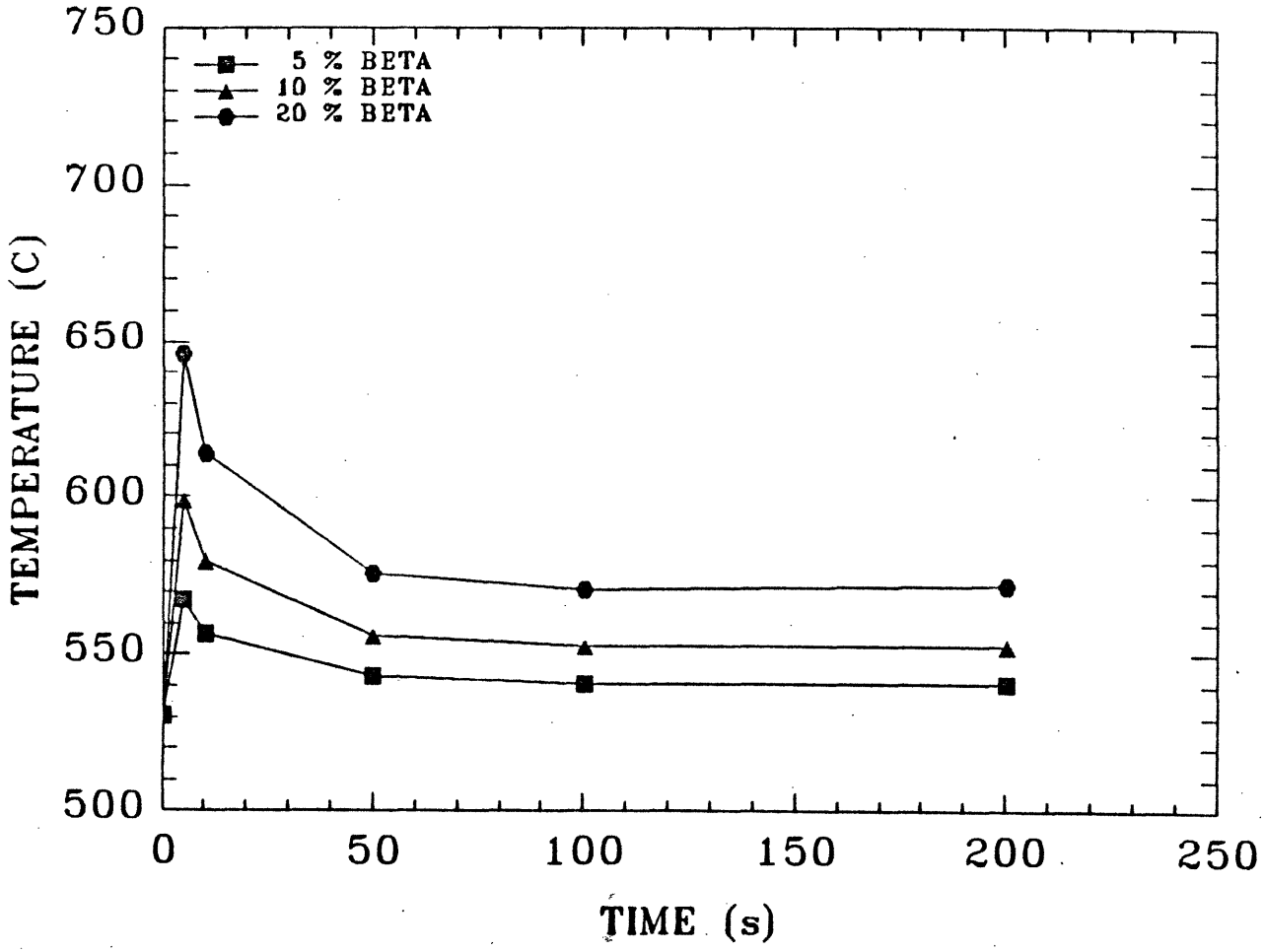

FIGURE 6.3:
INITIAL FIRST WALL TEMPERATURE RESPONSE DURING LOCA
10 % BETA DESIGNS

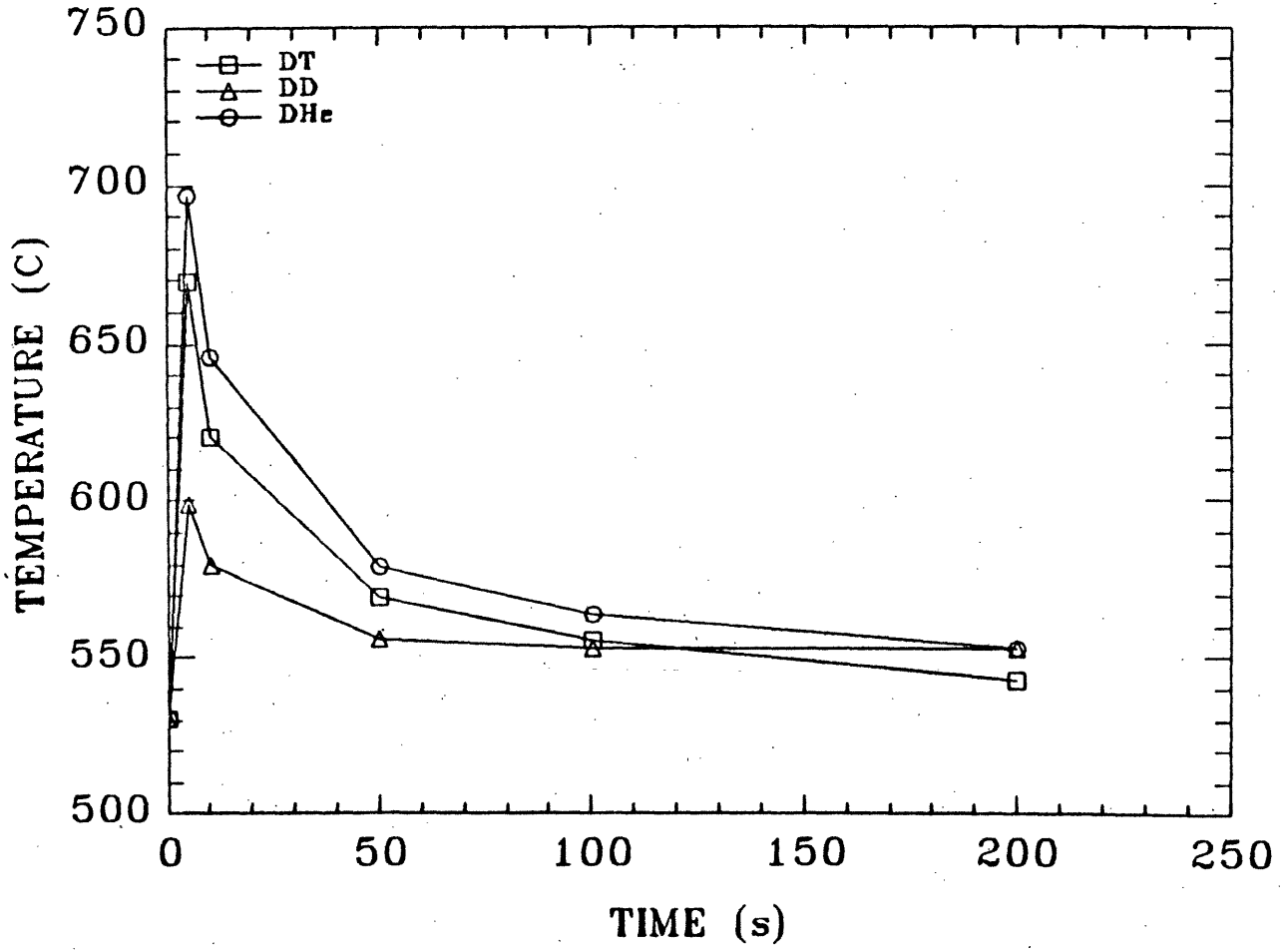

FIGURE 6.4: FIRST WALL TEMPERATURE DURING LOCA

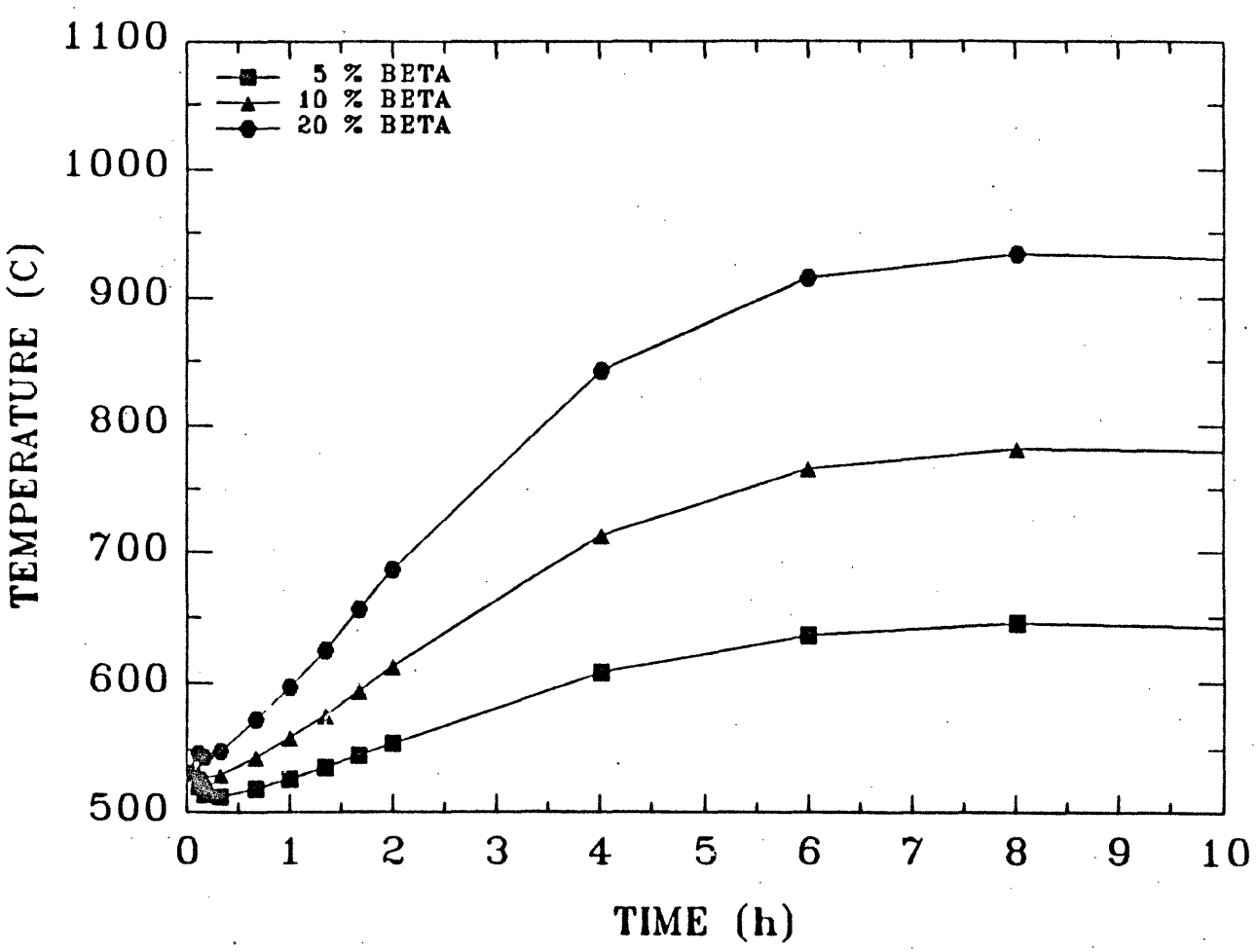

FIGURE 6.5: FIRST WALL TEMPERATURE DURING LOCA
DD DESIGNS

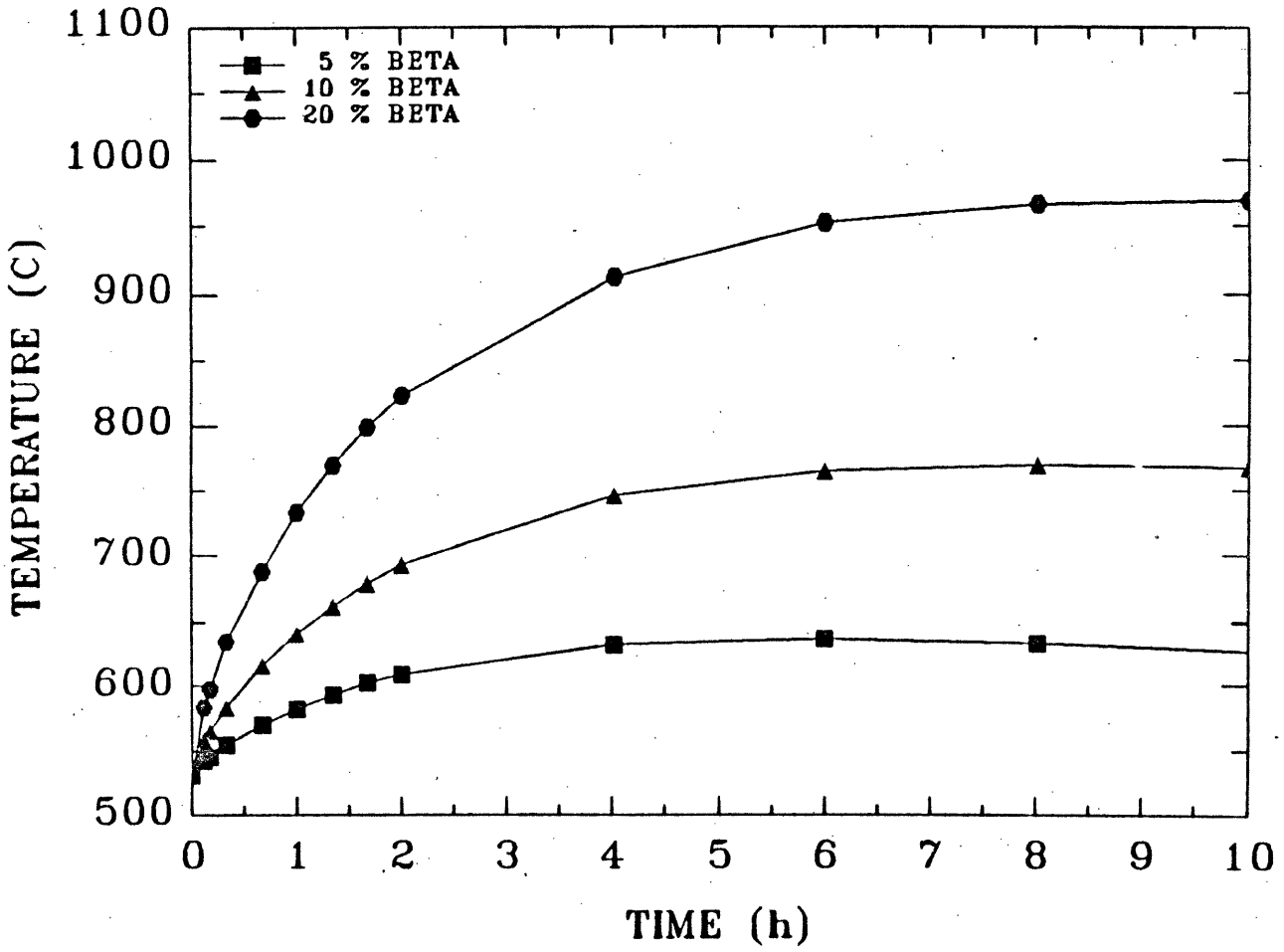

FIGURE 6.6: FIRST WALL TEMPERATURE DURING LOCA
10 % BETA DESIGNS

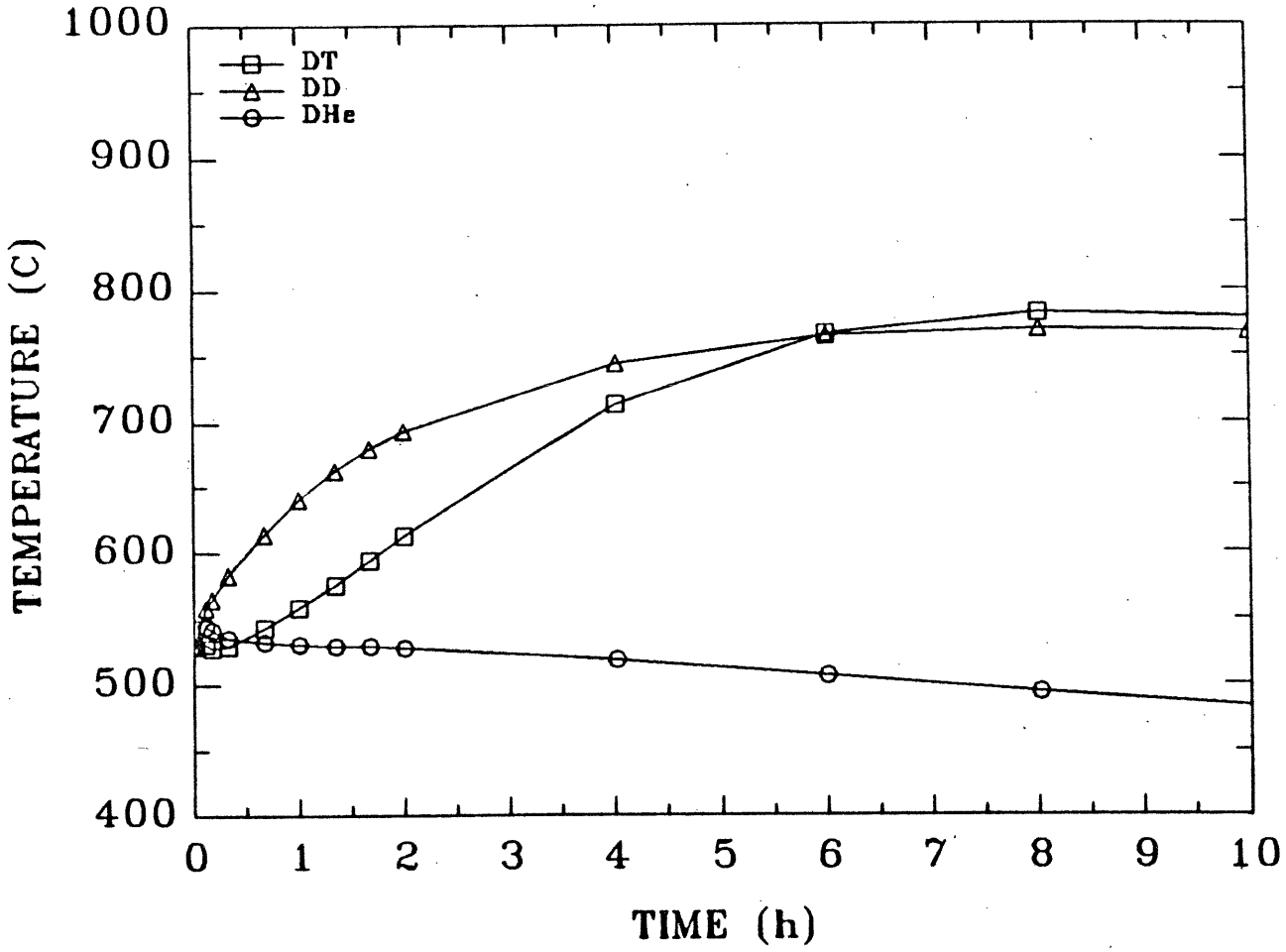

from the critical first wall area. Figures 6.7 and 6.8 show the blanket temperature as a function of position midway through the transient, for the various fuel cycles and values of beta. As can be seen, the DT blanket temperature profile has flattened, while a gradient still exists in the advanced fuel blankets. The decay heat density of the DD blankets is somewhat greater than that of the DT blankets (see table 5.11). However, the heat capacity per unit volume is greater for DD by about the same factor. Thus, the expected temperature rise would be roughly the same in both cases.

Given the temperature of the first wall as a function of time and the mobilization rates of the elements as a function of temperature, the quantities of each isotope released during the 10 hour transient can be determined. These are given in table 6.4 for each fuel cycle. No releases were assumed for temperatures below 600 °C. The quantities of nuclides released served as input to computer codes used to evaluate onsite and offsite health impacts of the event. These impacts are discussed in the next section.

The second major impact of the LOCA will be that of structural damage. This can be estimated by examining the combined effects of the elevated temperature and the presence of a stress on the first wall. The expected structural impact as described by the fraction of the rupture lifetime consumed is given in table 6.5. The residual stress and creep rate are also given. It can be seen that in all cases, a significant margin exists between the condition of the torus at the end of the transient and the point where rupture would occur. This is largely a consequence of the rapid relaxation of the stress. Thus, it appears that no further damage to the vacuum vessel other than the initial breach will result. An attempt to quantify the economic impact of this structural damage for all designs is made in section 4.3.5.

FIGURE 6.7:
BLANKET RESPONSES MIDWAY THROUGH LOCA
5 % AND 20 % BETA DT AND DD DESIGNS

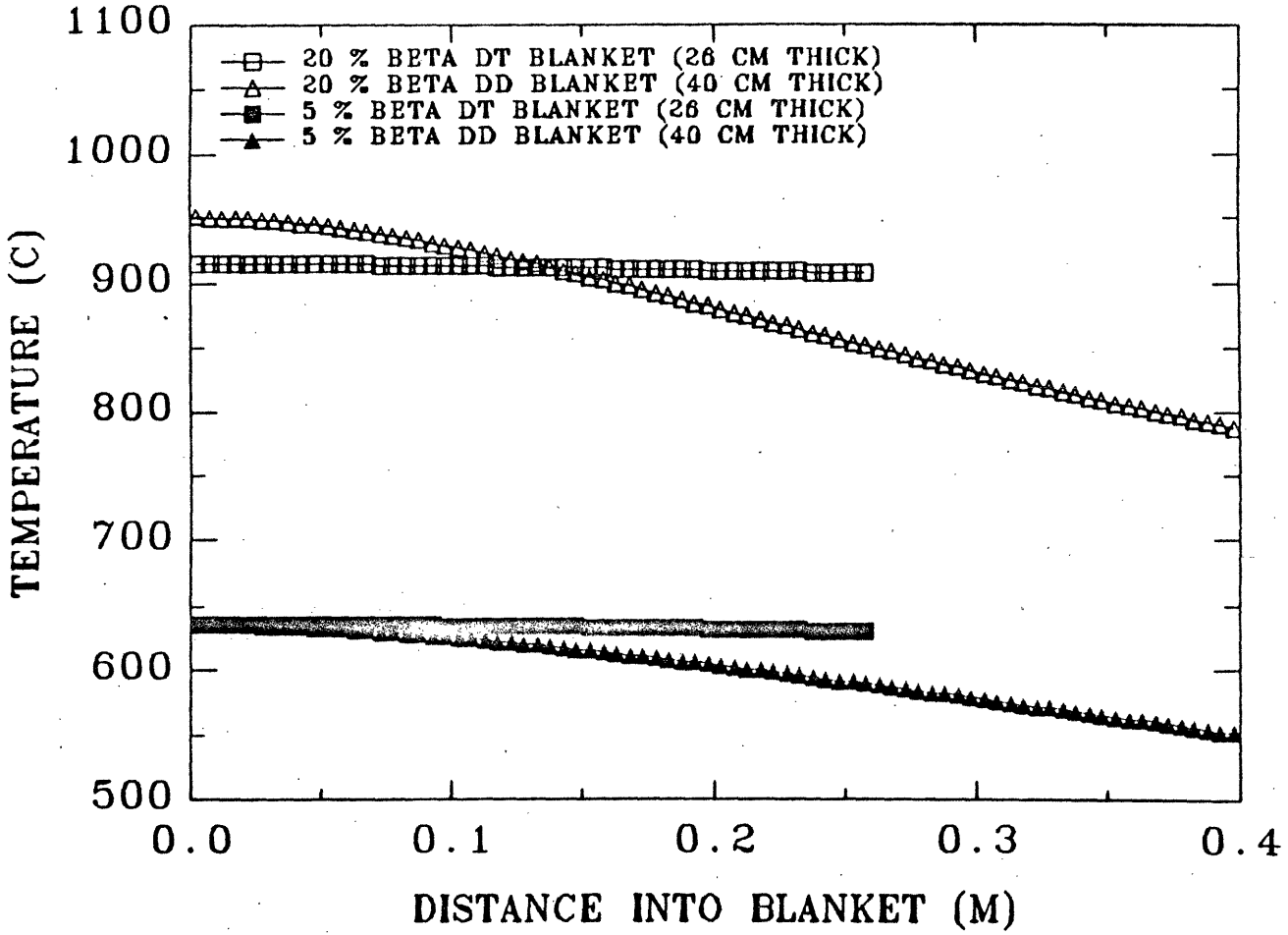

FIGURE 6.8:
BLANKET RESPONSES MIDWAY THROUGH LOCA
10 % BETA DESIGNS

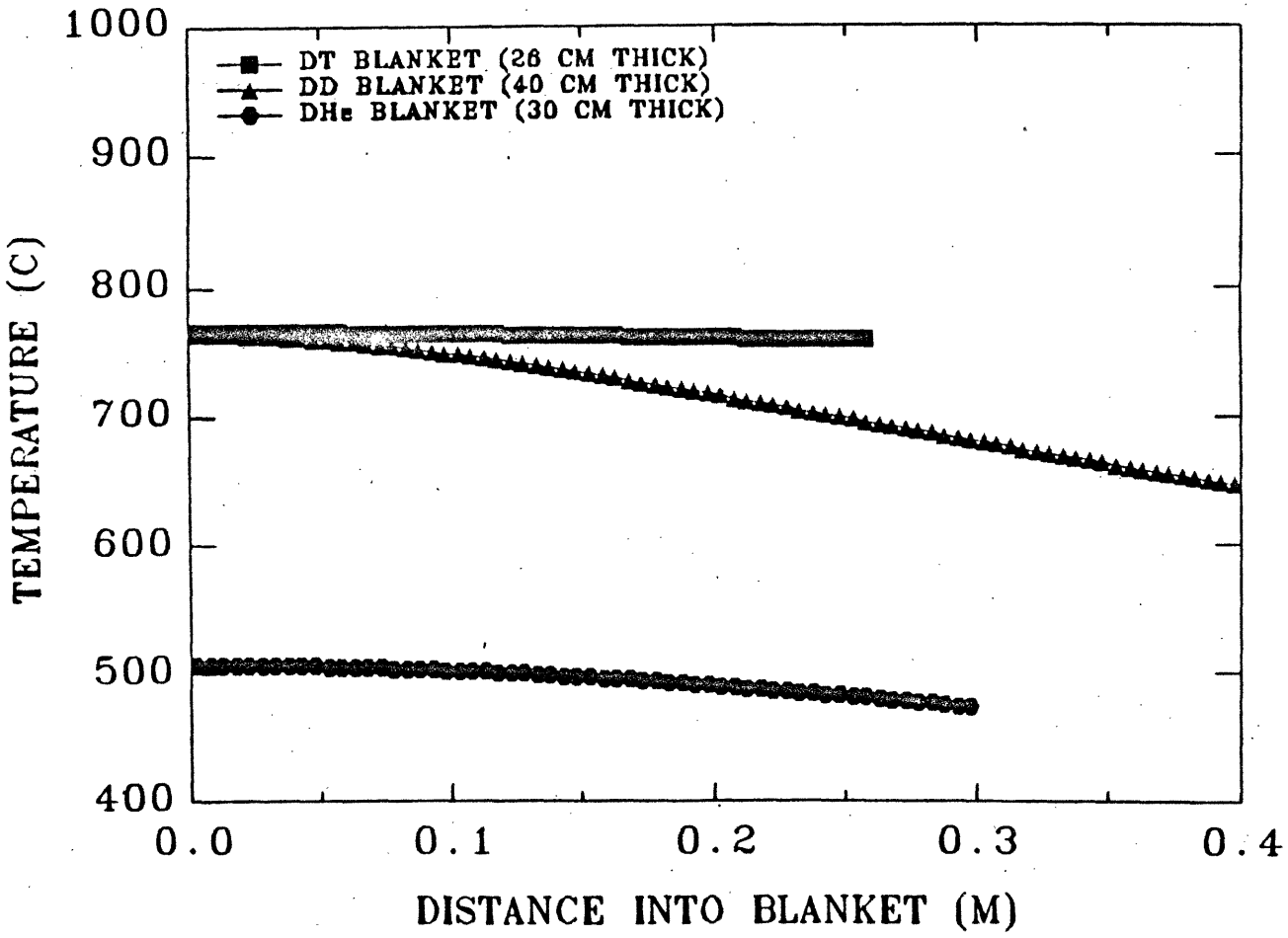

Table 6.4: Nuclides Released Subsequent to the LOCA

	DT			DD			DHe
	5 %	10 %	20 %	5 %	10 %	20 %	10 %
Peak Temperature During Plasma Heat Phase (K)	631	670	712	567	599	646	696
Peak Temperature During Transient (K)	645	781	934	636	769	969	696
Time of Peak Temperature (h)	8	8	8	6	8	10	0.00139
Isotopes Released:							
Total† (Ci)	4,700	8,600	12,200	6,320	8,840	12,500	2.0
P-32	3,540	6,100	7,920	3,230	4,660	6,020	0.90
P-33	36.3	62.7	81.3	31.7	53	68.4	1.03×10^{-2}
Ti-51	42.0	68.3	94.4	49.2	69.2	88.8	4.58×10^{-2}
V-48	0.39	1.26	3.65	0.34	0.99	3.04	1.17×10^{-4}
V-49	9.61	33.6	83.0	8.33	24.8	73.9	2.88×10^{-3}
V-52	65.4	229	575	60.2	185	538	2.11×10^{-2}
V-53	4.26	14.3	39.2	3.56	9.74	34.2	1.09×10^{-3}

† does not include any release of tritium; rapid pressurization of the torus will minimize permeation of tritium out of the structure

	DT			DD			DHe
	5 %	10 %	20 %	5 %	10 %	20 %	10 %
Cr-49	0.30	1.04	2.16	0.24	0.68	1.74	6.50×10^{-5}
Cr-51	54.2	188	454	41.9	125	351	1.17×10^{-2}
Cr-55	2.21	6.92	17.2	1.18	3.70	10.7	2.92×10^{-4}
Mn-52	0.38	0.61	0.76	0.12	0.24	0.29	1.06×10^{-4}
Mn-52m	0.33	0.53	0.66	0.10	0.21	0.25	9.19×10^{-5}
Mn-54	88.4	120	156	99.9	101	162	4.22×10^{-2}
Mn-56	220	341	424	321	397	503	0.15
Mn-57	3.09	4.23	6.01	3.89	3.32	6.92	1.40×10^{-3}
Fe-53	0.14	0.47	1.09	0.10	0.28	0.78	2.68×10^{-5}
Fe-55	221	679	1,360	188	514	1,270	5.03×10^{-2}
Fe-59	0.09	0.30	0.74	0.59	1.57	4.86	1.62×10^{-4}
Ni-57	0.10	0.35	0.71	8.38×10^{-2}	0.22	0.61	2.04×10^{-5}
Ni-59	3.15×10^{-5}	7.84×10^{-5}	1.43×10^{-4}	2.00×10^{-4}	2.70×10^{-4}	5.20×10^{-4}	5.07×10^{-8}
Ni-63	2.59×10^{-3}	6.80×10^{-3}	1.20×10^{-2}	1.70×10^{-2}	2.70×10^{-2}	5.37×10^{-2}	4.50×10^{-6}
Ni-65	1.10×10^{-3}	3.76×10^{-3}	8.96×10^{-3}	7.20×10^{-3}	1.92×10^{-2}	5.95×10^{-2}	2.00×10^{-6}
Mo-91	2.50×10^{-5}	6.12×10^{-3}	0.28	2.00×10^{-5}	4.20×10^{-3}	0.41	1.02×10^{-8}
Mo-93	2.61×10^{-7}	3.80×10^{-5}	1.58×10^{-3}	2.00×10^{-6}	2.20×10^{-4}	1.83×10^{-2}	1.04×10^{-9}
Mo-93m	4.00×10^{-4}	7.24×10^{-3}	0.46	2.70×10^{-4}	5.13×10^{-2}	7.43	1.27×10^{-7}
Mo-99	4.20×10^{-4}	9.25×10^{-2}	4.67	1.20×10^{-3}	0.26	30.9	6.98×10^{-7}
Mo-101	6.40×10^{-5}	1.43×10^{-2}	0.72	3.60×10^{-4}	7.93×10^{-2}	9.07	2.22×10^{-7}
W-181	147	290	411	29.6	19.6	11.7	1.66×10^{-2}
W-185	186	372	536	800	1,400	2,150	0.15
W-187	39.4	79.3	111	1,450	1,270	1,130	0.54

Table 6.5: Thermal Effects on First Wall During LOCA

Design	Residual Stress† (MPa)	Residual Strain Rate (h^{-1})	T_{max} (°C)	Fraction of Rupture Consumed
5 % beta DT	1.72	2.43×10^{-10}	645	5.82×10^{-6}
10 % beta DT	0.59	6.49×10^{-11}	781	2.37×10^{-6}
20 % beta DT	0.27	2.90×10^{-11}	934	7.79×10^{-5}
5 % beta DD	2.25	~ 0	636	6.44×10^{-6}
10 % beta DD	0.50	4.78×10^{-11}	769	2.31×10^{-6}
20 % beta DD	0.21	2.08×10^{-11}	969	2.34×10^{-4}
10 % beta DHe	38.7	~ 0	696	3.78×10^{-6}

† initial thermal stress at beginning of accident assumed to be $\sim$ 70 MPa

6.3.4 Health Effects due to the Loss of Coolant Accident

The amount of the first wall that is mobilized and transported out of the reactor will determine the health consequences of this accident. In this assessment, it was assumed that all of the material that was volatilized from the first wall escapes from the vacuum vessel and enters the reactor hall. Three scenarios were envisioned to give the range of possible onsite and offsite health consequences. Case (1) represents the anticipated course of action subsequent to the accident. Here, it was assumed that the radioactivity was contained within the reactor building until the accident was over and further mobilization has ceased. At this time, it was assumed that the ventilation system was re-activated and some release to the environment begins. It was also assumed that at 9 hours 45 minutes after the accident had occurred, 3 workers entered the reactor hall for 10 minutes to reestablish cooling of the torus (e.g. forced convection). As many of the operations as possible involved in reestablishing cooling will be performed remotely prior to this. However, it is expected that some contact assistance (a minimal amount) will be needed. Preceeding the time of worker entry, plant management would be assessing the situation i.e. determining the cause of the accident, estimating the consequences and devising a plan to minimize releases and occupational exposures. After worker entry, it was assumed that within 5 minutes, the situation was brought under control. At this time, it was assumed that plant management would decide to vent the building atmosphere to the environment at the normal ventilation rate. Workers were allowed to reenter the torus hall to begin clean up and repair operations once the dose rate fell to 1.25 rem/h. This would allow an unprotected worker to remain in the reactor building for 4 hours without exceeding his annual dose limit of 5 rem. These doses can be reduced through the use of protective equipment. Also, if there is a large labor pool to draw from, the dose can be spread out amongst workers, minimizing the individual exposures.

The other two scenarios examined served to bracket the maximum anticipated onsite and offsite effects. Case (2) assumed that the ventilation system was not re-activated after that accident so that all radioactivity was contained within the reactor building with no release to the environment. As will be shown, this results in high dose rates in the reactor hall over extended periods of time. The third scenario assumed immediate release of all radioactivity mobilized during the accident to the environment. This case would represent the worst offsite effects of the accident.

Onsite doses were assessed by following the decay of the released radionuclides (and build up of any radioactive daughters) from the beginning of the accident and during the time of worker entry into the reactor hall. External exposures are related to the activity concentration of the nuclide of concern through dose conversion factors. The total external dose due to exposure to this nuclide can be found from the dose rate if the time of exposure is known. External dose conversion factors are given in units of $\frac{\text{rem/h}}{\text{Ci/m}^3}$. The internal dose is related to the total quantity of a nuclide inhaled. To obtain the total dose incurred, knowledge of the breathing rate, airborne nuclide concentration and exposure time are needed. Internal dose conversion factors are given in units of $\frac{\text{rem}}{\text{Ci}}$. Fetter [6.17] gives whole body dose conversion factors for internal and external exposures as part of his FUSEDOSE package. Additional nuclides have been added to his library since the publication of the initial FUSEDOSE documentation (see appendix G). These factors have been used in determining doses incurred for this study. Knowing the time varying activity level of the nuclides, one can obtain the dose incurred by using the dose conversion factors and integrating over the exposure time. A breathing rate of 3.5×10^{-4} m^3/s was assumed. Additionally, the radionuclides in the reactor hall were taken to reside entirely in the air at a uniform concentration (i.e. no reduction in airborne concentrations was made to account for surface adsorption/absorption of radionuclides). The OCCDOSE code was written to follow the time variation of radionuclide activity in the reactor hall (see appendix G). The code calculates the total integrated dose to workers in the reactor hall subsequent to the release for a

specified exposure time.

Occupational exposures will result from decontamination and repair activities subsequent to the accident. Decontamination was assumed to begin as soon as the reactor hall dose rate fell below 1.25 rem/h. The duration of clean up was estimated from the clean up efforts performed at TMI. An appropriate estimate was obtained from the TMI clean up time by scaling with the total quantity of activity released (see section 6.3.5.2.3). After completion of the decontamination program, repair procedures began. It was assumed that the decontamination program removed surface adsorbed radionuclides only, and the airborne activity was unaffected by this effort. Hence, the dose rates encountered during repair would be reduced from those during decontamination by an amount determined only by the decay of the radionuclides and the building ventilation rate. Damaged equipment to be repaired includes only the single first wall/blanket module (not including breeder) which was damaged upon breaching the vacuum vessel. Single module repair/replacement time estimates were based on the times given in table 5.13 for blanket changeouts during maintenance outages (different fractions of the blanket are replaced annually for each design, depending on the blanket lifetime; a total of 20 modules comprise the blanket). The expected occupational exposure times for decontamination and repair for each of the fuel cycles for case (1) are given in table 6.6. Doses were evaluated using the OCCDOSE code, knowing the start and end times for decontamination and repair tasks (note that the unprotected worker doses are given). The 10 minute exposure of three people (0.5 man-hour) who entered to reestablish cooling of the first wall is also included. Onsite doses were not evaluated for case (2), where all radioactivity is contained in the reactor building. However, the dose rate after 2 years is indicated in table 6.6. As can be seen, the dose rate in some cases is still too high to allow worker entry for a useful amount of time. It is unlikely that this course of action will be chosen because of the long outage time (and hence, very large replacement power costs).

Table 6.6: Occupational Exposures Due to LOCA†

Task	DT 5 %	DT 10 %	DT 20 %	DD 5 %	DD 10 %	DD 20 %	DHe 10 %
Reestablish Cooling:							
Crew Size	3	3	3	3	3	3	3
Exposure Time (man-h)	0.5	0.5	0.5	0.5	0.5	0.5	0.5
Initial Dose Rate (rem/h)	40.9	70.8	93.1	39.1	55.9	74.0	0.011
Cumulative Exposure (man-rem)	20.4	35.4	46.6	19.6	28.0	37.0	0.0056
Clean Up:							
Crew Size	12	12	12	12	12	12	12
Exposure Time (man-h)	583	1074	1535	790	1105	1560	0
Initial Dose Rate (rem/h)	1.27	1.31	1.34	1.19	1.32	1.37	-
Cumulative Exposure (man-rem):							
Clean up	155	178	184	155	180	189	0
Waste Handling	26	29	30	26	30	31	0
Repair/Replacement:							
Crew Size	6	6	6	6	6	6	6
Exposure Time (man-h)	198	192	187	237	198	194	147
Initial Dose Rate (mrem/h)	128	22.9	4.44	57.2	20.8	4.17	11.2
Cumulative Exposure (man-rem)	13.5	2.4	0.45	6.8	2.2	0.43	1.02
Total (man-rem):	215	245	261	207	240	257	1.53
Dose Rate in Reactor Hall after 2 yr with no purge (rem/h) (case 2)	0.52	1.22	2.24	0.5	0.95	2.13	~ 0.0002

† release of activity to the environment begins after 10 hours for all but last row of the table, where no release to the environment occurs (case 2)

Public doses were assessed for cases (1) and (3). The release for case (1) was assumed to begin at the 10 h mark. The total quantity of radioactivity in the reactor hall at this time was assumed to be vented over a 100 h period at a rate equal to the normal ventilation rate of the reactor building (one air change per day or 4.6 m^3/s). All nuclides were assumed to be uniformly mixed in the reactor hall atmosphere prior to release. Decay during the release period was considered. For case (3), immediate release to the environment upon volatilization was assumed.

Offsite health effects were evaluated using the accident hazard analysis code (DOSE) included in the FUSEDOSE methodology developed by Fetter [6.17] †. The DOSE code applies the Gaussian plume dispersion model to a specified release of radionuclides under a specified set of meteorological conditions. The whole body doses to an individual downwind are calculated after consideration of radioactive decay, production of daughter products, plume rise, inversion layers, building wake effects, plume deposition and plume depletion. The code calculates doses for two exposure scenarios: (1) the acute dose to an adult, standing in the open performing light activity during the plume passage, who leaves the area afterwards; (2) the chronic dose to an adult who stays in the contaminated area for a specified length of time. Two dose integration times are considered for the acute exposure scenario: (1) the 50-year dose commitment resulting from the initial exposure, or the total dose during the lifetime of the individual, and (2) the critical dose, defined in reference [6.18] as the dose in the first seven days after the accident plus half the dose in the next 23 days. For the chronic exposure scenario, only the 50-year dose commitment is calculated. In the acute exposure scenario, inhalation of and direct radiation from contaminated air during the plume passage, and direct radiation from radionuclides deposited on the ground are considered. The calculation of the chronic dose considers the above mentioned pathways as well as inhalation of resuspended radionuclides. Exposures due to radionuclides deposited directly on

† Some new nuclides have been added to the libraries since the original documentation was published (see appendix G).

skin or clothes, or on vegetables that are subsequently consumed, are not included. Casualties‡ estimated by the DOSE code include the number of early illnesses and deaths and late cancer fatalities. Sterility, birth defects and genetic effects are not considered.

Input to DOSE includes the inventory of nuclides to be released at t=0, times of start and finish of the release, release height, initial plume size (i.e. size of building from which the release takes place) and weather conditions. The duration of the release determines the length of the plume and therefore the initial dilution of the activity in the direction of the wind. The atmospheric conditions during the release determine the dispersal of radioactivity. They include stability, plume centerline height, wind speed, deposition velocity and inversion layer height. Evacuation is not considered, so the population density is constant with time. The conditions assumed for the present study are summarized in table 6.7.

The results for the public health effects for cases (1) and (3) are given in table 6.8. The maximum dose rate at the site boundary (1 km) occurs at the onset of cloud passage. Because the release was assumed to take place over the same period of time (100 h for case (1) and 10 h for case (3)), dilution would occur to the same degree for each fuel cycle. Thus, the site boundary dose rate is a direct reflection of the radioactivity mobilized during the accident. For the average weather conditions assumed here, the critical, 50 year and chronic doses to an individual residing at the site boundary during plume passage are as given in table 6.8. As can be seen, the resulting doses are not large, being far below the NRC emergency guideline of 25 rem. In fact, the chronic dose to an individual, which considers effects over a 50 year period, only marginally exceeds the acceptable annual dose of 500 mrem for

‡ The dose response data used in FUSEDOSE were obtained from the Reactor Safety Study [6.18]: assuming supportive medical treatment, 200 rem would produce radiation sickness in 50 % of the exposed population; 510 rem would be lethal to 50 % of the exposed population after 60 days.

Table 6.7: Weather Conditions Assumed During LOCA

Stability Class:	D (neutral)
Release Height:	0 m (ground release)
Wind Velocity:	5 $\frac{m}{s}$
Deposition Velocity:	0.01 $\frac{m}{s}$
Height of Inversion Layer:	250 m
σ_y:	100 m (building y-dimension)
σ_z:	50 m (building z-dimension)

Table 6.8: Offsite Health Impacts of LOCA for Scenarios (1) and (3)

Effect	DT 5 %	DT 10 %	DT 20 %	DD 5 %	DD 10 %	DD 20 %	DHe 10 %
Maximum Dose Rate at Site Boundary (mrem/h):							
(1)*	0.31	0.53	0.70	0.38	0.48	0.62	1.2×10^{-4}
(3)†	2.37	4.83	6.36	2.98	4.08	5.32	9.04×10^{-4}
Individual dose at site boundary: (mrem)							
Critical:							
(1)	17	29	38	22	27	34	0.007
(3)	17	29	38	18	24	31	0.005
50 year:							
(1)	26	45	60	31	40	52	0.009
(3)	27	47	62	27	38	50	0.008
Chronic:							
(1)	360	510	690	400	400	640	0.17
(3)	370	520	690	410	420	680	0.17
Population Dose◇ (man-mrem):							
Critical:							
(1)	68	110	150	81	100	130	0.025
(3)	66	110	150	67	92	120	0.020
50 year:							
(1)	110	180	240	120	150	200	0.035
(3)	110	180	240	110	150	200	0.030
Chronic:							
(1)	1600	2300	3100	1700	1800	2900	0.72
(3)	1600	2300	3100	1800	1900	3000	0.74
Cancer Fatalities:							
(1)	0.20	0.28	0.38	0.22	0.22	0.36	8.9×10^{-5}
(3)	0.21	0.29	0.39	0.22	0.23	0.37	9.2×10^{-5}

* release occurs 10 h after accident initiation; release duration is 100 h

† immediate release occurs; release duration is 10 h

◇ population density of 100 persons/km^2

the worst case (high beta DT). Population doses were based on a density of 100 persons/km^2. These are also not large for the accident being considered here. There are no early deaths or illnesses, and less than one late cancer fatality expected in all cases. The time at which the release occurs (t=10 h for case (1) and t=0 for case (3)) and the release duration (100 h for case (1) and 10 h for case (3)) do not have a large impact on the accident consequences.

6.3.5 Economic Consequences of the Loss of Coolant Accident

Associated with fusion reactor accidents is a range of economic consequences and a certain level of economic risk. Generally, a risk spectrum in which low cost - low severity events are relatively frequent and high cost - high severity events are relatively infrequent can be envisioned. A recent study [6.19] categorized the economic consequences over the spectrum of possible events according to onsite and offsite impacts. These may range from minor repair and decontamination costs to significant costs associated with replacement of major plant components, replacement power and offsite evacuation and land decontamination costs. The cost components expected to contribute to the economic risk associated with the loss of coolant accident being considered here are outlined in this section. Estimates of the economic impact of the LOCA for each of the reactor designs are given. Evaluation is based on the methodology outlined in reference [6.19].

6.3.5.1 Onsite Economic Consequences

Onsite economic consequences are those cost elements which either occur at onsite locations or directly affect the plant licensee, the fusion power industry or the electric utility. These may include replacement power costs, plant decontamination costs, plant repair costs, plant capital costs, early decommissioning costs, plant

worker health impact costs, fusion power industry costs, electric utility business costs and litigation costs. It is expected that replacement power, decontamination, plant repair and health impact costs will contribute to the onsite costs due to the LOCA being studied here. These are discussed and estimates are made below. The other cost elements either don't apply or are difficult to quantify, and are not evaluated here. A discussion of these components can be found in reference [6.19].

6.3.5.1.1 Replacement Power

A significant contributor to onsite costs of reactor accidents is that of replacement power due to plant outage time. A simple model developed for fission plant outages can be used to estimate the replacement power costs [6.20]:

$$C_{RP} = \left(\frac{G\ C}{C'}\right) \int_0^{t_{out}} F_0\ e^{-rt}\ dt \tag{6.3}$$

where

C_{RP} = present value of the replacement power cost over the outage period ($)

G = electrical generation rating of the reactor (MWe)

C = actual capacity factor of the plant had the outage not occurred

C' = average capacity factor of the plant, obtained from operating data

t_{out} = outage duration (yrs)

F_0 = unit production cost increase of outage ($\frac{\$}{MW\ yr}$)

r = real discount rate

The model assumes that the option to purchase power during the outage is chosen and that no other methods for compensating for the lost generating capacity are implemented. Replacement power cost estimates for each design are given in table 6.11. The values assume a unit power production cost of $0.21 \text{x} 10^6 \frac{\$}{\text{MWe yr}}$ (from [6.20] updated to current dollars), corresponding to the expected mix of oil-fired and non-economy power sources for mid United States. The outage time runs from accident initiation until all clean up and repair operations have been completed.

6.3.5.1.2 Decontamination Costs

Decontamination and clean up operations will remove sources of potential radiation exposure posing risks to the health and safety of station workers and the public. Sources of radiation exist as airborne and surface contamination, as well as the damaged reactor. The clean up activities include building and equipment decontamination, treatment of radioactive liquids and packaging, handling, storage and disposal of radioactive wastes. Some general considerations are outlined here.

Following a radiation accident, radioactive contaminants may be transported or spread to areas other than locations immediately affected by the release. Airborne radioactivity may be spread via ventilation systems; liquid-borne radioactivity may leave the accident site as surface runoff. Additional mechanisms of spreading contamination include resuspension of radioactive particulates that have settled on floors and surfaces, transfer to the shoes, clothing or skin of personnel and transport to uncontaminated areas, and movement of contaminated equipment to uncontaminated areas. The control of the spread of radioactivity can greatly reduce subsequent decontamination efforts. The control problem can be minimized by using a minimum amount of equipment. Clean equipment will reduce contamination pick up as will minimizing equipment contact with contaminated surfaces (i.e. equipment should never be placed directly on the ground). Decontamination

of vehicles immediately after use can be accomplished by water hosing and brushing or vacuum cleaning. Procedures involving personnel should be well thought out beforehand. The use of anticontamination clothing and respiratory devices, and the establishment of proper area controls will effectively reduce the problems of personnel contamination and aid in preventing the spread of contamination to radiologically clean areas. Decontamination of persons subsequent to working in contaminated areas prevents further inhalation, ingestion or absorption of radioactivity through the skin. Procedures include removal of contaminated clothing and showering, with special effort given to scrubbing of skin and hair.

In highly contaminated areas, heavy-duty close-weave cotton-twill single-piece coveralls that cover all but the feet, hands and head can be worn by decontamination workers. These are effective in preventing most of the contamination from penetrating to the underclothing and skin. A second pair of coveralls is usually worn over the first pair to allow removal of highly contaminated clothing before preceeding to a primary decontamination facility. Plastic suits may be worn instead of the coveralls. These afford good protection from water and many gaseous toxic agents. Expendable shoes should be worn in highly contaminated areas; shoe covers may be sufficient in areas of low-level contamination. A surgeon's cap can be worn to minimize contamination of the hair and scalp. In grossly contaminated areas or areas with a great deal of airborne contamination, plastic or cloth hoods are worn. Gloves of cotton, canvas, leather or plastic are used, the type depending on the task and the level of contamination. To protect against radioactive air contaminants, present as either gases or particulates, respiratory protection may be needed. Their use should be minimized because they subject the wearer to additional stress and increase the risk of injury by impairing vision, freedom of motion and ability to communicate. Protection factors for respirators range from 10, for a facepiece with a half-mask and air-line respirator to 10,000 for a full facepiece with a self-contained breathing apparatus [6.21]. Selection of the appropriate respirator is influenced by the physical, chemical and radiological hazards present in the accident area, as well

as the nature of the task.

Decontamination efforts for buildings, equipment and other surfaces following an accident should be undertaken after considering whether the benefits would be sufficient to justify further exposure to personnel. Surface decontamination methods are summarized in table 6.9. For liquid contaminants, the surface to be decontaminated should be kept moist. Leaching several times with a minimum amount of a suitable reagent can provide decontamination factors of at least 100 on most non-porous surfaces. For dry powdered contaminants on porous surfaces, it is more efficient to try to remove as much contamination as possible by sweeping or vacuuming, provided this will not produce an inhalation hazard or spread contamination to unwanted areas. These methods require workers to wear protection clothing and respirators. The use of adhesive tapes or strippable paints can be effective for decontamination without causing air contamination or the spread of contamination to other areas. Wet methods on porous surfaces, such as concrete, will probably be effective only on the very loose contamination on the surface. Strong agents and excessive scrubbing may be effective to a certain extent, but may also tend to wash the contaminant further into the porous material. Removal of surface layers by abrasion or erosion may be effective in complete decontamination of porous materials. Coating of porous surfaces with varnished, lacquers or paints may increase future decontaminability by three or four orders of magnitude.

Because a release of radionuclides into the reactor hall occurs as a consequence of the LOCA being considered here, there is a need for decontamination subsequent to the accident. Costs incurred due to the decontamination effort will include the cost of removal and disposal of radioactive materials, decontamination materials and equipment operating costs and labor costs. Health detriment costs due to radiation exposure will also result; these are evaluated in section 6.3.5.1.4. It would be advantageous to implement and complete the clean up program in as short a time as possible. Regulatory concerns and financing issues may delay the program's commencement (these impedements to the clean up program were not considered

Table 6.9: Summary of Surface Decontamination Methods [6.22]

METHOD	SURFACES	ACTION	TECHNIQUE	ADVANTAGES	DISADVANTAGES
VACUUM CLEANING	Dry contaminated surfaces.	Removal of contaminated dust by suction.	Use conventional vacuum technique with efficient filter.	Good on dry porous surfaces. Avoids water reactions.	All dust must be filtered out of exhaust. Machine is contaminated.
WATER	All nonporous surfaces (· etal, paint, plastic, etc.). Not suitable for porous materials, such as wood, concrete, canvas, etc.	Solution and erosion.	Use gross decontamination employing water shot from high pressure hoses. Work from top to bottom to avoid recontamination; from upwind to avoid spray; 15 to 20 feet from the surface is the optimum operating distance. Vertical surface should be hosed at an incident angle of 30 to 45 degrees. Determine cleaning rate experimentally if possible. Otherwise, use a rate of 4 square feet per minute.	All water equipment may be utilized. Allows operation to be carried out from a distance. Contamination may be reduced by 50%. Water solutions of other decontaminating agents may utilize water equipment.	Drainage must be controlled. Porous materials will absorb contaminants. Oiled surfaces cannot be decontaminated. Not applicable on dry contaminated surfaces (use vacuum). Spray will be contaminated.
STEAM	Nonporous surfaces (especially painted or oiled surfaces).	Solution and erosion.	Work from top to bottom and from upwind. Clean surface at a rate of 4 square feet per minute. The cleaning efficiency of steam may be greatly increased by using detergents.	Steam reduces contamination by approximately 90% on painted surfaces.	Steam subject to same limitations as water. Spray hazard makes the wearing of waterproof outfits necessary
DETERGENTS	Nonporous surfaces (especially industrial film).	Emulsifying agent. Wetting agent.	Rub surface for 1 minute and wipe with dry rag. Use clean surface of the rag for each application. A powered rotary brush (with pressure feed) is more efficient. Moist application is all that is desired. Solution should not be allowed to drip onto other surfaces. Solution may be applied from a distance with a pressure proportioner.	Dissolves industrial film which holds contamination. Contamination may be reduced by 90%.	May require contact with surface. Mild method not efficient on long-standing contamination.
COMPLEXING AGENTS OXALATES CARBONATES CITRATES	Nonporous surfaces (especially unweathered surfaces; i.e., no rust or calcareous growth).	Forms soluble complexes with contaminated material.	Solution should contain 3% (by weight) of agent. Spray surface with solution. Keep surface moist for 30 minutes by spraying with solution periodically. After allotted time, flush material off with water. Agents may be used on vertical and overhead surfaces by employing mechanical foam.	Holds contamination in solution. Contamination (unweathered surfaces) reduced 75% in 4 minutes. Easily stored, carbonates and citrates are non-toxic, non-corrosive.	Requires application from 5 to 30 minutes. Little penetrating power; of small value on weathered surfaces.
ORGANIC SOLVENTS	Nonporous surfaces (greasy or waxed surfaces, paint or plastic finishes, etc.).	Solution of organic materials (oil, paint, etc.).	Entire unit may be immersed in solvent. Also may be applied by standard wiping procedures. (See Detergents.)	Quick dissolving action. Recovery of solvent possible by distillation.	Requires good ventilation and fire precautions. Toxic to personnel. Material bulky.

METHOD	SURFACES	ACTION	TECHNIQUE	ADVANTAGES	DISADVANTAGES
INORGANIC ACIDS	Metal surfaces, especially those with porous deposits (i.e., rust or calcareous growth). Circulatory pipe systems.	Strong dissolving power on metals and porous deposits.	Dip-bath technique is advisable for movable items. Acid should be kept at a concentration of from 1 to 2 Normal (9 to 18% hydrochloric, 3 to 6% sulfuric acid). Reaction time on weathered surfaces should be 1 hour. Pipe systems, 2 to 4 hours. Afterwards, surface should be neutralized and rinsed.	Corrosive action on metal and porous deposits. Corrosive action may be moderated by addition of corrosion inhibitors to solution.	Good ventilation required because of toxicity and explosive gases. Acid mixtures should not be heated. Possibility of excessive corrosion if used without inhibitors. Sulfuric acid not effective on calcareous deposits.
ACID MIXTURES HYDROCHLORIC SULPHURIC ACETIC ACID CITRIC ACID ACETATES CITRATES	Nonporous surfaces (especially those having porous deposits). Circulatory pipe systems.	Dissolving action.	Applied in same manner as inorganic acids. Mixture consists of: 0.1 gal. hydrochloric, 0.2 lb. sodium acetate, 1.0 gal. of water.	Dissolving action may reduce contamination 90% in 1 hour (unweathered surfaces).	Weathered surfaces may require prolonged treatment.
CAUSTICS LYE (SODIUM HYDROXIDE) CALCIUM HYDROXIDE POTASSIUM HYDROXIDE	Painted surfaces (horizontal).	Dissolving power softens paint (harsh method).	Lye paint-removal mixture: 10 gal. water, 4 lb. lye, 6 lb. boiler compound, 0.75 lb. cornstarch. Allow lye paint-remover solution to remain on surface until paint is softened to the point where it may be washed off with water. Remove remaining paint with long-handled scrapers.	Minimum contact with contaminated surfaces. Easily stored.	Personnel danger (painful burns). Reaction slow; thus, it is not efficient on vertical surfaces or overheads. Should not be used on aluminum or magnesium. Method is difficult on vertical or overhead surfaces.
TRI SODIUM PHOSPHATE	Painted surfaces (vertical, overhead).	Dissolving power (mild method).	Hot 10% solution applied by standard wiping technique. (See Detergents.) One-minute rub.	Reduces activity to tolerance in one or two applications.	Destructive effect on paint. Not to be used on aluminum or magnesium.
ABRASION	Nonporous surfaces.	Surface removal.	Use conventional procedures, but keep surface damp to avoid dust hazard.	Activity may be reduced to as low a level as may be desired.	Impracticable for porous surfaces because of surface penetration by moisture.
WET SANDBLASTING	Nonporous surfaces.		Wet sandblasting is most practical on large surface areas. Collect used abrasive.		Contamination spread over area must be recovered.
VACUUM BLASTING	Porous and nonporous surfaces.	Abrasion with controlled removal by vacuum suction.	Hold tool flush to surface to prevent escape of contamination.	Controlled disposal.	Contamination of equipment.

here).

The decontamination program assumed here was modeled after that followed in the TMI decontamination effort [6.22, 6.23]. The magnitude of the program should be somewhat reduced from that at TMI because there would be no need to remove fuel or decontaminate the primary coolant system. Also, different radionuclides would have been released, so slightly different techniques and procedures may be used (the ease of removal of the different radionuclides from surfaces is difficult to postulate). Methods used for decontaminating building and fixed equipment surfaces include washing with a high-pressure water jet, wet and dry vacuuming, and manual wiping (see table 6.9). The TMI staff estimated that decontamination of the reactor building would require a work effort in the range of 300,000 to 900,000 man-hours [6.23]. It is expected that the magnitude of the clean up effort for the accident considered here will be less than that for TMI, although similar activities are to be performed. The quantity of radioactivity released from TMI was calculated to be 2.4 MCi, based on readings from a stationary gamma monitor located at the base of and external to the stack [6.22]. It was assumed that the labor requirement for decontamination at the plants being considered here would scale from the lower TMI manpower estimate (300,000 man-hour) with the total quantity of radioactivity released during the accident. The manpower estimates for clean up are summarized in table 6.10. As with TMI, a 50 % productive in-building effort was assumed; the labor estimates given in table 6.10 refer to time spent in radiation fields.

It would be advantageous to begin the clean up effort as soon as possible. This would be allowed if radiation fields were not excessive (i.e. lethal for short exposure times), if workers were adequately protected, if there existed a labor force to draw from so that occupational exposure limits were not exceeded, if extra time was not needed to prepare for the decontamination program and if regulatory and financing considerations did not preclude immediate implementation of the program. Clean up efforts were assumed to begin when the dose rate fell to the 1.25 rem/h level. The cooldown time required before this dose rate is achieved is indicated for each

design in table 6.10. A crew of 12 men was used to perform all tasks, and crew replacement was assumed to occur when each crew member had incurred a dose of 5 rem. The total number of workers needed, assuming all crew members to replaced at the same time, is given in table 6.10 as well. Doses incurred are summarized in table 6.6 for case (1). Shielding would be used to protect workers from the ambient radiation fields while they are performing clean up tasks. Any reduction due to shielding or protective clothing has not been considered for the doses given in table 6.6.

Liquid wastes from decontamination must be treated prior to transport and disposal at a low-level radioactive waste disposal site. Processing alternatives include filtration, ion exchange, evaporation and bitumenization. The decontamination solutions must also be processed and stored or shipped offsite. Additional wastes will result from the accident and from decontamination activities. Blanket modules and other equipment can be handled as in the usual manner during regular blanket changeouts. No additional handling equipment or new procedures will be required for dealing with this waste (as is the case for many TMI tasks). Combustible trash can be incinerated to reduce volume; the resulting ash can be immobilized prior to disposal. Non-combustible trash can be compacted to reduce volume. Contaminated equipment and hardware can be disassembled and mechanically sectioned for volume reduction. These wastes must then be appropriately packaged before shipment to the waste disposal site.

The estimated occupational dose for building and equipment decontamination at TMI ranges from 1000 to 3600 man-rem [6.23]. Treatment of radioactive liquids and wastes is expected to result in a dose ranging from 115 to 640 man-rem. It can be anticipated that the same ratio of doses for building decontamination to waste handling will also result at the plants under consideration here. Thus, the dose for waste handling during decontamination can be taken as 16.5 % of that incurred during building decontamination. This factor has been applied in arriving at the dose estimates given in table 6.6.

Table 6.10: Decontamination Program

	DT			DD			DHe
Task	5 %	10 %	20 %	5 %	10 %	20 %	10 %
Time Spent in Radiation Fields (man-h)	292	537	768	395	553	780	0
Crew Size	12	12	12	12	12	12	0
Cooldown Time (d)	3.75	4.25	4.5	3.75	4.0	4.25	0
Total No. Workers	36	36	48	36	36	48	0

Labor costs for decontamination were based on a remuneration rate of 30 \$/h. In addition to these costs, other costs will be incurred due to: additional services, materials (chemicals, shielding, filters etc.), and additional equipment. These costs are roughly 25 % of the labor cost for decontamination [6.23]. The total cost for decontamination is given in table 6.11. This compares to $\sim$ 25 M\$ estimated for TMI contamination.

6.3.5.1.3 Repair Costs

Some damage to major components requiring replacement and/or repair will result from the LOCA. It was assumed that the damage was not extensive enough to render decommissioning the more attractive alternative (as opposed to repair). Repair was assumed to be possible. The repair costs include the replacement cost of any damaged components, the labor cost to replace them. The cost of health detriment for any worker exposure during the repair job is included in the estimate made in section 6.3.5.1.4. Before evaluating this cost, it was necessary to estimate the degree of damage to the reactor. From the temperature information, an estimate of the damage due to thermal creep was made (see discussion in section 6.3.3 and appendix G). In all cases, it appeared only necessary to replace the blanket module damaged during the initial breach of the vacuum vessel. Cost estimates for replacement were based on the algorithms given in appendix B. Single module replacement costs were taken to be one-twentieth of the total blanket cost. The cost of the breeder was not included in the DT blanket replacement costs (lithium was assumed to be reusable after the accident). Labor costs were assumed to be 25 \$/h (slightly lower than decontamination labor costs because of the reduced risk). Labor requirements are listed in table 6.6 and were based on estimates given in chapter 5 for module replacement. Since the repair costs are not incurred until after the completion of clean up, discounting to obtain the present value of this cost should be included. However, because of the relatively short duration of the decon-

Table 6.11: Economic Impact of LOCA

	DT			DD			DHe
Cost Contributor	5 %	10 %	20 %	5 %	10 %	20 %	10 %
Replacement Power Costs (M$)	5.2	6.7	8.0	5.9	6.6	7.9	1.0
Outage Duration (d)	7.6	9.7	11.6	8.6	9.6	11.4	1.5
Decontamination Costs:							
Labor (M$)	0.017	0.032	0.046	0.024	0.033	0.047	0
Materials (M$)	0.004	0.008	0.012	0.006	0.008	0.012	0
Total (M$)	0.021	0.040	0.058	0.030	0.041	0.059	0
Repair Costs:							
Equipment (M$)	0.924	0.703	0.561	37.9	23.1	14.8	0.553
Labor (M$)	0.005	0.005	0.005	0.006	0.005	0.005	0.004
Total (M$)	0.929	0.708	0.566	37.9	23.1	14.8	0.557
Health Effects Costs (M$)	0.009	0.010	0.010	0.008	0.010	0.010	6.0×10^{-5}
Total (M$)	6.16	7.46	8.62	43.8	29.8	22.8	1.56

tamination effort (on the order of days, as opposed to years), it was not necessary here. Estimates are given in table 6.11.

6.3.5.1.4 Health Effects Costs

The entry of workers into contaminated areas to perform clean up operations or repairs will result in exposure to radioactivity. There is an actual societal cost associated with the exposure of any individual to radiation. Studies have been carried out to estimate the costs and risks of radiation exposure [6.24, 6.25]. These are based on the costs associated with an incidence of cancer, including medical costs and lost income, and with genetically inherited abnormalities, including institutional care and lost earnings. The cost for exposure taken from reference [6.19] and updated to 1986 dollars is 40 $/man-rem. Health detriment costs, as indicated in table 6.11, are relatively minor.

6.3.5.2 Offsite Economic Consequences

As the results of section 6.3.4 indicate, offsite impacts of this accident will be very small. It is expected that the only cost which will result is the societal cost due to radiation exposure. From the population dose under the most conservative conditions, which assumes immediate release of all volatilized material to the environment, with no delay due to hold up in the reactor building, the cost is found to be insignificant relative to those incurred onsite.

Offsite accident costs are generally associated with population protective measures. Due to the negligible offsite dose, these costs are expected to be non-existent for the accident considered here. Nevertheless, a brief outline of the costs which may be considered for more severe events is given below. A more detailed discussion, along with models for estimating the costs, is given in reference [6.19].

Evacuation costs will result if there is the need to immediately move a population out of a threatened area. Evacuation may be invoked before a hazardous situation arises as a precautionary measure. If an area does receive unsafe radiation levels, it may be necessary to temporarily or permanently relocate the population. In addition to transportation, shelter and food costs for temporary relocation, a permanent relocation will involve lost income and productivity costs. Decontamination costs may be incurred to clean up and restore the land of an affected area. This is accomplished through the implementation of techniques which remove surface deposited radionuclides. Agricultural products in an affected area must be disposed of. A cost will result from the actual disposal of the contaminated material plus the cost to the farmers from the loss of produce or loss of feed for livestock. If an area is extremely contaminated, clean up may not be possible for an extended period of time. Prohibition of inhabitation or use of an area of land for an extended period of time may be necessary if decontamination efforts cannot reduce the activity to acceptable levels. "Land interdiction" costs can be evaluated using the concept of land wealth as outlined in references [6.26, 6.27, 6.28]. Other secondary offsite impacts include the effects on the local land values, prices of crops and dairy products and increased labor costs due to emigration. Additionally, the cost of electricity in a region will increase, affecting the local economy as reflected in prices, employment, incomes and productivity. Litigation costs will also result as affected parties will likely attempt to receive some compensation.

6.4 Accident Hazard Summary

The accident hazard associated with a fusion reactor is determined by the quantites of radioactive species associated with the design, the sources and magnitudes of the stored energy, and the credible accident scenarios where this energy could be liberated. The radioactive inventories were quantified in the previous chapter. Here, the sources and magnitudes of stored energy were examined and the consequences

of a loss of coolant accident were investigated.

The advanced fuels appear to have a greater store of energy. This is largely a consequence of the greater magnetic fields and the higher operating temperature associated with these designs. The DD fuel cycle is worst in terms of storage of decay heat, for the blanket materials used here (HT-9 and Fe2Cr1V). This is a result of the larger amount of structural material relative to DT and the higher neutron flux relative to DHe. An additional source of stored energy exists in the lithium blankets of the DT designs. The chemical energy which could be released upon burning lithium presents a potential concern for this fuel cycle.

To obtain some idea of the consequences of a potential accident for the various fuel cycles, the safety and economic effects of a loss of coolant accident were assessed. In terms of overall impact of the accident, the DHe fuel cycle presents the least hazard. The temperatures achieved during the transient, the quantities of radionuclides mobilized, clean up/repair efforts, occupational and public exposures are all significantly reduced for this fuel cycle. There is less of a disparity between the DT and DD fuel cycles.

The total quantity of radionuclides released is dependent on the first wall temperatures reached during the transient. For DHe, the declining temperature resulting from the low nuclear heating in the blanket leads to minimal releases. For the other fuel cycles, the first wall temperatures increase during the transient, and the maximum temperature reached increases with beta. There is not a large difference between the DT and DD fuel cycles. This is a consequence of the higher nuclear heating rate in the DD blankets due to the larger fraction of structural material despite the lower neutron flux. Although the relative amounts of the different nuclides released are different, the total amount volatilized is nearly the same for DT and DD. The total activity released for these cases is over three orders of magnitude higher than for the DHe fuel cycle.

The decontamination effort was assumed to be dependent on the total quantity of radioactivity released. This was greatest for the high beta DT and DD fuel cycles. However, it should be noted that relative to releases which occurred as a consequence of the incident at Three Mile Island, the releases which are considered here are orders of magnitude lower. The time at which the decontamination program can begin depends on the dose rate level in the reactor hall. The dose rate is determined by the quantities of specific radionuclides released, and will decrease at a rate dependent on the decay rate of these radionuclides. Worker entry was allowed when the dose rate had fallen to 1.25 rem/h. The longest cooldown time needed is for the high beta DT design. The duration of the clean up effort and the resulting occupational exposures are greatest for the high beta DT and DD designs, although there is not a large reduction at the lower values of beta. The small quantity of radioactivity released from the DHe reactor does not require a clean up program.

Doses incurred during repair activities depend on the time at which they take place relative to the beginning of the accident (i.e. dose rate) and the duration of the repair task. For those fuel cycles requiring less time for decontamination (this refers to decontamination of surfaces, not airborne activity which is removed through the ventilation system), the dose rate at which repair begins is higher. This is the case for the lower beta designs. The length of time needed for repair is largely determined by the size of the component to be replaced. This is greater for the low beta designs which have larger blanket modules. Thus, the dose incurred during repair is greatest for the low beta designs.

The total onsite dose incurred is due to either exposure while reestablishing cooling, during decontamination or during repair. There is not a large difference between the DT and DD fuel cycles. The doses are slightly greater for the high beta designs, although the variation over the range of betas examined is less than 20 % for both fuel cycles. There is a significant reduction in the onsite dose incurred for the DHe fuel cycle during the accident.

Offsite doses are small in all cases. However, if one wishes to examine trends, the same variations are exhibited with offsite effects as with onsite effects. The offsite impacts for the DHe fuel cycle are much reduced from the other cases. There is not a large difference between the DT and DD fuel cycles. The effects are greater at higher beta. It should be stressed that the impact of this accident is minimal. Even in the worst case (high beta DT and DD), the chronic dose (dose from all pathways except ingestion, over the individual's life) at the site boundary just exceeds the limiting annual dose for a member of the general public.

In terms of economic impact of the LOCA, the DD fuel cycle appears to have the most severe consequences. This is largely due to the replacement component costs. Because it was assumed that the first wall and blanket form an integral structure, the entire component must be replaced after the accident. This is relatively more expensive than for DT (in addition to the fact that the DD modules are larger) because the DT modules contain a large amount of lithium, which was assumed to be reusable after the accident, whereas the DD blankets contain a larger volume fraction of structure. It is the relatively more expensive structure which must be replaced in greater amounts for the DD fuel cycle. For the DHe fuel cycle, the replacement costs are similar to DT despite the large fraction of structure because the blanket segments are relatively small (i.e. the blanket is thin). Replacement power costs are also a significant contributor to the accident costs. These are fairly similar for the DT and DD designs at a given value of beta. The cost is somewhat lower for DHe because there is no need for a decontamination program and the outage duration is somewhat reduced.

The assessment was not performed for the DD design having an RAF first wall and Fe2Cr1V blanket. However, the impact of the LOCA can be inferred, knowing the magnitude of the decay heat source and the concentration of radionuclides in the first wall. It is expected that the first wall temperature history subsequent to the accident will be similar to the HT-9 case. This will occur because of the similar thermal properties of RAF and HT-9, and the fact that the shutdown decay heat

levels in the first wall and blanket are nearly the same. The first wall temperature rise may even exceed it because the RAF first wall and Fe2Cr1V blanket decay heat levels are slightly higher. Since the quantities of major contributors to the shutdown decay heat are similar in both first walls, it is expected that the decay heat as a function of time would follow a similar pattern. It is anticipated that a similar or slightly higher dose would result to clean up and repair crew members because major contributors to the dose are present in the RAF first wall in about the same concentration as in the HT-9 first wall (More may be released than for HT-9 if the first wall temperature rise is slightly greater. This assumes HT-9 volatilization rates are applicable to RAF). Offsite health impacts are expected to be small, as with the other cases. Economic consequences for the RAF case would be somewhat reduced because the cost to replace a single module in the alternate DD design is less than for the HT-9 design.

In summary, the DHe fuel cycle results in the least health and economic impacts due to the accident. Health hazards for the DT and DD fuel cycles are comparable at a fixed value of beta, both being significantly larger than for DHe. The economic impact of the DD fuel cycle is greater than for the DT fuel cycle. Thus, the DD fuel cycle appears least attractive in terms of the consequences of this accident. An improvement would result from using either a smaller volume fraction of structure or a lower activation material in the DD blankets.

6.5 References

(6.1) Y-K.M. Peng et al., Plasma Analysis of a Tokamak Fusion Engineering Device (FED), Proceedings of the 9th International Conference on Plasma Physics, 1982.

(6.2) S.J. Piet, M.S. Kazimi and L.M. Lidsky, Potential Consequences of Tokamak Fusion Reactor Accidents: The Materials Impact, M.I.T. Plasma Fusion Center, PFC/RR-82-18, June 1982.

(6.3) R.J. Onega et al., Thermal Consequences to the First Wall of a DT Fueled Tokamak due to a Major Plasma Disruption, Nuclear Science and Technology, 75, p. 243, 1980.

(6.4) E.C.Selcow, Safety and Deterministic Failure Analyses in High Beta DD Tokamak Reactions, Columbia University, DOE/DT/53016-T3, 1984.

(6.5) F. Arendt and P. Komarek, Potential Failures and Hazards in Superconducting Fusion Reactors, Nuclear Technology/Fusion, 1, p. 552, 1981.

(6.6) D. Okrent et al., On the Safety of Tokamak-Type, Central Station Fusion Power Reactors, Nuclear Engineering and Design, 39, p. 215, 1976.

(6.7) D.A. Dube and M.S. Kazimi, Analysis of Design Strategies for Mitigating the Consequences of a Lithium Fire Within the Containment of Controlled Thermonuclear Reactors, Massachusetts Institute of Technology, MITNE-219, 1978.

(6.8) D.W. Jeppson and L.D. Muhlestein, Fusion Reactor Breeder Materials Safety Comparison Studies, Nuclear Technology/Fusion, 4, p. 277, 1983.

(6.9) J.P. Holdren, Findings of a U.S. National Committee on Environmental, Safety and Economic Aspects of Magnetic Fusion Energy, Draft March 1987.

(6.10) S. Barnett, Massachusetts Institute of Technology, private communication, March 1987.

(6.11) P.H. Sager et al., FED Baseline Engineering Study Report, Oak Ridge National Laboratory, ORNL/FEDC-82/2, April 1983.

(6.12) J.B. Cannon, Background Information and Technical Basis for Assessment of Environmental Implications of Magnetic Fusion Energy, U.S. Department of Energy, DOE/ER-0170, August 1983.

(6.13) J. Massidda, Thermal Design Considerations for Fusion Reactor Inherent Safety, Doctoral Dissertation, Nuclear Engineering Department. M.I.T., expected completion in 1987.

(6.14) S.J. Piet et al., Modelling of Fusion Activation Product Release and Reactor Damage from Rapid Structural Oxidation, Nuclear Technology/Fusion, 4, p. 1115, 1983.

(6.15) S.J. Piet et al., Oxidation/Volatilization Rates in Air for Candidate Fusion Reactor Blanket Materials, PCA and HT-9, Journal of Nuclear Materials, p. 24, November - December 1986.

(6.16) G.M. Barrow, PhysicalChemistry, Fourth Edition, McGraw-Hill Book Company, 1979.

(6.17) S. Fetter, Radiological Hazards of Fusion Reactors: Models and Comparisons, Doctoral Dissertation, University of California, Berkeley, May 1985.

(6.18) Reactor Safety Study, An Assessment of Accident Risks in U.S. Commercial Nuclear Power Plants, U.S. Nuclear Regulatory Commission, WASH-1400 (NUREG-75/014), October 1975.

(6.19) S.J. Brereton and M.S. Kazimi, A Methodology For Cost/Benefit Safety Analyses for Fusion Reactors, M.I.T Plasma Fusion Center, PFC/RR-85-3, March 1985.

(6.20) W.A. Buehring and J.P. Peerenboom, Loss of Benefits Resulting from Nuclear Power Plant Outages, Argonne National Laboratory, NUREG/CR-3045, (ANL/AA-28), Vols 1 & 2, March 1982.

(6.21) B. Shleien, Preparedness and Response in Radiation Accidents, HHs Publication FDA 83-8211, August 1983.

(6.22) T.H. Moss and D.L. Sills, Eds, The Three Mile Island Nuclear Accident: Lessons and Implications, Annals of the New York Academy of Sciences, volume 365, 1981.

(6.23) Programmatic Environmental Impact Statement (Final) Related to Decontamination and Disposal of Radioactive Wastes Resulting from March 28, 1978 Accident Three Mile Island Nuclear Station, Unit 2, U.S. Nuclear Regulatory Commission, NUREG-0683-VI, March 1981.

(6.24) M.X. Hartunian et al., The Incidence and Economic Costs of Cancer, Motor Vehicle Injuries, Coronary Heart Disease and Stroke: A Comparative Analysis, American Journal of Public Health, 70, p. 1249, 1980.

(6.25) T. Straume and R.L. Dobson, Leukemia and Cancer Risk Estimates from Recalculated Hiroshima and Nagasaki Doses, Proceedings of the 26th Annual Meeting of the Health Physics Society, Louisville Kentucky, 1981.

(6.26) R.P. Burke, Economic Risks of Nuclear Power Reactor Accidents, Doctoral Dissertation, Nuclear Engineering Department, Massachusetts Institute of Technology, October 1983.

(6.27) J.W. Kendrick, The Formation and Stocks of Total Capital, National Bureau of Economic Research, No. 100, General Series, Columbia University Press, New York, 1976.

(6.28) J.W. Kendrick et al., The National Wealth of the United States: By Major Sectors and Industry, A Research Report from the Conference Board's Division of Economic Research, Conference Board Report No. 698, New York, 1976.

(6.29) M.S. Kazimi, Safety Aspects of Fusion, Nuclear Fusion, Vol. 24, No. 11, p. 1461, 1984.

(6.30) U.S. Atomic Energy Commission, Radiological Emergency Operations - Student's Manual, USAEC Report TID-24919.

(6.31) D.C. Baxter et al., DD Tokamak Reactor Assessment, Nuclear Technology/Fusion, 4, p. 246, September 1983.

(6.32) Y. Fujiie et al., Safety Ensuring Principle for Fusion Systems, Proceedings of the Technical Committee Meeting on Fusion Safety, Culham U.K., November 1986.

(6.33) Fusion Safety Status Report, International Atomic Energy Agency, IAEA-TECDOC-388, 1986.

(6.34) B.K. Jenson and R.D. Endicott, Utility Evaluation of the DT STARFIRE and DD WILDCAT Reactors, Nuclear Technology/Fusion, 4, p. 290, September 1983.

(6.35) S. Fetter, A Calculational Methodology for Comparing the Accident, Occupational and Waste Disposal Hazards of Fusion Reactor Designs, Fusion Technology, 8, p. 1359, July 1985.